P-07-227

Oskarshamn site investigation

Structural characterization of deformation zones (faults and ductile shear zones) from selected drill cores and outcrops from the Laxemar area – Results from Phase 2

Giulio Viola, Guri Venvik Ganerød
Geological Survey of Norway, Trondheim, Norway

December 2007

Svensk Kärnbränslehantering AB
Swedish Nuclear Fuel
and Waste Management Co
Box 250, SE-101 24 Stockholm
Tel +46 8 459 84 00

ISSN 1651-4416
SKB P-07-227

Oskarshamn site investigation

Structural characterization of deformation zones (faults and ductile shear zones) from selected drill cores and outcrops from the Laxemar area – Results from Phase 2

Giulio Viola, Guri Venvik Ganerød
Geological Survey of Norway, Trondheim, Norway

December 2007

Keywords: Oskarshamn, AP PS 400-06-098, Structural geology, Shear zone, Fault, Fault rocks, Kinematics.

Abstract

A study of predominantly brittle structures, i.e. brittle deformation zones, faults, fractures and associated fault rocks, was carried out on a number of drill cores and outcrops of the Laxemar area, Oskarshamn. The main aim of the study is to document from a geometric and kinematic point of view the brittle deformational history of the region. The study deals with the detailed characterization of the observed deformation zones and fault rocks were systematically investigated in order to improve our understanding of the deformation mechanisms that controlled the local brittle structural evolution. Striated surfaces were used to constrain the kinematics of fault zones. Such data were obtained from outcrops and, to a variable extent, from several oriented deformation zones in the drill cores.

DZ1 of **KLX03** is composed by three different cores. Fault products vary from foliated cataclasites to cataclasites. Clear evidence for structural reactivation occures throughout the section. The three cores have different orientations and the available kinematic evidence gathered during the study does also differ from core to core. In more detail, whereas the uppermost core strikes consistently NE-SW and dips gently to the SE and striated planes within it and in its upper transition zone suggest a normal sense of shear towards the SE, the intermediate and deepest cores strike SE-NW, almost at 90° from the uppermost core, and are possibly characterized by reverse kinematics.

KLX04 was logged from 223 to 358 m depth. Deformation style is similar throughout the section and, in general, there is convincing evidence of a complex, long-lived brittle deformation history. Hydrofracturing and fluidization are inferred to have been important deformation mechanisms in this section, which lacks any sign of ductile precursors. The orientation of the fractures and cataclastic cores is rather consistent for all of the investigated deformation zones. The strike of these features is generally SE-NW and their dip is gentle to moderate to the NE and SW. Striated planes indicate the predominance of oblique reverse faulting, with top-to-the-N/NE or S/SW sense of shear. There are, however, also a few extensional fault planes, with slickensides generally coaxial with the reverse faulting direction.

KLX08 had DZ 6 and DZ 7 logged during this study. Deformation style is brittle throughout the inspected depth interval and structural evidence suggests multiple cataclastic episodes and a complex reactivation history. The cores of both deformation zones contain fault rocks that cover the whole spectrum of brittle fault products. DZ 6, including its upper and lower transition zones, is characterized by generally NNE-SSW striking and very gently ESE and WNW dipping fractures and striated planes, which bear primarily evidence of reverse faulting. These gently dipping fractures are interpreted, on the ground of the mineral infill, to postdate a set of steep conjugate E-W trending fractures. Fractures within DZ 7 have a similar orientation and dip very gently but no striated planes were observed.

KLX09: DZ 13 was logged in detail. DZ 13 is characterized by the presence of an extremely thick fault core (c. 30 m) formed by cataclastic rocks. No evidence of ductile precursors is observed. DZ 13 contains numerous striated planes that strike roughly NW-SE and dip very consistently to the NE. Kinematic constraints indicate both compression and extension, with top-to-the-SW and top-to-the-NE senses of shear, respectively.

Only DZ 9 was logged in **KLX10** during this study. DZ 9 has a remarkable core, c. 5 m thick, which consists of a complex sequence of fault rocks, with cataclasites, ultracataclasites and gouge. Orientation data from this depth interval are inconclusive, except for a series of systematic S/SSE-dipping open fractures within the upper transition zone.

In this study we have logged the whole of **KLX11A**. DZ 3, 6, 7, 8, 11, 12 and DZ 14 were identified as real deformation zones. Within these zones there is evidence of pervasive brittle deformation and multiple reactivation. Apart from DZ 11, where most fractures and striated planes strike NW-SE and bear evidence for sinistral and dextral strike-slip and low-obliquity shearing, the remaining deformation zones are oriented roughly WSW-ENE to E-W.

KLX12A: DZ 10, 11 and 12 were logged in detail during this study. The three zones are developed predominantly within intermediate to mafic rock types, varying from quartz monzodiorites to diorites and gabbros. The deformation style that characterizes these deformation zones is fully ductile, with mylonitic shear zones forming the cores of the deformation zones. Only in DZ 11 there is evidence of cataclasis, whereby mylonites overprint previously formed cataclasites. Whereas the mylonitic fabric in DZ 10 dips moderately to the SW, within the cores of DZ 11 and 12 mylonites dip consistently c. 50–55° to the SE/ESE.

In **KLX18A** we have interpreted as real deformation zones DZ 3, 5, 6, and 9. They are invariably characterized by cataclasites, highly fractured intervals and crush zones. Microstructures indicate multiple episodes of brittle deformation and structural reactivation. In general, fractures and cataclastic bands within these deformation zones strike E-W and dip gently to moderately to the S, SSW.

Four different deformation zones (DZ 1 to DZ 4) were logged in **KLX20A**. DZ 1, 2 and 3 contain fault cores and significant crush zones, whereas we do not interpret DZ 4 as a proper deformation zone. The most interesting and relevant zone is DZ 1, which contains a large dolerite dyke. Numerous striated planes (particularly within the dolerite) were measured, and two significant and systematic families of fault planes were identified. Generally E-W striking and moderately N- and S-dipping planes show both normal and reverse kinematics, with low obliquity. These are crosscut by sub vertical planes striking from NNW to NNE with predominantly strike-slip kinematics.

Sammanfattning

Et undersøkelse av overveiende sprø strukturer, dvs sprø deformasjonssoner, forkastninger, brudd og tilhørende forkastningsbergarter, er utført på flere borekjerner og blotninger i Laxemar-området, Oskarshamn. Hovedformålet med undersøkelsen er fra et geometrisk og kinematisk synspunkt å dokumentere den sprø deformasjonshistorien i området. Undersøkelsen omfatter detaljert karakterisering av de observerte deformasjonssonene, og forkastningsbergarter ble systematisk undersøkt for å forbedre forståelsen av deformasjonsmekanismene som kontrollerte den lokale sprø utviklingen av strukturene. Overflater med glidestriper ble brukt for å bestemme kinematikken til forkastningssonene. Slike data ble skaffet til veie fra blotninger, og i en del tilfeller også fra flere orienterte deformasjonssoner i borekjernene.

Deformasjonssone DZ1 fra borekjerne **KLX03** ble logget i denne undersøkelsen. Sonen består av forskjellige områder med deformasjon. Forkastningsproduktene varierer fra folierte kataklasitter til kataklasitter. Det ble funnet klare tegn for strukturell reaktivering gjennom hele lengden**.** De tre områdene har forskjellig orientering, og de tilgjengelige kinetiske bevisene samlet gjennom denne undersøkelsen varierer også fra kjerne til kjerne. I mer detalj viser det seg at den øverste kjernen stryker konsekvent mot NØ-SV og faller slakt mot SØ, og planene med glidestriper i den og den dens øvre overgangssone antyder en normal skjærbevegelse mot SØ. Den midtre og dypeste kjernen derimot, stryker mot SØ-NV, nesten 90° fra den øverste kjernen og er muligens karakterisert av revers kinematikk.

KLX04 ble logget fra 223 m til 358 m dybde. Deformasjonsstilen er lik gjennom hele lengden, og generelt er det overbevisende indikasjoner for en kompleks, langlivet, sprø deformasjonshistorie. Brudd på grunn av høyt vanntrykk og fluidisering er antatt å ha vært viktige deformasjonsmekanismer i denne delen, som ikke har noen tegn på duktile forløpere. Orienteringen på bruddene og de kataklastiske delene i kjernene er temmelig ensartet for alle undersøkte deformasjonssoner. Strøket på disse dannelsene er generelt SØ-NV og fallet er slakt til moderat mot NØ og SV. Glidestriper viser en dominans av skrå reversforkastninger, med topp mot N/NØ eller S/SV skjærbevegelse. Imidlertid er det også noen få plan som viser ekstensjonsforkastninger, generelt med samme akseretning som retningen på reversforkastningene.

KLX08 inneholdt DZ 6 og DZ 7 som ble logget i denne undersøkelsen. Deformasjonsstilen er sprø gjennom det hele undersøkte dybdeintervallet og strukturelle bevis antyder gjentatte kataklastiske episoder og en kompleks reaktiveringshistorie. Kjernene fra begge deformasjonssonene inneholder forkastningsbergarter som dekker hele spekteret av sprø forkastningsprodukt. DZ 6, inkludert både den øvre og nedre overgangssonen, er karakterisert av generelt NNØ-SSV-strykende brudd og glidestripeplan som heller svært svakt mot ØSØ eller VNV og viser hovedsakelig antydning til reversforkastning. På grunn av mineralfyllinger er disse svakt hellende bruddene tolket til å postdatere et sett av steilt konjugerte Ø-V gående brudd. Brudd innenfor DZ 7 har samme orientering og har svært slakt fall, men ingen glidestripeplan ble observert.

KLX09: DZ 13 ble logget i detalj. DZ 13 er karakterisert med et ekstremt tykt forkastningsområde (ca 30 m) dannet av kataklastiske bergarter. Ingen tegn på forutgående duktil bevegelse ble observert. DZ 13 inneholder tallrike plan med glidestriper som stryker omtrent NV-SØ og faller svært konsekvent mot NØ. Kinematiske indikatorer viser både kompresjon og ekstensjon, med henholdsvis topp-mot-SV og topp-mot-NØ rettet skjærbevegelse.

Bare DZ 9 ble logget i **KLX10** i denne undersøkelsen. DZ 9 har en bemerkelsesverdig kjerne, ca 5 meter tykk, som består av en kompleks sekvens av forkastningsbergarter med kataklasitter, ultrakataklasitter og sleppebergarter (=gouge). Data for orienteringen på dette dybdeintervallet er ikke entydige unntatt for en serie av åpne brudd som faller systematisk S/SSØ innen den øvre overgangssonen.

I denne undersøkelsen har vi logget hele **KLX11A**. DZ 3, 6, 7, 8, 11, 12 og DZ 14 ble identifisert som reelle deformasjonssoner. Innenfor disse sonene er det tegn på gjennomgående sprø deformasjon og gjentatt reaktivering. Bortsett fra DZ 11, hvor de fleste bruddene og planene med glidestriper stryker NV-SØ og viser tegn på (både) venstrelengs- og høyrelengsbevegelse og en liten komponent av skrå skjærbevegelse, er de resterende deformasjonssonene orientert omtrent VSV-ØSØ til Ø-V.

KL12A: DZ 10, 11 og 12 ble logget i detalj i denne undersøkelsen. De tre sonene er utviklet hovedsakelig i intermediære til mafiske bergartstyper som varierer fra kvartsmonzodioritter til dioritter og gabbro. Deformasjonsstilen som karakteriserer disse deformasjonssonene er fullstendig duktile, med mylonittiske skjærsoner som danner kjernene av deformasjonssonene. Bare i DZ 11 er det tegn på kataklase, der mylonittene overpreger tidligere dannede kataklasitter. Mens den mylonittiske teksturen i DZ 10 faller moderat mot SV, faller mylonittene i de sentrale delene av DZ 11 og 12 konsekvent ca 50–55° mot SØ-ØSØ.

I **KLX18A** har vi tolket at sonene DZ 3, 5, 6, og 9 har reell deformasjon. De er fortsatt karakterisert av kataklasitter, sterkt knuste intervaller og knusningssoner. Mikroteksturer antyder flere episoder med sprø deformasjon og strukturell reaktivering. Generelt stryker bruddene og de kataklastiske båndene innenfor disse deformasjonssonene Ø-V, og faller slakt til moderat mot S og SSV.

Fire forskjellige deformasjonssoner (DZ 1 til DZ 4) har blitt logget i **KLX20A**. DZ 1, 2 og 3 inneholder forkastningskjerner og betydelige knusningssoner, mens vi ikke tolker DZ 4 som en ekte deformasjonssone. Den mest interessante og relevante sone er DZ 1, som inneholder en tykk dolerittgang. Tallrike plan med glidestriper (spesielt innenfor doleritten) ble målt, og to betydelige og systematiske grupper av forkastningsplan ble identifisert. Plan som generelt stryker Ø-V og faller moderat mot N og S viser både normal og revers kinematikk, med en liten komponent skråforkastning. Disse er skåret av subvertikale plan som stryker fra NNV til NNØ med dominerende sidelengs kinematikk.

Contents

1 Introduction

This report provides the detailed characterization, in terms of deformation characteristics, geometry and, when possible, kinematics of selected brittle deformation zones at the Oskarshamn investigation site (Figure 1-1). This report forms the continuation of a similar study by the same authors /Viola and Venvik Ganerød 2007/. Detailed logging and structural characterization were performed on several depth intervals from a series of chosen drill cores, selected for their complexity and for the structural relevance of the deformation zones (from here on referred to as "DZ" and identified as such in the geological single-hole interpretation studies) they intersected. In addition, a limited number of outcrops were also investigated.

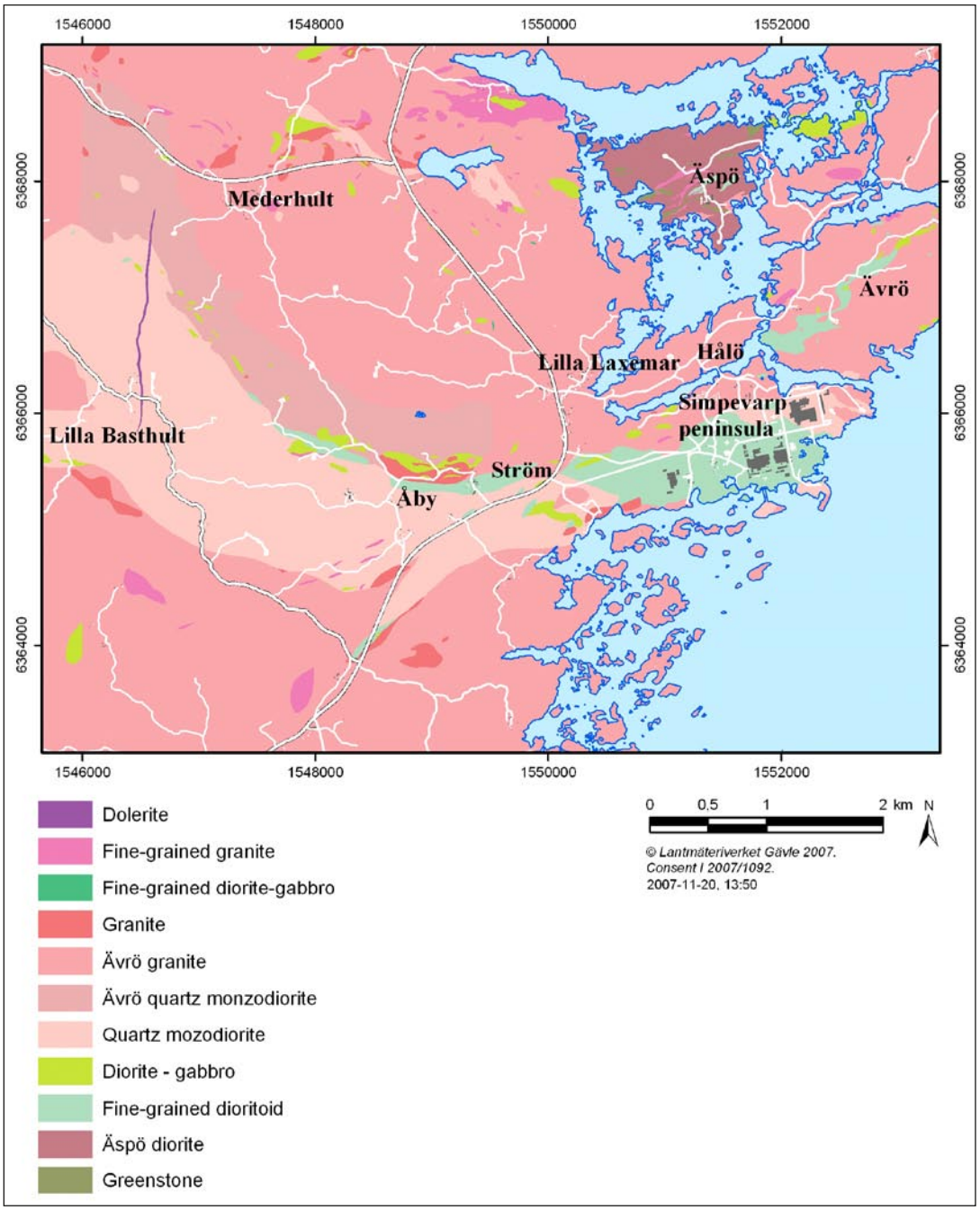

Figure 1-1. *Geology map of the Oskarshamn site investigation area.*

This study forms one of the activities performed within the site investigation process at Oskarshamn. The work was carried out in accordance with activity plan AP PS 400-06-098. Controlling documents for performing this activity are listed in Table 1-1. Both activity plan and method descriptions are SKB internal controlling documents.

Table 1-1. Controlling documents for the performance of the activity.

Activity plan	**Number**	**Version**
Karaktärisering av spröda deformationszoner steg 2	AP PS 400-06-098	1.0
Method descriptions	**Number**	**Version**
/Braathen 1999/	Tectonophysics 302, 99–121	
/Braathen et al. 2002/	Norwegian Journal of Geology, 82, 225–241	
/Braathen et al. 2004/	Tectonics, 23, TC4010, doi:10.1029/2003TC001558	
/Munier et al. 2003/	SKB R-03-07	
/Nordgulen et al. 2002/	Norwegian Journal of Geology, 82, 299–316	
/Osmundsen et al. 2003/	Journal of the Geological Society, London 160, 1–14	
/Petit 1987/	Journal of Structural Geology 9, 597–608	

2 Objective and scope

The aim of this study was to document, describe and characterize structurally, by means of detailed geometric and kinematic analyses, a number of brittle deformation zones from selected drill cores and from a few outcrops in the field. Fault rocks associated with these deformation zones, if present, were also investigated in order to improve our understanding of the deformation mechanisms that controlled the local brittle structural history. Data from drill cores and from the field, combined with observations from selected thin sections, form the basis for the results and conclusions of this study.

3 Equipment

3.1 Description of equipment/interpretation tools

During the drill core logging stage and during the field work we used the standard equipment for structural investigations, including hammer, compass, hand lens, diluted HCl, digital camera, and GPS for locating observation points according to SKB standards (Swedish Grid). Samples collected in the field and from drill cores were cut in the core laboratory, and selected oriented slabs were marked and sent in for preparation of polished thin sections.

4 Execution

4.1 Methodology

Standard structural field techniques were used during field work. The standard procedure for obtaining the true orientation of linear structures (lineations, striations, etc) on fault surfaces in drill cores with known orientation is as follows:

1. Fractures of potential interest are identified by visual inspection of drill cores from selected deformation zones, as defined previously by the geological single hole interpretations.
2. Individual fractures are identified on the BIPS image of the borehole wall, which provides a mirror image of the core itself. Care has to be taken to ensure that the fracture selected on the image matches the one from the drill core. In some cases this can be challenging, particularly where abundant fractures cut the core at different angles. Independent checks that the correct fracture is chosen can be carried out by using information contained in the drill core database, as, for example, the properties of the fracture itself, the acute angle α between the fracture and the core axis, and the angle β, which is the angle (measured counter-clockwise) from the lower intersection of the fracture with the core wall, to the top of the drill core.
3. Having identified the fracture of interest, the top of the drill core is marked based on visual inspection of the BIPS image and on the angle β. Fractures' orientation (strike and dip) is obtained using the information contained in the drill core database.
4. The core is positioned the right way up and at the true inclination using a core holder supplied by SKB. This device allows the accurate adjustment of the core inclination as given in the database.
5. The orientation of the linear structure is determined by measuring its plunge direction and plunge.
6. When the sense of slip can be determined with confidence, the true movement of the hanging wall with respect to the footwall of the fault is established.
7. Relevant data are recorded in a database.

Thin section samples were collected from some of the drill cores, and their polished sections were studied at the Geological Survey of Norway (Trondheim) using standard petrographic techniques.

4.2 General

Literature studies preceded the investigations, which were carried out at the Oskarshamn core-logging facility on March 20–23 and September 19–22 2006 for a total of ten working days. The following drill cores and relative deformation zones were inspected during this study (Table 4-1).

Two days in September 2006 were devoted to structural fieldwork in the Laxemar area aimed at unravelling brittle structural patterns at a number of selected outcrops (PSM007661–PSM007668).

Table 4-1. Drill cores and sections studied in this report.

Drill core	Logged length (m)	Deformation Zone
KLX03	722.5–814	DZ 1
KLX04	227–355	DZ 1 to 5
KLX08	385–487.5	DZ 6 and 7
KLX09	100–880	DZ 1 to 18
KLX10	690.5–706	DZ 9
KLX11A	142–975	DZ 1 to 18
KLX12A	445–600	DZ 10 to 12
KLX18A	137–489	DZ 1 to 9
KLX20A	234–416.5	DZ 1 to 4
Total:	674.41	

4.3 Data handling and processing

Structural data were analysed at the Geological Survey of Norway (NGU) in Trondheim and plotted using the commercial package Tectonics FP. Thin sections were analysed in several steps:

1) Scanning at high resolution of the entire section using a standard slide scanner.
2) Printing of the scanned jpg-images as A4 colour prints in order to aid in establishing general structural and textural relationships and to locate critical sites for further detailed microscopic study.
3) Petrographic analysis and documentation of textural and micro-structural relationships using a petrographic microscope and a digital camera attached to it.

4.4 Analysis and interpretation

The working methods used are described in /Braathen 1999, Braathen et al. 2002, Nordgulen et al. 2002/ and /Osmundsen et al. 2003/. In this report, the definition of fault rocks follows the classification scheme of /Braathen et al. 2004/. Criteria for identifying kinematic indicators in the brittle regime are presented, for example, in /Petit 1987/.

A systematic analysis of fault slip data at the micro- and meso-scale has been made aiming towards an improved understanding of kinematic patterns in the area of interest. The approach consists in the analysis of strike and dip of fault planes and of azimuth and plunge of their striations. This allows the determination of the complete kinematics of fault trends (even major fault trends). It also provides the basis for paleo-stress inversion calculations that can aim at the reconstruction of the stress field evolution through time. Figure 4-1 provides the key to read the conventions used in the stereonets to represent the orientation and the kinematics of individual fault plane/striation pairs.

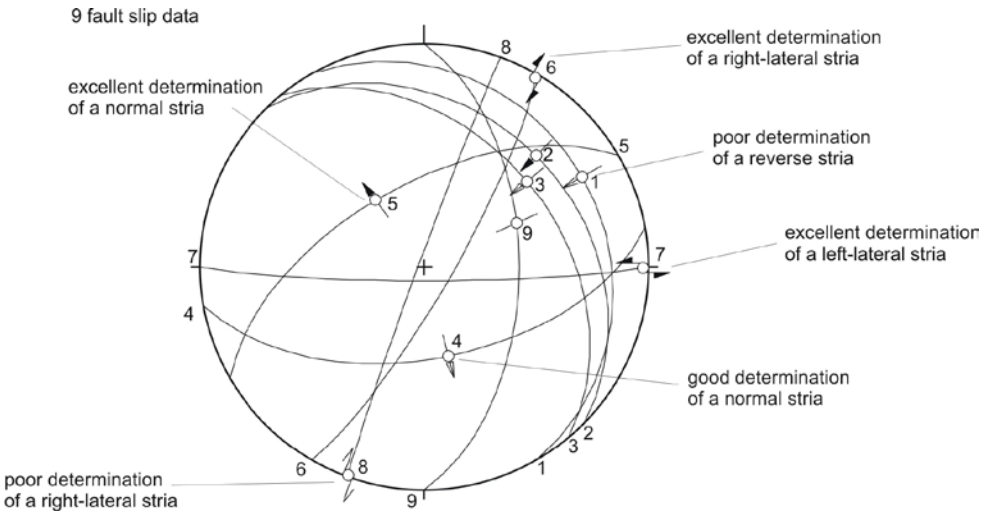

Figure 4-1. *Example of a stereonet plotting kinematic information for striated fault planes (Schmidt projection, lower hemisphere). Keys for striae: outward-directed arrow: normal striation (numbers 4 and 5 on the stereonet); inward directed arrow: reverse striation (numbers 1, 2 and 3); couple of arrows: strike-slip striation (numbers 6, 7 and 8); full black arrowhead: excellent constraints on the sense of shear (numbers 2, 5, 6 and 7); empty arrowhead: good constraints on the sense of shear (numbers 3 and 4); open arrowhead: poor constraints on the sense of shear (numbers 1 and 8); thin line without any arrowhead: no constraints on the sense of shear (number 9).*

4.5 Nonconformities

Problems with BIPS orientations

By pure coincidence there were two BIPS loggings made at different stages in the same borehole. Although the two different loggings should have provided identical results as regards the orientation of planar elements, this was not the case. Apparent discrepancies were discovered and this finding led to a systematic study and investigation of the problem and of its possible causes. It was discovered that early loggings, which used a gravitational steel ball to indicate the lower side of the borehole, were more affected then later loggings, which used instead an air bubble to indicate the upper side of the borehole. Furthermore, steeper (close to vertical) boreholes were more affected than less inclined boreholes, due to the spinning tendency of the probe. This tendency was also increased by the torsion built up in the logging cable during the logging operation. The spinning of the probe made it hard for the logging operator to perform the orientation adjustments, which had to be done manually.

The identification of these problems has led to a major effort towards the correction of the acquired orientations with all possible means. The main method adopted was the utilization of the raw videotapes so as to study and record the offset of the orientation in relation to the air bubble. In early boreholes, where the steel ball was used, other logging methods, like acoustic televiewer, were used to correct the error. Orientation mismatches were generally small, up to 10°, but usually less. In some rare short sections, mostly in the uppermost parts of the cores, the error was, however, much larger and a few of these sections had to be finally reported as not oriented.

This report uses the orientations that were officially in use at the time of logging and no correction has been used.

4.6 Fault architecture and nomenclature

Faults occur on all scales in the lithosphere. They control the spatial arrangement of rock units, affect the topography, control the permeability of rocks and sediments and, more importantly, accommodate deformation (strain, plus rotation plus translation) during plate interaction and intraplate movements. The term fault zone is generally used for brittle structures in which loss of continuity and slip occurs on several discrete faults within a band of definable width. Shear zones, on the other hand, are ductile structures, across which a rock body does not lose continuity so that strain is progressively distributed across a band of definable width. Based on this definition, a fault zone is a volume of rock where strain is highly localized.

Commonly fault zones can be subdivided into a series of distinctive constituent elements (Figure 4-2 and Figure 4-3). These are 1) the *undeformed host rock*, 2) the *transition zone* /Munier et al. 2003/ (corresponding to the "damage zone" of e.g. /Gudmundsson et al. 2001/) and 3) the proper *fault core* /e.g. Caine et al. 1996, Evens et al. 1997, Braathen and Gabrielsen 2000/. The host rock consists of undeformed rock with low fracture frequency of < 4 fractures/m /Munier et al. 2003/ (Figure 4-2). The transition zone still contains undeformed rock, but the fracture frequency generally increases up to 9 fractures/m (Figure 4-2). Narrow zones or bands of fault rock may occur, especially closer to the boundaries to the fault core. The width of the transition zone varies with the size of the fault zone and the style of deformation, and can range from a few meters to tens of meters. The fault core is identified by the occurrence of fault rock or intensively fractured rock (Figure 4-2 and Figure 4-3). Fault rocks may occur in lenses alternating with pods of relatively undeformed rock /Caine et al. 1996, Braathen and Gabrielsen 2000/. The width of the fault core may vary from cm to m /Braathen and Gabrielsen 2000/.

Rocks that occur within fault zones provide primary evidence for the processes that have occurred there. It is therefore of great importance to fully characterize fault rock occurrences, so as to better understand faulting processes and mechanisms at all scales. Fault rocks form in response to strain localization within fault and shear zones and reflect the interplay of a variety of physical and environmental parameters such as, for example, the finite amount of strain, lithology, style of deformation (i.e. frictional or plastic flow), presence or absence of fluids, strain rate, temperature, pressure and so on. Figure 4-4 reports the classification scheme proposed by /Braathen et al. 2004/ that we will use in this study to classify fault rock occurrences.

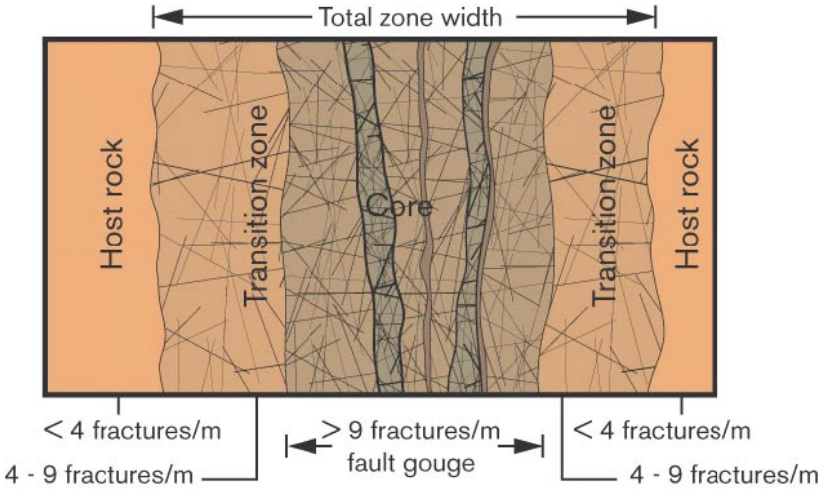

Figure 4-2. *Schematic illustration of a brittle deformation zone according to SKB definition /after Munier et al. 2003/.*

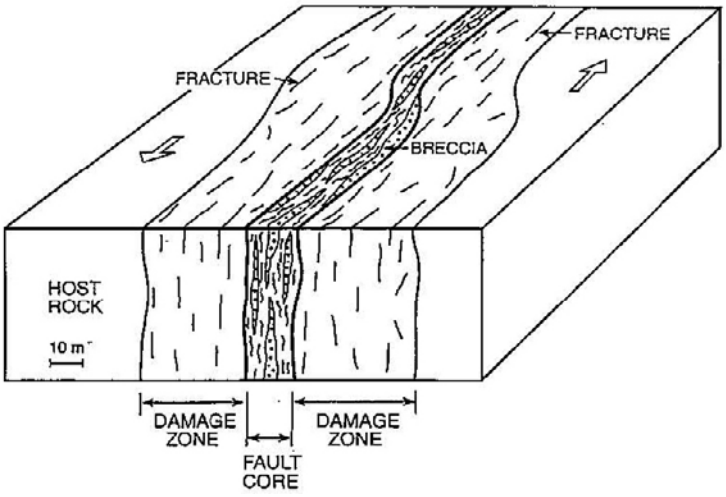

Figure 4-3. *Schematic illustration of the architecture of an idealized fault zone /Gudmundsson et al. 2001/. Note that the term "damage zone" used in this scheme corresponds conceptually to the term "transition zone" of Figure 4-2.*

Brittle ← *Deformation style* → **Ductile**									
Frictional flow ← *Dominant deformation mechanism* → **Plastic flow**									
Non-cohesive			Secondary cohesion		Primary cohesion				*% matrix and grain-size*
			Cemented HB	Indurated HB			*> 50% phyllosilicate*	*< 50% phyllosilicate*	
Hydraulic breccia (HB)	Breccia series	Proto-breccia	Cemented proto-breccia	Indurated proto-breccia	Cataclasite series	Proto-cataclasite	Proto-phyllonite	Proto-mylonite	*0-50% matrix*
		Breccia	Cemented breccia	Indurated breccia		Cataclasite	Phyllonite	Mylonite	*50-90% matrix*
		Ultra-breccia	Cemented ultra-breccia	Indurated ultra-breccia		Ultra-cataclasite	Ultra-phyllonite	Ultra-mylonite	*90-100% matrix*
	Gouge		Cemented gouge	Indurated gouge					*Sub-microscopic matrix*
			Pseudotachylyte						

Figure 4-4. *Fault rock classification scheme proposed by /Braathen et al. 2004/.*

5 Drill core investigations

In the following section, the character and structural relationships of the deformation zones studied in the drill cores are described with particular emphasis on the occurrence of fault cores and associated fault rocks, transition zones and systematic sets of sealed and open fracture networks. When possible, the sense of shear along striated planes was established in order to add kinematic constraints to the brittle evolution of the area. Observed crosscutting relationships between fractures and faults with different orientations and mineral infill are pointed out, thus providing tighter constraints to the model of the geological history of the investigation area. The kinematic data are described in relation to the mineralogy of the faults and fractures. The geographic location of the cores investigated in this study is shown in Figure 5-1.

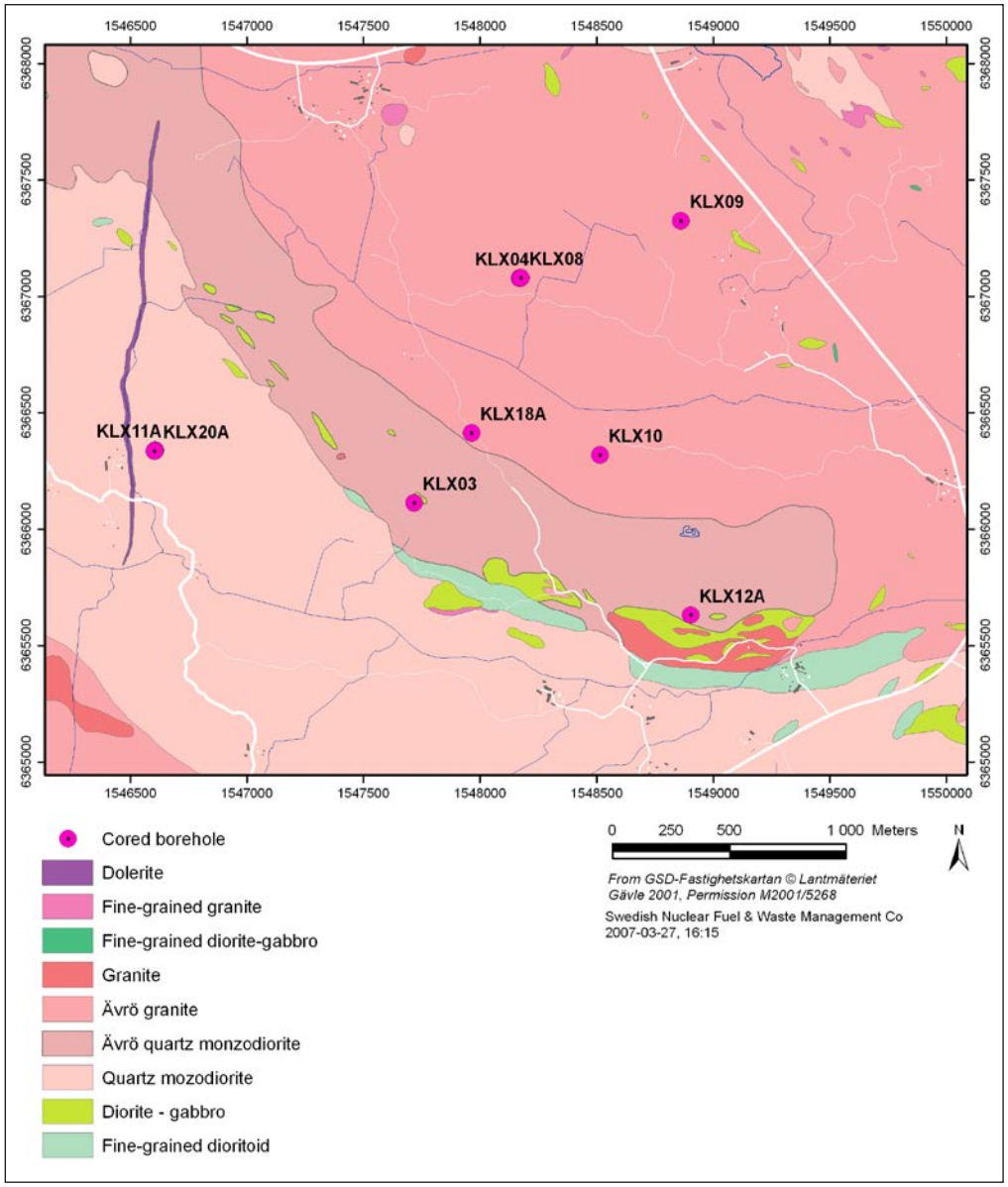

Figure 5-1. *Location of the drill cores described in this report.*

5.1 Summary of drill core data

The characteristics and the main structural features of each deformation zone logged during this study are conveniently summarized in concise descriptive tables reported at the end of every DZ chapter. These tables, together with the schematic log drawn for each DZ, provide a very useful tool for a rapid characterization of the deformation zones. In order to summarize the main observations and the content of this long chapter, in this section we lay out a synoptic structural summary of each of the drill cores by pointing out the most relevant and interesting aspects of the study and we thus provide elements for further work and comparative analyses.

KLX03

One single DZ (DZ1, 720–820 m) was logged during this study. It contains three distinct cores and their respective transition zones, separated by intervals of undeformed host rock. Deformation style within this DZ varies with depth: foliated cataclasites form the first core at depth 732.2 m, purely brittle features are instead found within the second core, at depth 767.5 m, whereas foliated cataclasites are found again in the lowest core at depth 795 m. Clear evidence for structural reactivation is found throughout the section.

Although the three cores are part of the same DZ in the single-hole interpretation by /Carlsten et al. 2005/, it is useful to point out that they have different orientations and that the kinematic evidence gathered during the study does also differ from core to core. In more detail, whereas the uppermost core strikes consistently NE-SW and dips gently to the SE (Figure 5-6), and striated planes within it and in its upper transition zone suggest a normal sense of shear towards the SE (Figure 5-3 and Figure 5-6), the intermediate and deepest cores strike SE-NW, almost at 90° from the uppermost core, and are possibly characterized by reverse kinematics (e.g. Figure 5-12 and Figure 5-14). It is therefore suggested that a more detailed and critical assessment of DZ 1 would be required in order to account for the structural variability within the DZ. A set of very characteristic, c. N-S trending, epidote-decorated brittle-ductile shear zones is intersected by KLX03 (Figure 5-17). These structures are very common in the Laxemar area and have been described in several drill cores and outcrops by /Viola and Venvik Ganerød 2007/.

KLX04

The depth interval logged extends from 223 to 358 m. The single-hole interpretation by /Carlsten et al. 2004/ describes 5 different deformation zones within this section and our study confirms their presence on the base of structural criteria. In addition, between DZ 2 and DZ 3 we have identified two other significant fault cores, characterized by fault rock occurrences, and their relative transition zones (Figure 5-20).

Deformation style is similar throughout the section and, in general, there is convincing evidence of a complex, long-lived brittle deformation history. Hydrofracturing and fluidization are inferred to have been important deformation mechanisms in this section, which lacks any sign of ductile precursors. The orientation of the fractures and of the cataclastic cores is rather consistent for all of the investigated deformation zones. The strike of these features is generally SE-NW and their dip is gentle to moderate to the NE and SW. Striated planes indicate the predominance of oblique reverse faulting, with top-to-the-N/NE or S/SW sense of shear. There are, however, also a few extensional fault planes, generally coaxial with the reverse faulting direction. No age relationships were observed. It is interesting to point out that DZ 3 of KLX04 is a potential intercept of the moderately S-dipping seismic reflector M1. Our logging confirms the presence of a c. 3–4 m thick cataclastic core in DZ 3, which dips moderately to the SSW (Figure 5-34). Fracture frequency also increases within DZ 3.

KLX08

KLX08 has the same geographic location of KLX04, but has a different orientation. Two DZ's were logged within KLX08, DZ 6 extending from 385 to 427 m and DZ 7 from 476 to 487 m depth. /Viola and Venvik Ganerød 2007/ have reported on DZ 1 and 2. The deformation style remains brittle throughout the inspected depth interval and structural evidence suggests multiple cataclastic episodes and a complex reactivation history. The cores of both deformation zones contain fault rocks that cover the whole spectrum of brittle fault products. DZ 6, including its upper and lower transition zones, is characterized by generally NNE-SSW-striking and very gently ESE- and WNW-dipping fractures and striated planes, which bear primarily evidence of reverse faulting. These gently dipping fractures are interpreted, on the ground of the mineral infill, to postdate a set of steep conjugate E-W trending fractures (Figure 5-42). Fractures within DZ 7 have a similar orientation and dip very gently but no striated planes were observed. Seismic reflector M1 passes through KLX08 and has a theoretical intercept at depth 459 m.

KLX09

Although in this report we describe seven different deformation zones (DZ 7, 9, 10, 11, 12, 13 and DZ 14), only DZ 13, extending from depth 634 m down to 743 m, was logged in detail. DZ 13 is characterized by the presence of an extremely thick fault core (c. 30 m) formed by cataclastic rocks. No evidence of ductile precursors is observed. DZ 13 contains numerous striated planes that strike roughly NW-SE and dip very consistently to the NE. Kinematic constraints indicate both compression and extension, with top-to-the-SW and top-to-the-NE senses of shear, respectively.

KLX10

Only DZ 9, extending from 690 to 706 m depth, was logged during this study. /Viola and Venvik Ganerød 2007/ have described DZ 6 and DZ 7. DZ 9 has a remarkable core, c. 5 m thick, which consists of a complex sequence of fault rocks, with cataclasites, ultracataclasites and gouge. Orientation data from this depth interval is inconclusive, except for a series of systematic S/SSE-dipping open fractures within the upper transition zone (Figure 5-62).

KLX11A

In this study we have logged the whole of KLX11A. Although eighteen deformation zones are described by the single-hole interpretation study by /Carlsten et al. 2007a/, during our study we have defined only seven of these as real deformation zones. These are DZ 3, 6, 7, 8, 11, 12 and DZ 14. They are mostly found in the central part of the core. Within these zones there is evidence of pervasive brittle deformation and multiple reactivation.

Apart from DZ 11, where most fractures and striated planes strike NW-SE and bear evidence for sinistral and dextral strike-slip and low-obliquity shearing (Figure 5-79), the remaining deformation zones are oriented roughly WSW-ENE to E-W. Seismic reflector M1 passes through KLX11A and has a theoretical intercept at depth 551 m.

KLX12A

Three deformation zones (DZ 10, 11 and 12) were logged in detail during this study. The three zones are developed predominantly within intermediate to mafic rock types, varying from quartz monzodiorites to diorites and gabbros. The deformation style that characterizes these deformation zones is entirely ductile, with mylonitic shear zones forming the cores of the deformation zones. Only in DZ 11 there is evidence of cataclasis, whereby mylonites overprint previously formed cataclasites. Whereas the mylonitic fabric in DZ 10 dips moderately to the SW, within the cores of DZ 11 and 12 mylonites dip consistently c. 50–55° to the SE/ESE.

KLX18A

According to /Carlsten et al. 2007d/ the interval extending from 137 to 490 m depth contains nine different deformation zones. Out of these, however, we have interpreted as real deformation zones only DZ 3, 5, 6, and 9. They are invariably characterized by cataclasites, highly fractured intervals and crush zones. Microstructures indicate multiple episodes of brittle deformation and structural reactivation. In general, fractures and cataclastic bands within these deformation zones strike E-W and dip gently to moderately to the S, SSW.

KLX20A

Four different deformation zones (DZ 1 to DZ 4) were logged. DZ 1, 2 and 3 contain fault cores and significant crush zones, whereas we do not interpret DZ 4 as a proper deformation zone. The most interesting and relevant zone is DZ 1, which contains a large dolerite dyke. Numerous striated planes (particularly within the dolerite) were measured, and two significant and systematic families of fault planes were identified. Generally E-W striking and moderately N- and S-dipping planes show both normal and reverse kinematics, with low obliquity (Figure 5-131). These are crosscut by sub vertical planes striking from NNW to NNE with a predominantly strike-slip kinematics.

5.2 KLX03

The drilling site of KLX03 is located in the central part of the Laxemar area, where Ävrö quartz monzodiorites crop out extensively (Figure 5-1). The drill core has a length of 1,000.42 m and is oriented 223/77 within the depth interval investigated during this study /Carlsten et al. 2005/. We have logged only DZ 1 (720.5–820 m) and this is therefore the only deformation zone discussed in this report for KLX03.

5.2.1 DZ 1: depth interval 720–820 m

DZ 1 is an approximately 100 m thick, rather heterogeneous section consisting of three spatially distinct fault cores, each defined by fault rock occurrences and their relative transition zones (Figure 5-2). Red staining, thin cataclastic bands and a general increase in fracture frequency are the most diagnostic structural features of the transition zones.

Structural data for the uppermost transition zone between 723 and 732 m are shown in Figure 5-3. Several striated surfaces were observed and characterized kinematically, but do not provide a clear picture. Apart from a few steep strike-slip shear fractures, there are several transtensional planes dipping moderately to the SSE. These fractures are coated invariably by chlorite and epidote, with minor calcite and hematite. Red great circles plot a faint ductile tectonic planar fabric that occurs at depth c. 730 m.

The first prominent fault core of DZ 1 is located at approximately 732.20 m depth. It is about 1 m thick and contains foliated cataclasites and ultracataclasites. A faint foliation is visible (Figure 5-4). Later quartz and/or calcite veins crosscut the core fault rocks (Figure 5-5).

Sample KLX03-1 was collected at depth ~732.60 m in order to further investigate the deformation mechanisms in this DZ core. Figure 5-5 shows the image of its scanned thin section. The fault rock is a weakly foliated protocataclasite formed from severely altered amphibole-bearing granites. Its faint foliation dips consistently to the SSE-SE (Figure 5-6). A striated shear fracture (visible in Figure 5-4) displays sinistral transtensional kinematics with a top-to-the-SW sense of shear along a SE-dipping plane.

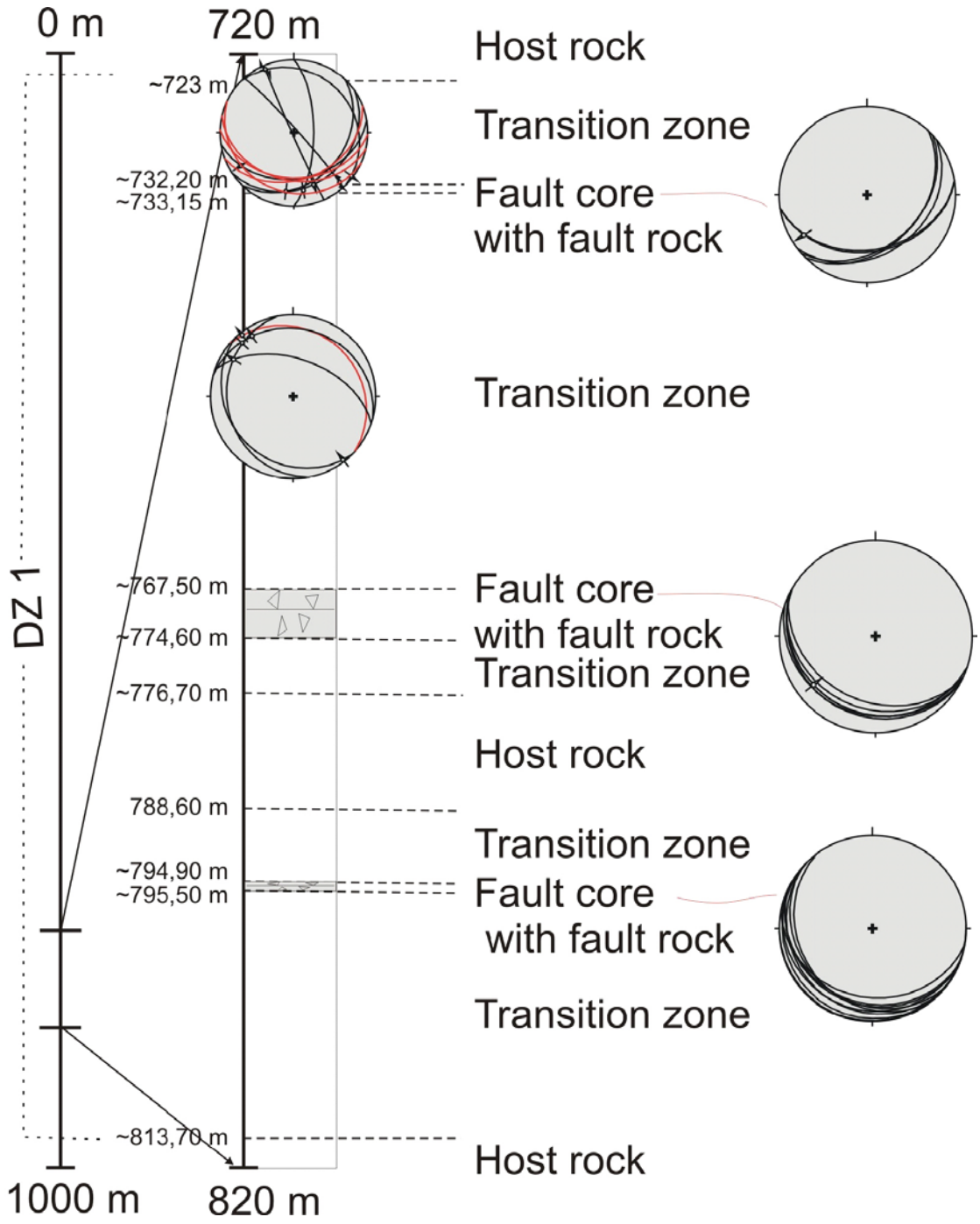

Figure 5-2. *Drill core KLX03 with schematic structural log of DZ 1 (720–820 m). Details on the stereonets can be found in the text.*

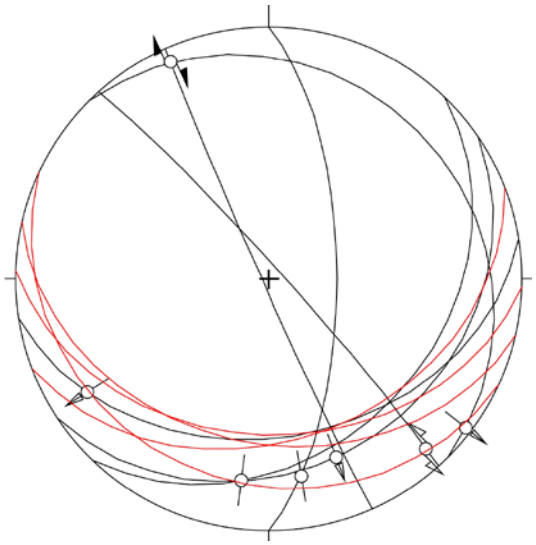

Figure 5-3. *Structural information for striated fracture planes (black great circles) and a zone of pervasive foliation (red great circles) in the depth interval 720–732 m.*

Figure 5-4. *Cataclasites from the uppermost fault core located at depth c. 732.5 m.*

Chlorite is widespread throughout the section and is invariably associated with foliation and shear band planes, thus constraining shearing to the lowermost greenschist facies conditions. The upper part of the sample shows a rather pervasive dextral extensional crenulation cleavage (ECC), with chlorite-decorated shear bands cutting through the foliation and affecting also thin dark-brown ultracataclastic bands (Figure 5-5). K-feldspars are deformed in a brittle fashion and cataclasites were formed by granular flow mechanisms; clast rigid-body rotation is commonly observed. Ultracataclasites form bands and pockets that are generally oriented subparallel to the foliation planes.

From these microscopic observations deformation in this DZ appears to have been accommodated predominantly by processes operating at the brittle ductile transition, as demonstrated by the coexistence of ductile (pervasive foliation, shear bands, small asymmetric folds within the cataclasites) and brittle features (evidence of granular flow mechanisms and rigid-body rotation). Later calcite veins cut discordantly the foliated protocataclasites.

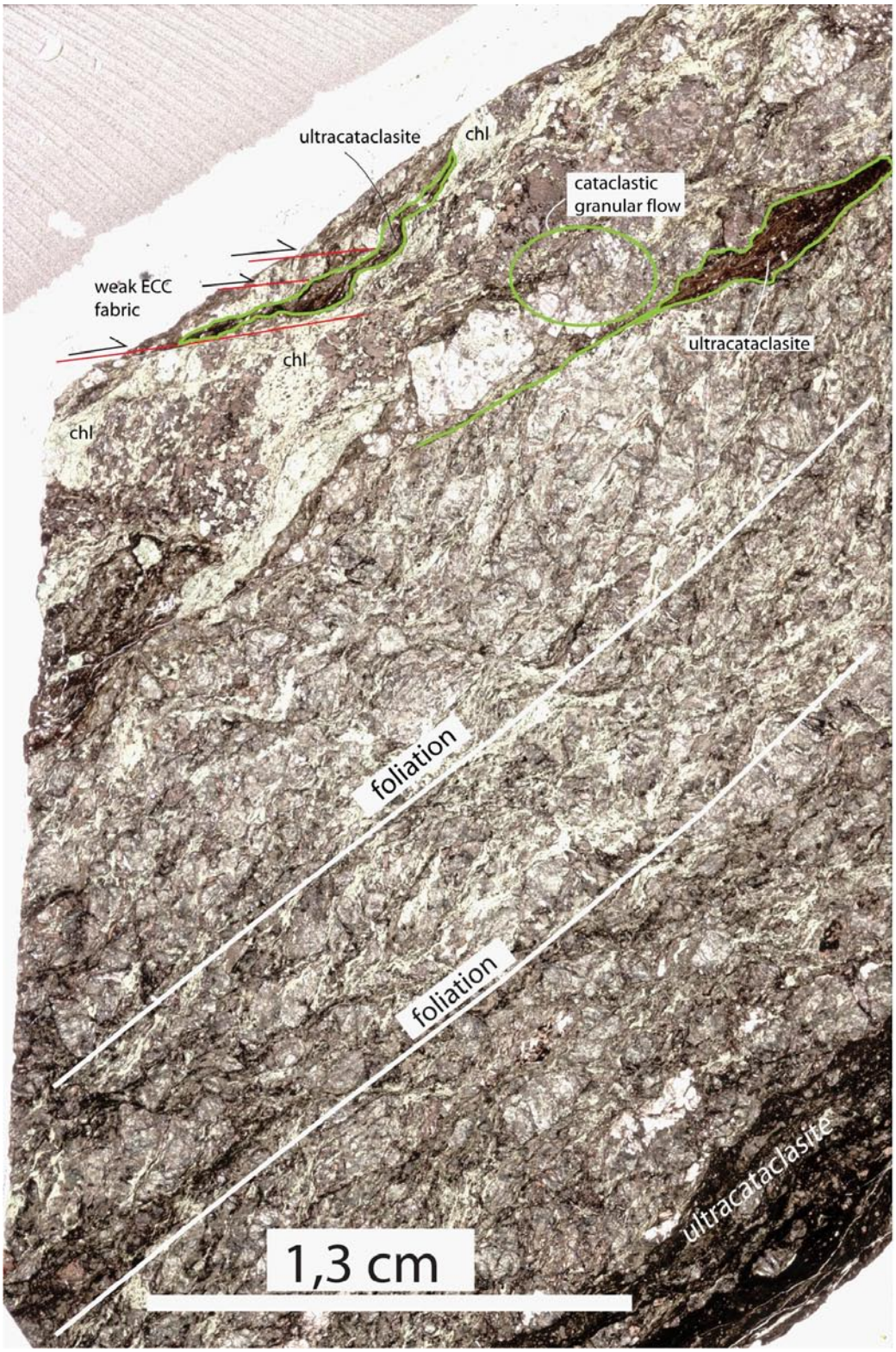

Figure 5-5. *Scanned thin section of sample KLX03-1 from depth 732.60 m. The fault rock is a weakly foliated protocataclasite. Deformation under brittle-ductile conditions is suggested.*

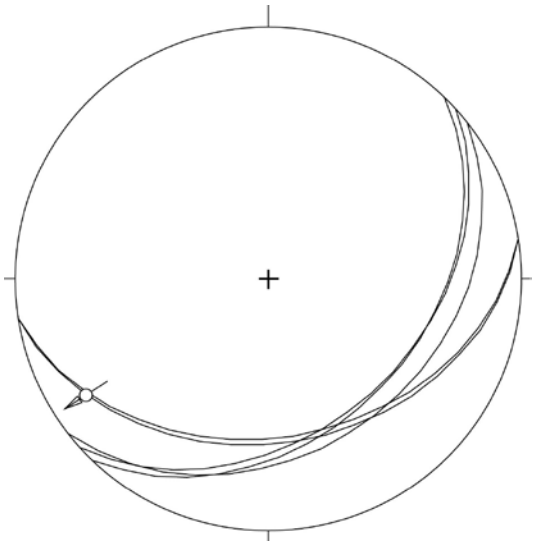

Figure 5-6. *Orientation of the fault core at depth 732.5 m in KLX03.*

The transition zone dividing this upper core from a deeper second fault core starts at approximately 733.15 m depth; it is characterized by localized red staining and abundant calcite and epidote veins and networks. Veins are generally associated with calcite- and epidote-rich millimetric bands of cataclasites and cemented microbreccias (Figure 5-7). It is suggested that the material forming the veins precipitated during dilational episodes connected to the presence of over pressured fluids.

Some chlorite- and epidote-coated striated planes were constrained kinematically within this transition zone. Figure 5-8 shows that these planes dip moderately to the NE and SW and that they accommodated predominantly strike-slip kinematics. The red great circle is an epidote-coated plane at depth 741.755 m located immediately above an epidote-rich sealed dilatant network (Figure 5-9).

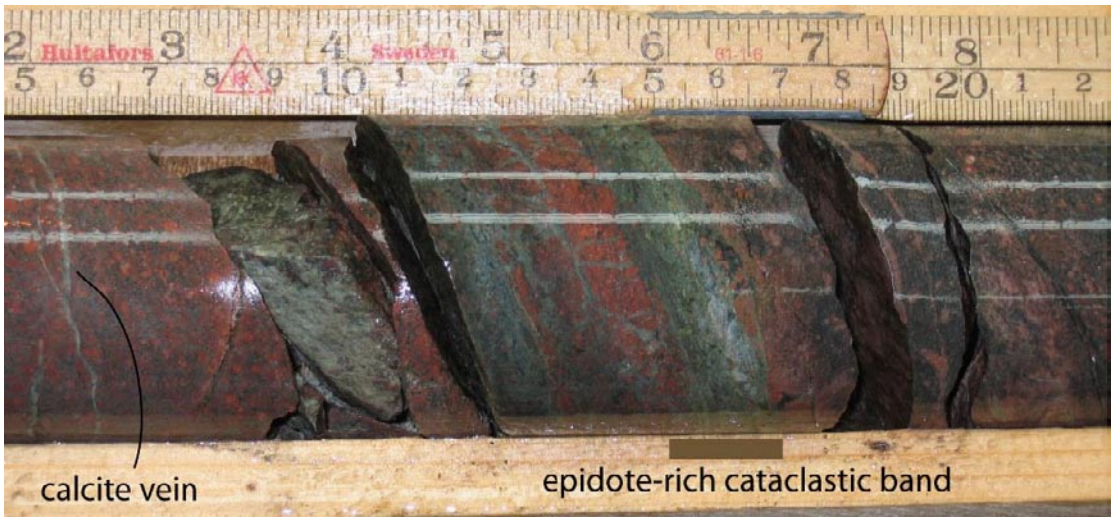

Figure 5-7. *Cataclastic band at depth 750.67 m.*

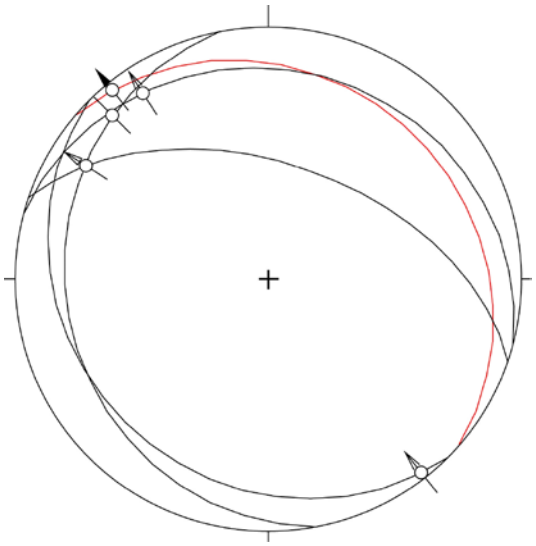

Figure 5-8. *Fault slip data for striated planes in the transition zone between 733 and 767 m depth. The red great circle shows the orientation of the striated plane at the top of the epidote-sealed dilatant network shown in Figure 5-9.*

Figure 5-9. *Epidote-rich dilatant network (possibly a cemented breccia) at depth 741.755 m with a gently NE-dipping striated plane above it. The plane and its kinematics are shown by the red great circle and the associated arrow in the stereonet of Figure 5-8.*

Striated planes are found in otherwise relatively undeformed host rock, although thin cataclastic bands are a common structural feature of the transition zones of DZ 1. As an example, sample KLX03-2 from depth ~750.68 m is a protocataclastic granite characterized by an anastomosing network of thin cataclasite bands and a discrete, c. 10 mm thick cataclastic/ultracataclastic horizon.

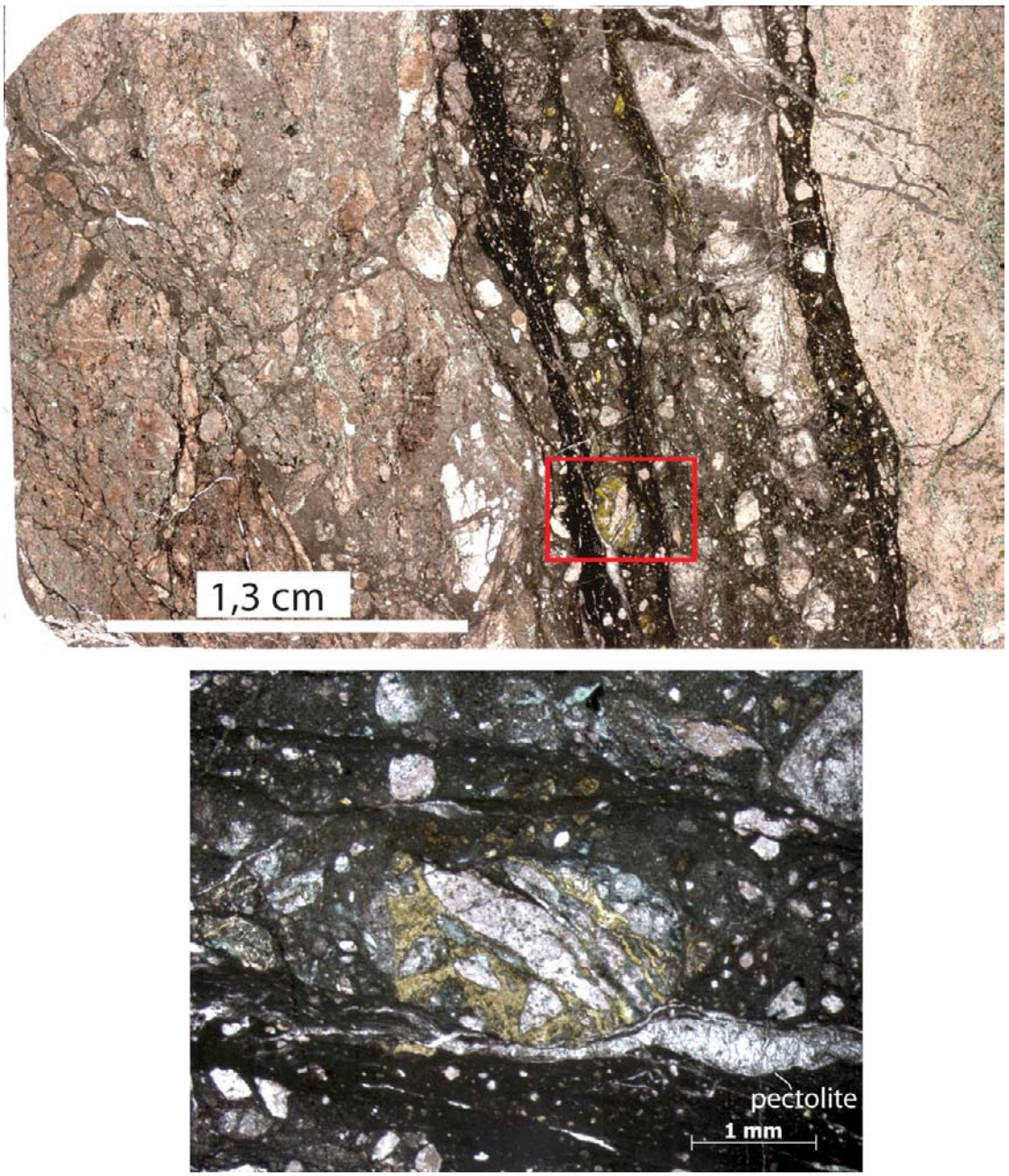

Figure 5-10. *Above: scanned thin section of sample KLX03-2. The rock is a protocataclastic granite (to the left hand side of the thin section) crosscut by a c. 15 mm thick cataclastic/ultracataclastic band. The microphotograph shows a relatively large K-feldspar clast within the cataclastic/ultracataclastic band crosscut by pre-to syn-cataclasis veins of a deep yellow-green ferric epidote.*

A deep yellow-green ferric epidote ("julgoldite", with maximal Fe 3+ substitution) is found associated with the cataclastic products of an earlier brittle deformation phase. It is in fact found invariably associated with clasts of cataclasites reworked by later brittle processes, thus suggesting multiple brittle deformational pulses.

The second fault core of DZ 1 starts at an approximate depth of 767.50 m. It is about 8.5 m thick (it is the thickest of DZ 1) and contains complex structural relationships and textures defined by abundant protocataclasites "crosscut" by epidote veins and bands (Figure 5-11a) together with ultracataclasites and gouge levels (Figure 5-11b). In contrast to the upper and lower cores, it lacks foliated intervals and evidence of brittle-ductile deformation features. The fault core dips consistently to the SW with a gentle dip and one striated plane, coated by chlorite and hematite, suggests a reverse, top-to-the-NE sense of shear for this brittle deformation zone (Figure 5-12).

The lower part of this core shows very complex structural relationships (Figure 5-13), which suggest multiple episodes of cataclasis and brecciation.

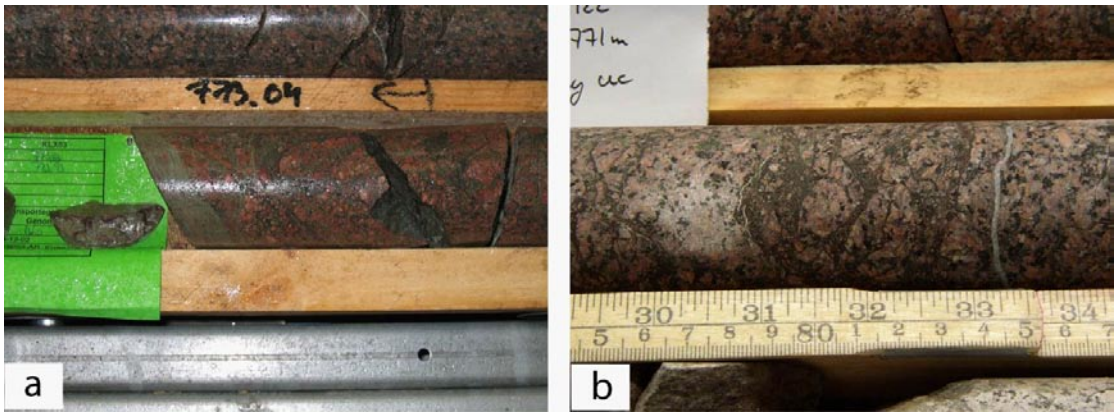

Figure 5-11. *Examples of the complex textural relationships observed in the fault core at depth 767–775 m. Coarse protocataclasites deform the Ävrö granite and are in turn crosscut by later epidote-rich bands (a) and thin dark ultracataclasites/gouge veins (b).*

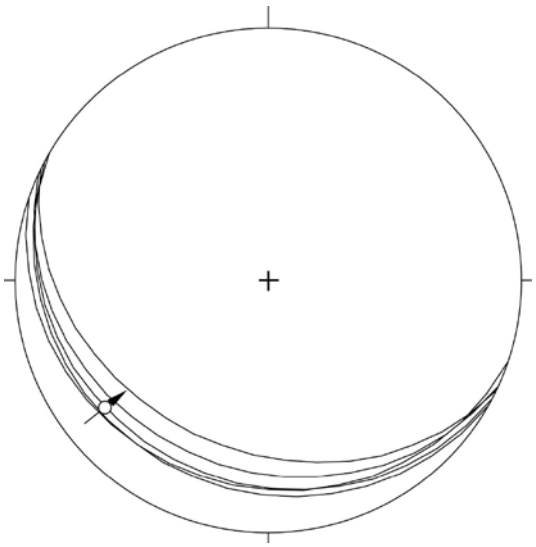

Figure 5-12. *Orientation of the fault core at depth interval 767–775 m. A striated plane at depth 773.91, coated by chlorite and hematite, indicates reverse, top-to-the-NE kinematics.*

Figure 5-13. *Detail of the lower part of the deformation zone central core. A brown ultracataclasite/ gouge (to the right hand side) cuts across epidote-rich brecciated granites. Note the poor sorting of the clasts and their angular shapes.*

We locate the beginning of the following transition zone at approximately 788.60 m depth. It is again characterized by red staining and thin bands of ultracataclasites. At approximately 792.20 m there is a lithological change from the Ävrö granite to a foliated quartz monzodiorite.

The third and last DZ 1 fault core is located at approximately 795 m depth, is about ~50 cm thick and consists mainly of foliated cataclasites that deform foliated quartz monzodiorites. The core of the deformation zone dips very shallowly southwest, which is also the dip direction of the ductile foliation within the quartz monzodiorites (Figure 5-14 and Figure 5-15).

Calcite and quartz veins are found in abundance within the core. Some of them are subparallel to the foliation planes, others are coarse and cut across discordantly, suggesting their late formation in the deformation history of this deformation zone (Figure 5-15).

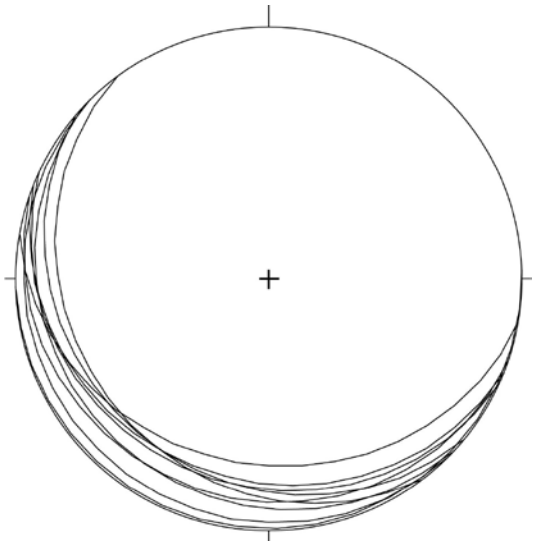

Figure 5-14. *Orientation of the c. 30 cm thick deformation zone core at depth 797 m.*

Figure 5-15. *Foliated cataclastic quartz monzodiorites form the core of this very gently SW-dipping deformation zone core at depth 797–798 m.*

Figure 5-16 shows the foliated cataclasites as seen in sample KLX03-4, from depth ~795.20 m. Foliation planes are defined by chlorite wrapping around brittly reworked K-feldspars and plagioclase clasts. Late, discordant calcite veins belong to at least two different generations as can be inferred from mutual crosscutting relationships. The microphotograph of Figure 5-16 indicates a long lasting and complex brittle history, whereby calcite veins are themselves affected by cataclasis along the edges; here, calcite clasts are fragmented, rotated and dispersed in an extremely fine-grained ultracataclasite.

At depth 798.01 m there occurs a brittle-ductile epidote shear zone that strikes c. N-S and is characterized by weakly foliated epidote-rich ultracataclasites in its core (Figure 5-17).

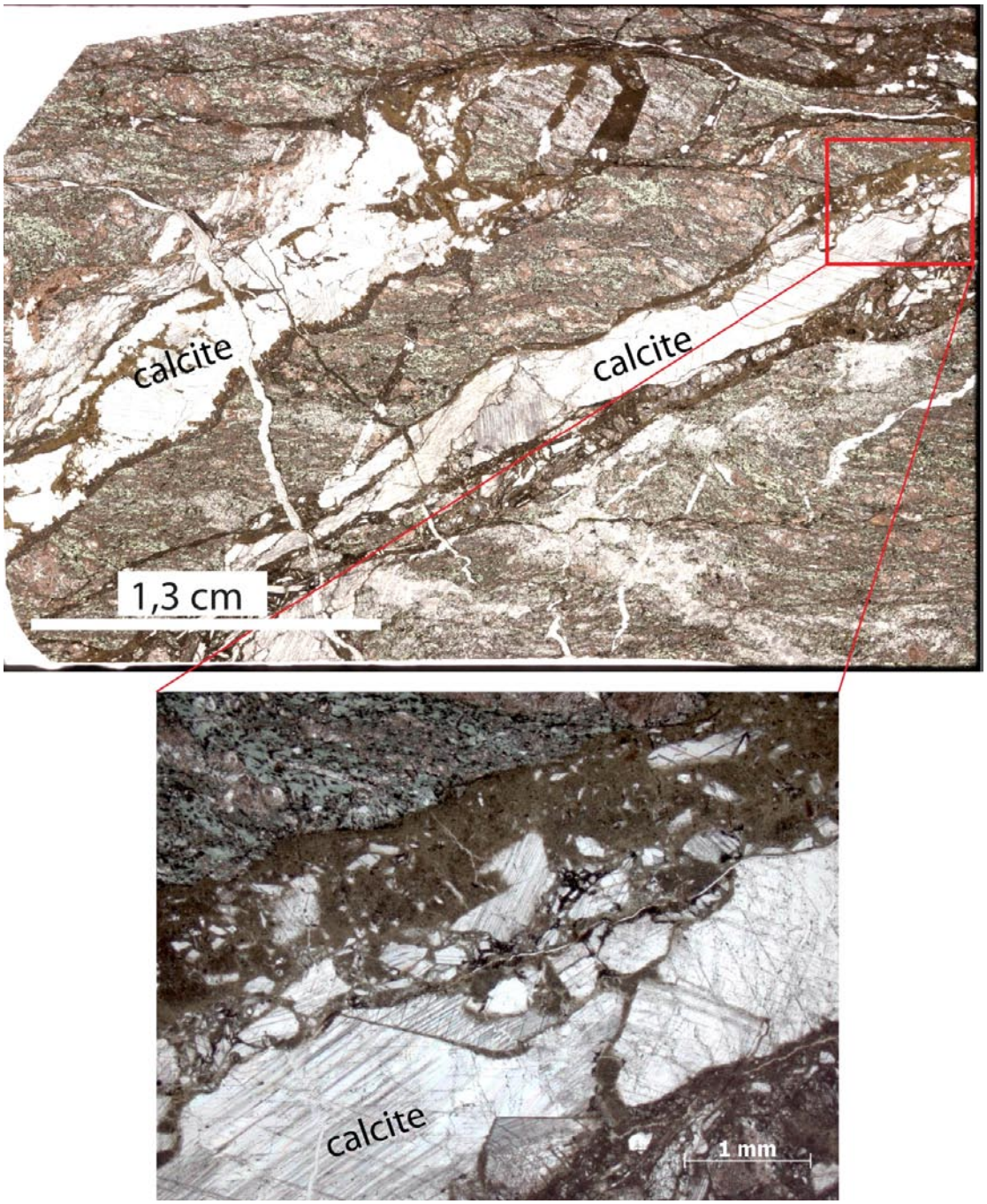

Figure 5-16. *Foliated cataclasites of sample KLX03-4 are injected by at least two different generations of discordant calcite veins. The microphotograph shows that calcite veins were also affected by brittle reworking.*

Figure 5-17. *Steep, N-S trending fault with cataclasites and abundant epidote alteration. The stereonet plots the orientation of the structure.*

The core is followed by a transition zone (795.50–813.70 m) that contains localized red staining and limited occurrences of thin brittle-ductile faults with the same orientation as the fault shown in Figure 5-17. One of these, oriented 186/88, was sampled for thin section inspection (sample KLX03-5 from depth ~798.013 m) and is shown in Figure 5-18. The fault developed under brittle-ductile conditions and is characterized by epidote, chlorite and millimetric ultracataclastic bands striking parallel to the fault zone boundaries.

At 806 m depth there occurs an interesting structural feature, whereby thin faults cut across steeper epidote-decorated brittle-ductile shear zones (similar to those shown in Figure 5-17 and Figure 5-18), establishing a relative chronology of events.

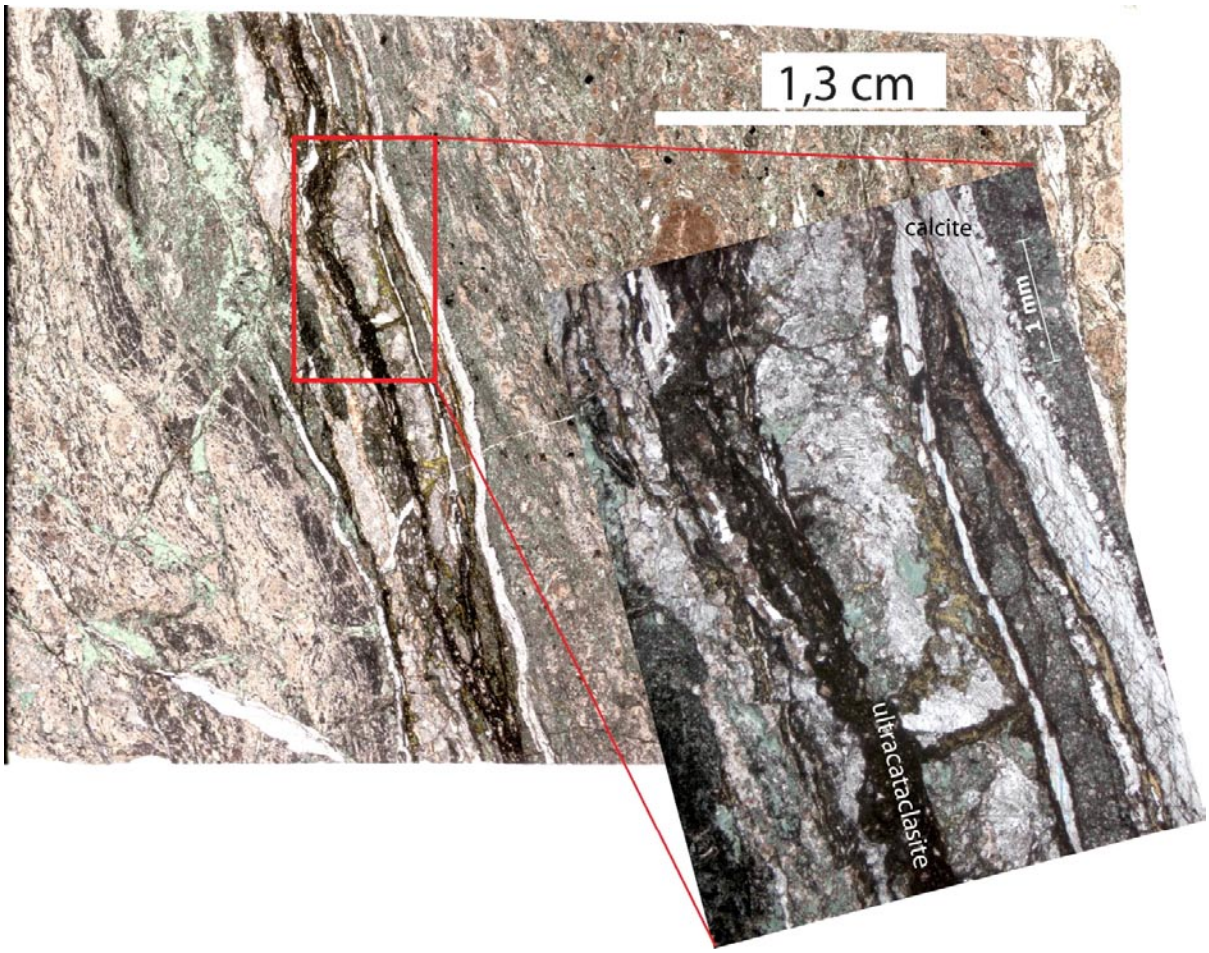

Figure 5-18. *Scanned thin section and microphotograph of sample KLX03-5. A steep epidote- and chlorite-decorated brittle-ductile shear zone deforms the granitic host rock. Note the incipient foliation developed to the right of the fault zone. Thin ultracataclasites and calcite veins occur parallel to the strike of the deformation zone.*

Figure 5-19. *An epidote-decorated brittle ductile shear zone is offset along a flatter discrete brittle fault at depth 806 m.*

Table 5-1. Summary of DZ 1.

Depth (m)	Box number	Interpretation	Description
720	113	Host rock	Undeformed rock.
Approx. 723	113	Transition zone	Red staining in bands due to red altered feldspar and grain size reduction. Red staining affects otherwise relatively undeformed granites (host rock). S-dipping ductile fabric at depth 730 m.
Approx. 732.20	115	Fault core	The fault core is approximately 1 m thick and contains pervasively foliated cataclasites and ultracataclasites. Deformation constrained at brittle/ductile conditions.
Approx. 733.15	115	Transition zone	Red staining in discrete bands. Some calcite veins, usually associated with thin (mm) bands of ultracataclasite (gouge) and fragments of cataclasite or host rock, commonly cemented by minerals such as calcite and epidote. The occurrence of red staining and ultracataclasite bands increases towards the fault core. Sample KLX03-2 at depth ~750.68 m of calcite-cemented breccia.
Approx. 767.50	121	Fault core	8.5 m thick brittle core formed by protocataclasites crosscut by fluidized ultracataclasites and possibly gouge. The occurrences of ultracataclasites/gouge increase progressively towards the “centre” of the core at depth ~773–774 m.
Approx. 774.60	122	Transition zone	Red staining.
Approx. 776.70	123	Host rock	Undeformed host rock.
Approx. 788.60	125	Transition zone	Red staining, bands of ultracataclasite and foliated mafic rock.
Approx. 794.90	126	Fault core	Foliated cataclasite ~50 cm thick. Brittle-ductile deformation conditions.
Approx. 795.50	126	Transition zone	Red staining. Brittle-ductile fault occurrence.
Approx. 813.70	130	Host rock	Undeformed host rock.

5.3 KLX04

The location of KLX04 is shown in Figure 5-1. The core is 993.49 m long, is oriented 010/80 and penetrates in Ävrö granites. The section logged during this study extends from 223 to 358 m depth and includes eight small fault zones with their respective transition zones (Figure 5-20). Five of these zones are mapped as DZ zones in the single-hole interpretation by /Carlsten et al. 2004/. The transition zones between the fault cores are generally characterized by increasing fracture frequencies towards the core and the occurrence of networks and thin bands of cataclasites and ultracataclasites. Red staining occurs throughout the section.

5.3.1 DZ 1: depth interval 227–230 m

The fault core at depth 227.60 m consists of a ~1 m thick interval of crushed, non-cohesive rock, with a sharp contact to the undeformed host rock (Figure 5-21). Fractures within the core dip generally about 60° to the SW or more gently to the NE, thus defining a conjugate system (see stereonet in Figure 5-21).

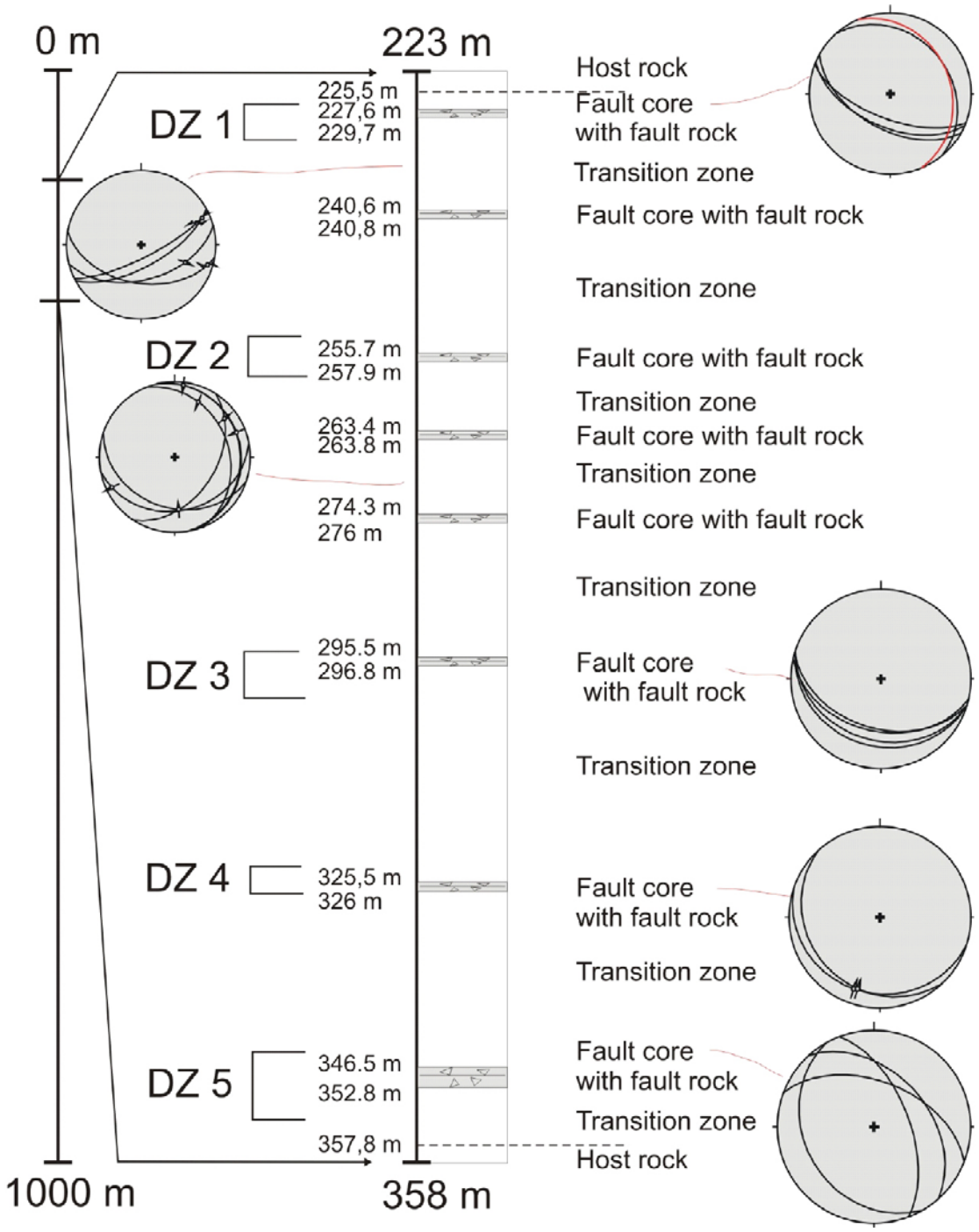

Figure 5-20. *Schematic log of KLX04 deformation zones DZ 1 to 5. Details on the stereonets can be found in the body text.*

Figure 5-21. *Brittle fault core and associated crush zone at depth 227.60 m in KLX04. The stereonet shows the orientation of selected fracture planes within the DZ core. The red great circle is the fracture oriented 337/26 at the base of the zone. Note the cataclastic texture of the core (inset on the top right-hand side) and the anastomosing sealed network of thin cataclastic and gouge bands in the lower transition zone immediately below the red oval.*

The DZ core is formed by anastomosing, wavy ultracataclasite or gouge bands injected into the bedrock, and thus form a dense network (see inset in Figure 5-21). The transition zone that occurs immediately below the core is characterized by the presence of an identical sealed network of anastomosing cataclastic bands that disrupts the integrity of the coarse-grained granitic host rock, but does contain neither systematic fracture sets nor a discrete crush zone (Figure 5-21).

An interesting structural relationship is observed at depth 240.044 m, where a steep quartz, epidote and chlorite vein (orientated 172/86) is crosscut and offset by thin and shallower brittle bands (orientation 012/44; Figure 5-22).

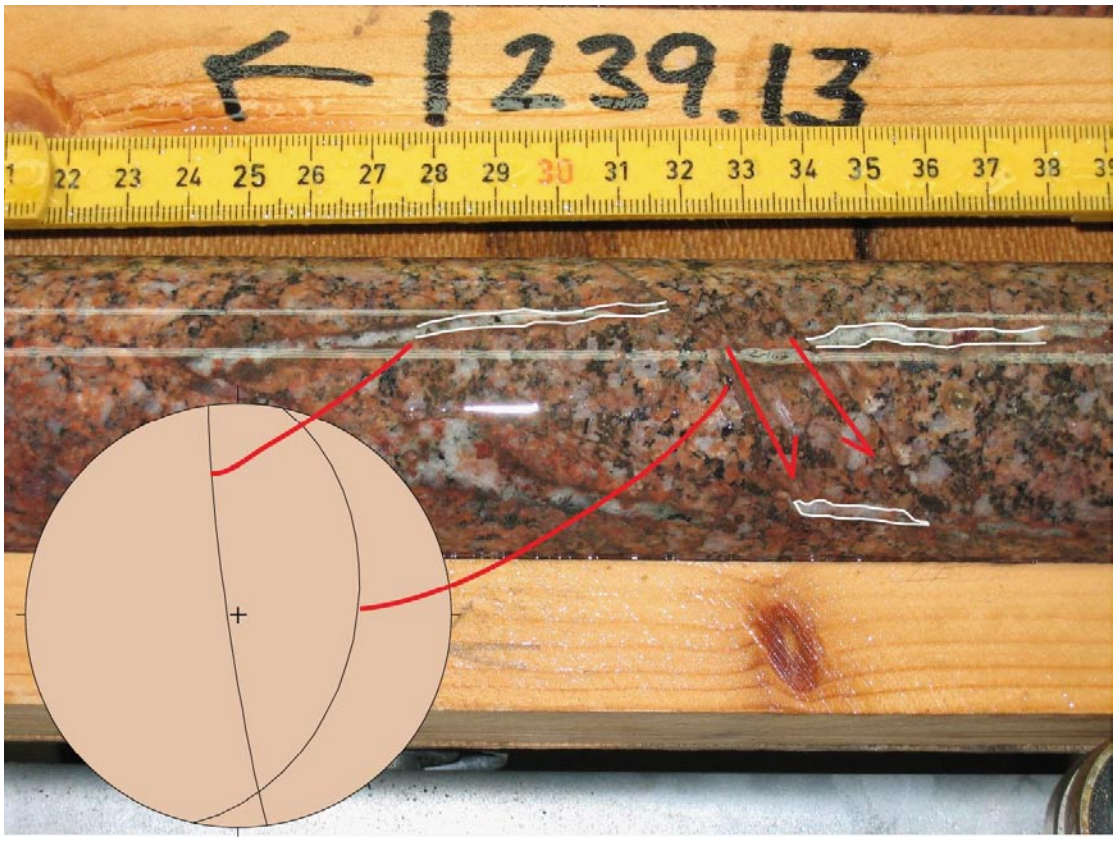

Figure 5-22. *A steep vein (highlighted by the white outline) is offset by a set of moderately E/ESE-dipping brittle faults. The red arrows show the sense of displacement along the two fault structures.*

At depth 240.65 m there occurs a discrete, 15–20 cm thick fault core (oriented 351/59) defined by cataclasites, ultracataclasites and gouge (Figure 5-23). This localized brittle zone is characterized by a complex fault rock occurrence; gouge pockets (possibly pseudotachylyte; Figure 5-24a) are dispersed in a strongly cataclastically overprinted granite. Figure 5-24b–c illustrate the details of the progressive textural evolution observed in the thin section of sample KLX04-8, from depth 240.75 m. A gradual transition from pristine host rock to ultracataclasites is observed over a very short distance. Granular flow is the dominant deformation mechanism, whereby dilation and cataclasis led to the nucleation and progressive comminution of fragments of K-feldspars and plagioclase in epidote-rich bands. During the early stages of the process, clasts are still very poorly sorted, have irregular shapes and are separated by thin veins of ultra-cataclastic material formed in response to the first increments of the brittle strain accommodation history (Figure 5-24b). Continuous deformation reduces progressively the grain size of the fragments and smoothes their corners (Figure 5-24c) down to the formation of an extremely fine-grained ground mass containing only very few rounded and fine clasts (Figure 5-24d).

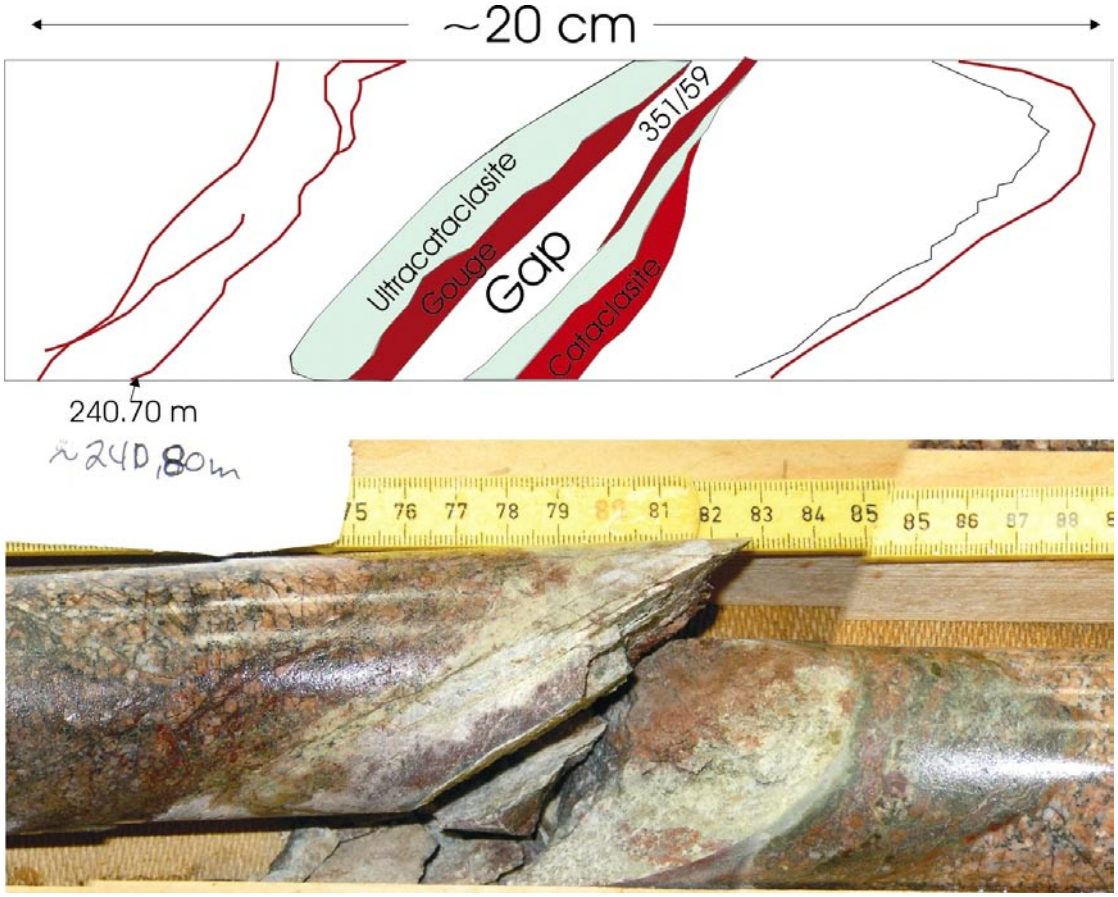

Figure 5-23. *Photograph and interpretative sketch of the fault rock occurrence at 240.8 m depth.*

Figure 5-25 illustrates more details of the deformational history, indicating multiple episodes of cataclasis. The upper microphotograph of Figure 5-25 shows in fact a later "injection" of an extremely fine-grained ultracataclasite (possibly even a pseudotachylyte) that intrudes, along very irregular contacts, upon a previously formed cataclasite. The injected material is extremely fine-grained (hence very dark), very homogeneous and almost devoid of clasts. Local, late veins cutting through the ultracataclastic pocket (bottom microphotograph of Figure 5-25) also generate more localized cataclasis. This deformation zone is not recorded in the single-hole interpretation /Carlsten et al. 2004/.

A transition zone containing several striated planes follows in the section. The fracture planes strike roughly EW and dip S, SSE. No clear kinematic picture emerges from the analysis of this statistically limited dataset (Figure 5-26).

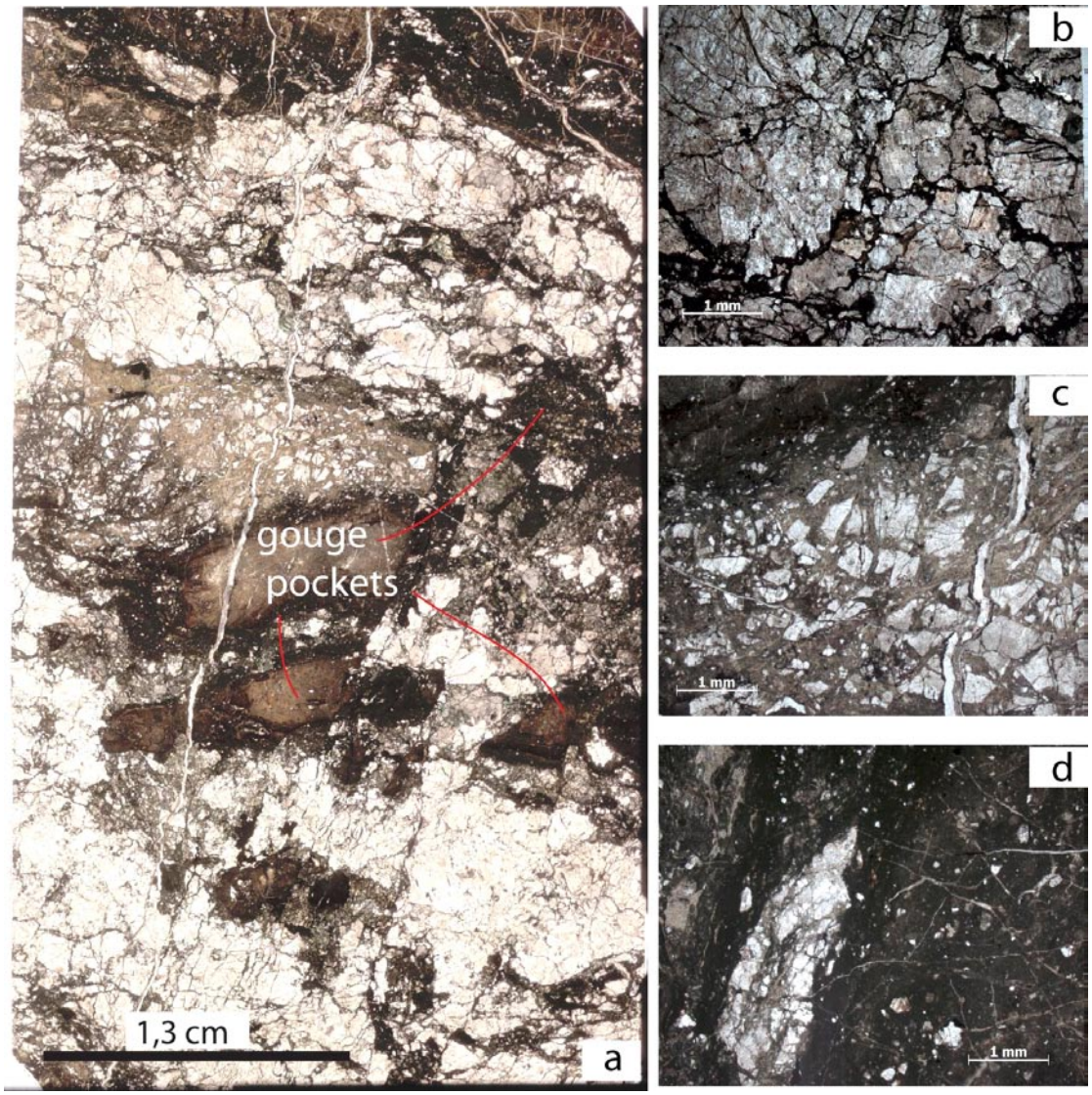

Figure 5-24. *Scanned thin section of sample KLX04-8 (a). (b) to (d) illustrate the progressive textural evolution of the host rock to a proper ultracataclasite via dilation, granular flow and mechanical comminution of the fragments.*

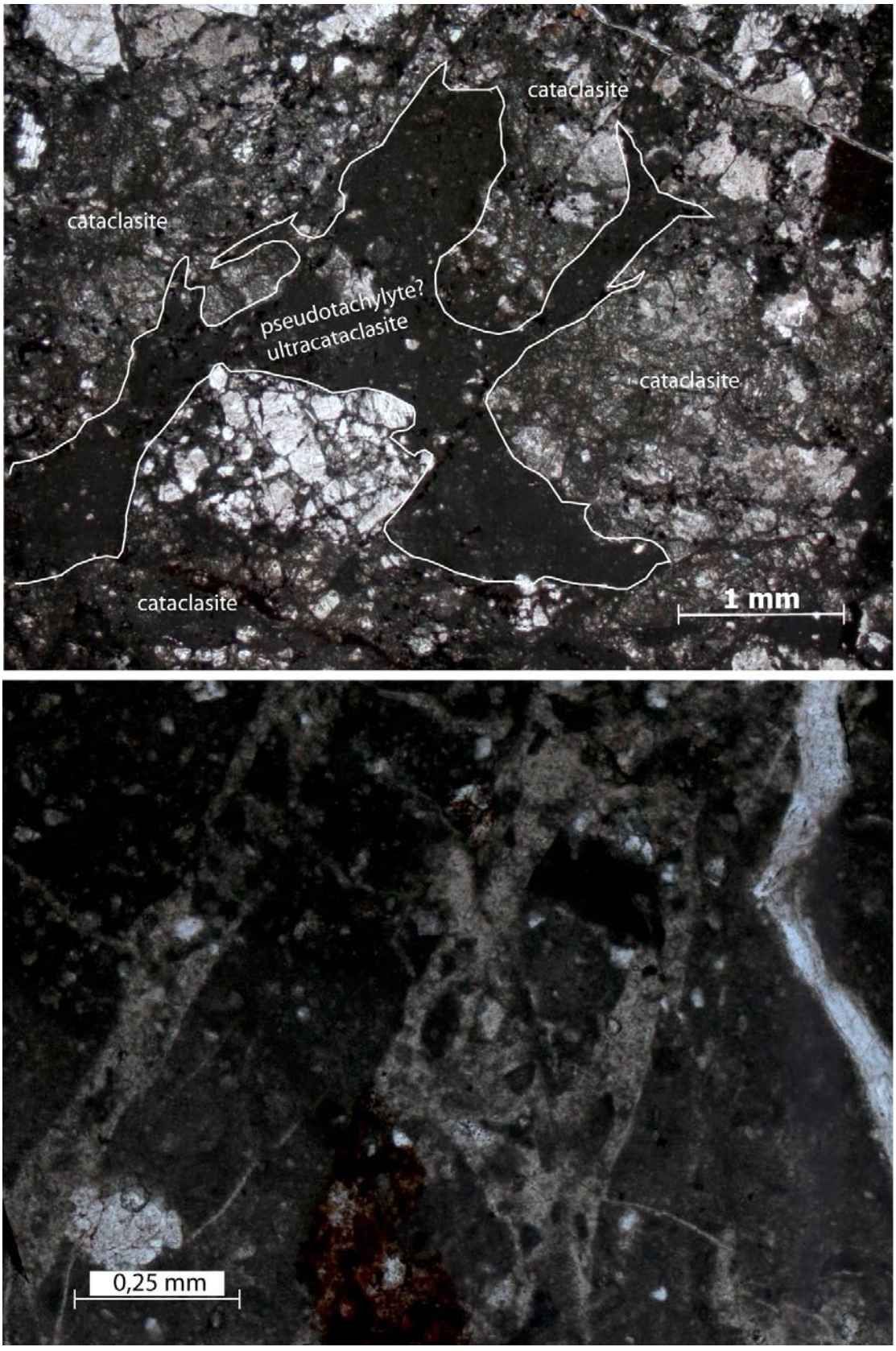

Figure 5-25. *Details of the several episodes of cataclasis recognised in sample KLX04-8.*

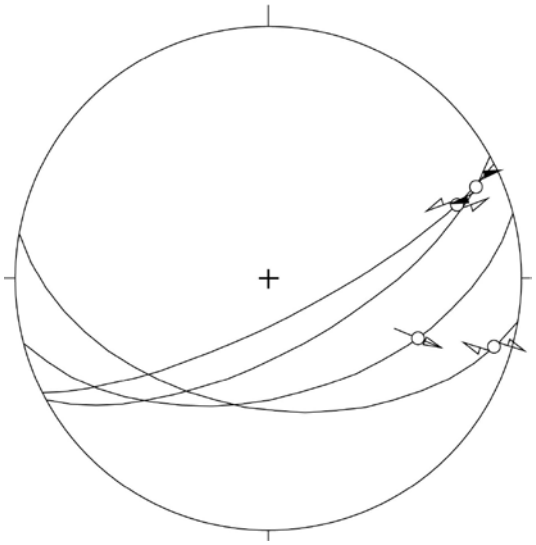

Figure 5-26. *Fault slip data for the transition zone between depths 240 and 255 m. Transtensional kinematics is recorded for the observed striated planes.*

Table 5-2. Summary of DZ 1.

Depth (m)	Box number	Interpretation	Description
223.87	23	Host rock	Ävrö granite with low fracture frequency. Localized red staining.
225.50	23	Transition zone	Increasing fracture frequency and red staining.
227.60	23	Fault core	The fault core consists of crushed, non-cohesive rock for ~1 m. Transition to cohesive fault rock. Fault rock composed of “injections” of ultracataclasite or gouge that “intruded” into the bedrock, forming a cataclastic network in otherwise undeformed bedrock.
229.70	24	Transition zone	Undeformed bedrock with cataclastic network. Localized red staining.
240.65	26	Fault core	~5 cm thick interval of cataclasites, ultracataclasites and gouge. Increasing occurrence of ultracataclastic networks both above and below the fault rock-dominated zone.
240.80	26	Transition zone	Thin transition zone to undeformed host rock.
241.05	26	Host rock	Rock with low fracture frequency, 1–3 f/m. Narrow crush zone likely due to drilling technical problems.

5.3.2 DZ 2: depth interval 254–258 m

A second, distinct DZ begins at depth 253.95 m with a noticeable increase in fracture frequency. The central fault core can be subdivided into two subzones with 1) SZ (subzone) 1, at depth 256.10–256.45 m, containing foliated cataclasites passing laterally to a crush zone formed at the expense of the cataclasites themselves (Figure 5-27); 2) SZ2, at depth 256.65–257.88 m, consisting of a zone of crushed, non-cohesive rock.

A transition zone with progressively decreasing fracture frequency, localized red staining and a few, isolated ultracataclasite bands, follows in the drill core. It contains several striated planes that were constrained kinematically. The striated planes are invariably coated by epidote, chlorite and to a lesser extent calcite.

Good quality slickensides indicate either reverse or normal sense of shear along ENE or S-dipping planes (Figure 5-28).

Figure 5-27. *Foliated cataclasites form the core of subzone 1 in DZ 2.*

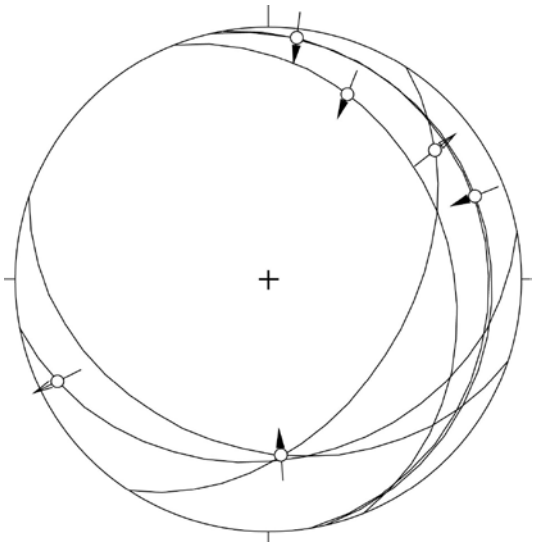

Figure 5-28. *Fault slip data for chlorite-, epidote- and calcite-coated striated fractures in depth interval 259–261 m.*

In our opinion two more localized deformation zones occur, although they are not registered in the single-hole interpretation by /Carlsten et al. 2004/. The first zone begins at depth 261.3 m, and is introduced by a transition zone defined by a progressive increase in fracture frequency and localized red staining. The deformation zone core (depth interval 263.42–263.65 m) consists of:

i) A narrow zone, ~20 cm thick, of fault rock containing cataclasites, ultracataclasites and gouge, with red gouge being the most prominent feature (Figure 5-29). Sample KLX04-10, which straddles the sharp boundary between the ultracataclastic core and the granitic host rock (Figure 5-30a), demonstrates a complex, long-lived brittle deformation history. The spectacular microstructures indicate a prolonged series of reactivation events, whereby older indurated ultracataclasites are themselves cataclastically reworked by younger brittle deformation events (Figure 5-30b, c and d). The contact between the granitic host rock and the deformation zone core is very sharp and is defined by a thin dilatant quartz vein (0.2 mm thick) and a protocataclastic band containing angular clasts of the granite K-feldspars and plagioclase (Figure 5-30c). The internal structure of the core is defined by subparallel bands of different types of fault rock, from epidote-dominated ultracataclasites to proper gouge layers, which locally wrap around cataclastic pockets containing large, highly fractured, clasts of granite. Late quartz and calcite veins cut discordantly the fault core.

ii) Highly fractured, non-cohesive crush zone containing also a sealed network of ultracataclasites and/or gouge. A ~1 m thick zone of cohesive cataclasites and ultracataclasites follows. The transition from fault core to transition zone is sharp. The transition zone contains sealed networks of ultracataclasite/gouge bands. The deformation zone is followed by otherwise undeformed granitic rock.

The second deformation zone is about 5 m thick and begins with a transition zone at 271.85 m marked by an increase in fracture frequency and sporadic occurrences of ultracataclasite/gouge networks. At depth 272.77 m there occurs a steep epidote-decorated brittle-ductile shear zone oriented 241/76. The shear zone contains in its middle part an open fracture infilled by calcite and epidote, and evidence of localized cataclasis (Figure 5-31).

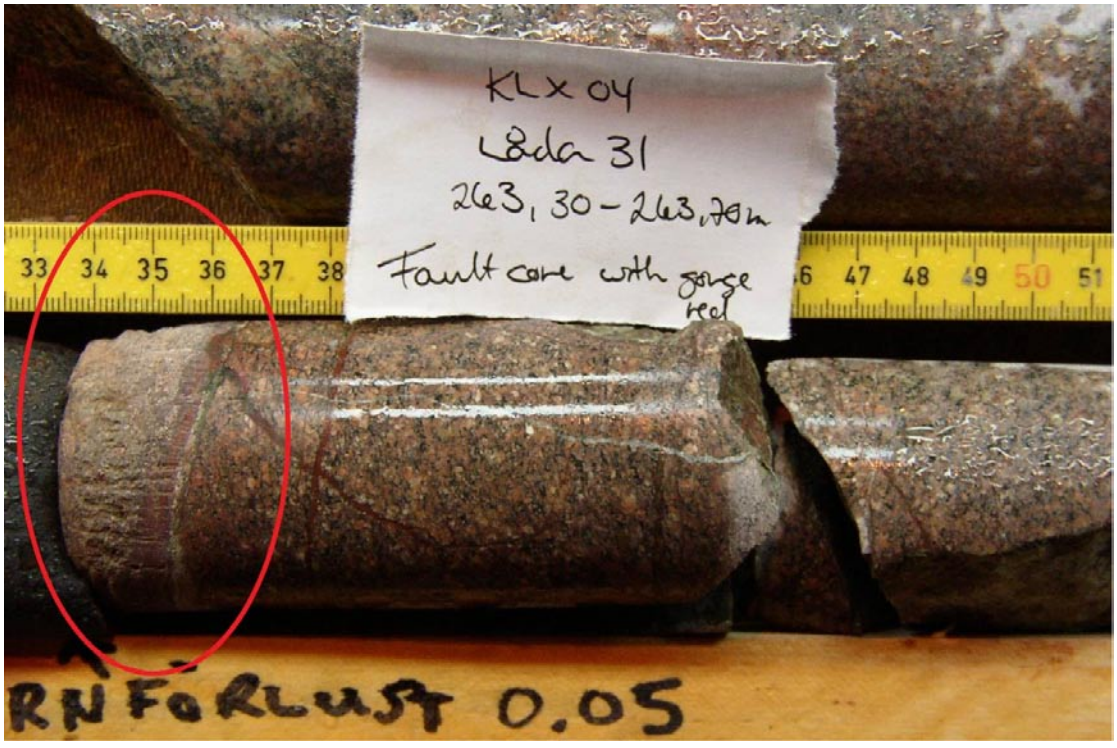

Figure 5-29. *Sharp lower contact between red gouge (circled in red) and protocataclasites. The contact is oriented 140/17.*

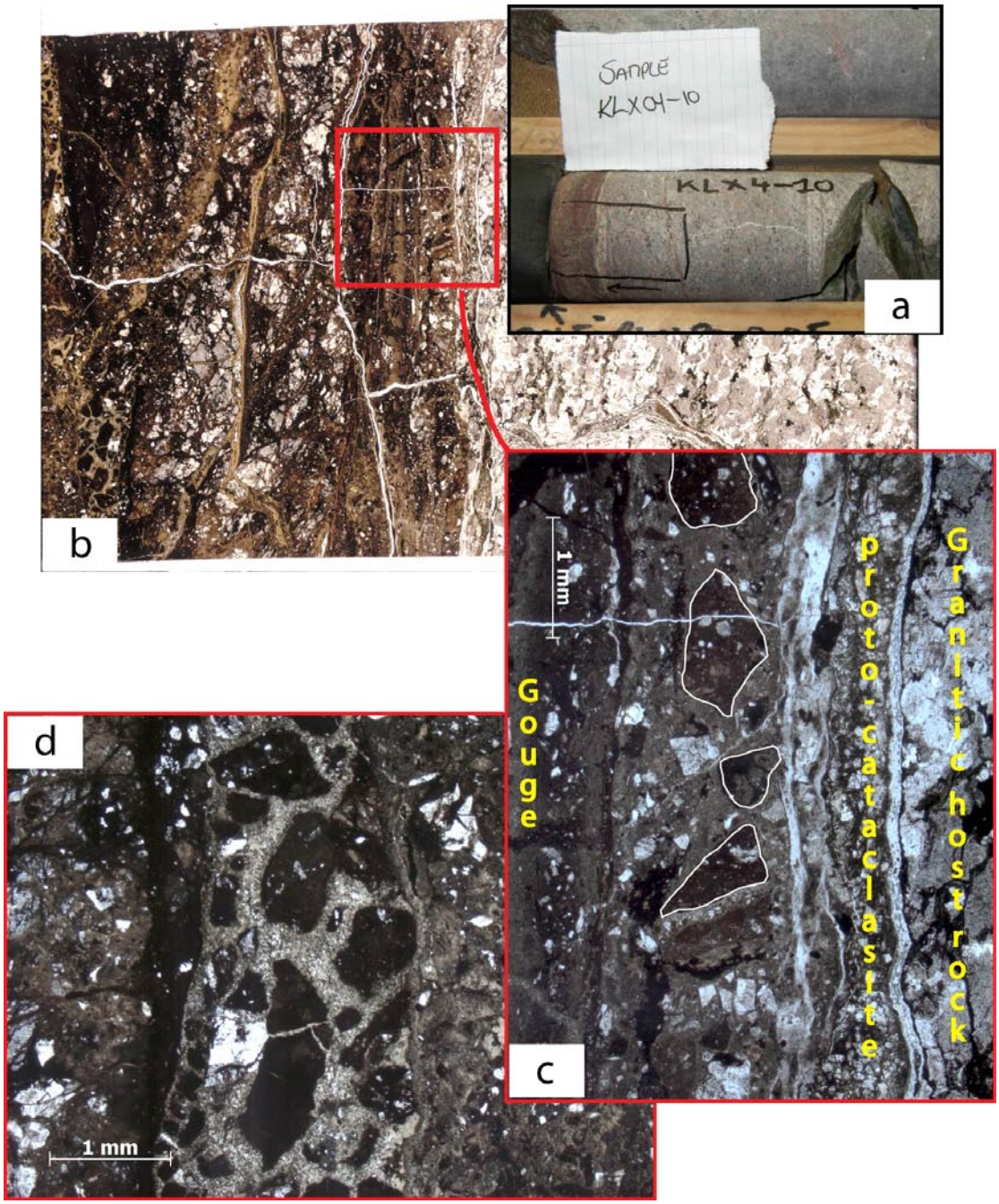

Figure 5-30. *(a): Location of sample KLX04-10 and (b) scanned thin section. The DZ core is formed by alternating subparallel bands of ultracataclasites and gouge that locally wrap around relatively less deformed cataclastic domains. (c): Detail of the sharp transition between the core and the host rock. Note the ultracataclasite clasts (with a white outline) fragmented and disrupted by a subsequent ultracataclastic episode. (d): Evidence of two distinct cataclastic events: dark, angular fragments of an early ultracataclasite float in a recrystallized epidote-dominated and fine-grained matrix genetically linked to a subsequent brittle event.*

The thin fault core (274.3–276 m) of this deformation zone consists of a complex ultracataclasite/gouge sealed network. Sample KLX04-11 (Figure 5-32) shows the microscopic details of such network and its associated, localized grain size reduction. The random distribution of the cataclastic bands and their irregular shape strongly suggest high pore-pressure and hydrofracturing as the likely mechanism for the generation of the network.

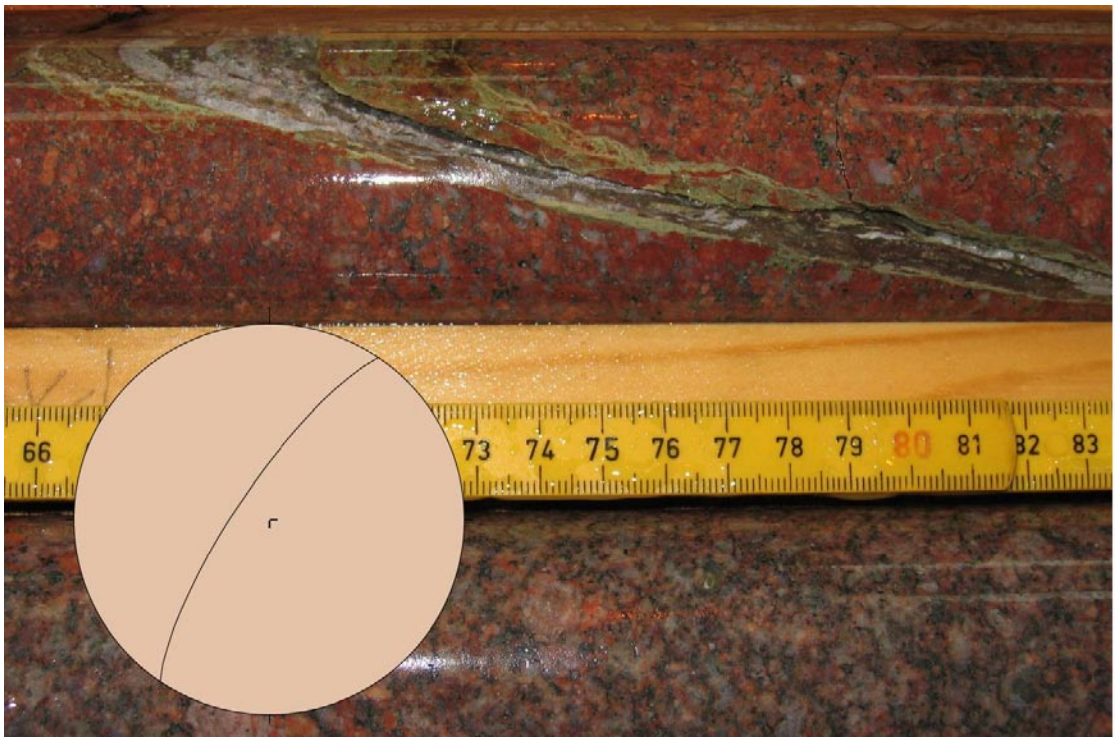

Figure 5-31. *Brittle-ductile epidote and calcite-decorated shear zone at depth 272.77 m. The structure dips steeply to the NW.*

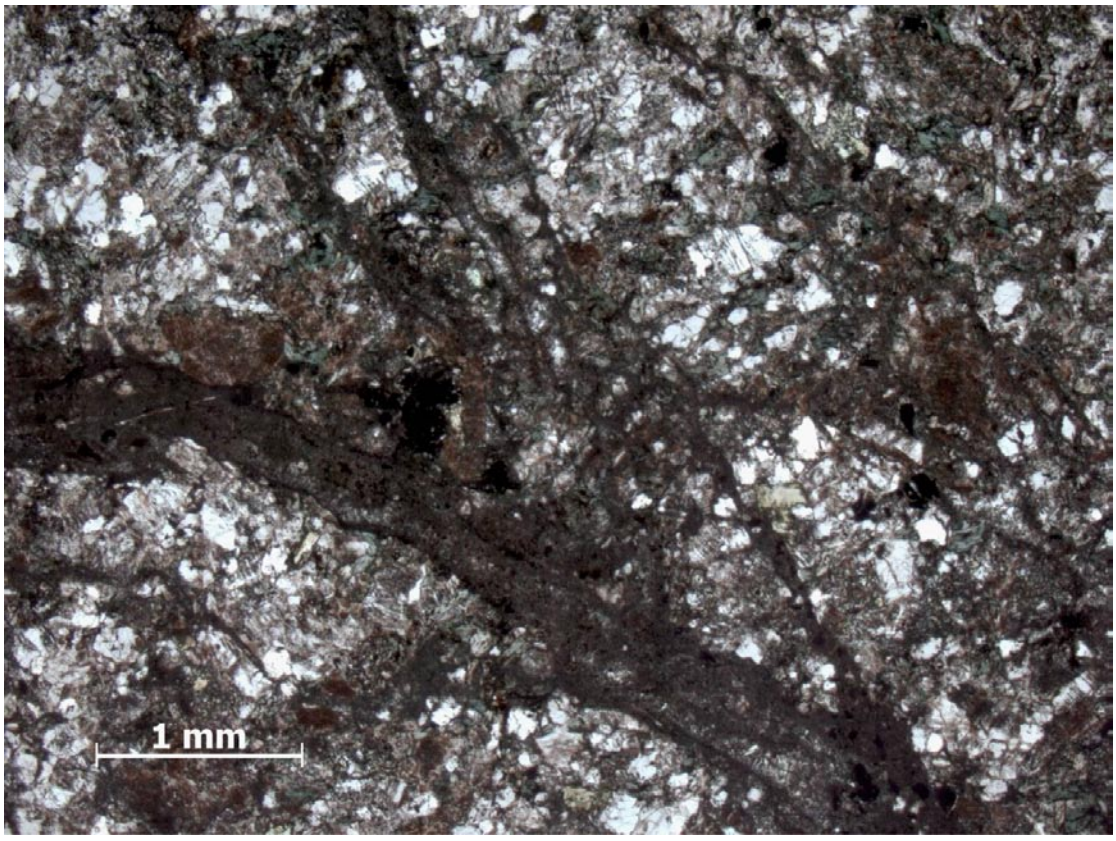

Figure 5-32. *Detail of the sealed cataclastic network of sample KLX04-11. Note the grain size reduction within and in proximity of the individual branches of the network.*

Table 5-3. Summary of DZ 2.

Depth (m)	Box number	Interpretation	Description
253.95	30	Transition zone	Increase in fracture frequency.
255.70	30	Fault core	Foliated cataclasites; crush zone developed at the expense of the cataclasites. Sample KLX04-9 of foliated cataclasite.
		Subzone FZ 1: 256.10–256.45	
		Subzone FZ 2: 256.65–256.76	Zone of crushed, non-cohesive rock. Not defined as fault rock due to the lack of structural/textural criteria.
		Subzone FZ 3: 256.92–257	Zone of crushed, non-cohesive rock. Not defined as fault rock due to the lack of structural/textural criteria.
		Subzone FZ 4: 257.65–257.88	Zone of crushed, non-cohesive rock. Not defined as fault rock due to the lack of structural/textural criteria.
257.88	30	Transition zone	Fracture frequency 8 f/m. Localized red staining. A few strands of ultracataclasites/gouge.
259.10	30	Host rock	Changes in lithology. Fracture frequency 3–5 f/m, minor increase towards the following transition zone.
261.31	31	Transition zone	Increase in fracture frequency up to 5–9 f/m. Red staining.
263.42	31	Fault core	The fault core consists of 2 generations of fault rock and crushed, non-cohesive rock (not breccia): 1) Small zone, ~20 cm thick, of cataclasites/ultracataclasites/gouge, with red gouge as the most prominent. 2) Highly fractured rock and crush zone, non-cohesive, but not defined as fault rock. Network of ultracataclasites/gouge. 3) Zone of cohesive fault rock, subsequently affected by a crush zone, ~1 m wide. Sample KLX04-10. The transition from the fault core to following transition zone is highly fractured and contains abundant sealed networks of ultracataclasites/gouge strands.
263.65	31	Transition zone	Numerous sealed networks of ultracataclasites/gouge strands.
263.85	31	Host rock	Fracture frequency down to 3–5 f/m.
271.85	33	Transition zone	Progressive increase of fracture frequency and of occurrences of ultracataclasites/gouge networks.
274.30	33	Fault core	Very prominent, 5–10 cm thick network of ultracataclasites/gouge. The rest of the zone consists of a network of cataclasite bands. Sample KLX04 11 and 12.
276	34	Transition zone	Network of ultracataclasites/gouge and lithological changes.
276.50	34	Host rock	Low fracture frequency, 3–5 f/m, and undeformed rock.

5.3.3 DZ 3: depth interval 295–298 m

DZ3 begins at depth 293.60 m with an upper transition zone defined primarily by an increase in fracture frequency up to 8–12 f/m. Figure 5-33 provides an overview of the deformation zone.

The fault core begins at 295.48 m and can be subdivided into three distinct subzones: i) FZ1 (295.48–295.68 m), a zone of crushed, non-cohesive rock. ii) FZ2 (295.83–296.03 m), a cataclastic zone with discrete ultracataclastic/gouge occurrences (Figure 5-33). The upper contact of the cataclastic core dips moderately SE (Figure 5-34). iii) FZ3 (296.03–296.25 m), a second crush zone, probably due to a very high fracture frequency. The transition zone that follows from depth 296.80 m contains a high fracture frequency. The deformation zone terminates at depth 297.58 m and is transitional to undeformed granitic host rock. Overall, the DZ is asymmetric in strain distribution, with most of the observed brittle features located in the hanging wall.

Figure 5-33. *Overview of DZ 3 in KLX04. The red oval highlights the position of part of the cataclastic core of the deformation zone, a detail of which is shown in the inset. The core is strongly cataclastic and is rich in green ultracataclasites/gouge.*

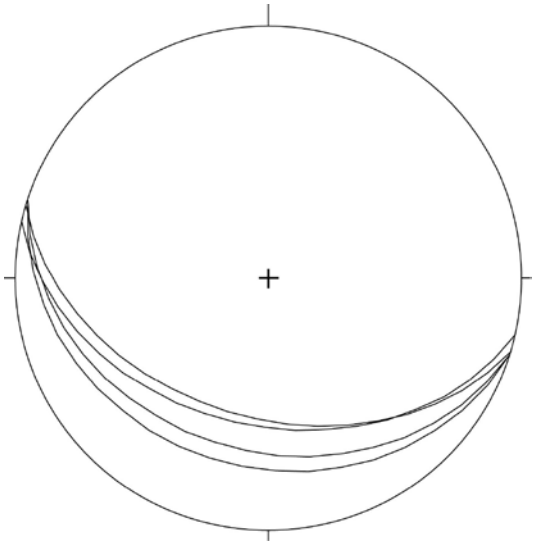

Figure 5-34. *Orientation of the upper contact of the cataclastic core of DZ 3.*

Table 5-4. Summary of DZ 3.

Depth (m)	Box number	Interpretation	Description
293.60	37	Transition zone	Progressive increase in fracture frequency, up to 8–12 f/m.
295.48	37	Fault core	Zone of crushed, non-cohesive rock. Not defined as fault rock due to the lack of structural/textural criteria.
		Subzone FZ 1: 295.48–295.68	
		Subzone FZ 2: 295.83–296.03	Cohesive fault rock with cataclasites/ultracataclasites/ gouge occurrences.
		Subzone FZ 3: 296.03–296.25	Zone of crushed, non-cohesive rock. Not defined as fault rock due to the lack of structural/textural criteria.
296.80	37	Transition zone	High fracture frequency, up to 9 f/m, and some lithological changes.
297.58	37	Host rock	Low fracture frequency, 3–5 f/m, otherwise undeformed rock.

5.3.4 DZ 4: depth interval 325–326 m

DZ 4 is c. 30 cm thick, starts at depth 325.50 m and has no clear transition zone. The fault core consists of epidote-rich cohesive cataclasites, ultracataclasites and gouge (Figure 5-35), followed by a crush zone at depth 325.87 m. Kinematic analysis of striated fractures associated with the DZ core indicates a reverse, top-to-the-NNE sense of shear along fractures that dip gently to the SW (stereonet in Figure 5-35). The section ends at depth 326 m with a transition back to undeformed host rock with low fracture frequency.

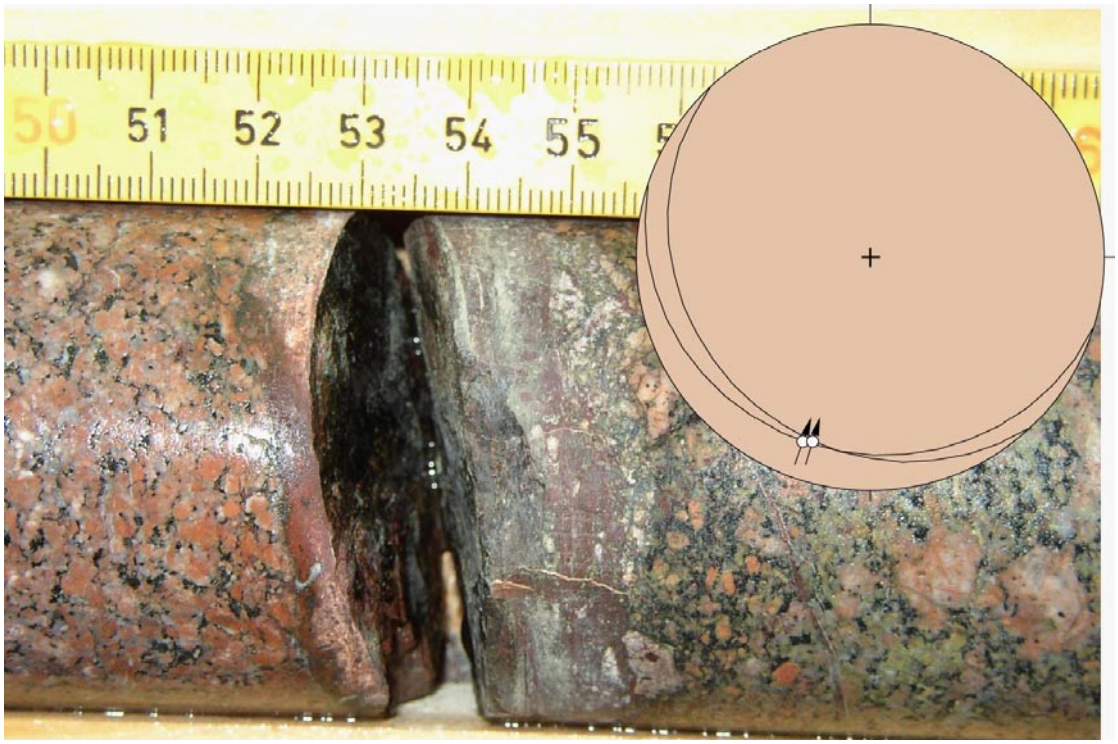

Figure 5-35. *Core of DZ 4 at depth 325.5 m, with protocataclasites, ultracataclasites and bands of brown gouge. Two striated surfaces constrain reverse top-to-the-NNE kinematics along gently SW-dipping planes.*

Table 5-5. Summary of DZ 4.

Depth (m)	Box number	Interpretation	Description
325.50	43	Fault core	No clear transition zone. The fault core consists of cohesive fault rock (protocataclasites/cataclasites/ gouge).
326	43	Host rock	Undeformed sequence with low fracture frequency, 3–5 f/m.

5.3.5 DZ 5: depth interval 346–355 m

The section starts at depth 346.26 m with a c. 20 cm thick upper transition zone. The fault core, from depth 346.46 m, is characterized by c. 35 cm of cataclasites and both green and red gouge. Ultracataclasites/gouge are arranged in a complex, sinuous and anastomosing sealed network with associated grain size reduction (Figure 5-36).

Systematic fractures within the core strike roughly NW-SE (Figure 5-37). The fault core ends with a narrow zone of ultracataclasite and/or gouge, from where a thin section sample was collected (KLX04-13b). Figure 5-38 shows the location of KLX04-13b, which samples effectively the pervasive sealed cataclastic network. The scanned thin section of Figure 5-38 shows

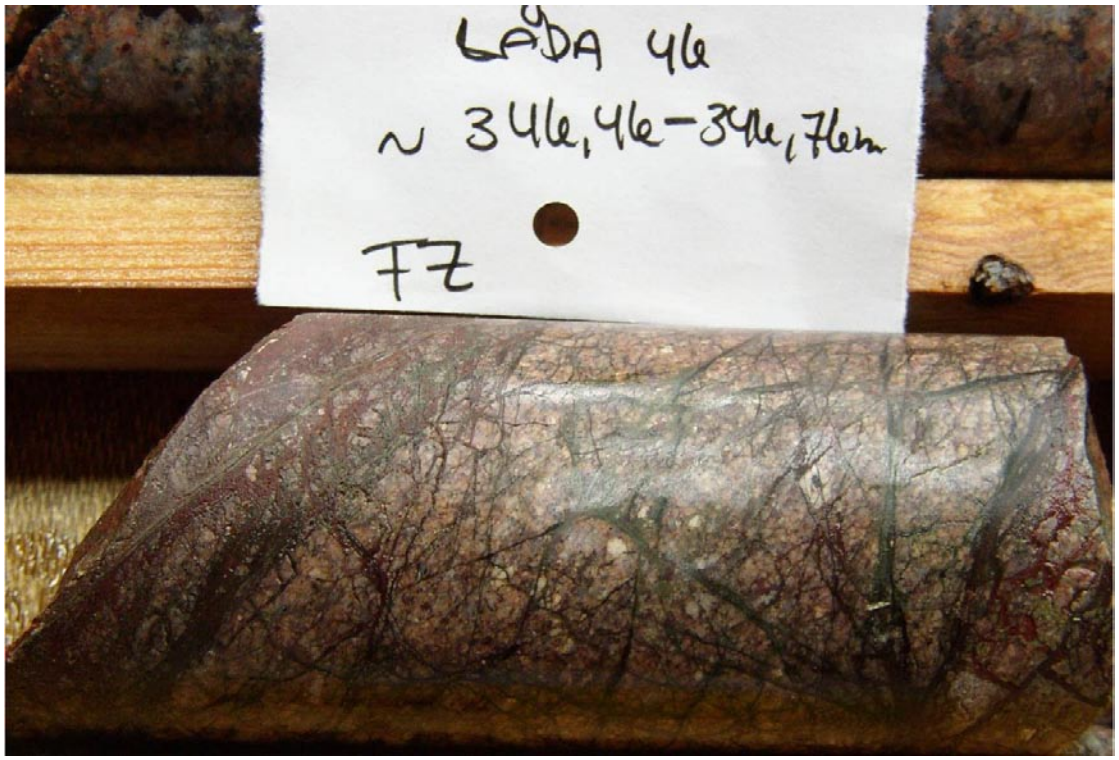

Figure 5-36. *Detail of the core of DZ 5, defined by a complex sealed network of ultracataclasite/gouge bands and a distinct interval of brown/green gouge at depth 346.66 m.*

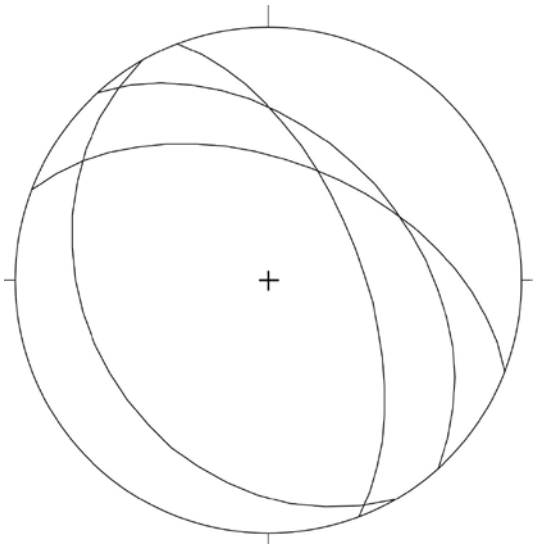

Figure 5-37. *Orientation of discrete systematic fractures within the core of DZ 5.*

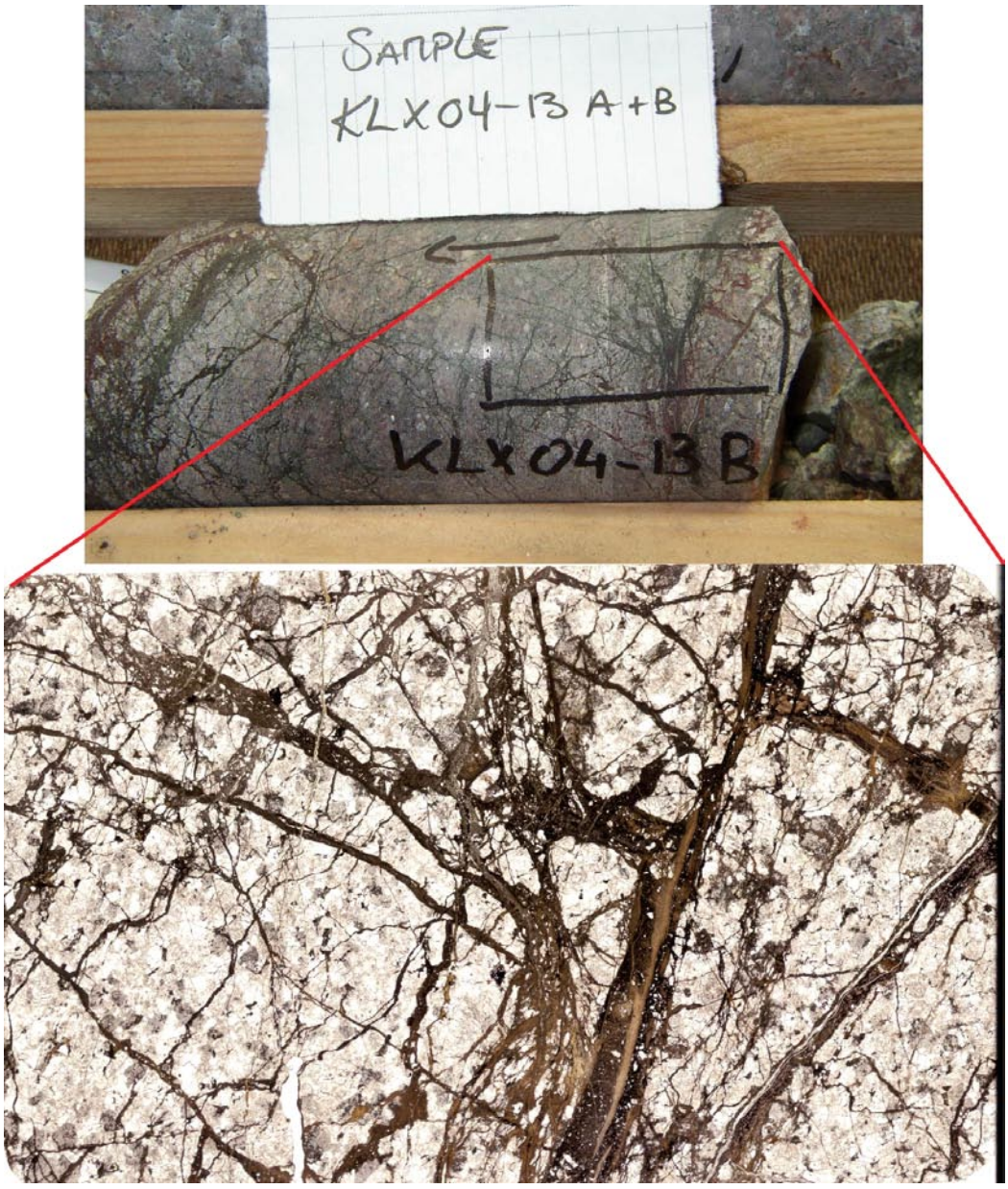

Figure 5-38. *Sample KLX04-13b illustrates the complexity of the dilatant fluidised network of ultracataclasites that define the core of DZ 5.*

a very interesting structural pattern, whereby the granitic host rock is completely disrupted by the injection of a very dense, anastomosing dilatant network of fluidized ultracataclasites. It is clear that the injected material does not follow any preferential direction, but forms instead a mesh of randomly oriented "dykes". Cataclasis and granular flow are invariably associated with the dilatant network, and it is remarkable how well sorted the cataclastic injections are. Hydrofracturing and fluidization are believed to be the mechanisms responsible for the formation of this DZ core, although more investigations would be necessary to fully unravel the complexities of the mechanism that generated the fault rock.

A crush zone follows within the fault core. A transition zone begins at 352.81 m with abundant ultracataclasite and/or gouge strands and fractured rock. The transition zone contains numerous striated planes. Figure 5-39 shows that no clear kinematic pattern emerges, though, with highly dispersed fracture planes (generally dipping to the west) and predominance of very oblique shearing. Undeformed host rock is logged again at depth 357.77 m.

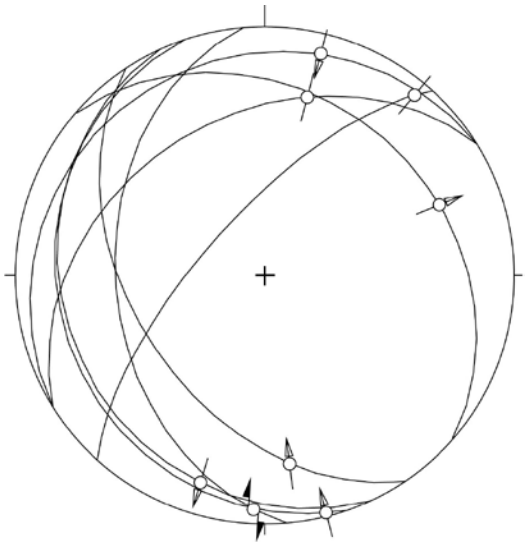

Figure 5-39. *Fault-slip data for the transition zone following the core of DZ 5. No clear kinematic pattern emerges from the data.*

Table 5-6. Summary of DZ 5.

Depth (m)	Box number	Interpretation	Description
346.26	46	Transition zone	Narrow zone, max 20 cm in thickness, with some alternation in lithology.
346.46	46	Fault core	~35 cm thick cataclastic interval. Transition to a crush zone formed by non-cohesive rock (highly fractured). The fault core ends with a narrow zone of ultracataclasites/gouge. Sample KLX04-13.
352.81	48	Transition zone	Numerous ultracataclasite/gouge strands. Fractured sequence.
357.77	48	Host rock	Low fracture frequency, 3–5 f/m, otherwise generally undeformed rock.

5.4 KLX08

The location of KLX08 is shown in Figure 5-1. The core is 1,000.41 m long. In the depth interval logged for this study the core plunges 80° towards 211° and penetrates in Ävrö granite. /Viola and Venvik Ganerød 2007/ characterized structurally DZ 1 and 2 of the single-hole interpretation of KLX08 /Carlsten et al. 2005/. This report will describe DZ 6 (385–427 m) and DZ 7 (476.5–486.5 m) shown in Figure 5-40.

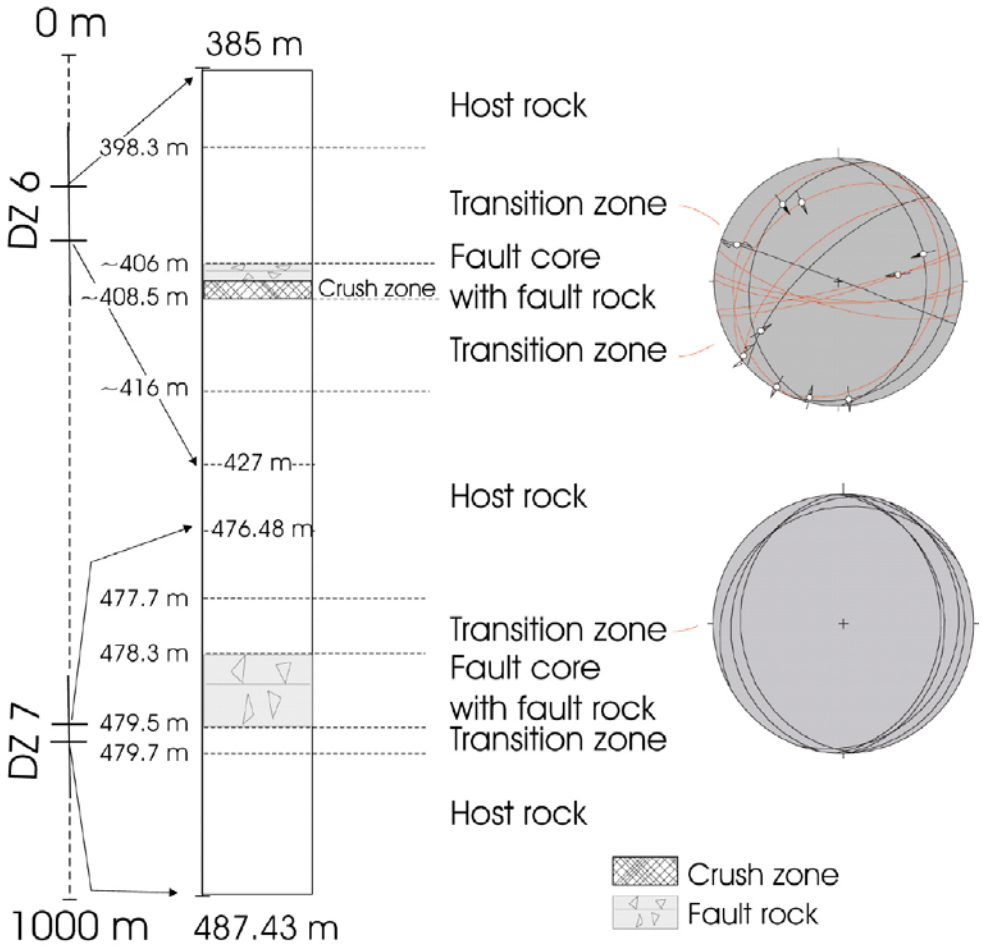

Figure 5-40. *Schematic interpretative log of DZ 6 and DZ 7 of KLX08. Details about the stereonets can be found in the text.*

5.4.1 DZ 6: depth interval 385–427 m

The host rock in this section is a porphyritic facies of the Ävrö granite, with centimetric K-feldspar phenocrystals. DZ 6 is characterized by a ~2.5 m thick fault core with 2 symmetrically arranged transition zones (Figure 5-41). The upper and lower transition zones show increasing and decreasing fracture frequency towards and away from the fault core, respectively. The stereonet of Figure 5-42 shows the fault slip data observed and measured within the two transition zones; red great circles represent striated planes of the upper transition zone, whereas black great circles represent planes of the lower transition zone. The steep, roughly EW trending fractures are generally coated by epidote, whereas the shallower planes are coated by chlorite, clay minerals and calcite, which in turn may suggest the steep fractures to be older (thus formed under higher T conditions) than the gently-dipping ones. No direct crosscutting relationships were, however, observed. No straightforward kinematic framework can be obtained from these few measurements. In general, highly oblique or strike-slip kinematics is accommodated along moderately WNW or ESE dipping planes (Figure 5-42). The steep E-W epidote-coated fracture planes suggest instead strike-slip displacements along moderately plunging lineations.

The occurrence of discrete and localized cataclasites is common throughout both transition zones. The upper boundary of DZ 6 fault core is located at approximately 405.77 m depth. The core consists of ~50 cm of cohesive cataclasites, ultracataclasites and gouge, and a ~2 m thick crush zone affecting the undeformed host rock. At depth 406.18 m there occurs a narrow, cataclastic zone characterized by a c. 3 cm thick green ultracataclasite and gouge (Figure 5-43). An open fracture, coated by epidote and clay minerals is oriented 150/41 and runs parallel to the ultracataclasite.

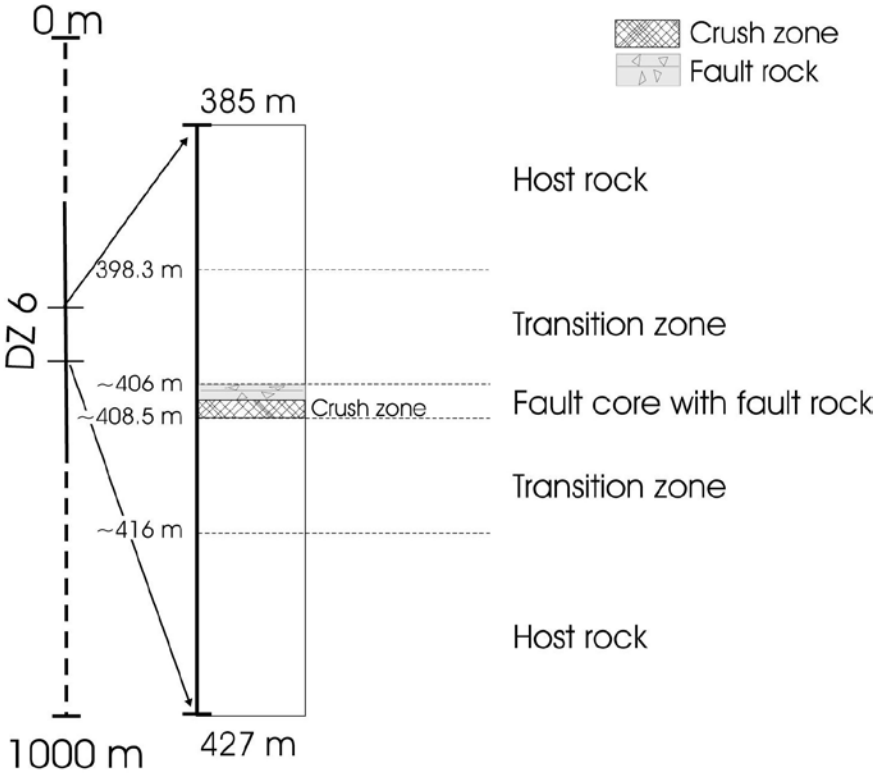

Figure 5-41. *Schematic interpretative log of DZ 6 of KLX08.*

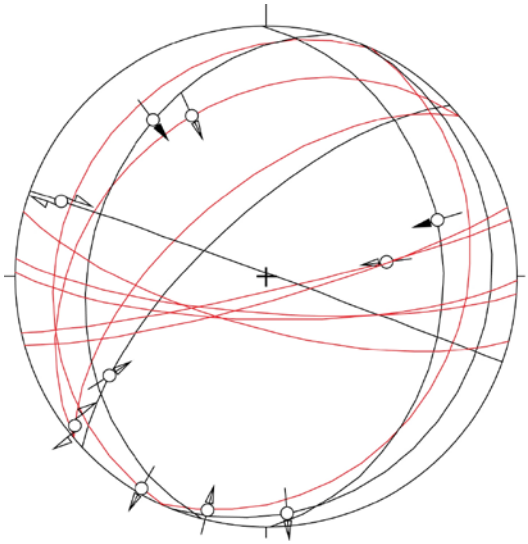

Figure 5-42. *Fault–slip data and orientation of striated planes and fractures in the transition zones above and below the core of DZ 6. Red great circles plot structures from the upper transition zone, black from the lower.*

Sample KLX08-1 comes from this part of the DZ core and preserves complex textural characteristics (Figure 5-44) indicative of multiple cataclasis episodes. For example, the microphotograph of Figure 5-44 zooms into a thin, light brown ultracataclasite cutting across a coarser-grained cataclasite along a straight, sharp contact. While the older cataclasite is darker in colour and contains poorly sorted and angular clasts, the crosscutting ultracataclasite is extremely homogeneous and fine-grained. The texture of sample KLX08-1 is very variable and consists of alternating layers and pockets of protocataclasites and proper cataclasites and gouge. Late, discordant quartz and calcite veins are abundant.

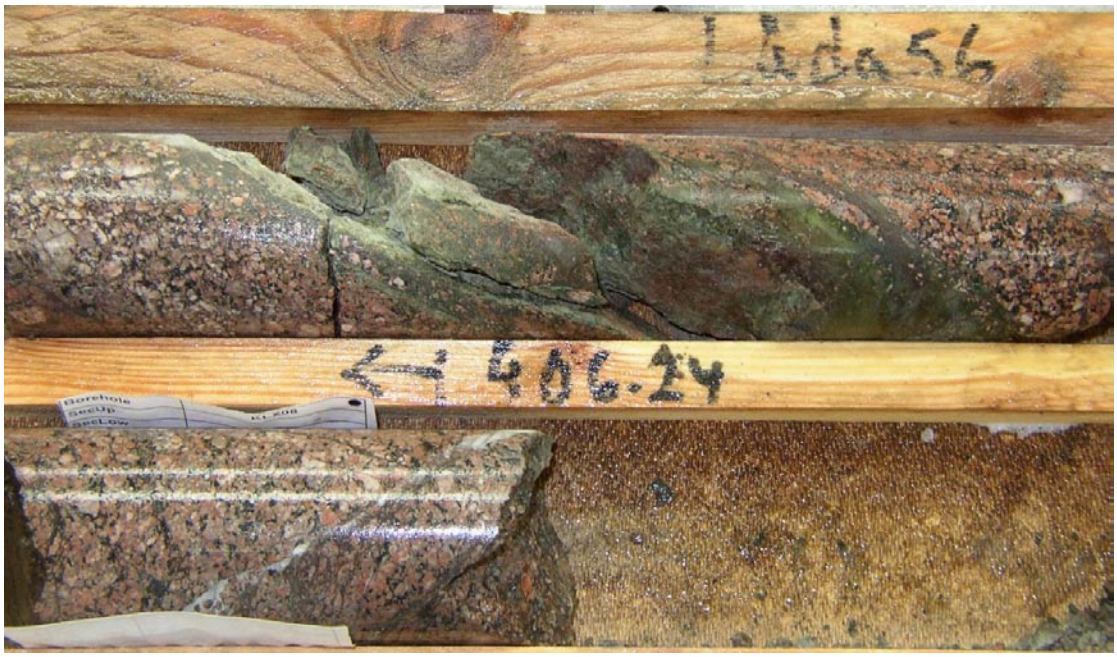

Figure 5-43. *Epidote ultracataclasite at depth 406.18 m. The ultracataclasite and the open fracture are oriented 150/41.*

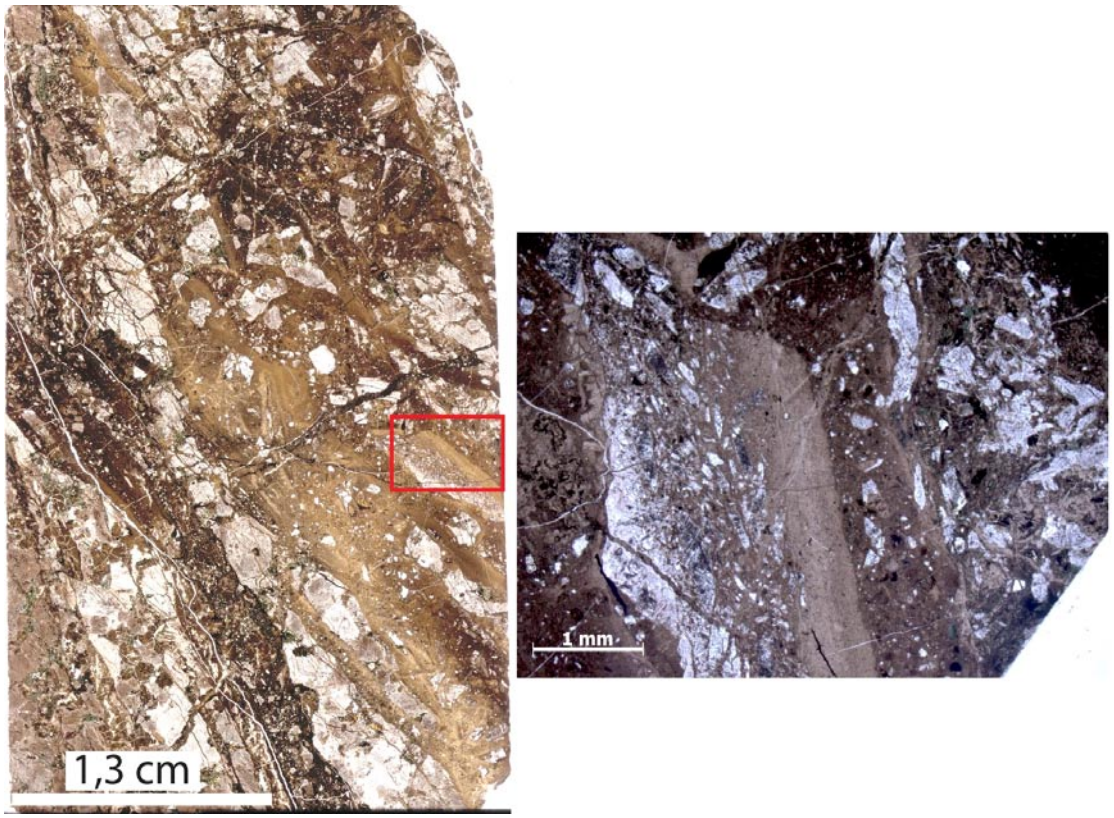

Figure 5-44. *Scanned thin section of sample KLX08-1 (to the left) and microphotograph of the cataclastic/ultracataclastic texture of part of the sample (to the right). The red rectangle shows the area covered by the microphotograph.*

Table 5-7. Summary of DZ 6.

Depth (m)	Box number	Interpretation	Description
385	52	Host rock	Undeformed rock with low fracture frequency, 1–3 f/m.
398.30	54	Transition zone	Progressive increase in fracture frequency, up to 5–15 f/m. Increase in occurrence of narrow, discrete cataclastic bands.
405.77	56	Fault core	Occurrence of cohesive cataclasites, ultracataclasites and gouge and discrete crush zones. Occurrence of a pervasive cataclastic sealed network. The most distinct zone is ~45 cm thick, while the whole fault core is ~2.5 m in thickness. Sample – KLX08-1.
408.48	56	Transition zone	Highly fractured transition zone. Sporadic occurrences of ultracataclastic narrow bands in relatively undeformed Ävrö granite.
			Undeformed rock with low fracture frequency, 1–6 f/m.

5.4.2 DZ 7: depth interval 476.5–487.5 m

DZ 7 is a deformation zone defined by a c. 1 m thick fault core and its two upper and lower, slightly asymmetric transition zones (Figure 5-45). The upper transition zone (depth interval 477.668–478.31 m) is thicker than the lower counterpart and is characterized by an increase in fracture frequency towards the fault core and several discrete ultracataclasite and/or gouge bands (Figure 5-46).

It contains very gently dipping open fractures, striking roughly NS and dipping shallowly either E or W (Figure 5-47).

The DZ fault core (depth 478.31–479.505 m) is ~1.2 m thick and is formed by a network of ultracataclasite and/or gouge bands. The most prominent zone in the core is located at depth 479.14 to 479.41 m.

The lower transition zone extends from 479.505 m depth down to 479.696 m and consists of fractured host rock and sporadic cataclasites, including a c. 20 cm thick sealed network at depth 479. 505 m. The drill core enters undeformed host rock at depth 479.696 m, with low fracture frequency, localized red staining and a few epidote veins.

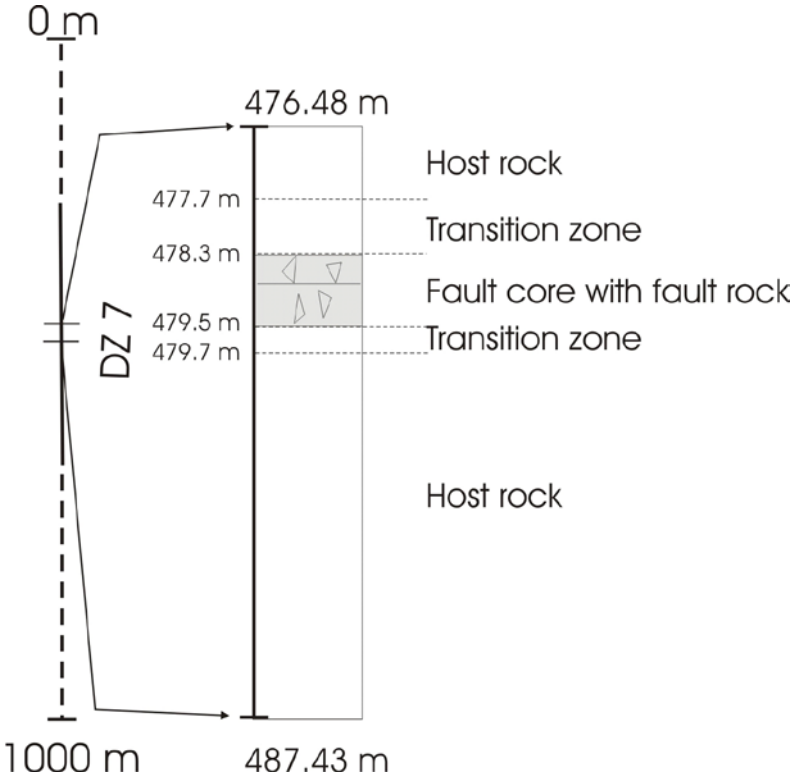

Figure 5-45. *Schematic structural log of DZ 7 of KLX08.*

Figure 5-46. *DZ 7. Uppermost transition zone, with gently dipping open fractures and a discrete olive-green ultracataclastic band.*

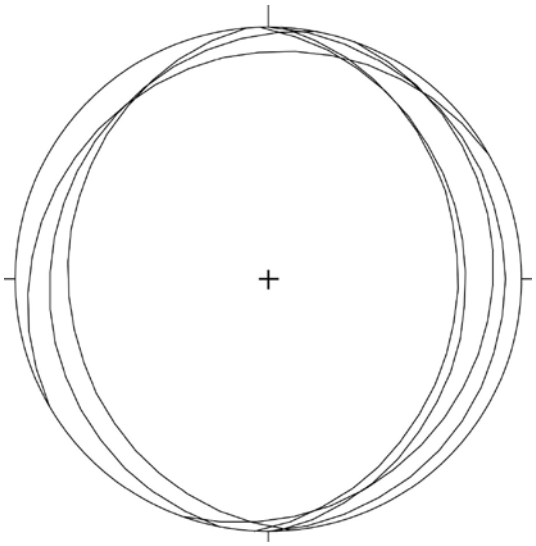

Figure 5-47. *Orientation of open fractures of the upper transition zone of DZ 7.*

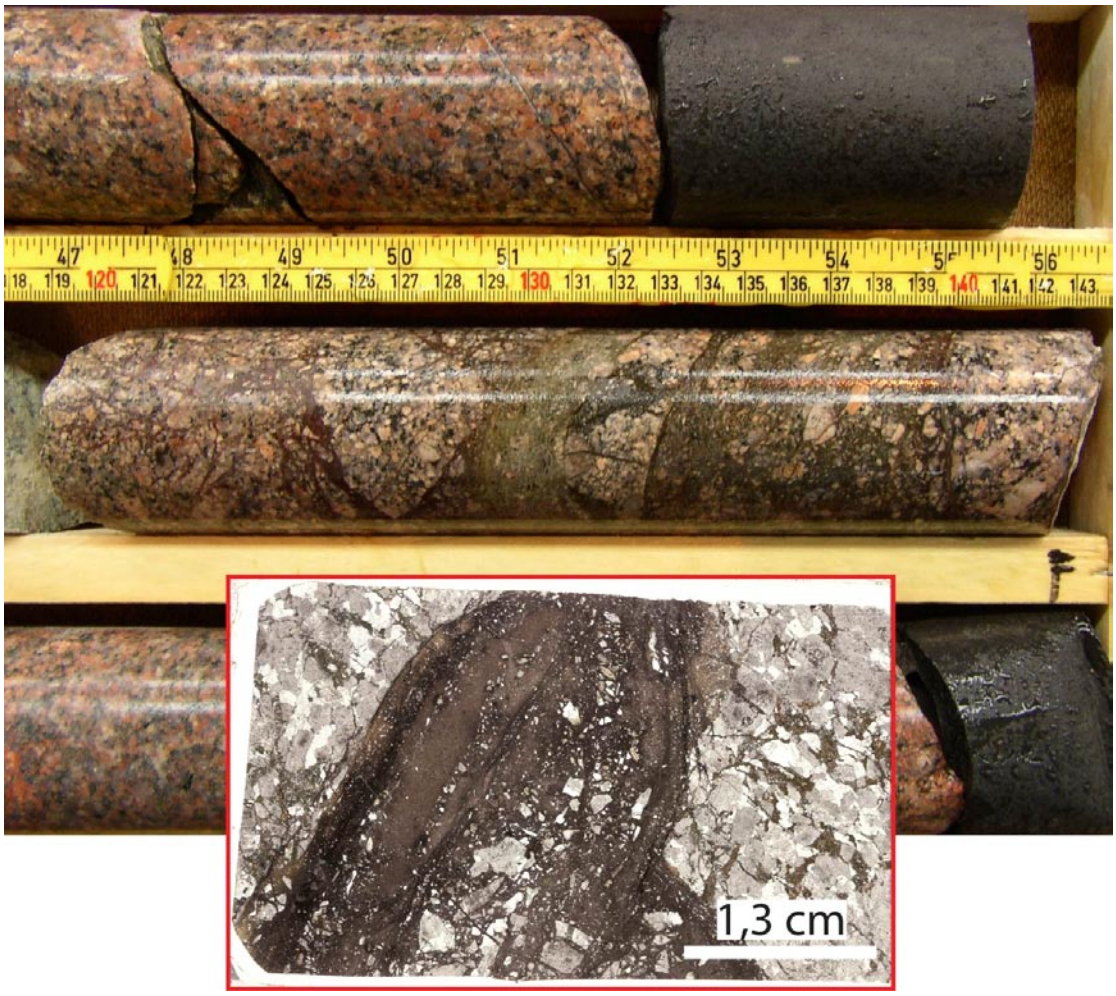

Figure 5-48. *DZ 7 fault core and scanned thin section of sample KLX08-2. Protocataclasites, ultra-cataclasites and gouge bands form a sealed anastomosing network. The thin section illustrates the heterogeneous textural characteristics of the DZ core, with very fine-grained ultracataclasites coexisting with poorly sorted cataclasites.*

Table 5-8. Summary of DZ 7.

Depth (m)	Box number	Interpretation	Description
476.48–477.668	69	Host rock	Undeformed rock with low fracture frequency.
477.668–478.31	69	Transition zone	Progressive increase in fracture frequency towards the fault core, and increase in the occurrence of ultracataclasite/gouge bands.
478.31–479.05	69	Fault core	Occurrence of sealed ultracataclastic networks and increasing occurrence of discrete horizons of brittle fault products. The most distinct zone is from 479.14–479.41 m, while the whole fault core is ~1.2 m thick. Sample – KLX08-2.
479.505–479.696	69	Transition zone	Cataclastic network ~20 cm thick.
479.696–	70	Host rock	Undeformed rock with low fracture frequency. Some red staining and occurrence of epidote veins.

5.5 KLX09

KLX09 is located in the easternmost part of the Laxemar investigation area, where Ävrö granites outcrop (Figure 5-1). The drill core has a length of 992.29 m and is oriented 265/85 /Carlsten et al. 2007e/. The section logged and described in this report extends from depth 105.83 down to 870 m (Figure 5-49). According to the single-hole interpretation /Carlsten et al. 2007e/ this section contains seven distinct deformation zones separated by relatively undeformed rock. Apart from DZ 13, which was logged in great detail and for which numerous structural and kinematic observations were made and are reported in this section, the analysis of the remaining core was made at a cursory level and therefore only very schematic descriptions are given in this report. Generally, the undeformed host rock contains bands and anastomosing networks of cataclastic rock that vary in thickness from millimeter to centimeter, possibly foliated protocataclasites and narrow crush zones. Red staining is common, especially in proximity to cataclastic networks or bands.

5.5.1 DZ 7: depth interval 313–323.2 m (314.50–321.95 m)

In the single-hole interpretation /Carlsten et al. 2007e/ DZ 7 is limited to the depth interval 313–323.2 m. From our logging DZ 7 begins with a transition zone at 314.50 m depth, which extends down to 321.95 m and is characterized by pervasive red staining and localized networks of ultracataclasite and/or gouge bands (Figure 5-50).

The DZ fault core (at depth interval 321.95–323.20 m) contains a ~50 cm thick cataclastic horizon cored by thin ultracataclastic bands, followed by a ~75 cm thick crush zone.

Table 5-9. Summary of DZ 7.

Depth (m)	Box number	Interpretation	Description
314.50–321.95	39	Transition zone	Zones of red staining, and networks of ultracataclasites/gouge at depth interval 314.50–314.82 m and 317.10–317.95 m. The zone is 7.45 m thick.
321.95–323.20	40	Fault rock	~50 cm thick interval formed by a cataclastic zone cored by ultracataclasites, followed by ~75 cm of crushed rock, possibly reworking cataclasites. The thickness of the zone is 1.25 m.

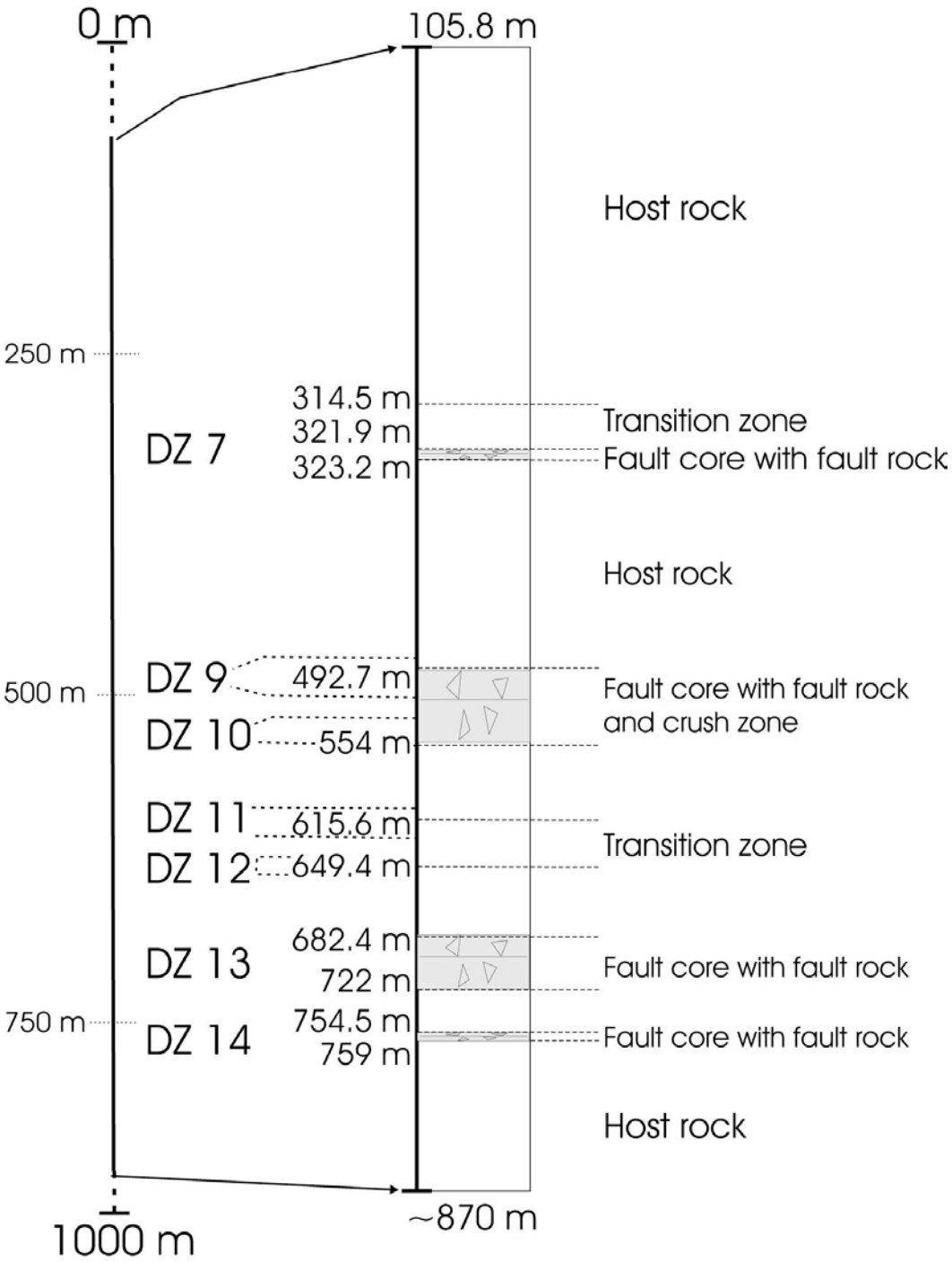

Figure 5-49. *Schematic illustration of the logged depth interval of KLX09. There are seven deformation zones identified and characterized by the single-hole interpretation /Carlsten et al. 2007e/. Their cores invariably contain fault rock; DZ 9 also contains a significant crush zone.*

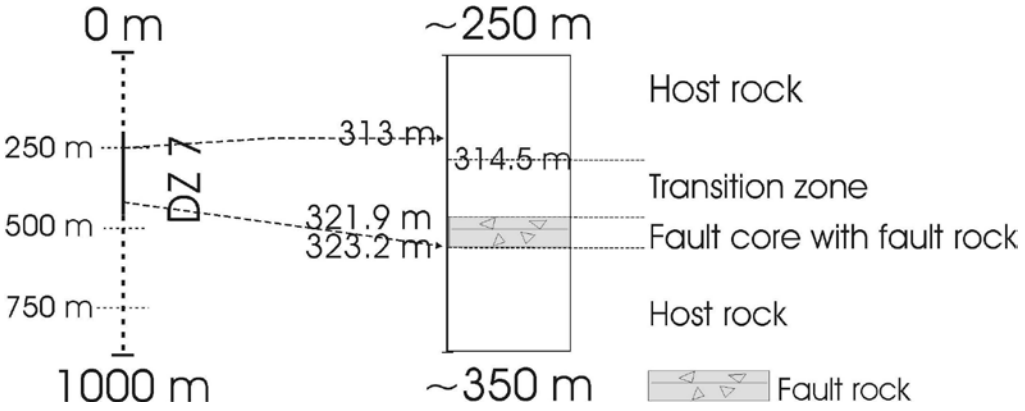

Figure 5-50. *Schematic log of DZ 7.*

5.5.2 DZ 9 and 10: depth interval 492.4–554 m (492.7–584 m)

From our logging these deformation zones occur between 492.7 and 584 m depth, slightly different from what reported in the single-hole interpretation/Carlsten et al. 2007e/, and can be grouped into a single zone containing several subzones. The deformation zone begins with an upper transition zone at depth 492.70–494.35 m, with the occurrence of cataclastic rock in thin bands, and a proper fault core extending from 494.35 to 499.80 m (Figure 5-51). The fault core consists itself of three localized zones: (1) An 8 cm wide crush zone in a cataclastic protolith; (2) A 10–12 cm thick sequence of red gouge and green ultracataclasites; (3) A 4.5 m thick interval of cohesive rock containing abundant networks of cataclasites and/or protocataclasites and minor occurrences of gouge/ultracataclasites. From depth 499.80 m there follows a lower transition zone characterized by a progressively decreasing number of networks of ultracataclastic bands and pervasiveness of red staining.

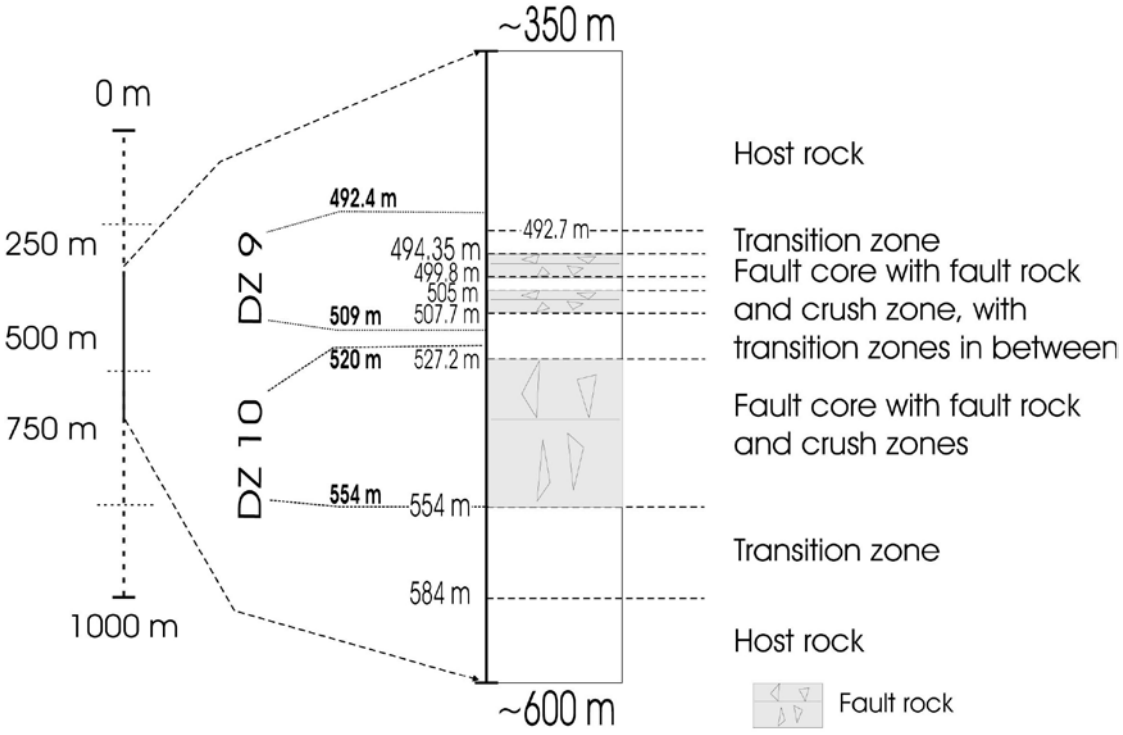

Figure 5-51. *Schematic structural log of DZ 9 and 10.*

A second, distinct fault core is located at depth 505 m and consists of a ~25 cm thick crush zone, possibly formed from pre-existing cataclasites and/or ultracataclasites; below it there follows an heterogeneous sequence of green cataclasites and/or protocataclasite, varying in thickness from 0.5 to 2 cm, interspersed with lenses of less deformed rock. Another transition zone occurs from depth 507.70 m, lacking significant deformation but displaying pervasive red staining.

A third fault core is found at 527.20 m depth. It consists of three discrete sub-zones: (1) A subzone characterized by an increase in fault rock occurrence such as protocataclasite and/or cataclasite and networks of thin ultracataclasite/gouge bands. (2) A 20 cm thick subzone between 527.50 and 527.70 m containing a sequence of ultracataclasite, gouge, cataclasite and ultracataclasite, and in addition a crush zone in the "center of the subzone", and finally (3) a complex variety of fault rock occurrences and crush zones.

A last transition zone begins at depth 554 m and is characterized by progressively decreasing deformation and diffuse red staining (Figure 5-51).

Table 5-10. Summary of DZ 9 and 10.

Depth (m)	Box number	Interpretation	Description
492.70–493	70	Transition zone	Undeformed rock with localized occurrences of cataclasites. The total thickness of the zone is 61 m.
494.35	71	Fault core: subzone 1)	8 cm of crushed cataclastic rock.
		subzone 2)	10–12 cm of red gouge and green ultracataclasites.
		subzone 3)	4.5 m of cataclasite and protocataclasite networks.
499.80	72	Transition zone	Decrease in networks of ultracataclasite/gouge and red staining.
505	73	Fault core	~25 cm thick crush zone, possibly formed by the reworking of pre-existing cataclasites/ultracataclasites. Transition to cohesive c/pc with lenses of less deformed rock. Bands of green ultracataclasites, 0.5–2 cm thick.
507.70	73	Transition zone	Red staining, decreasing deformation.
527.20	77	Fault core	Increase of fault rock occurrence as protocataclasites/cataclasites and network of ultracataclasites/gouge.
		527.50–527.70	Zone of ultracataclasites/gouge/cataclasites, and in addition crushed rock in the "center of zone".
	82		Variety of fault rock occurrences and crush zones.
554–	82	Transition zone	Decreasing deformation intensity and diffuse red staining.

5.5.3 DZ 11 and 12: depth intervals 611–618.3 m and 648.6–649.6 m (615.60 –649.40 m)

From the single interpretation hole this section is mapped as DZ 11 and 12 within depth intervals 611–618.3 (DZ 11) and 648.6 to 649.6 m (DZ 12). From our logging, however, this DZ begins at 615.70 m and extends down to 649.40 m (Figure 5-52). It lacks a proper core and consists principally of a transition zone characterized by pervasive red staining and thin occurrences of fault rock covering the whole spectrum from proto- to ultracataclasites.

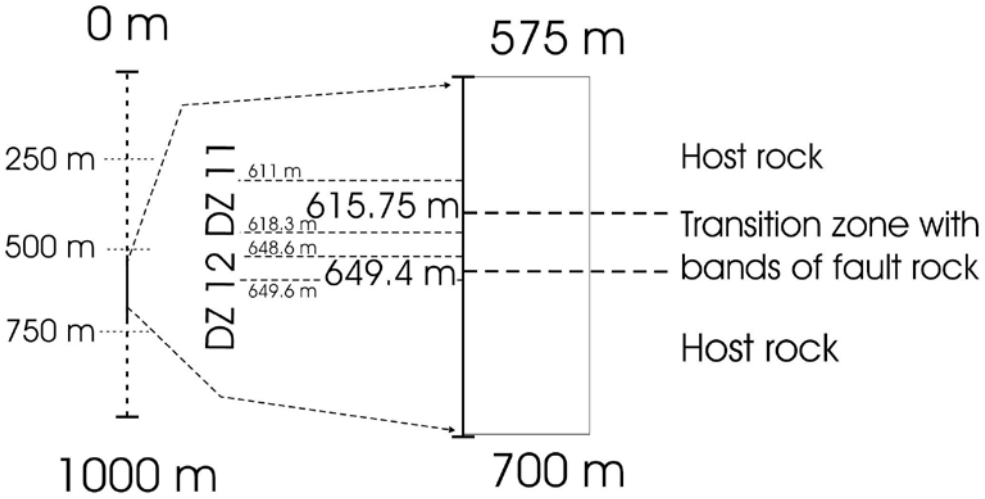

Figure 5-52. *Structural log of DZ 11 and 12.*

Table 5-11. Summary of DZ 11 and 12.

Depth (m)	Box number	Interpretation	Description
615.60–616.70	93	Transition zone	~1 m of red staining and cataclastic (proto- to ultra) occurrences. The thickness of the zone is c. 34 m.
628.75–629.30	96		Red staining and bands of cataclastic fault rock.
642.94–644.19	98		Bands of ultracataclasites and cataclasites.
648.95–649.40	99		Millimetric bands of ultracataclasites.

5.5.4 DZ 13: depth interval 682–722 m (634–743 m)

DZ 13 begins at depth 682 m and extends down to 722 m (Figure 5-53). It is a major deformation zone that contains different types of fault rocks and is rich in kinematically unambiguous striated planes (Figure 5-54).

The deformation zone begins with a c. 7 m thick upper transition zone defined by red staining and sporadic occurrences of bands of ultracataclasite/gouge arranged in sealed networks. Deformation intensity increases significantly towards the core, the upper boundary of which we locate at depth 689.50 m.

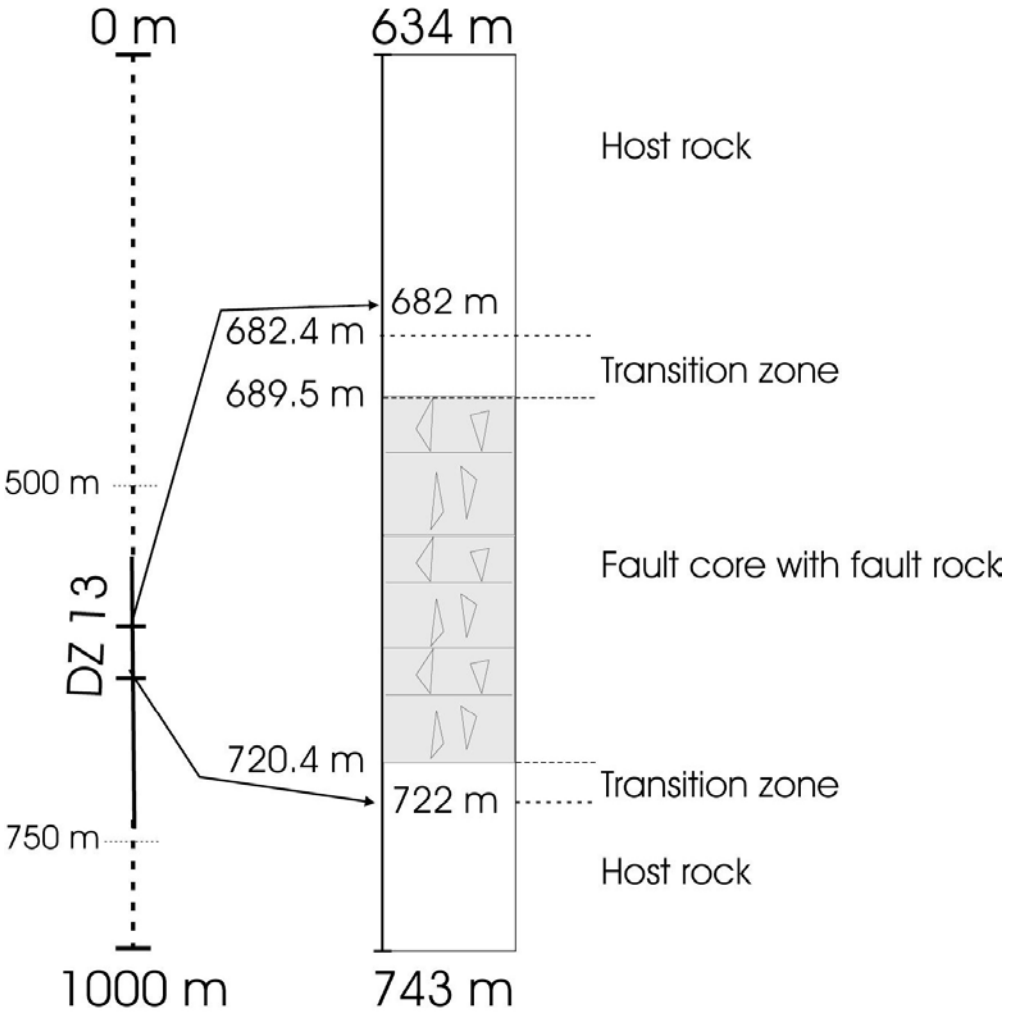

Figure 5-53. *Detailed interpretative log of DZ 13 in KLX09.*

Figure 5-54. *Example of a striated plane at depth 701.676 m. Chlorite, calcite and clay minerals coat the surface. Slickensides indicate that the hanging wall to this plane moved up parallel to the striations.*

At depth 689.67 there occurs a c. 3 cm thick green/brown ultracataclastic/gougy horizon associated with a striated plane. The slickenside-bearing plane dips moderately to the S/SSE and kinematic analysis indicates an overall dextral strike-slip motion with only a very minor S-side-up component (Figure 5-55). The contact between the faulted horizon and the host rock is very sharp (Figure 5-55).

At depth 692.80 there occurs an indurated breccia cemented by calcite. Analysis of the individual clasts suggests that it formed at the expense of already protocataclastic granites (Figure 5-56).

Immediately below there is a discrete, highly deformed sequence with ~20 cm of red gouge at its center (sample KLX09-1; Figure 5-57). KLX09-1 shows localized cataclastic zones affecting medium-grained granites. Deformation by granular flow mechanisms is concentrated in narrow bands within which there occurs extreme grain size reduction and disruption of the protolith by mechanical grinding of the granite (Figure 5-58).

Figure 5-55. *Ultracataclasites/gouge at depth 689.67 m.*

Figure 5-56. *Cemented breccia derived from protocataclastic granites.*

At depth 720.20 m there occur ~25 cm of red gouge and green ultracataclasite (sample KLX09-2; Figure 5-57 and Figure 5-58). The cataclasites are oriented 030/14. KLX09-2 thin section analysis reveals a spectacular ultracataclasite band, characterized by a darker colour than the surrounding rock that "injects" into preexisting cataclasites, thereby suggesting a prolonged, if not multiple, cataclastic activity. The granitic protolith is heavily reworked. Mechanical grinding and comminution generated a fine ultracataclasite with extremely angular and poorly sorted clasts.

Pectolite fills in later fractures and cavities that deform and affect both ultra- and cataclasites (Figure 5-58).

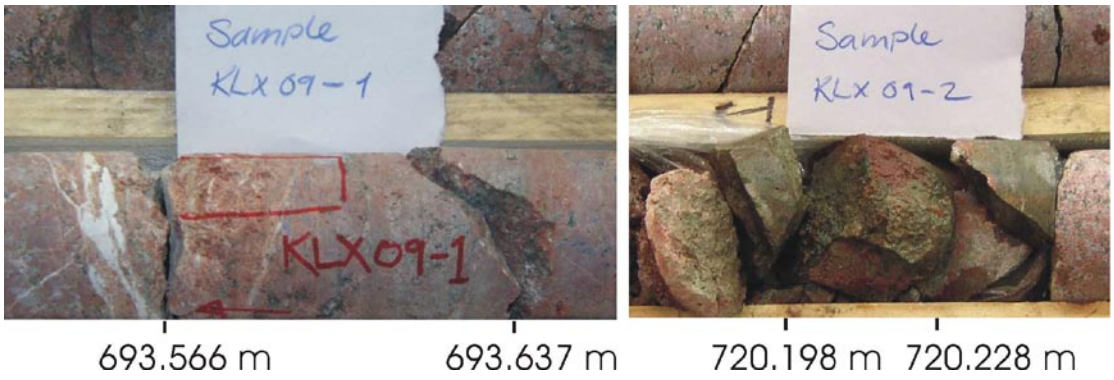

Figure 5-57. *Samples from DZ 4. KLX09-1 is of a porous cataclasite or cemented breccia, with cross cutting calcite veins. KLX09-2 is of a cataclasite with epidote or chlorite (green) matrix and fragments of granite (host rock), cataclasite and ultracataclasite.*

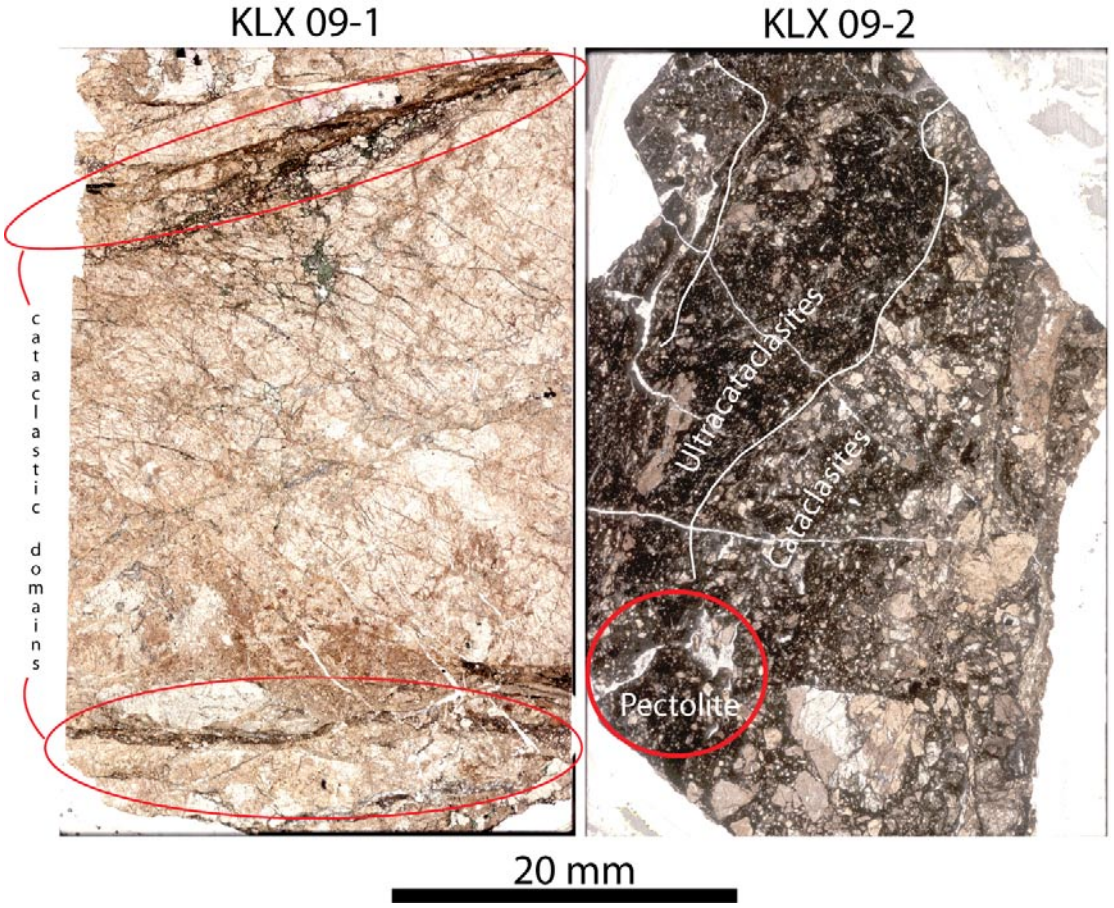

Figure 5-58. *Scanned thin sections of sample KLX09-1 (to the left) and KLX09-2 (to the right). KLX09-1 shows localized cataclasis characterized by significant grain size reduction and strain accommodation only within relatively narrow bands (circled in red). KLX09-2 is a spectacular cataclastic rock. A central ultracataclastic domain is recognized. It is characterized by darker colour, probably reflecting the fine grain size of the cataclasite matrix, and it "injects" and crosscuts a proto- to cataclastic sequence. The red circle shows later fractures infilled by pectolite.*

DZ 13 core is followed by a c. 2 m thick transition zone starting at depth 720.40 m. The zone is characterized by diffuse red staining and by the progressive decrease of the fracture frequency.

As mentioned above, DZ 13 is particularly rich in striated planes. The whole of our observations and kinematic analyses for the DZ is shown in Figure 5-59. A rather complex kinematic picture emerges from the analysis of the dataset, whereby there is clear indication of sets of both compressional and extensional faults. Given the relatively large number of fault planes, a preliminary kinematic analysis for DZ 13 was run. The analysis (strain inversion) of these meso-scale faults was carried out using so-called "paleostress analysis" techniques. The analysis of

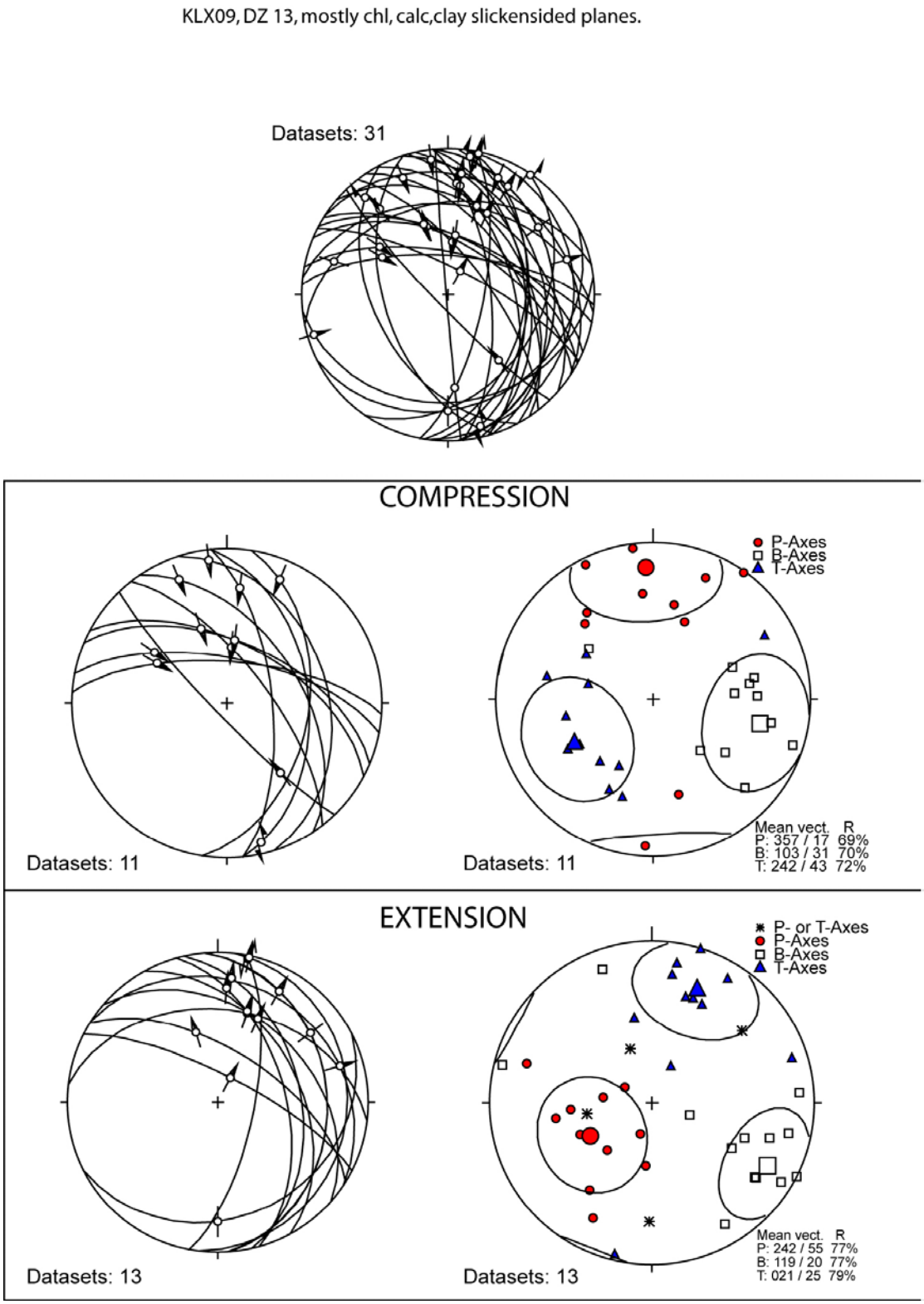

Figure 5-59. *Stress tensor analysis for the striated planes measured for DZ 13 in KLX09.*

fault slip data yields information concerning the orientation of the strain tensor. The aim of this procedure was 1) to determine if all fault movements are compatible with a single stress field and 2) to derive a "paleostress" tensor from the data that can be compared in future studies to regional fault patterns. The results of Figure 5-59 indicate that the measured fault surfaces can be assigned to two discrete faulting events, although no indication is provided as to their relative timing. A subhorizontal compression oriented roughly NS would account for the reverse faults measured in DZ 13 that strike from W-E to N-S and display systematically top-to-the-S, -SE reverse faulting. The extensional faults that strike from NW-SE to NS may instead have formed in response to a SW-NE-oriented extensional phase.

Table 5-12. Summary of DZ 13.

Depth (m)	Box number	Interpretation	Description
682.37	105	Transition zone	Increasing deformation and alternation in bedrock plus pervasive red staining. Fracture frequency up to 5–8 f/m. Bands of ultracataclasites/gouge arranged in networks. The total thickness of the zone is 39.6 m.
689.50	107	Fault core	Complex fault core with abundant fault rock occurrences and crush zones. 2 highly deformed zones 1) ~20 cm at ~690 m with distinct red gouge at the center. Sample KLX09-1; 2) ~25 cm at 720.20 m with distinct red gouge (possibly non-cohesive) and green ultracataclasite. Sample KLX09-2.
720.40	113	Transition zone	"Thin" transition zone with red staining and alternation in bedrock lithology.
721–722	113	Transition zone	Decreasing fracture frequency. Changes in lithology. Some ductile fabric. Occurrence of undeformed rock.

5.5.5 DZ 14: depth interval 744.50–760.50 m

DZ 14 begins with a transition zone characterized by an increase in the occurrence of cataclastic deformation bands and red staining. The DZ fault core begins at 754.50 m (Figure 5-60) and it contains two sub-zones: (1) subzone 1 contains brittle-ductile textures, and a sequence of cataclasites, ultracataclasites and protocataclasites. (2) Subzone 2, extending from 755.60 to 757.61 m depth, contains a crush zone and a highly fractured rock interval formed by cataclasites and/or ultracataclasites. A lower transition zone starts at depth 759 m and follows the section.

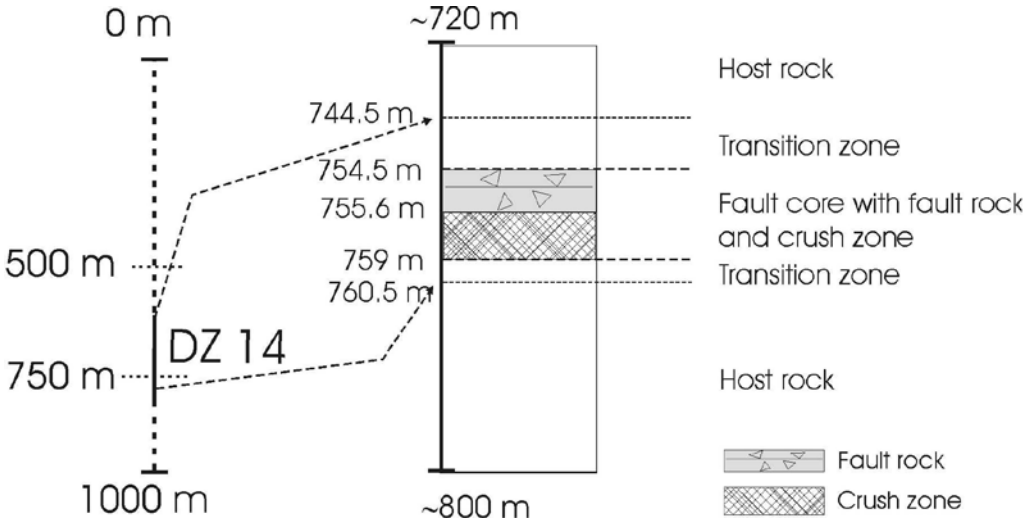

Figure 5-60. *Schematic log of DZ 14.*

Table 5-13. Summary of DZ 14.

Depth (m)	Box number	Interpretation	Description
744.50	118	Transition zone	Increasing deformation bands of cataclasites and red staining.
754.50	119	Fault core	Ductile-brittle fabrics, cataclastic products occurring in variable intensity. The thickness of the zone is 4.5 m.
		755.60–757.61	Crushed/highly fractured rock interval developed at the expense of cataclastic rocks.
759	119	Transition zone	

5.6 KLX10

KLX10 is located centrally in the Laxemar investigation area, where at the surface outcrop Ävrö granites. In this report we describe the structural logging of deformation zone DZ 9, which extends between 690.5 and 706 m depth /Carlsten et al. 2007b/. In this depth interval the core plunges 84° towards direction 268°.

5.6.1 DZ 9: depth interval 690.5–706 m

DZ 9 begins with an upper transition zone at 698.3 m characterized by a progressive increase of fracture frequency and the number of occurrences of cataclastic networks towards the deeper fault core (Figure 5-61).

Fractures are generally open with a systematic S/SSE dip direction (Figure 5-62). Discrete crush zones also occur within the highly fractured transition zones.

The DZ core begins at ~699 m depth. It is a remarkable core, c. 5 m thick, which consists of a complex sequence of fault rocks, varying from cataclasites to ultracataclasite and locally minor gouge occurrences. Due to the intense deformation and some core loss during recovery, we experienced major difficulties with the adjusted lengths of the observable structural features within the depth interval 699–704 m.

Figure 5-63 shows the complex structural features characteristic of the core, where there is evidence of several generations of cataclasites and ultracataclasites and mutual crosscutting relationships. Sample KLX10-1 was collected from the contact between a protocataclasite and an ultracataclasite. The black matrix in the thin section is extremely fine grained (hence the black colour) and is the equivalent to the grey-coloured matrix in the drill core (Figure 5-63). In this specific case, the transition from cataclasites to ultracataclasites is gradual and is likely to be the result of the progressive mechanical reworking of the protocataclasites. A second, lower transition zone follows the fault core and extends from 704.13 to 705.187 m depth.

The host rock that follows from depth 705.187 m has low fracture frequency, some localized red staining and a few, thin scattered cataclastic networks.

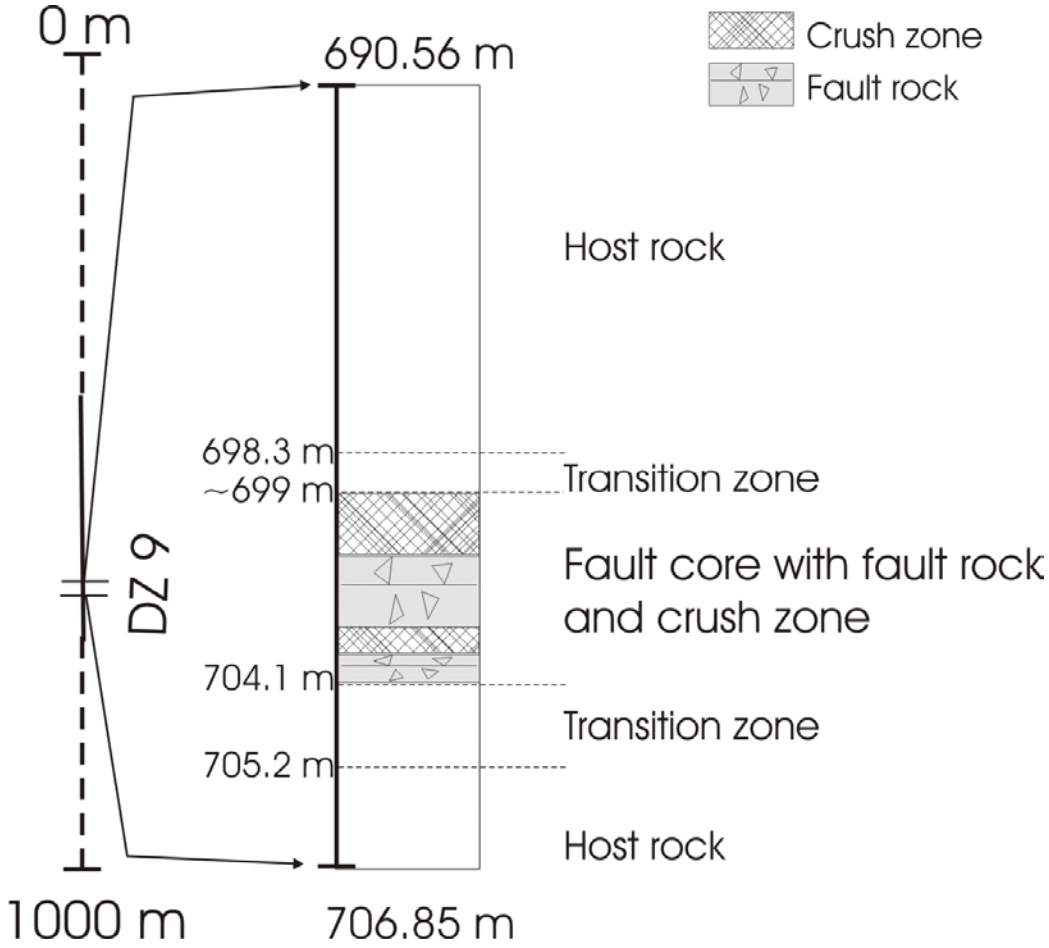

Figure 5-61. *DZ 9 of KLX10.*

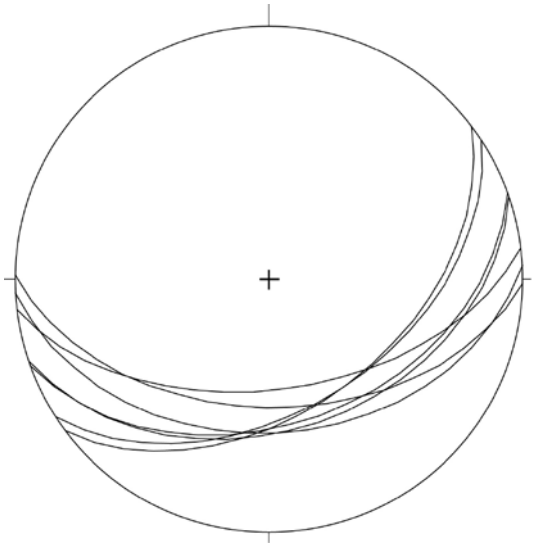

Figure 5-62. *Orientation of open fractures within the upper transition zone of DZ 9 in KLX10.*

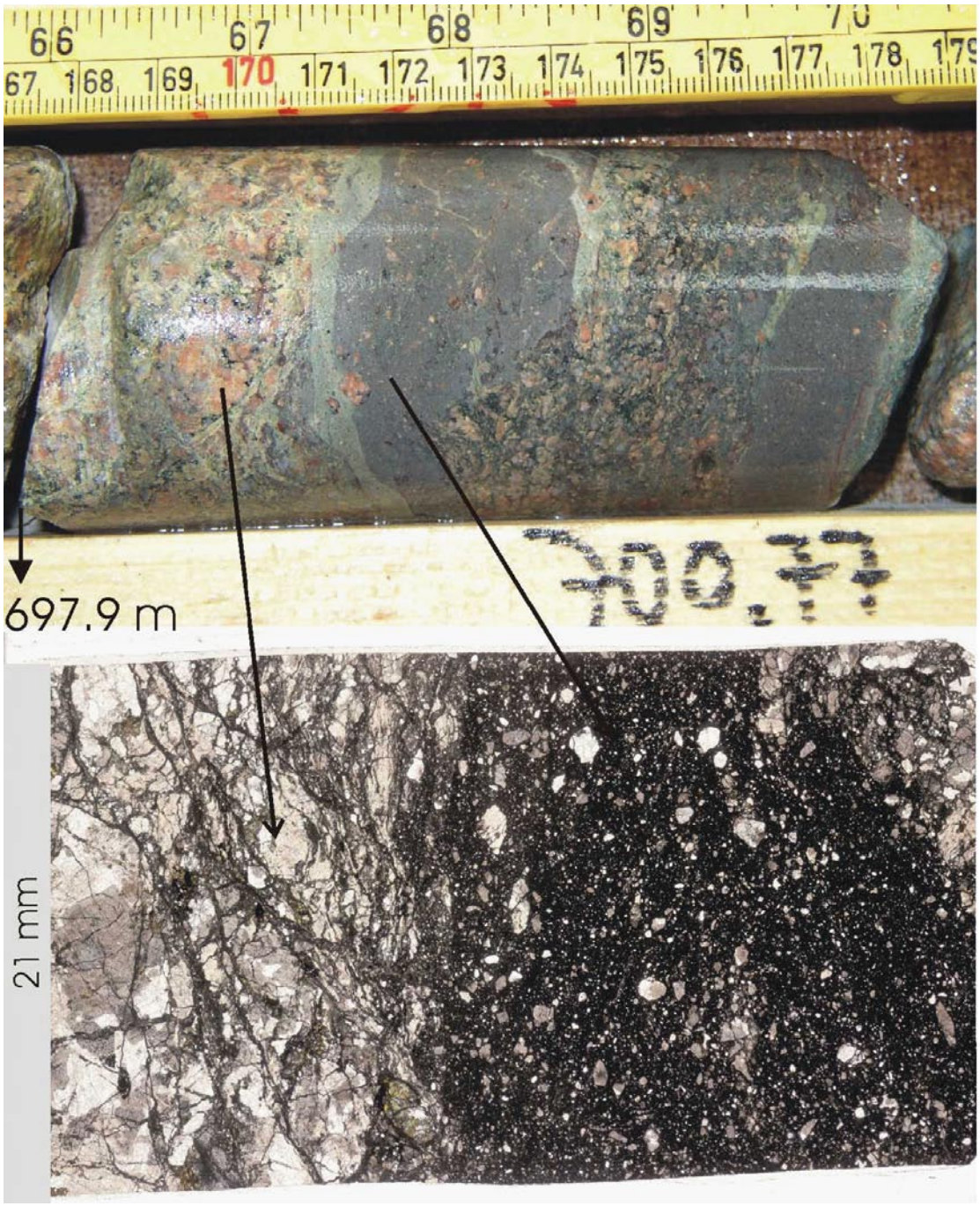

Figure 5-63. *Sample KLX10-1 from depth 697.9 m illustrates the existence of several generations of cataclasites and ultracataclasites, with the fine-grained (grey) ultracataclasite containing fragments of "older" cataclasites in turn formed at the expense of the hosting granite. The black matrix in the thin section is extremely fine grained (hence the black colour) and is the equivalent to the grey-coloured matrix in the drill core. The transition from the cataclasite to the left to the ultracataclasite to the right is gradual and is the result of the progressive mechanical reworking of the protocataclasites.*

Table 5-14. Summary of DZ 9.

Depth (m)	Box number	Interpretation	Description
690.56– 698.321	110–111	Host rock	Weak red staining.
698.321– ~699	111	Transition zone	Progressive increase in fracture frequency towards the fault core, and increase in the number of occurrences of cataclastic networks. The thickness of the zone is 6.85 m.
~699–704.13	111–112	Fault core	The core consists of a variety of fault rock products, from cataclastic networks to pc/c/uc and (minimal) gouge, plus crush zones. Sample – KLX10-1.
704.13–705.187	112	Transition zone	High fracture frequency.
705.187	112	Host rock	Low fracture frequency. Some red staining and occurrence of a cataclastic network.

5.7 KLX11A

The drill site is located in the westernmost part of the Laxemar investigation area in the quartz mozodiorite (Figure 5-1). The drill hole has a length of 992.29 m and is oriented 088/73 /Carlsten et al. 2007a/. Eighteen deformation zones (DZ 1-18; Figure 5-64) are described by the single-hole interpretation report /Carlsten et al. 2007a/ within KLX11A. During our study, however, only seven of those were positively identified as proper deformation zones (according to the general criteria listed in the introduction of this report; highlighted in red colour in Figure 5-64). The remaining deformation zones of the single-hole interpretation report /Carlsten et al. 2007a/ in our opinion do not fulfill the structural criteria to be classified as such, because, apart from the sporadic occurrence of very discrete, thin cataclastic/gouge bands, a few fractures and red staining, they are characterized predominantly by undeformed rock. In the following section we describe our main observations and conclusions for each of the eighteen zones described in the single-hole interpretation.

5.7.1 DZ 1: depth interval 142.25–142.9 m

The depth interval corresponding to DZ 1 of the single-hole interpretation /Carlsten et al. 2007a/ is characterized by generally undeformed granite, with only a few occurrences of thin bands of cataclasite. These mm- to cm-thick bands occur for example at depth 142.27 m, between 142.475 and 142.52 m, 142.61 and 142.62 m, 142.80 and 142.86 m and again between 142.96 and 142.97 m. Cataclasites are rich in epidote and are generally foliated, with foliation planes defining a sinuous, undulating planar fabric and forming anastomosing networks (Figure 5-65).

The transition from the undeformed host rock to the cataclastic bands is generally sharp and often coincides with open fractures coated by calcite, hematite and clay minerals. A gradual increase of red staining both above and below the cataclastic bands is also commonly observed. Foliation planes dip gently to the WSW (Figure 5-66). Unfortunately, no kinematics could be established for the foliated cataclasites. Due to the very localized and discrete character of these foliated cataclastic bands, we do not interpret DZ 1 as a significant deformation zone.

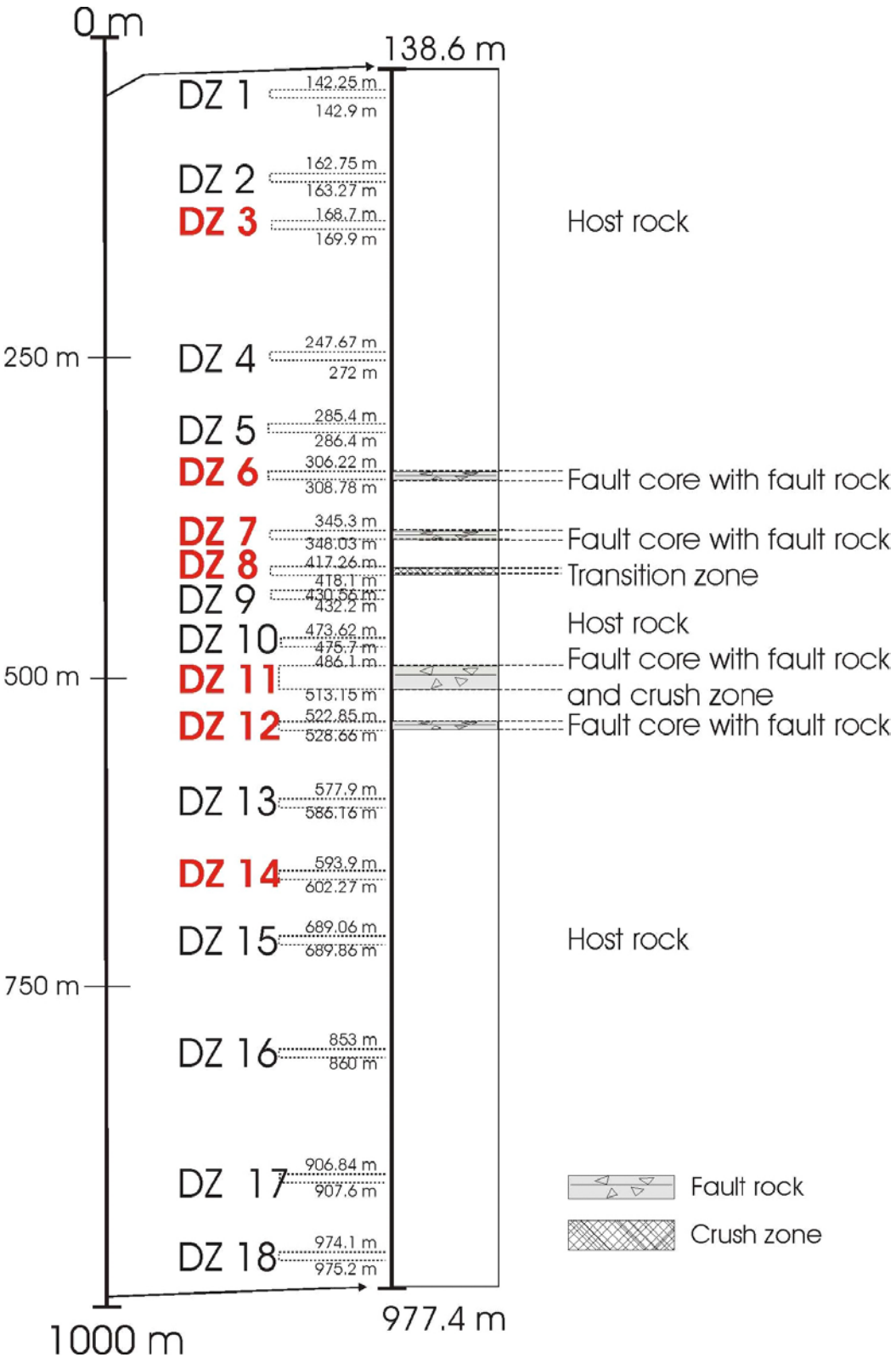

Figure 5-64. *Schematic illustration of the logged depth interval of KLX11A. In red are the depth intervals from the single-hole interpretation that we classify as proper deformation zones.*

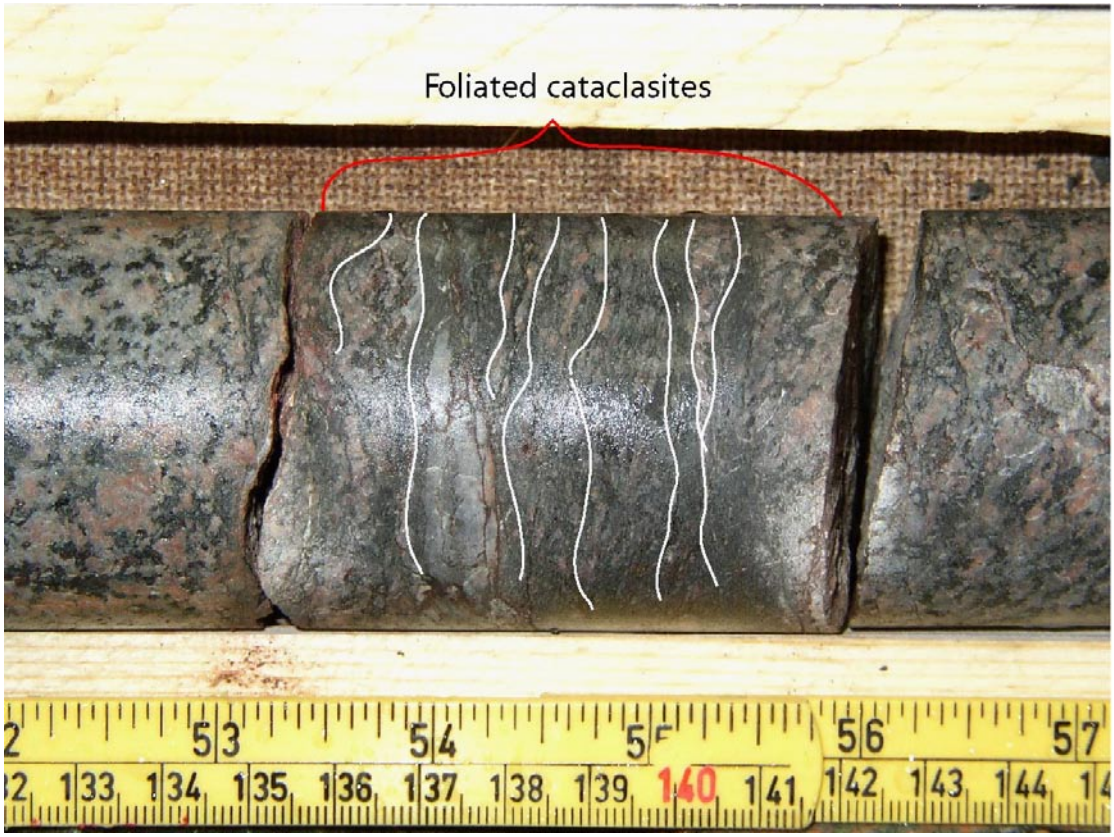

Figure 5-65. *Foliated cataclasites at depth 142.475 m in KLX11A.*

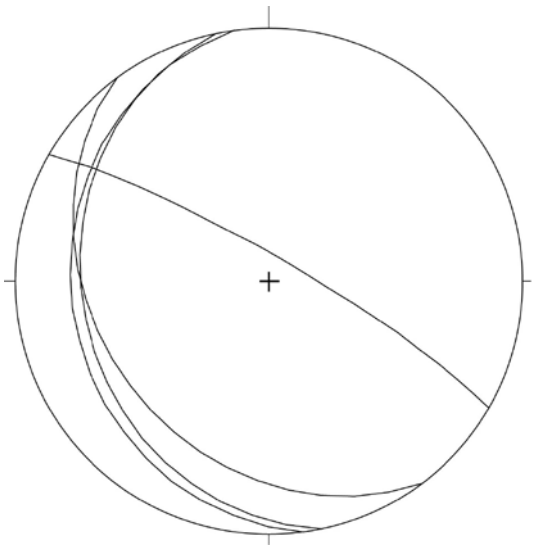

Figure 5-66. *Equal area projection, lower hemisphere stereonet of the orientation of foliated cataclasites in DZ 1 of KLX11A. The steep, NE-dipping great circle shows the orientation of an epidote-coated fracture at depth 143.399 m.*

Table 5-15. Summary of DZ1.

Depth (m)	Box number	Interpretation	Description
138.64 –144.17	8	Host rock	Undeformed rock with low fracture frequency. A few occurrences of foliated cataclastic bands. Localized red staining around the bands.

5.7.2 DZ 2: depth interval 162.75–163.27 m

Apart from the two slickensided planes shown in Figure 5-67, the depth interval corresponding to DZ 2 of the single-hole interpretation does not contain relevant structural features. In our opinion this section should not be classified as a deformation zone.

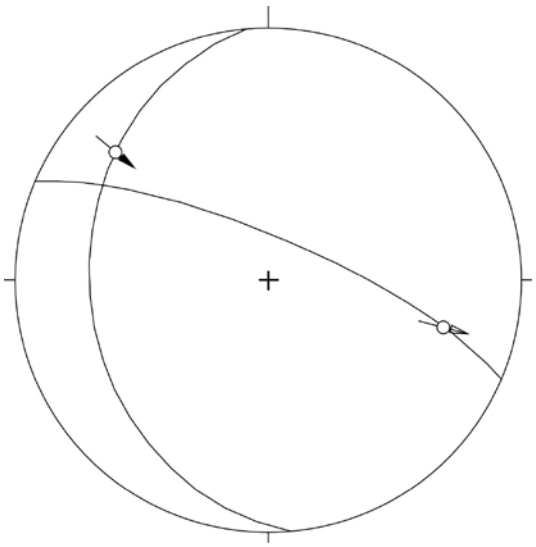

Figure 5-67. *Kinematically constrained planes found in DZ 2 of KLX11A. A W-dipping oblique thrust and a steep NE-dipping dextral transtensional fracture are the only structurally interesting features of DZ 2.*

Table 5-16. Summary of DZ 2.

Depth (m)	Box number	Interpretation	Description
160.77–171.70	12–13	Host rock	Undeformed rock with low fracture frequency. A few occurrences of cataclastic bands arranged spatially in anastomosing networks. Localized red staining around the bands in the section 168.20–169.79 m.

5.7.3 DZ 3: depth interval 168.7–169.9 m

This depth interval consists of fresh, practically undeformed rock, with the exception of one structurally interesting section of foliated granite from depth 169 m. The foliation strikes on average WSW/ENE and dips moderately northwest (Figure 5-68).

The zone is up to 1.5 m thick and is composed by cataclasite and/or ultracataclasite bands arranged in networks that also contain thin gouge layers. The section is characterized by diffuse red staining but also by a very discrete crush zone. The dilatant crush zone is very well seen in the BIPS image at the contact with a crosscutting coarse-grained granite dike. The zone is ~10 cm thick (196.70–169.80 m) and is developed at the expense of one of the cataclastic networks. Thin gouge strands/bands occur at the marginal contact to the pristine undeformed rock. Due to the foliated granites, the overprinting cataclasites and the prominent crush zone, DZ 3 is considered to be a real deformation zone.

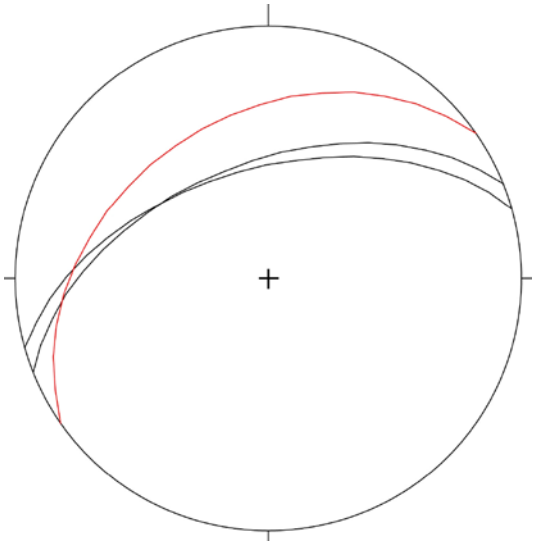

Figure 5-68. *Black great circles represent the orientation of foliated granites in DZ 3, whereas the red great circle is a thin cataclastic band at adjusted depth 168.772 m.*

Table 5-17. Summary of DZ 3.

Depth (m)	Box number	Interpretation	Description
168.7–169.9 m	13	Weak deformation zone	Undeformed rock with low fracture frequency containing a 1.5 m thick, NW-dipping interval of foliated granite. 10 cm-thick crush zone at depth 196.70 mm overprinting a cataclastic sealed network.

5.7.4 DZ 4: depth interval 247.67–272 m

This section shows pervasive red staining throughout. Long and steep, undulating shear fractures with a NNE-SSW trend (Figure 5-69) occur within the upper part of the section and, when open, are generally coated by hematite, chlorite and calcite.

They exploit an older sealed network of calcite and epidote veins (Figure 5-70). At depth 263.83 m there occurs a lithological change from granite to fine-grained dolerite, which extends down to depth 267.698 m. The contact is oriented 196/05. A crush zone affects the dolerite in the depth interval 265.597–266.127 m. Its upper contact dips subhorizontally to the E, whereas the lower dips gently to the SW (Figure 5-69).

Within the fine-grained dolerite there are a few thin, discrete faults, subparallel to the open fractures observed in the upper part of the section that offset small-scale granitic enclaves trapped within the dolerite. This section is not interpreted here as a deformation zone. No definable core or transition zone can be identified and no significant and systematic increase in fractures frequency is observed towards the crush zone.

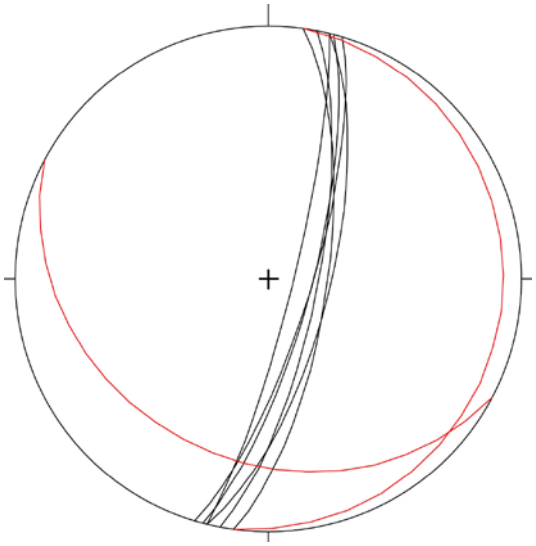

Figure 5-69. *Orientation of the steep fractures that characterize the upper part of DZ 4 in KLX11A (black great circles) and of the upper and lower contact (subhorizontal and gently dipping, respectively) of the crush zone in the fine-grained dolerite at depth 265.597 m.*

Figure 5-70. *Steep open fracture exploiting a pre-existing sealed network of epidote veins.*

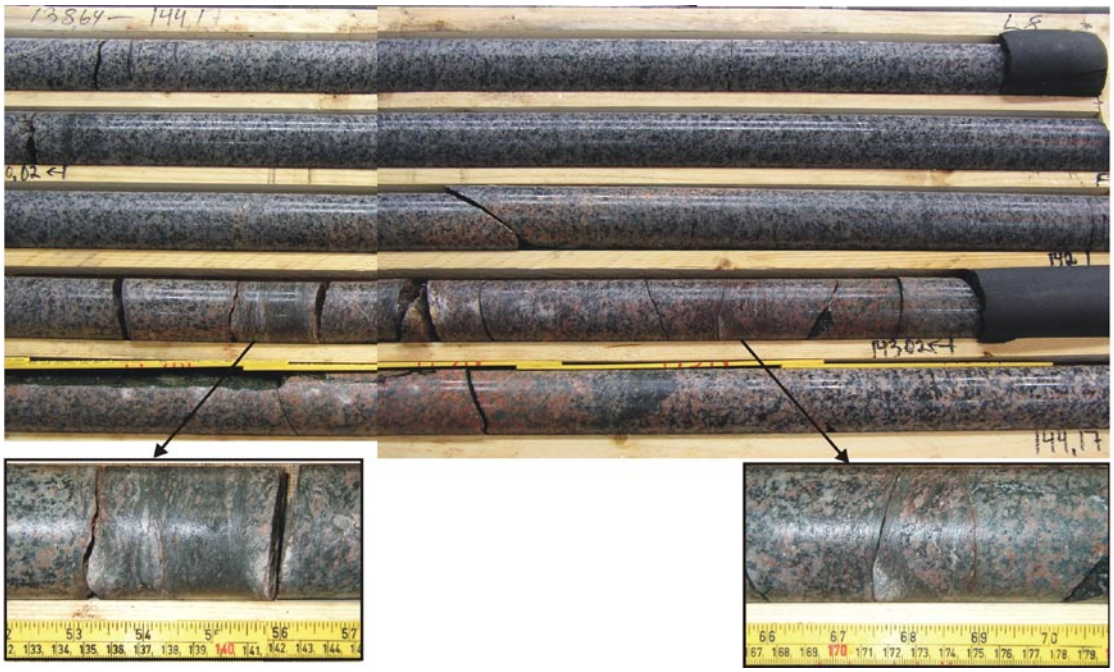

Figure 5-71. KLX11A 143 m.

Table 5-18. Summary of DZ 4.

Depth (m)	Box number	Interpretation	Description
244.5–271.58	27–31	Host rock	Undeformed rock with low fracture frequency, mostly related to steep, NNE/SSW striking fractures. Red staining throughout the section. Crush zone at depth 265.597–266.127 m.

5.7.5 DZ 5: depth interval 285.4–286.4 m

The inspected section does not contain any significant structural feature and is therefore not considered a deformation zone.

Table 5-19. Summary of DZ 5.

Depth (m)	Box number	Interpretation	Description
282.81–288.07	34	Host rock	Undeformed rock with low fracture frequency. Fractures are not systematic.

5.7.6 DZ 6: depth interval 306.22–308.78 m

DZ 6 is a thin, weak deformation zone (2–2.5 m thick) containing a weakly foliated cataclasite (~6 cm thick, Figure 5-72) oriented 209/34 and a 25–30 cm thick crush zone (crush zone upper limit orientation 233/35; lower limit 046/41). The latter occurs at a lithological contact between the Ävrö granite and a microgranitic dike. There is pervasive red staining throughout this section.

Figure 5-72. Foliated cataclasite in DZ 6.

Table 5-20. Summary of DZ6.

Depth (m)	Box number	Interpretation	Description
305.18–306.07	38	Host rock	Undeformed rock with low fracture frequency.
306.07–308.82	38	Fault core	Small zone (6 cm) of fault rock, cataclasite, and crushed rock (25–30 cm). The fault core occurs at a lithological contact between Ävrö granite and a microgranite dike.
308.82–310.56	38	Host rock	Undeformed rock with low fracture frequency.

5.7.7 DZ 7: depth interval 345.3–348.03 m

DZ 7 has a well-defined fault core characterized by thin, discrete bands of cataclasites and anastomosing networks of cataclasite/ultracataclasite and gouge bands (Figure 5-73). The fault core extends from depth 346.21 m to 346.69 m. Cataclasites are red-brown in colour and are alternated with gouge bands from mm to cm thick (up to a maximum of 3 cm; Figure 5-73).

The central part of the deformation zone core is defined by an epidote-rich cataclasite/ultracataclasite (~10 cm thick) oriented 220/49. Figure 5-74 shows the scanned thin section of sample KLX11A-1, an epidote-rich cataclasite collected from the core of the deformation zone. The upper part of the image (with part of it enlarged in the microphotograph to the right) shows a strongly fractured portion of the host rock. The microphotograph to the right shows that the host rock is made up of foliated, intensively recrystallised quartz-feldspars granitoids, thus suggesting the existence of a precursor ductile fabric. The intense fracturing process led to dilation and rigid body rotation of individual fragments. Dilatant openings are infilled by carbonates. The lower part of the scanned thin section contains a proper cataclasite, with an epidote-rich, fine-grained matrix and poorly sorted clasts of the host rock floating in it. The contact to the fractured host rock is sharp and truncates the carbonate-infilled veins, although observations at large magnification reveal that the carbonates are in part smeared along the sharp contact, thus suggesting a possible syn-cataclasis genesis of the carbonates. Similar dilatant fractures with calcite are also present in the main cataclasite. Red staining occurs pervasively throughout the core.

DZ 7 is asymmetric as far as strain distribution with respect to the central fault core is concerned, because no obvious transition zone exists above the core. Below it, however, pervasive red staining and several steep fractures striking NE/SW (Figure 5-75) define a proper transition zone to undeformed host rock.

Figure 5-73. *Detail of the network of proto-, ultra-cataclasites and gouge bands in the core of DZ 7 of KLX11A. Mechanical comminution has generated extremely fine-grained clasts. The cataclastic band is oriented 259/63.*

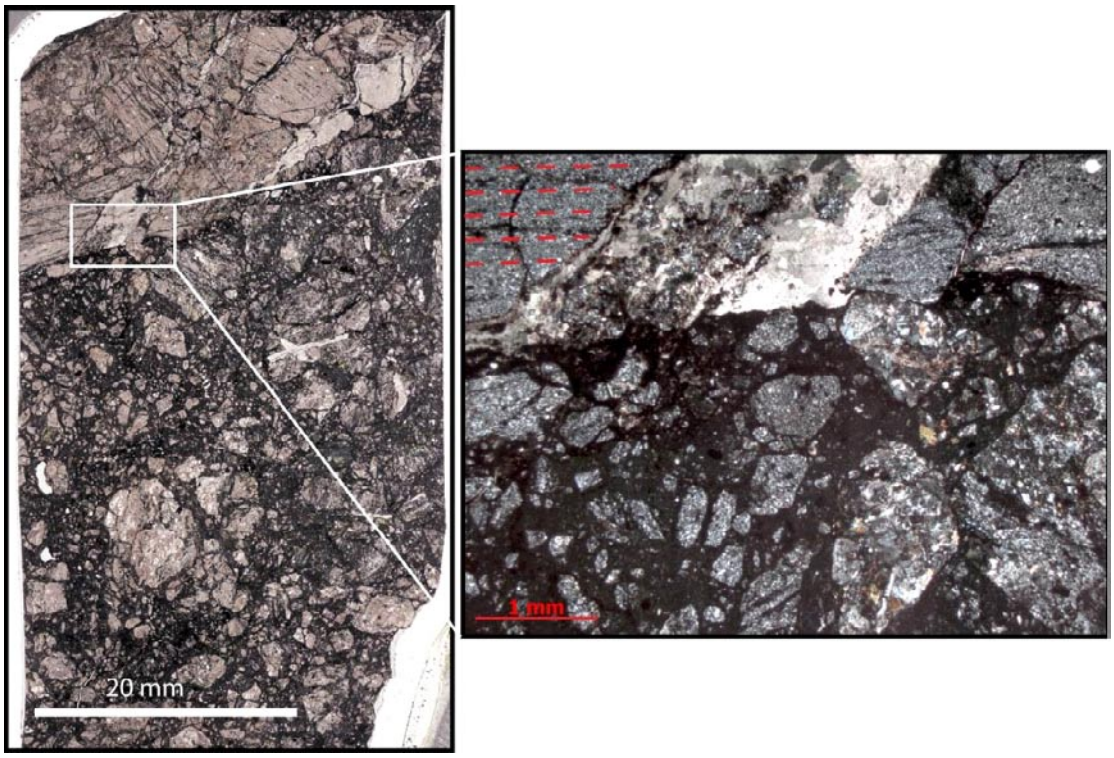

Figure 5-74. *Left: Scanned thin section of sample KLX11A-1, showing a classic cataclasite formed by an epidote-rich fine-grained matrix and poorly sorted, angular clasts of the host rock. Right: Detail of the sharp contact between the cataclasite and the strongly fractured host rock. The host rock, apart from carbonate infilled dilatant veins, is made off by foliated, strongly recrystallised quartz-feldspar metagranitoids. The dashed red lines highlight the pervasive foliation in the fractured host rock.*

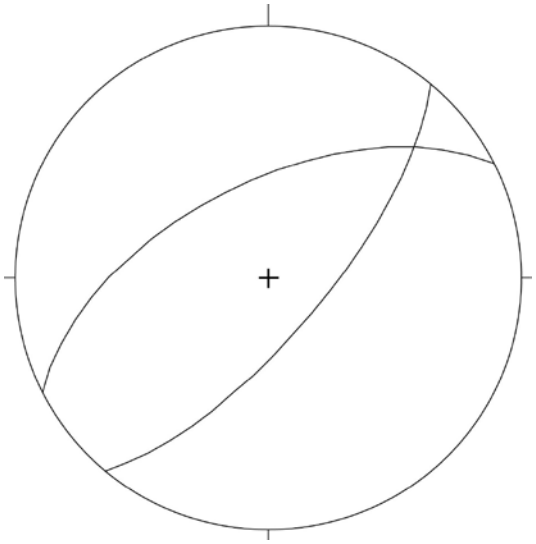

Figure 5-75. *Orientation of selected fractures in the transition zone of DZ7.*

Table 5-21. Summary of DZ 7.

Depth (m)	Box number	Interpretation	Description
344.02–346.21	45	Host rock	Undeformed rock with low fracture frequency. Red staining.
346.21–346.69	45	Fault core	Thin zone (3 cm) of epidote-rich cataclasites (see thin section KLX11A-1). Networks of cataclasites/ ultracataclasites/gouge and epidote veins.
346.69–348.04	45	Transition zone	Red staining. Steep NW/SE open fractures.
348.04–349.35		Host rock	Undeformed rock with low fracture frequency.

5.7.8 DZ 8: depth interval 417.26–418.1 m

DZ 8 is characterized by thoroughgoing red staining and networks of epidote-rich cataclastic domains similar to those observed in DZ 7. A thin crush zone is found at depth 417.991 m, it extends down to 417.99 m and defines the centre of this deformation zone at 417.91 to 417.99 m (Figure 5-76). The crush zone contains a slickensided plane that dips to the S and has top-to-the-N kinematics (Figure 5-77).

Figure 5-76. *The crush zone shown in the picture is the most interesting structural feature of DZ 8. It dips to the south, as shown in Figure 5-77.*

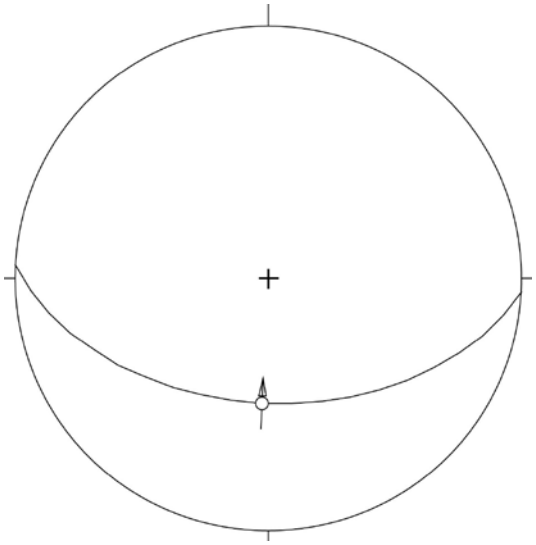

Figure 5-77. *Fault slip data for a slickensided surface associated with a prominent crush zone at depth 417.991 in DZ 8.*

Table 5-22. Summary of DZ 8.

Depth (m)	Box number	Interpretation	Description
411.87–417.27	57	Host rock	Undeformed rock with low fracture frequency.
417.27–418.1	57–58	Transition zone	Red staining and a network of epidote veins.
418.1–423.39	58	Host rock	Undeformed rock with low fracture frequency.

5.7.9 DZ 9: depth interval 430.56–432.2 m

This section is not a deformation zone. The depth interval contains interfingering leucogranites and quartz monzonites to monzodiorites /Carlsten et al. 2007a/.

Table 5-23. Summary of DZ 9.

Depth (m)	Box number	Interpretation	Description
428.99–434.68	60	Host rock	Undeformed rock with low fracture frequency.

5.7.10 DZ 10: depth interval 473.62–475.7 m

This depth interval does not contain a deformation zone, but only a lithological contact at depth 475.117 m between monzogranite and fine-grained dolerite and back to granite at depth 475.687 m.

Table 5-24. Summary of DZ 10.

Depth (m)	Box number	Interpretation	Description
468.65–479.93	67–68	Host rock	Undeformed rock with low fracture frequency. Lithological changes at depth 475.117–475.687 m from monzogranite/granite to fine-grained dolerite and again granite.

5.7.11 DZ 11: depth interval 486.1–513.15 m

This depth interval contains an asymmetric deformation zone (due to the lack of a well-defined transition zone below the core) with a distinct fault core defined by fault rock occurrences and a highly fractured rock interval. The deformation zone is entirely developed in granites and is accompanied by pervasive red staining (Figure 5-78).

The first 20 to 25 m of the section do not present structurally interesting features, with non-systematic fractures and a generally low fracture frequency. A well-defined transition zone starts at depth 502.13 m and extends down to 509.003 m. Fracture frequency increases progressively and there are numerous occurrences of thin bands and networks of cataclasites, ultracataclasites and epidote veins. Fractures dip gently to moderately to the E, SE, S and SW (Figure 5-79a). There occurs also a steep NNW trending epidote, calcite and phrenite-coated fracture.

The fault core, located at depth interval 509.003 to 510.710 m, consists predominantly of fault rocks such as protocataclasites to cataclasites and bands of ultracataclasites and gouge. It contains numerous broken fractures, with millimetric apertures, and several striated planes (Figure 5-80).

The orientation of the fractures measured in the core is in general agreement with that of the fractures in the transition zone and defines a set of conjugate fractures striking roughly NW/SE and with antithetic dip direction to the NE and SW (Figure 5-79b). A steep transtensional dextral fracture is oriented similarly to the steep epidote-coated fracture measured in the transition zone and likely overprints the conjugate set. The DZ core terminates with a zone of crushed rock and c. 15 cm of core loss. The core has a sharp lower contact to the host rock, characterized by red staining.

Figure 5-78. *Overview of the core of DZ 11.*

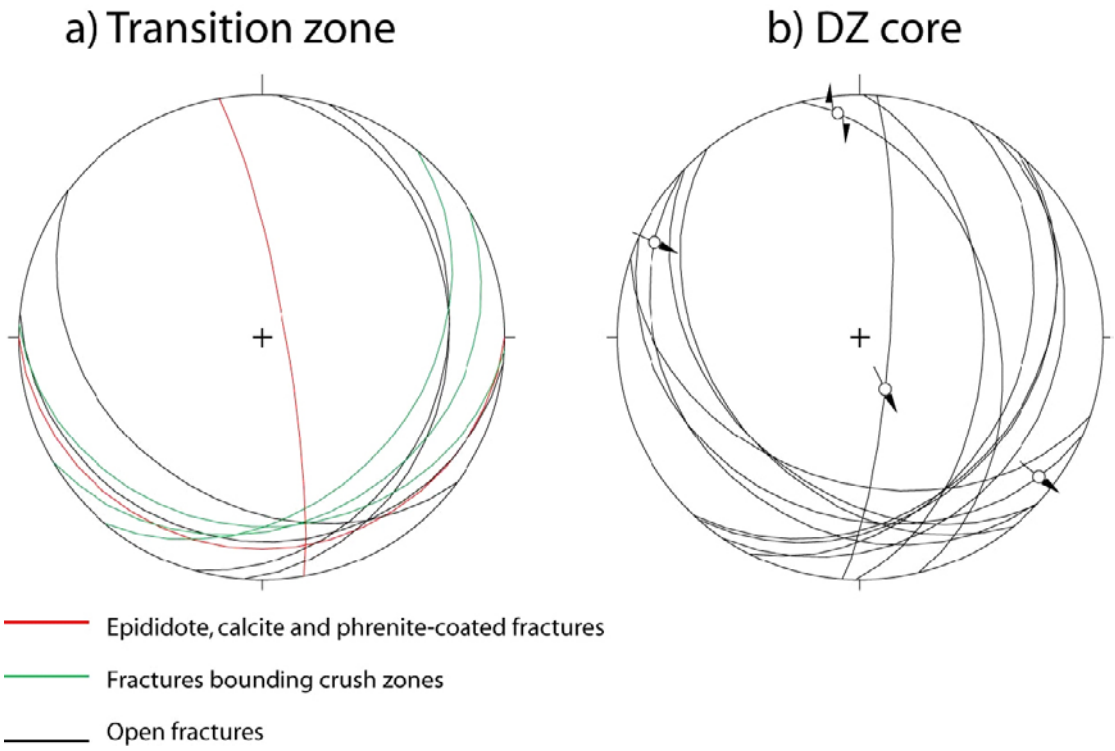

Figure 5-79. *Orientation of fractures for the transition zone (a) and the core (b) of DZ 11. 4 striated planes were constrained kinematically.*

Figure 5-80. *Detail of the deformation zone core. Note the protocataclastic nature of the granite and the numerous epidote and calcite-coated broken fractures.*

Table 5-25. Summary of DZ 11.

Depth (m)	Box number	Interpretation	Description
479.93–502.13	69–73	Host rock	Undeformed rock with low fracture frequency.
502.13–509.003	73–74	Transition zone	Transition zone at 503.13–509.003 m defined by increasing fracture frequency and occurrence of bands/network/strands of cataclasites/ultracata-clasites and epidote veins. A thin crush zone also occurs.
509.003–510.71	74	Fault core	Brittle core defined by abundant fault products (protocataclasites, cataclasites and bands of gouge). The core ends at a crush zone, which caused c. 15 cm core loss during core recovery. Several slickensided planes. Set of c. NE/SW striking conjugate fractures.
510.71–517.34	74–75	Host rock	Sharp contact to host rock with some red staining and farther below undeformed rock.

5.7.12 DZ 12: depth interval 522.85–528.66 m

This depth interval contains a c. 6 m thick fine-grained, foliated quartz monzodiorite that intrudes otherwise undeformed granites. The quartz monzodiorite hosts a distinct brittle-ductile core between depths 525.269 and 525.691 m.

The boundaries to the deformation zone core are sharp, both above and below. The core itself is ~45 cm thick and made by intensively foliated and gently crenulated quartz monzodiorites. The core is strongly fractured (Figure 5-83a); the fractures are, however, not visible in the BIPS images of the corresponding depth interval, possibly suggesting that they may have been produced by the drilling and recovery process. Foliation planes dip gently to moderately to the S (Figure 5-82). Samples KLX11A-3 and KLX11A-4 were collected in order to investigate the characteristics of this deformation zone (Figure 5-83b and d). Thin section analysis revealed that what was initially interpreted as foliated cataclasites is actually only a package of foliated, and gently crenulated (Figure 5-83c and d) quartz monzodiorites. There is no sign of penetrative cataclasis. They are separated from the undeformed granite by a thin ultracataclastic layer (Figure 5-83e and f) and its associated chlorite-decorated fractures. Later quartz-filled fractures crosscut the ultracataclasites (Figure 5-83e). It is not obvious what actually localized the brittle core within the foliated quartz monzodiorites.

Figure 5-81. *Highly fractured brittle core in DZ 12. The core is located in a pervasively foliated quartz monzodiorite.*

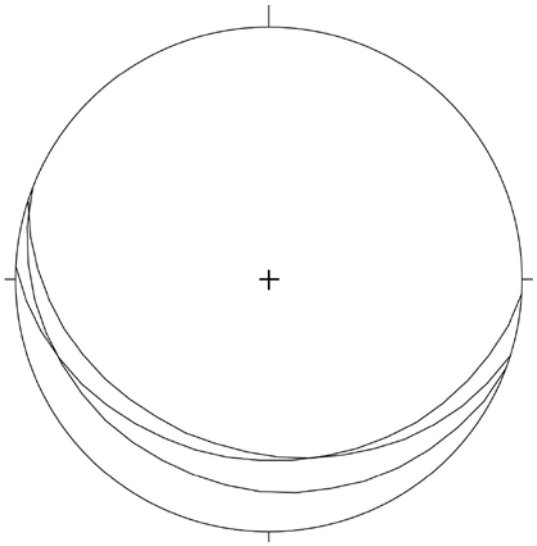

Figure 5-82. *Orientation of selected foliated cataclasites in the core of DZ 12.*

Table 5-26. Summary of DZ 12.

Depth (m)	Box number	Interpretation	Description
517.34–525.269	76–77	Host rock	Undeformed rock with low fracture frequency. Lithological change from granite to quartz monzodiorite (foliated) at ~521 m.
525.269–525.691	77	Fault core	The core itself is ~45 cm and consists of S-dipping foliated quartz monzodiorite. Numerous fractures overprint the foliated rock but are not observed in the BIPS images for the same depth interval.
525.691–532	77–78	Host rock	Sharp contact from the DZ brittle core to foliated quartz monzodiorites. Lithological change from foliated quartz monzodiorite to undeformed granite at ~527 m.

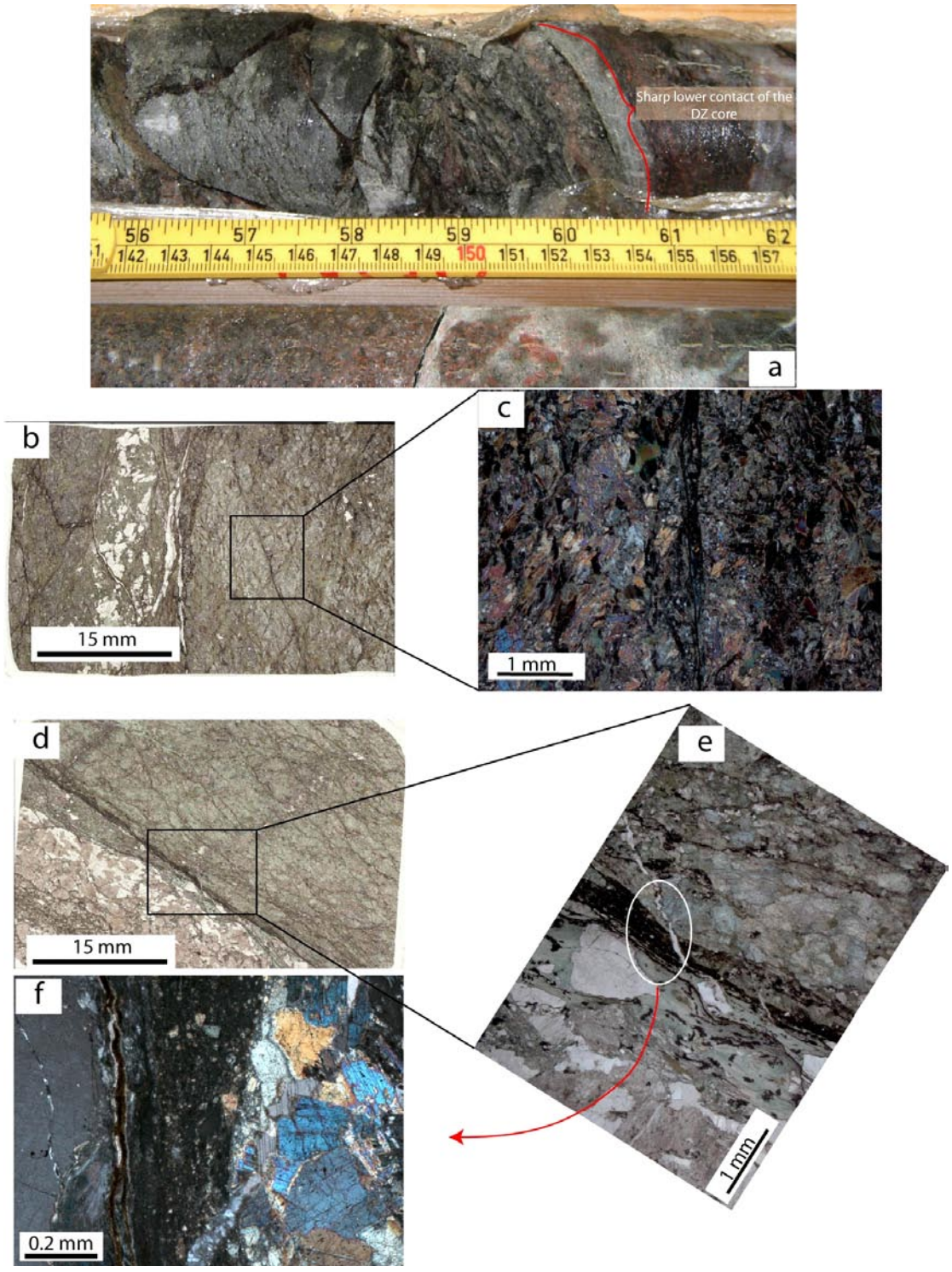

Figure 5-83. *(a): Detail of the sharp transition between the foliated and brittly overprinted quartz monzodiorites and the host rock. (b): Scanned thin section of sample KLX11A 3. The sample comes from the core of the DZ. Although logged as a core of foliated cataclasites, microscopic investigation has excluded the presence of foliated cataclasites. (c): Detail of the texture of the foliated and slightly crenulated quartz monzodiorite. Thin fractures, coated by epidote and chlorite, are common and impart a disjunctive foliation to the rock. (d): Scanned thin section of sample KLX11A-4. It shows the transition between the foliated quartz monzodiorite and the undeformed granite. The contact is very sharp and is defined by a very thin ultracataclastic band. (e) Detail of the thin ultracataclasite. A late generation of quartz-filled fractures crosscuts the ultracataclasite. (f): Blow up of the ultracataclasite to illustrate the extremely fine-grained nature of the rock.*

5.7.13 DZ 13: depth interval 577.9–586.16 m

This section is not interpreted as a deformation zone, although red staining is pervasive through it. It does not contain particularly relevant structural features except for two highly fractured intervals (depth 579.644 and 582.859 m, Figure 5-84) and a few discrete, narrow bands of epidote at depth 580.570 m (Figure 5-85), 582.86 m, 582.859 m and at 582.97 m.

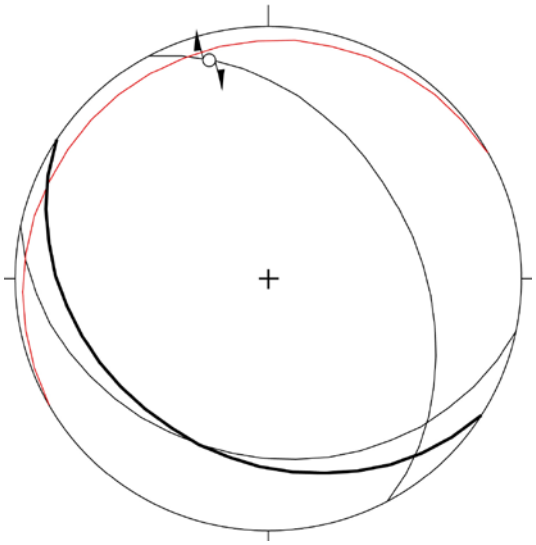

Figure 5-84. *Red great circle: orientation of the epidote band shown in Figure 5-85. Black great circle: orientation of the upper contact of a c. 20 cm thick crush zone at depth 579.644. Bold black circle: orientation of a second crush zone at depth 582.859. The slightly transpressional dextral striated epidote-coated surface is located at depth 579.223.*

Figure 5-85. *Epidote-rich band at depth 580.570 m, with a thin quartz vein in the middle. The band is oriented 240/07.*

Table 5-27. Summary of DZ 13.

Depth (m)	Box number	Interpretation	Description
576.15–586.56	87–88	Host rock	Undeformed rock with low fracture frequency. Sporadic occurrence of epidote bands with possible fault rock, especially at depth 582.86 m (orientation 154/66), 582.859 m (orientation 123/30) and at 582.97 m. Two minor crush zones at depth 579.644 and 582.859 m.
581.85–586.12	88		Pervasive red staining.

5.7.14 DZ 14: depth interval 593.9–602.27 m

This section is characterized by the presence of a penetratively foliated ductile core. At depth 597.72 m there occurs a lithological contact between the undeformed, yet red-stained, Ävrö granite and strongly foliated quartzdiorites and monzonites interfingered with thin granitic layers (Figure 5-86). The ductile foliation trends on average NS and dips gently to the west (Figure 5-87). It is suggested that the foliated portion of the section forms a ductile deformation zone core. There is however evidence of a distinct brittle deformation event that overprints the ductile fabric (for example Figure 5-86). Cataclasites and gouge in thin, mm to cm-thick bands are widespread in the remaining part of the section. The thin bands of brittle fault rock form a brittle core, whose transition zone is characterized by an interval of red staining between depths 598.17 and 599.07 m.

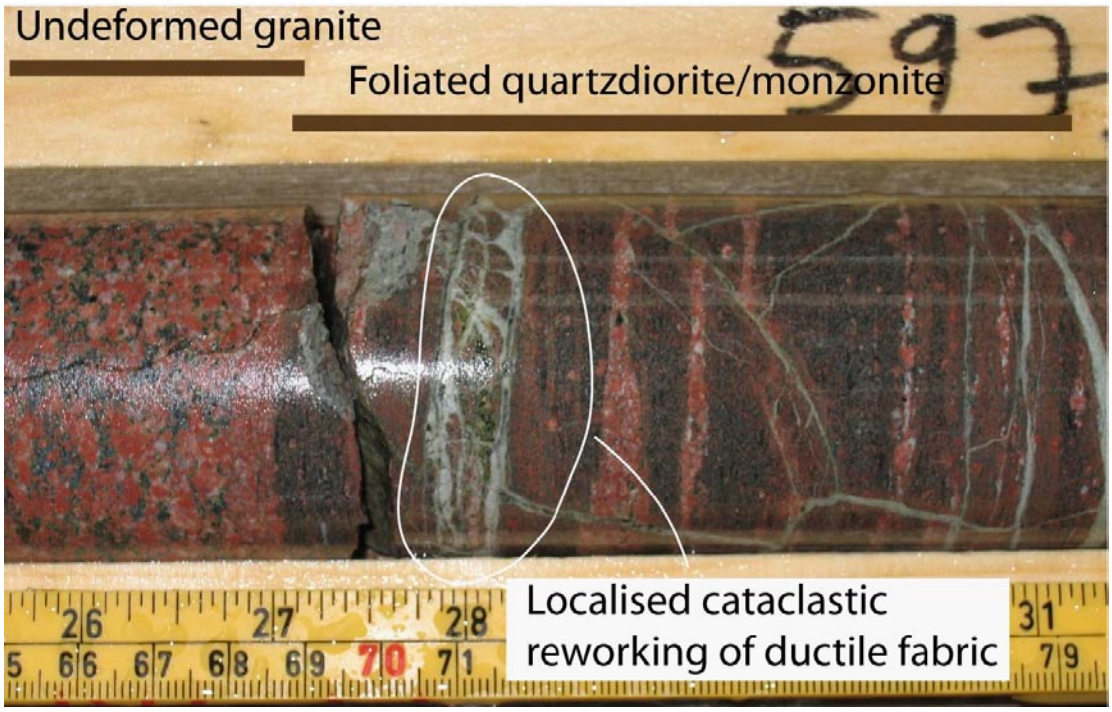

Figure 5-86. *Sharp contact between undeformed granite above and strongly foliated quartzdiorite/monzonite below. The ductile, foliated core is locally reworked by brittle, cataclastic deformation.*

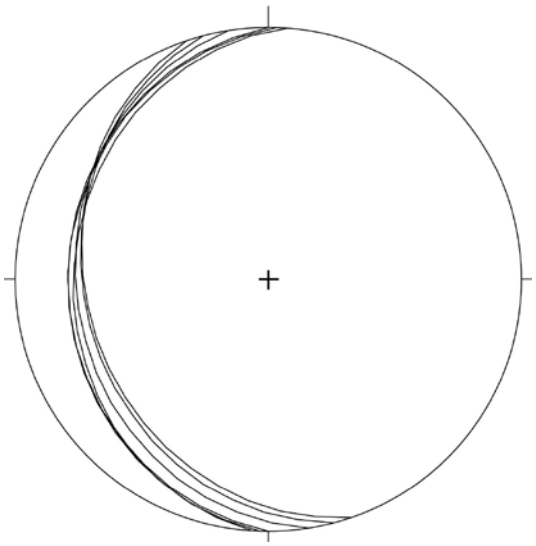

Figure 5-87. *Orientation of the pervasive foliation within the ductile core of DZ 14.*

The scanned thin section image of Figure 5-88a shows in detail some of the structural characteristics of the later brittle reworking of the pervasive foliation. The foliation, defined by aligned amphiboles, is crosscut by a "feeder" calcite and phrenite vein that, in the upper part of the thin section (also visible in Figure 5-86), leads to dilation and brecciation in a direction parallel to the foliation. The interpretation is that of an overpressured fluid phase that injects the host rock but locally exploits the mechanical anisotropy of the preexisting ductile foliation to generate "sill-type" hydrofracturing, causing dilation and disruption of the existing foliated quartzdiorites and monzonites in bands subparallel to the foliation itself.

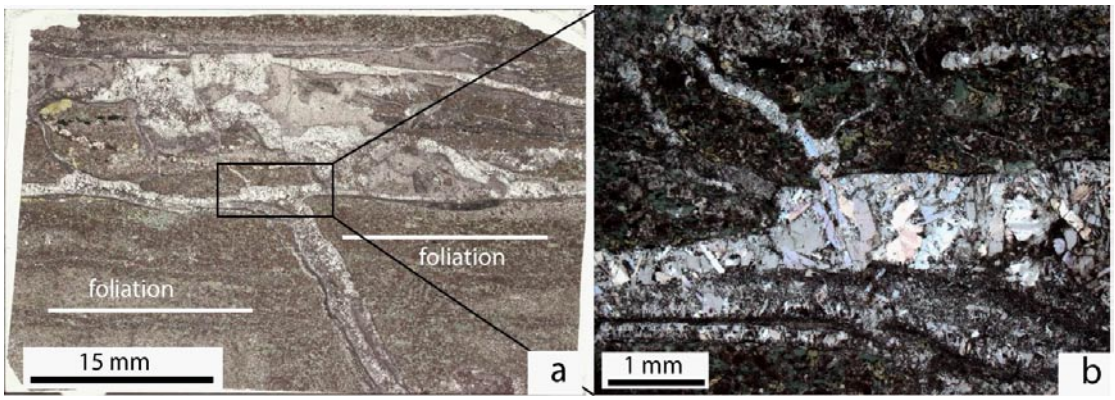

Figure 5-88. *(a) An overpressured fluid phase injected discordantly the foliated host rock and caused disruption and brecciation in a band parallel to the foliation. (b). Pectolite fills one of the dilatant veins parallel to the foliation, defined predominantly by plagioclase and amphibole.*

Table 5-28. Summary of DZ 14.

Depth (m)	Box number	Interpretation	Description
592.07–598.17	90	Host rock	Undeformed rock with low fracture frequency.
598.17–599.07	90–91		Red staining.
597.706–602.28	91	Ductile deformation zone core overprinted by discrete brittle features.	Lithological change from granite to foliated quartzdiorites and monzonites and back to granite. Phrenite, calcite and epidote veins led to localized hydrofracturing and disruption of the foliated host rock in bands parallel to the foliation.
602.28–602.90	91	Host rock	Undeformed granite with low fracture frequency.

5.7.15 DZ 15: depth interval 689.06–689.86 m

This depth interval is characterized by diffuse red staining and localized networks and thin bands of cataclasites and ultracataclasites. At depth 689.626 m there occurs a significant example of intense cataclasis, expressed by a mesh of extremely fine-grained black ultracataclasites containing angular clasts of the surrounding red granites and of earlier epidote-rich cataclasites (Figure 5-89).

Thin section KLX11A-5 was studied in order to further investigate the composition and the characteristics of the fine-grained dark ultracataclastic matrix. Figure 5-90a shows an image of the scanned thin section. The contact between the cataclasite and the host Ävrö granite is very sharp. Mechanical grinding and comminution generated a fine ultracataclasite with extremely angular and poorly sorted clasts. The study of the thin section has, however, revealed that the dark fine-grained matrix of the ultracataclasite does not reflect the usually observed composition of epidote-dominated cataclasites observed in many cores, but is instead formed by low-temperature (zeolite facies) fluid–related babingtonite and pectolite (Figure 5-90b, c and d). Babingtonite is a calcium-iron-manganese inosilicate mineral with the formula $Ca_2(Fe,Mn)FeSi_5O_{14}(OH)$.

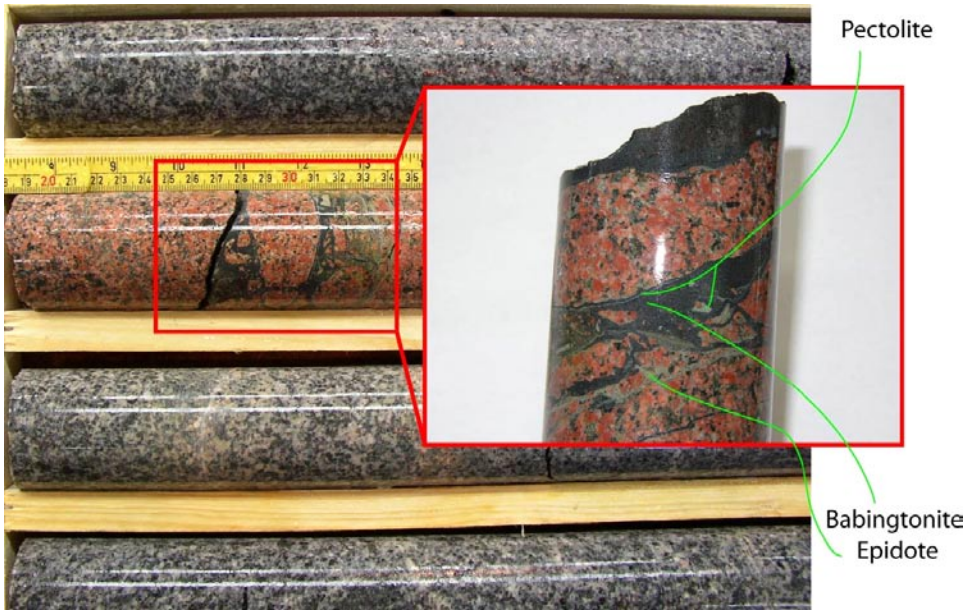

Figure 5-89. *Cataclastic network at depth 689.626 m. Thin section analysis has revealed that the dark, fine-grained ultracataclasite matrix is composed of babingtonite and pectolite, which replaced the initial matrix during a post-cataclasis phase of hydrothermal activity.*

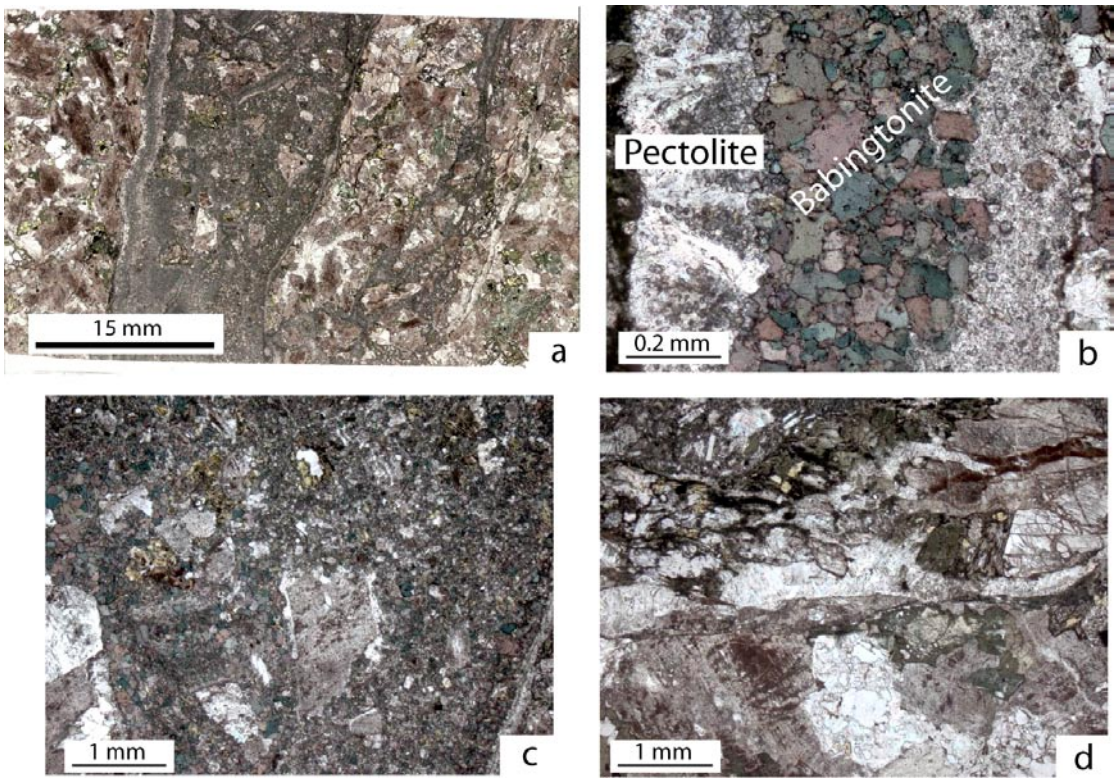

Figure 5-90. *(a): Scanned thin section KLX11A-5. The Ävrö granite is cut discordantly by an ultracataclasite containing poorly sorted, angular granite clasts and a fine-grained matrix formed by babingtonite and pectolite. (b): Pectolite forms a thin, continuous layer at the contact to the host rock. It occurs in radiated and fibrous crystalline masses. Babingtonite has high relief and interference colours. (c): The cataclastic texture is preserved in the cataclastic bands despite the likely replacement of the initial matrix by babingtonite. (d): Pectolite also occurs in dilatant veins in the granite.*

It is a very dark green to black translucent (in thin crystals or splinters) mineral crystallizing in the triclinic system with typically radial short prismatic clusters and druzy coatings. It generally occurs with zeolite minerals in cavities in volcanic rocks or in late hydrothermal veins crosscutting granites. Pectolite is a white to gray mineral, $NaCa_2Si_3O_8(OH)$, sodium calcium inosilicate hydroxide. It crystallizes in the triclinic system typically occurring in radiated or fibrous crystalline masses. It is found as transparent, colourless crystals and grains in veins and cavities in magmatic rocks and is generally associated with zeolites, phrenite, calcite, fluorite, and serpentine.

Figure 5-90a is the scanned thin section of sample KLX11A-5. Pectolite forms the thin layers along the walls of the cataclastic band. Figure 5-90b shows undeformed crystal of babingtonite, with high relief and very high interference colours and a thin layer of pectolite located right at the sharp contact between the host granite (to the left, out of the image) and the babingtonite crystals. In the studied samples, pectolite occurs invariably along the edge of the cataclastic veins or as a thin rim around the edge of some of the cataclasite clasts (see, for example, the details of Figure 5-89). Textural relationships, such as undeformed crystals and abundance of triple junctions among babingtonite crystals, suggest that babingtonite replaced an earlier phase and grew statically in the dilatant space of the cataclastic band. Figure 5-90c shows that the original clast-rich texture of the ultracataclasite is still preserved, in spite of the likely replacement of the initial matrix by babingtonite. Pectolite, in contrast to what observed for babingtonite, is not entirely confined to the cataclasite bands, but is also found in dilatant spaces within the host Ävrö granite, as shown in Figure 5-90d.

Apart from the peculiarity of the occurrence of these two relatively rare minerals, these observations would indicate that fluid circulation and hydrothermal activity have been active post-cataclasis and that fluids exploited high-permeability conduits, as indeed the case of a dilatant cataclastic zone.

Table 5-29. Summary of DZ 15.

Depth (m)	Box number	Interpretation	Description
687.34–693.06	107	Host rock	Undeformed rock with low fracture frequency. A cataclastic network shows replacement of the initial matrix by babingtonite and pectolite, two quite rare minerals forming in relatively low temperature hydrothermal environment (zeolite facies).

5.7.16 DZ 16: depth interval 853–860 m

This section is not interpreted as a real deformation zone, but as pristine host rock interval that contains discrete and localized sealed, cataclastic dilational networks with evidence for multiple reactivation and some minor fractured intervals. Fracture frequency is relatively low and does not increase towards the cataclastic bands with a few exceptions at 853.207 m (see orientation of fractures in Figure 5-91) and 858.321 m. The cataclastic bands are oriented roughly N-S and dip steeply to the W. An example of a broken fracture parallel to a calcite-epidote-infilled vein, which in turn dilated a cataclastic band, is seen in Figure 5-92.

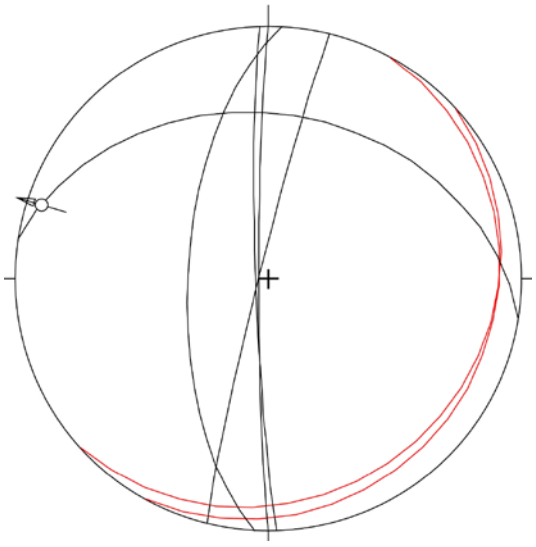

Figure 5-91. *Red great circles show the orientation of a minor fracture zone at depth 853.207 m. Black great circles plot the orientation of calcite, epidote and clay minerals sealed networks or of broken fractures parallel to them. A sinistral transtensional N-dipping fault was measured at depth 852.770.*

Figure 5-92. *A broken fracture, coated by calcite, epidote and clay minerals and oriented 180/87, follows a dilational calcite epidote vein and exploits a pre-existing protocataclastic band. A faint foliation is visible, suggesting deformation at the brittle-ductile transition.*

Table 5-30. Summary of DZ 16.

Depth (m)	Box number	Interpretation	Description
850.74–861.37	136–137	Host rock	Undeformed rock with low fracture frequency. Occurrence of sealed networks of epidote veins, cataclasites and ultracataclasites with mm to cm thickness. Localized red staining.

5.7.17 DZ 17: depth interval 906.84–907.6 m

This depth interval is not a deformation zone. It nonetheless contains an interesting structural feature at depth 907.033 m (Figure 5-93). A steeply W/WNW-dipping cataclastic band, c. 5 cm thick, was the site of several deformation episodes, whereby continuing post-cataclasis dilation led to the generation and emplacement of epidote, chlorite and calcite veins, all intruded sub-parallel to the cataclastic band (strike 203/80). Crosscutting relationships indicate that calcite veins belong to the latest event, because they cut discordantly both epidote and chlorite layers. The cataclastic network at the sides has mirror-image symmetry with respect to the central calcite veins and is c. 10 cm thick. Pervasive red staining occurs.

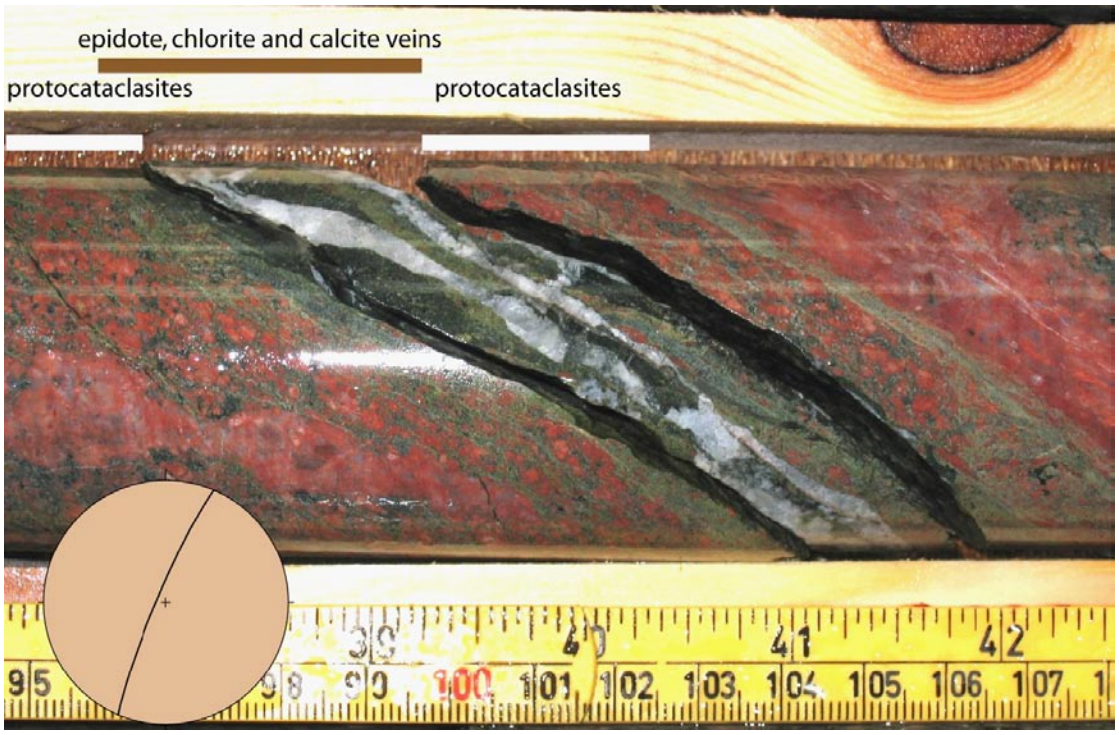

Figure 5-93. *A protocataclastic network localized repeatedly dilational strain leading to multiple intrusions of epidote, chlorite and calcite veins. Calcite veins are the latest feature. The stereonet shows the orientation of the protocataclastic network.*

Table 5-31. Summary of DZ 17.

Depth (m)	Box number	Interpretation	Description
905.85–911.33	146	Host rock	Undeformed rock with low fracture frequency. Occurrence of a sealed network of cataclasites intruded repeatedly by multiple vein generations. Site of localized, repeated dilation.

5.7.18 DZ 18: depth interval 974.1–975.2 m

This section is not interpreted as a deformation zone. It hosts a "rock occurrence" at depth 974.45 m consisting of cataclasites arranged in a thin, epidote-rich network oriented 206/65 close to the upper lithological contact to a coarse pegmatite dike (Figure 5-94). No increase in fracture frequency toward the cataclastic occurrence is recorded. However, pervasive red staining occurs around the pegmatite and the cataclastic band.

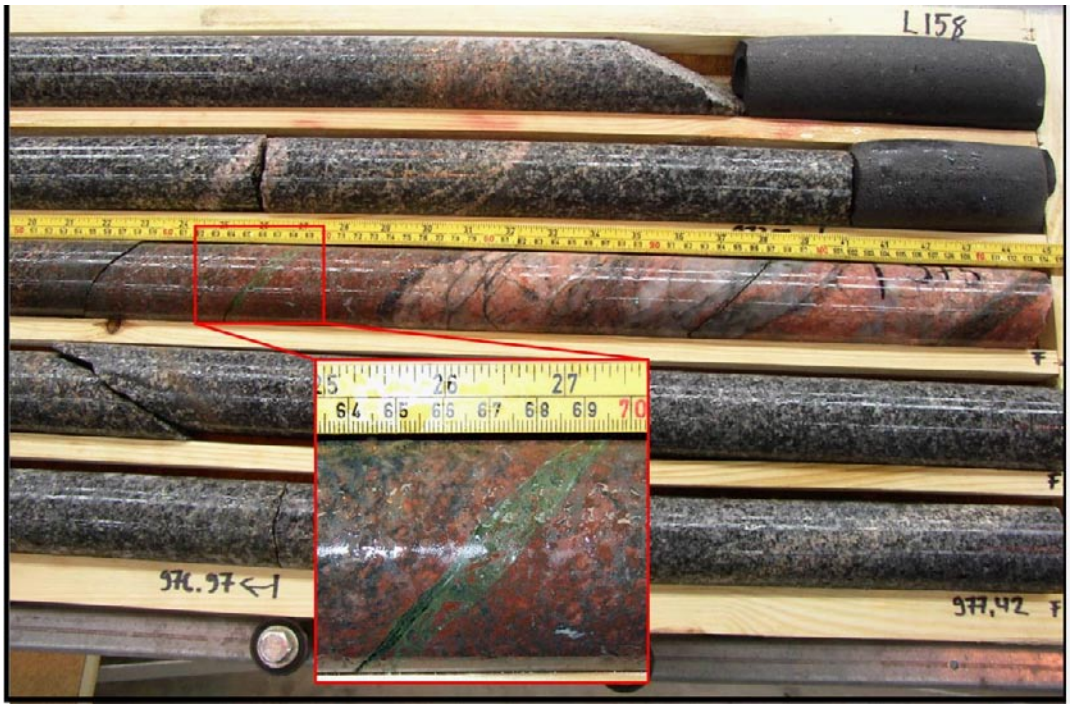

Figure 5-94. *Detail of the thin, epidote-rich cataclastic band immediately above a pegmatitic intrusion in DZ 18.*

Table 5-32. Summary of DZ 18.

Depth (m)	Box number	Interpretation	Description
971.88–977.42	158	Host rock	Generally undeformed rock with low fracture frequency. Occurrence of one discrete sealed network of cataclasites (0.5 –1 cm, Figure 5-94) and a band of cataclasite, ~1–1.5 cm thick. Localized red staining.

5.8 KLX12A

KLX12A drill site is located in the southern part of Laxemar, close to the lithological boundary between Ävrö quartz monzodioritic and dioritic-gabbroic bedrock (see Figure 5-1 for its geographical location). The drill hole has an orientation of 75° towards 305°. Three deformation zones, DZ 10, 11 and 12 (as per the single-hole interpretation report by /Carlsten et al. 2007c/), were logged and are reported here.

5.8.1 DZ 10: depth interval 445.6–447.55 m

DZ 10 is developed within dioritic to gabbroic rocks and consists of two distinct fault cores (Figure 5-96). The first, narrow fault core extends from 446.769 m to 446.774 m depth. It is characterized by the presence of a brittle/ductile shear zone, in which epidote defines a penetrative foliation that overprints, over a several cm thick interval, a protocataclastic/cataclastic component (Figure 5-97). Open fractures, with thick chlorite coating, exploit the trend of the shear zone.

The epidote-defined shear zone strikes NS-NNW/SSE (Figure 5-98). One striated surface parallel to one of these zones suggests strike-slip kinematics along these zones during later brittle reactivation (Figure 5-98).

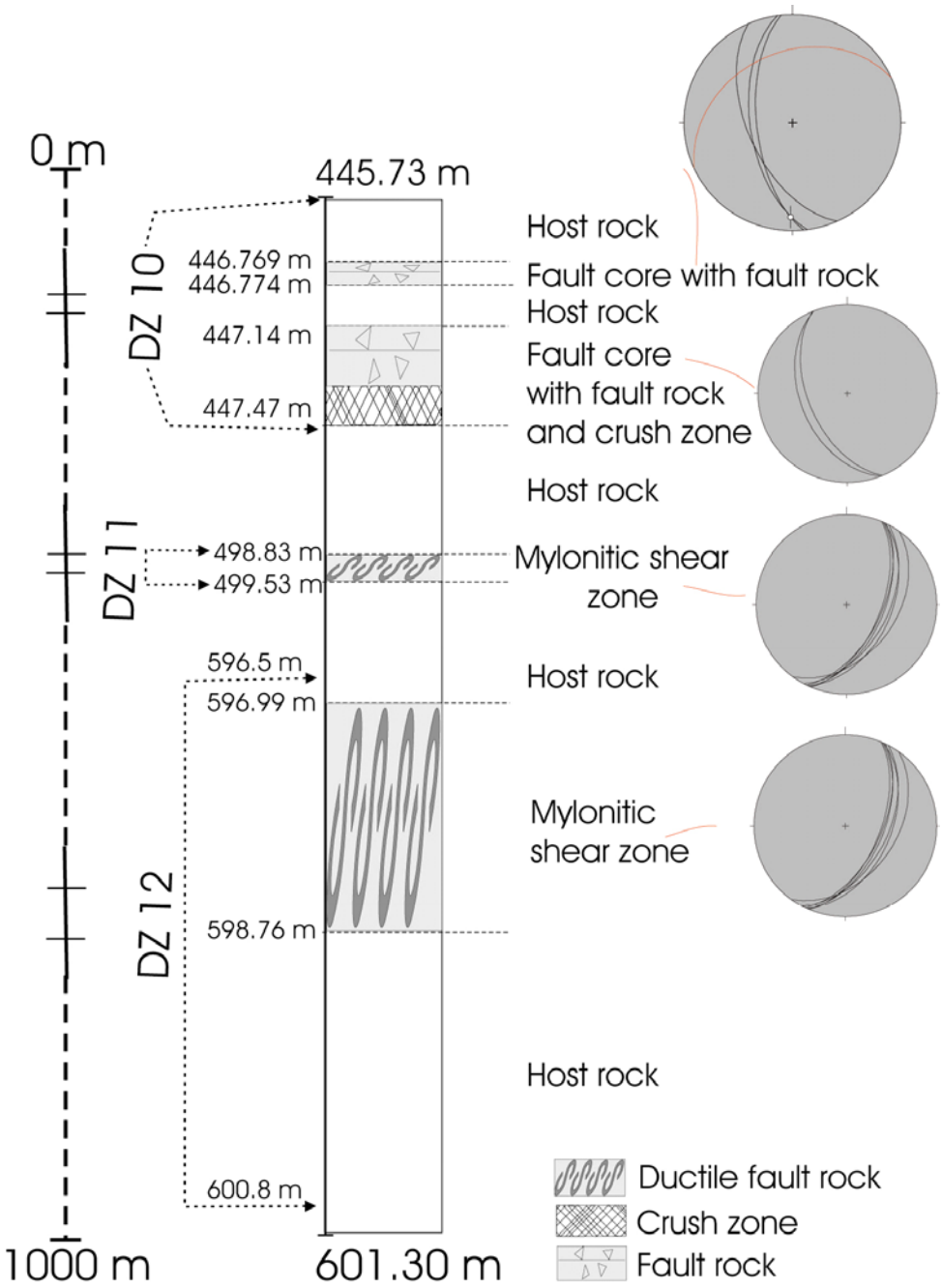

Figure 5-95. *Schematic interpretative log of DZ 10, 11 and 12 of KLX12. See the text for more details about the stereonets.*

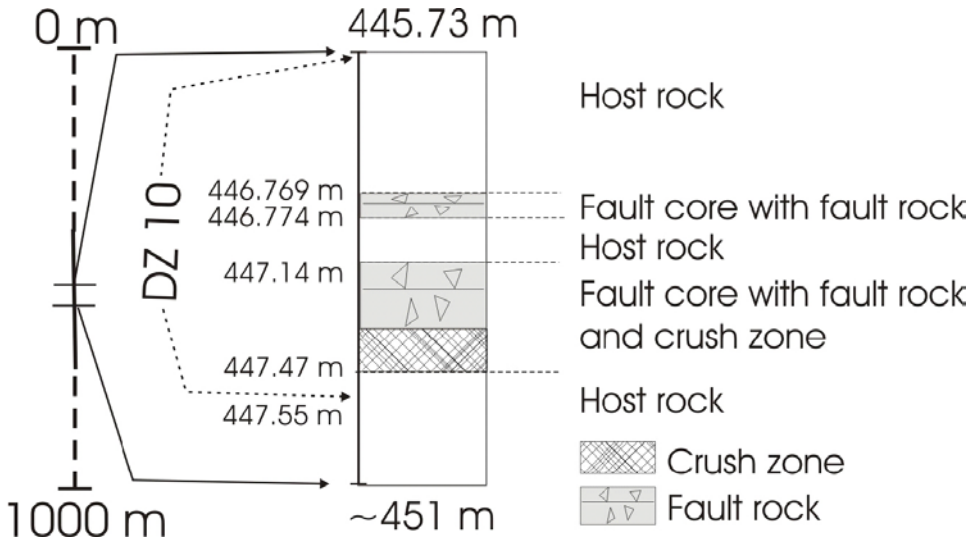

Figure 5-96. *Structural log of DZ 10.*

Figure 5-97. *Epidote shear zone overprinting earlier protocataclastic/cataclastic fabrics in DZ 10 upper core.*

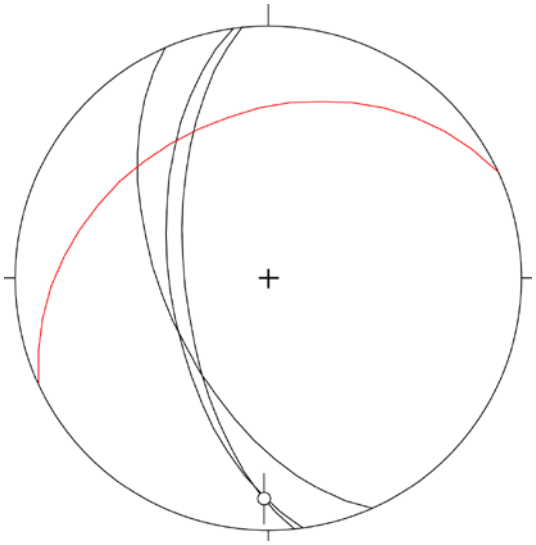

Figure 5-98. *Orientation of the epidote-defined foliation (black great circles), of a striated open fracture exploiting the ductile fabric (black great circle with striation) and of an earlier protocataclastic/ cataclastic band overprinted by the foliation (red great circle) observed in the central part of DZ 10. Strike slip movement is established for the open fracture.*

The core has a sharp contact with the host rock both preceding and following the fault core. Between the upper and the lower cores there occurs a narrow interval of basically undeformed host rock (446.774–447.14 m). The second core extends from 447.14 m down to 447.47 m depth. It is characterized by similar structural relationships and has the same orientation of the upper, thin core (Figure 5-98). It confirms that the penetrative ductile fabric overprints earlier protocataclasites, oriented 245/45 (red great circle of Figure 5-98). There follows a crush zone, which exploits a pre-existing network of fine sealed fractures (Figure 5-99). The upper and lower contacts of the zone are oriented identically and dip c. 50° to the SW (Figure 5-99).

There follows dioritic host rock. Three striated surfaces were observed (Figure 5-100), but no clear or consistent kinematic framework emerges from their analysis.

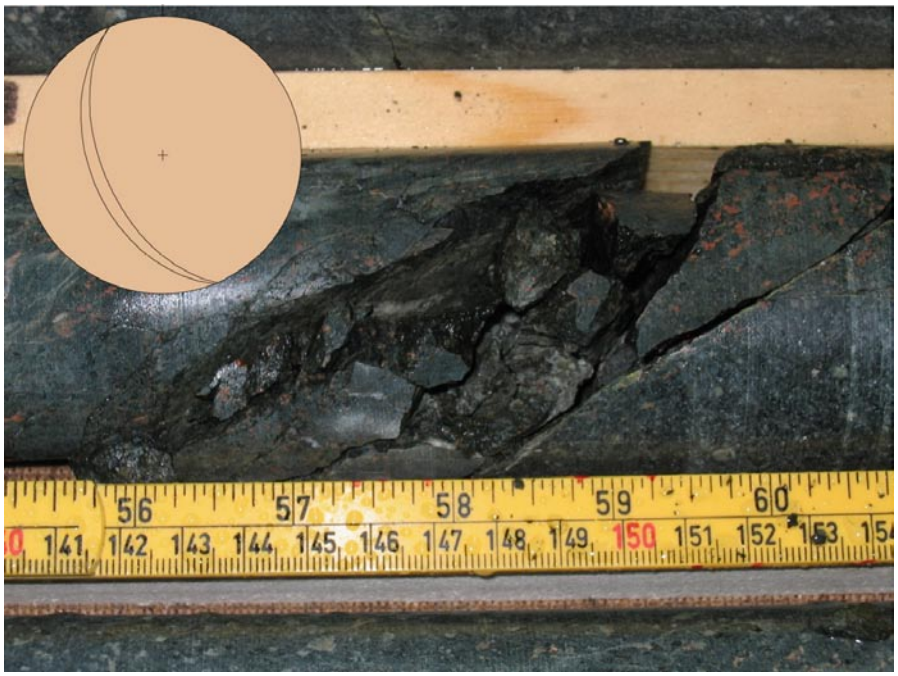

Figure 5-99. *Crush zone at depth 447.460 and orientation of its upper and lower contacts.*

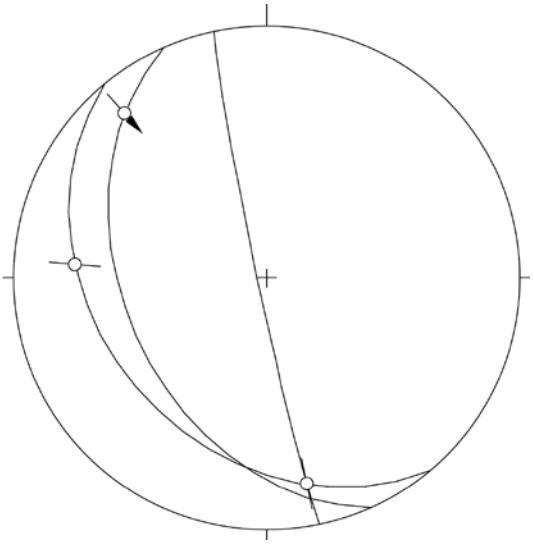

Figure 5-100. *Stereoplot of fault slip data below the core zone of DZ 10.*

Table 5-33. Summary of DZ 10.

Depth (m)	Box number	Interpretation	Description
445.73	65	Host rock	Undeformed host rock with low fracture frequency, 1–3 f/m.
446.769–446.774	65	Fault core	Upper thin fault core, 3–5 cm thick, characterized by a ductile, epidote-defined shear zone that overprints protocataclasites/cataclasites.
446.774–447.14	65	Host rock	
447.14–447.47	65	Fault rock	Brittle-ductile fault core characterized by ductile planar fabrics reworking older protocataclasites/cataclasites (similar to the upper fault core). This zone is followed by a crush zone, which exploits a pre-existing network of fine, sealed fractures and possibly also the ductile fabric (~4 cm).
447.5–451	65	Host rock	Undeformed dioritic to gabbroic rock.

5.8.2 DZ 11: depth interval 498.85–499.54 m

This section is developed within dioritic to gabbroic rocks and contains an approximately 25 cm thick mylonitic sequence, which we interpret as a ductile DZ core. The section extends from depth 498.83 m down to 499.06 m (Figure 5-102) and is characterized by a penetrative mylonitic foliation that dips on average 55° to the ESE.

Thin section KLX12A-1 shows a compositional banding given by the alternation of amphibole-dominated and granitic layers (Figure 5-103). The rock is indeed penetratively foliated and the microscopic analysis allowed the identification of kinematic indicators (asymmetric sigma clast and mica-decorated shear bands) that indicate sinistral shearing at the scale of the thin section (Figure 5-103). Unfortunately, no lineation is associated with the mylonitic planar fabric, thus precluding the determination of the regional significance of the sinistral sense of shear. The mylonite zone has very sharp boundaries to the host rock and the contact dips parallel to the mylonitic foliation.

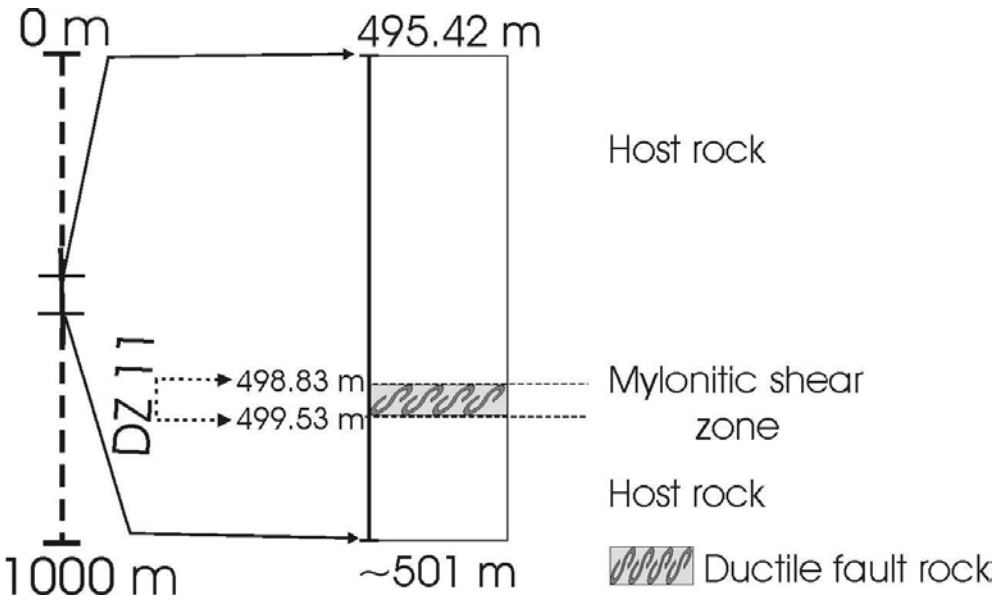

Figure 5-101. *Simplified structural log of DZ 11.*

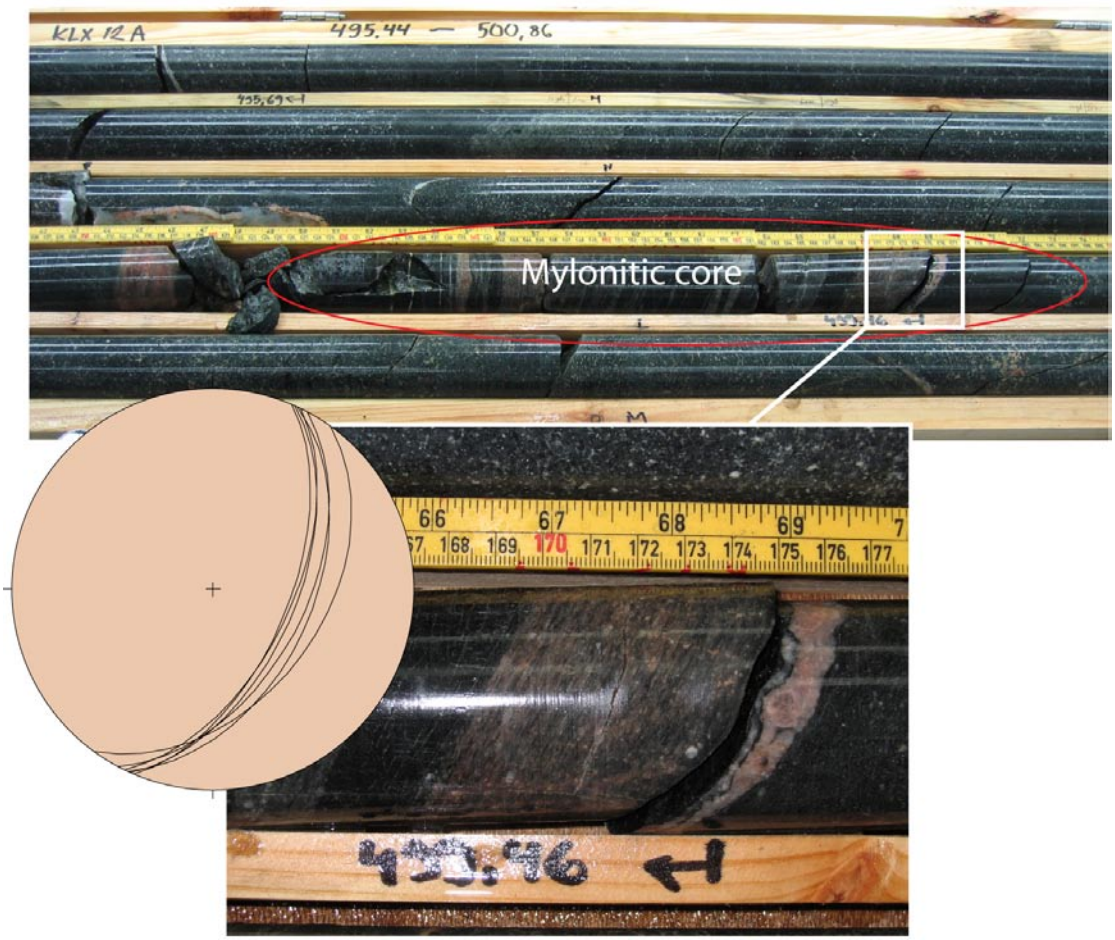

Figure 5-102. *Mylonitic core of DZ 11 within Box number 75 of KLX12 A. The bottom photograph shows the presence of an extremely well developed foliation and a proper mylonitic texture. The mylonitic foliation dips c. 55° to the ESE (see the stereonet).*

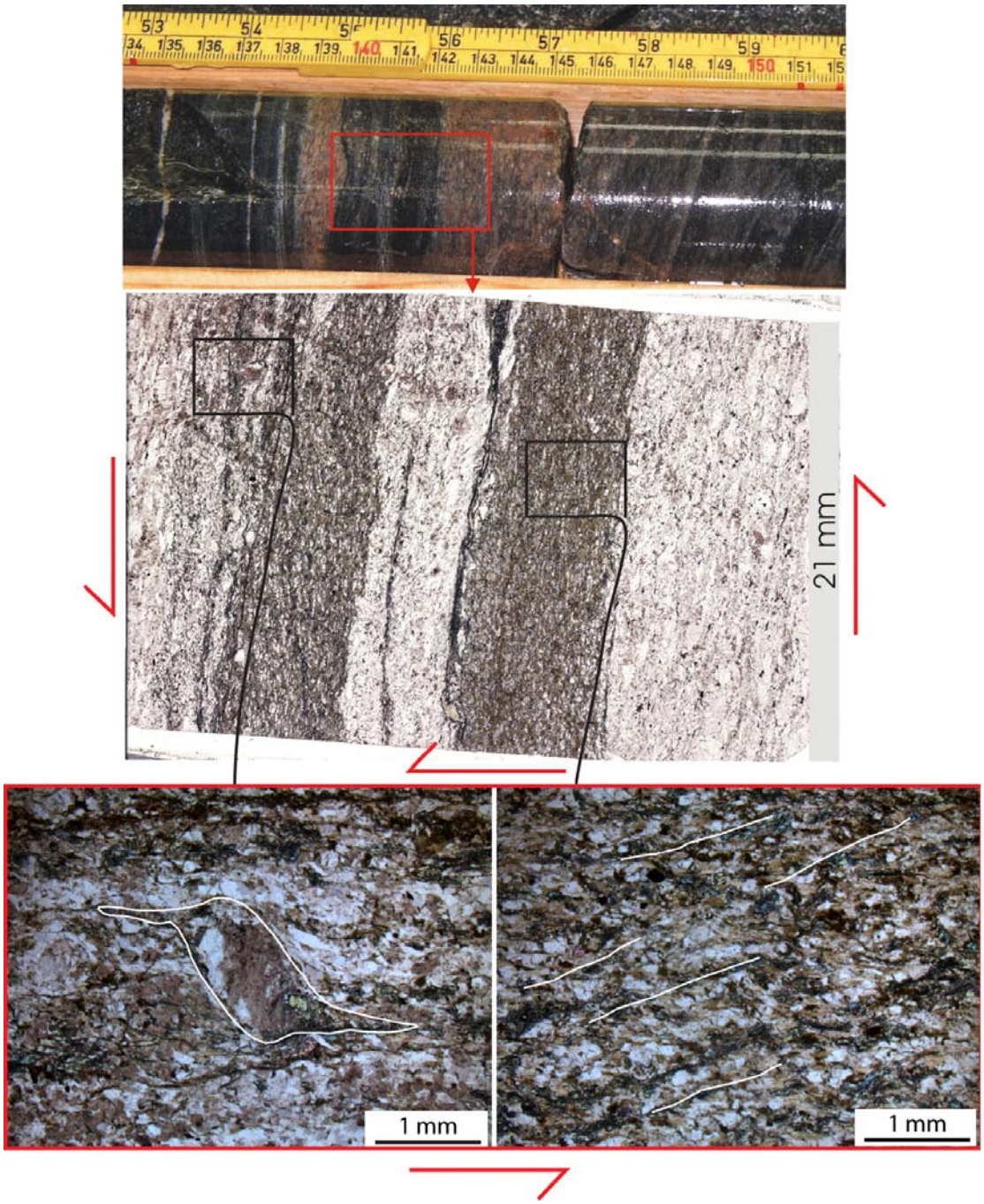

Figure 5-103. *Position of sample KLX12-1 at 499.4 m depth within DZ 11 in KLX12 A (upper photograph). The scanned thin section (in the middle) shows ductile deformation within a strongly compositionally banded rock. Kinematic indicators (sinistral sigma clast, bottom left, and oblique mica shear planes, bottom right) point to sinistral kinematics.*

Table 5-34. Summary of DZ 11.

Depth (m)	Box number	Interpretation	Description
495.42–498.83	75	Host rock	Undeformed dioritic to gabbroic rock with low fracture frequency, 1–3 f/m. Thin granitic layers occur throughout the DZ.
498.83–499.06	75	Ductile shear zone/ deformation zone	Mylonite zone, with average dip of 55° to the ESE. The ductile zone has very sharp boundaries to the host rock. Thickness of zone is 0.25 m.

5.8.3 DZ 12: depth interval 596.5–600.8 m

DZ 12 deforms a rock interval formed by diabase and medium-grained porphyritic granitoids. A mylonitic shear zone, very similar to that described in DZ 11, forms the core of DZ 12 (Figure 5-104 and Figure 5-105). The mylonitic core extends from c. 597 m to 598.76 m depth; its mylonitic foliation dips moderately to the SE (Figure 5-106). Mylonites are locally overprinted by brittle epidote networks and epidote-coated broken fractures, which dip c. 60° to the SW (green great circles in Figure 5-106).

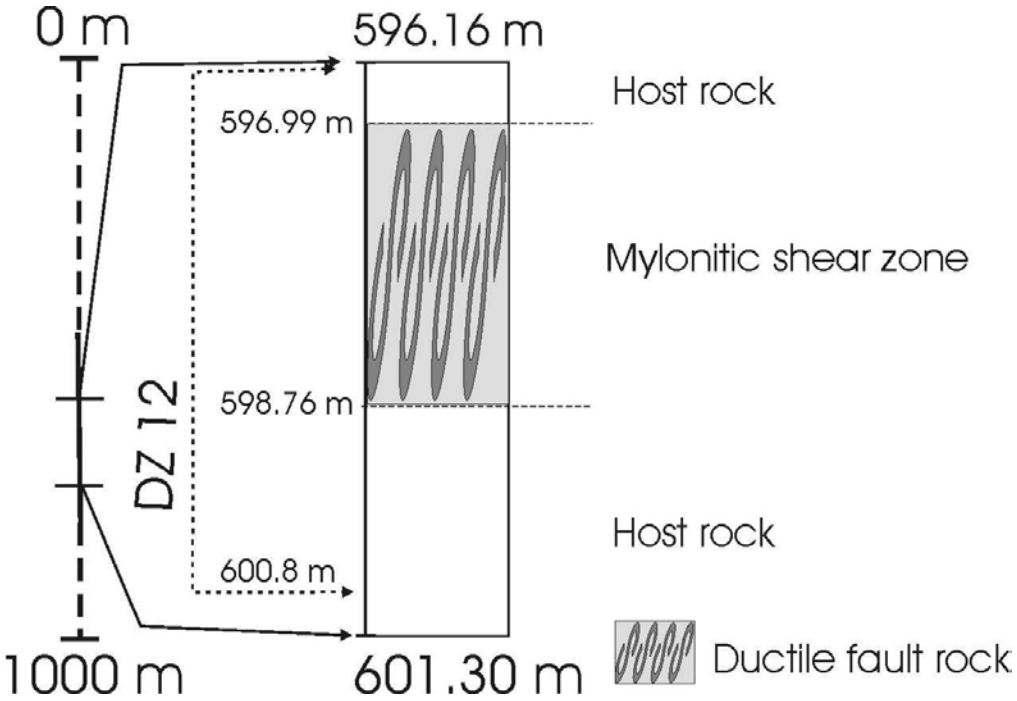

Figure 5-104. *Simplified structural log of DZ 12.*

Figure 5-105. *Penetrative mylonitic foliation in the core of DZ 12 of KLX12A.*

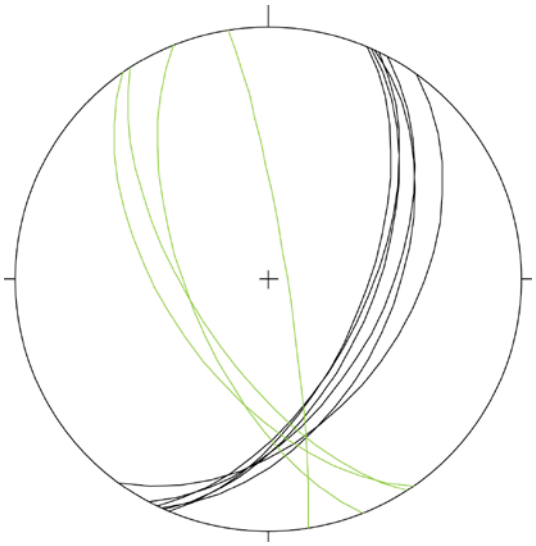

Figure 5-106. *In DZ 12 the mylonitic foliation trends ENE with a moderate dip (~50°) to the SE (black great circles) and is overprinted by a set of systematic fractures with NW trend and steep dip angles (~60°) towards the SW (green great circles).*

Table 5-35. Summary of DZ 12.

Depth (m)	Box number	Interpretation	Description
596.16–596.99	94	Host rock	Lithologically heterogeneous box, with changes from diabase to porphyritic granites. Undeformed rock with low fracture frequency.
596.99–598.76	94	Ductile shear zone/ deformation zone	Mylonitic shear zone characterized by pervasive mylonitic foliation overprinted by millimetric brittle epidote cataclastic networks.
598.76–	94	Host rock	Dioritic to gabbroic bedrock.

5.9 KLX18A

KLX18A is located in the middle of the Laxemar investigation area (Figure 5-1). We have logged a depth interval extending from 138 m down to 490 m (Figure 5-107), in which there are nine different DZ described by the single hole interpretation study by /Carlsten et al. 2007d/. The core is oriented 271/81.

5.9.1 DZ 1: depth interval 137.8–143.9 m

Although described as a DZ in the single-hole interpretation, in our opinion this depth interval does not contain structural features of particular interest. Diffuse red staining and a few, scattered and millimetric cataclastic bands are the key features of the section (Figure 5-108).

Fractures have generally a southwesterly dip, as shown in Figure 5-109. No striated planes were observed.

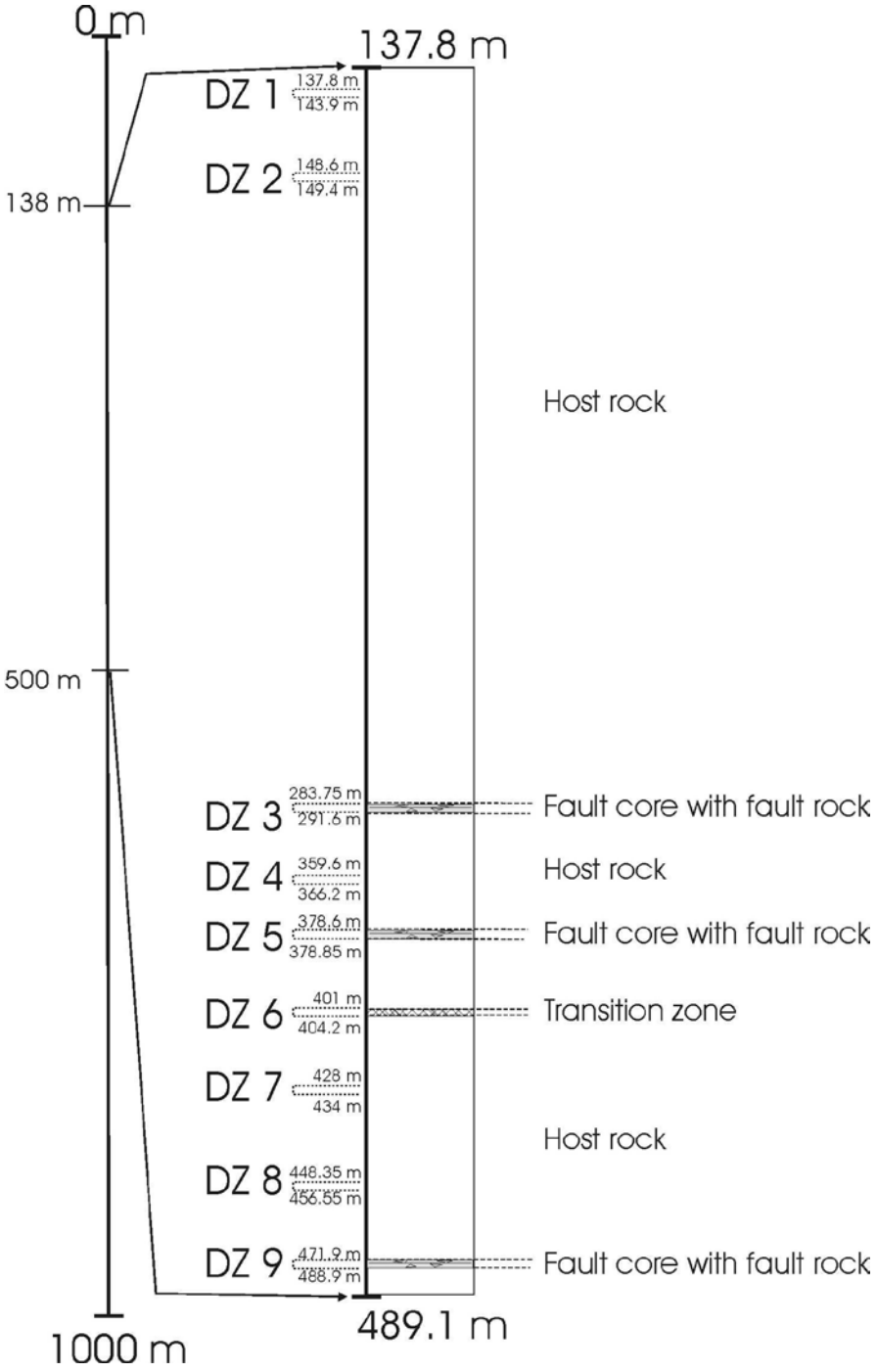

Figure 5-107. *KLX18A DZ 1 to DZ 9.*

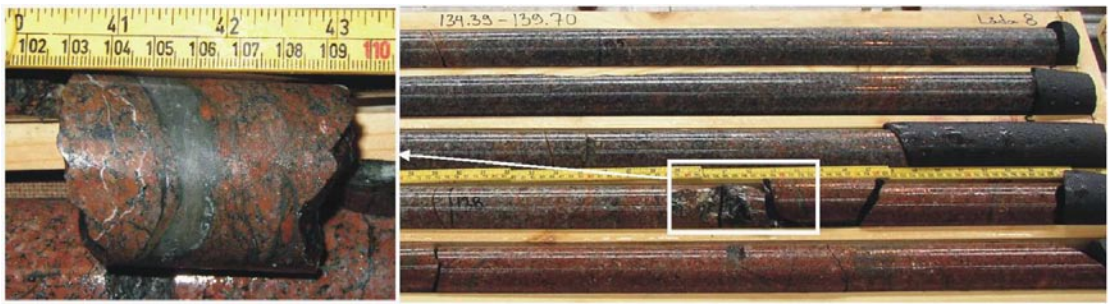

Figure 5-108. *Red staining and a few scattered epidotized cataclastic bands characterize DZ 1.*

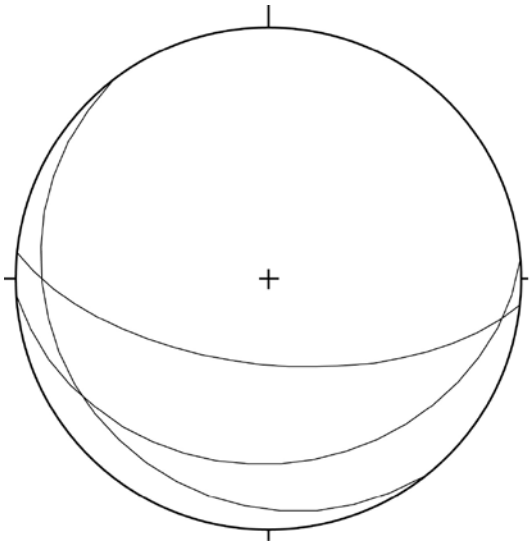

Figure 5-109. *Orientation of selected fractures in DZ 1 of KLX18A.*

Table 5-36. Summary of DZ 1.

Depth (m)	Box number	Interpretation	Description
134.39–139.70	8	Host rock	Undeformed host rock with only red staining and a few millimetric to centimetric cataclastic bands.

5.9.2 DZ 2: depth interval 148.6–149.4 m

Similarly to DZ 1, DZ 2 is not characterized by relevant structural features. Of interest are only a few thin cataclastic bands, and an open fracture filled with green clay minerals (Figure 5-110 and Figure 5-111).

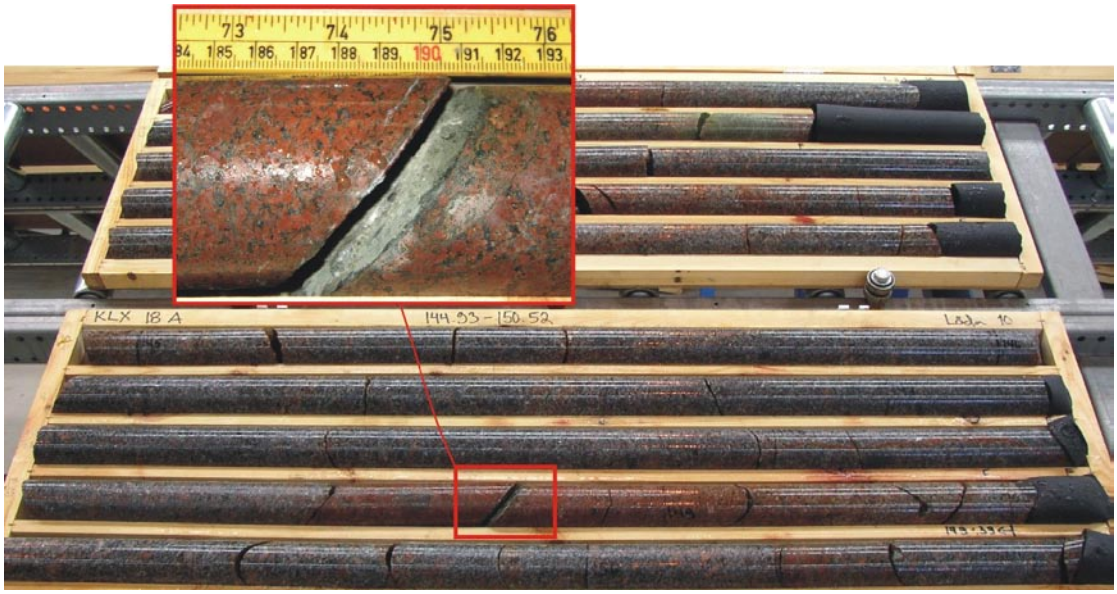

Figure 5-110. *Overview of DZ 2 in KLX18A and detail of one open fracture filled in by clay minerals and oriented 092/40 at depth 148.690.*

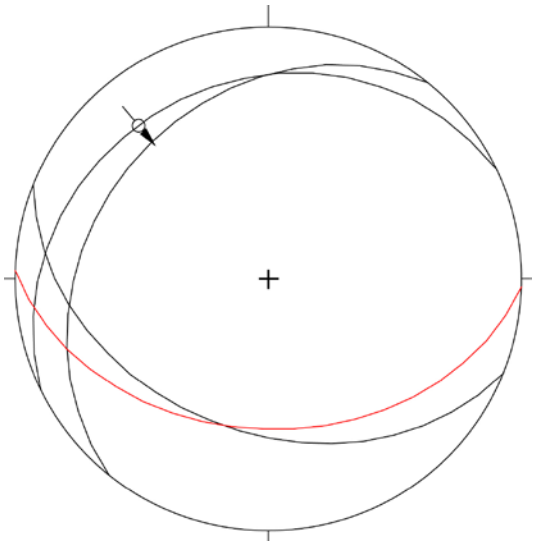

Figure 5-111. *Orientation of fractures in DZ 2. A NW-dipping striated surface indicates reverse top-to-the-SE kinematics. The red great circle represents the open fracture shown in Figure 5-110.*

Table 5-37. Summary of DZ 2.

Depth (m)	Box number	Interpretation	Description
139.70–150.52	9, 10	Host rock	Undeformed host rock with diffuse red staining and a few thin cataclastic bands.

5.9.3 DZ 3: depth interval 283.75–291.6 m

This section contains a c. 16 m wide deformation zone consisting of an upper transition zone, a proper core and a lower transition zone. The upper transition zone extends from 284.85 to 287.288 m depth and displays a progressive increase in fracture frequency towards the fault core and includes a 20 cm thick crush zone and a zone of core loss, also 20 cm thick. Fractures, invariably coated by chlorite, calcite and clay minerals, are oriented consistently NE-SW and dip steeply to the SE (Figure 5-112).

The DZ fault core (287.288–290.701 m) has a sharp upper boundary separating the upper transition zone from its protocataclasites, which develop progressively over a 20 to 25 cm thick interval into cataclasites and ultracataclasites. The cataclastic texture of the rock is best seen in the scanned image of sample KLX18A-1 thin section. A faint foliation, which is defined by the alternation (at the thin section scale) of protocataclastic and cataclastic bands (Figure 5-113), is also recognizable within the cataclasites. The core continues with intensively epidotized rock, intense fracturing, crush zones and an 87 cm core loss interval. Sample KLX18A-2 shows that the texture of the rock remains protocataclastic throughout, with pervasive red staining, localized bands of more intense cataclasis and diffuse chloritization. Later dilatant calcite veins are common in this interval. The DZ lower transition zone (290.701–291.42 m) is shorter than the upper one, is characterized predominantly by diffuse epidotization and is transitional to undeformed granitic host rock at 291.42 m depth.

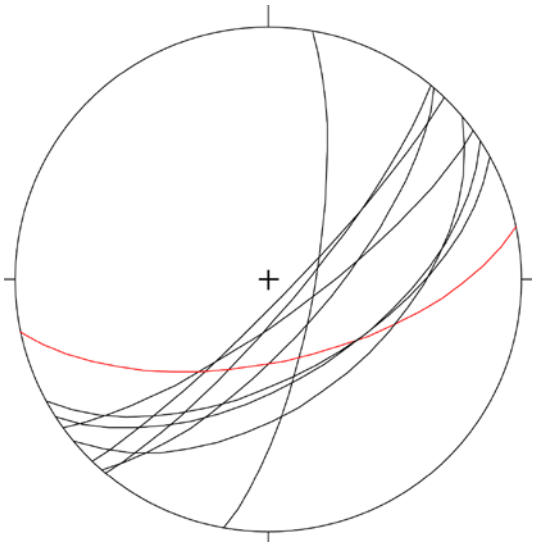

Figure 5-112. *Fracture orientation within the upper transition zone of DZ 3. The red great circle is the fracture that defines the upper contact of the crush zone extending from 285.453 down to 285.624 m depth.*

Figure 5-113. *Sample KLX18-1 from cataclastic granites at depth 287.4 m. The scanned thin section shows a faint foliation within the sample (white dashed lines), which is defined by the alternation of protocataclastic and cataclastic domains.*

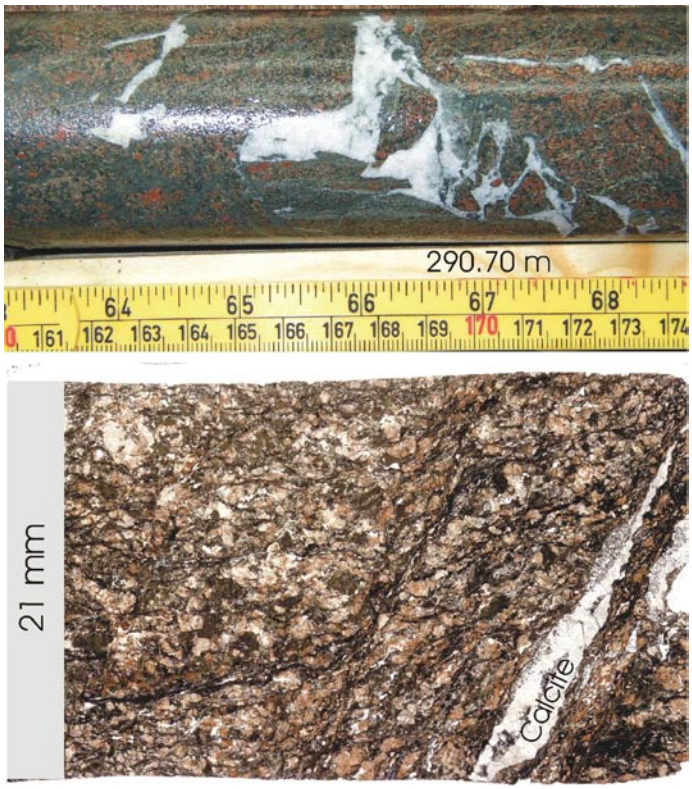

Figure 5-114. *"Late" dilational calcite veins cut across altered protocataclastic granites, as shown by the scanned thin section of sample KLX18A-2.*

Table 5-38. Summary of DZ 3.

Depth (m)	Box number	Interpretation	Description
284.85–287.288	36	Transition zone	Increasing fracture frequency, 20 cm thick crush zone and core loss; no major fault rock (just thin bands and networks). Thickness of zone is 6.60 m.
287.288–290.701	36, 37	Fault core	Protocataclasites that pass laterally into cataclasites and ultracataclasites over a 20–25 cm thick interval. The core continues with heavily altered rock, with epidotization and intense fracturing, crush zones and c. 87 cm of core loss. The lower part of the core includes altered protocataclasites.
290.701–291.42	37	Transition zone	This transition zone is shorter and contains epidotization.

5.9.4 DZ 4: depth interval 359.6–366.2 m

Based on structural criteria, this depth interval is hardly definable as a deformation zone. It consists of basically undeformed rock with only localized red staining and a few minor cataclastic bands and/or networks, often associated with calcite-infilled fractures.

Figure 5-115. *DZ 4 359.6–366.2 m (Box number 50 and 51). This DZ consists of moderately to little fractured rock with localized red staining. The bedrock is Ävrö granite.*

Table 5-39. Summary of DZ 4.

Depth (m)	Box number	Interpretation	Description
356.71–367.66	50, 51	Host rock	Undeformed granitic rock with limited occurrences of cataclastic bands/networks and localized red staining.

5.9.5 DZ 5: depth interval 378.6–378.85 m

The most relevant structural feature of DZ 5 is the presence of a thin cataclastic core, extending from 378.795 to 378.850 m depth. This core follows a narrow zone of heavily fractured rock, with open fractures dipping very shallowly to the S/SSE (Figure 5-116).

The core is defined by a cataclastic, locally ultracataclastic interval (Figure 5-117). Its detailed analysis reveals that fault rocks bear evidence of multiple cataclastic reactivation; this is undoubtedly proven by the presence of i) cataclasites and ultracataclasites with a fine-grained, dark green matrix containing angular granite fragments; ii) ripped off fragments of component i) dispersed in a light green chlorite matrix, and iii) ripped off fragments of components i) and ii) dispersed in an extremely fine-grained purple coloured matrix. Sample KLX18A-3 is a thin section, 8×4 cm in size, that covers the whole core.

Figure 5-118 shows microscopic details of selected portions of the DZ core. The upper microphotograph zooms into the “transition zone” between the undeformed granite (to the right) and the dark green cataclasite to the left. The transition is very sharp and is outlined by quartz-calcite dilatant veins striking parallel to the contact. The dark green colour of the cataclastic matrix is due to the presence of epidote. Clasts are poorly sorted and have angular and irregular shapes. The middle and the lower microphotographs (parallel and crossed nicols images, respectively, of the same detail) zoom instead onto the detail of a relatively large ultracataclastic/cataclastic clast reworked by a younger cataclastic episode. The fine-grained ultracataclastic portion of the clast shows evidence of banding and foliation. The pale green colour is due to chloritization.

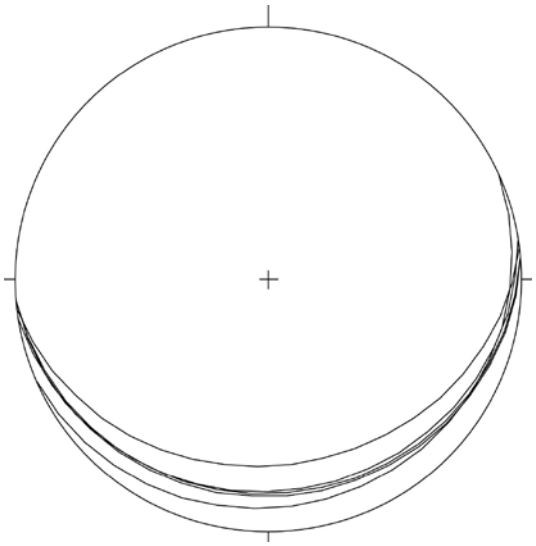

Figure 5-116. *Very shallow, S/SSE-dipping fractures are observed immediately above DZ 5 core.*

Figure 5-117. *DZ core, extending from 378.795 to 378.850 m depth. The core consists of cataclasites and ultracataclasites with differently coloured matrix. The outer rim of the core has a dark green colour and contains fragments of the granitic host rock. The ultracataclasite with the greyish-green matrix contains fragments of a previously formed and indurated cataclasite and clasts of the hosting granite, while the purple coloured ultracataclasite also contains fragments of the greyish-green ultracataclasite.*

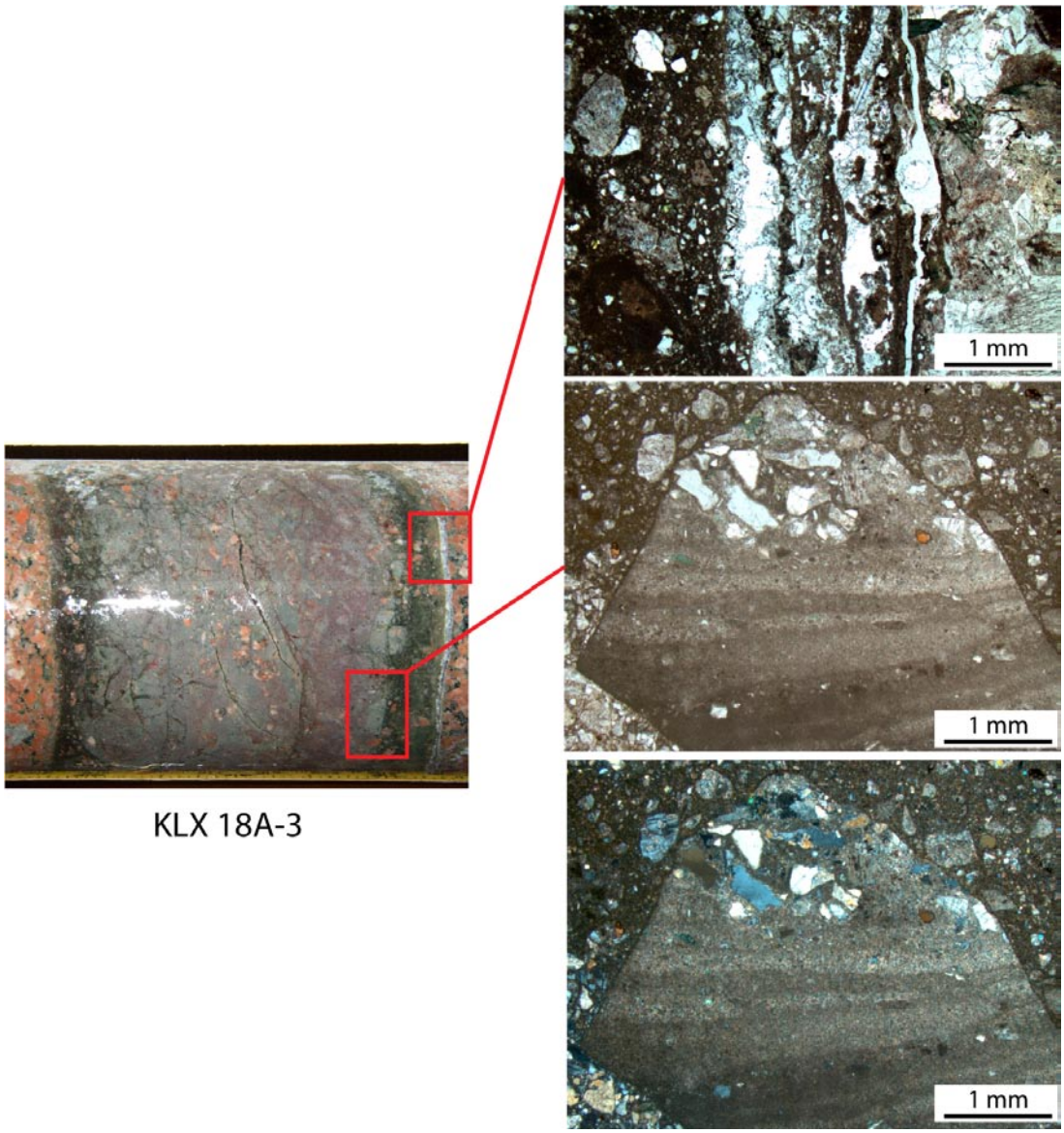

Figure 5-118. *Microphotographs from sample KLX18A-3. The top microphotograph illustrates the details of the contact between the undeformed granite (to the right) and the dark green epidote-rich cataclasites. In the middle and bottom photos are the details of a foliated/banded cataclastic and ultracataclastic clast reworked by a subsequent cataclastic phase.*

Table 5-40. Summary of DZ 5.

Depth (m)	Box number	Interpretation	Description
373.23–378.795	53	Host rock	Undeformed rock, red staining begins at depth 378.50 m and extends to 379.60 m.
378.795–378.850	54	Fault core	Cataclastic band of ~6.5 cm thickness, with evidence for multiple cataclastic reactivation.
378.850–	54	Host rock	Undeformed rock with localized red staining.

5.9.6 DZ 6: depth interval 401–404.2 m

This section contains a transition zone (402.498–403.324 m) characterized by highly fractured granites and quartz monzodiorites, by the presence of a crush zone and diffused red staining. A couple of cataclastic bands and cataclastic sealed epidote networks occur within the DZ (Figure 5-119). This transition zone is controlled by the lithological change from granite to quartz monzodiorites at depth 402.498 m. Granites are found again at 403.324 m depth.

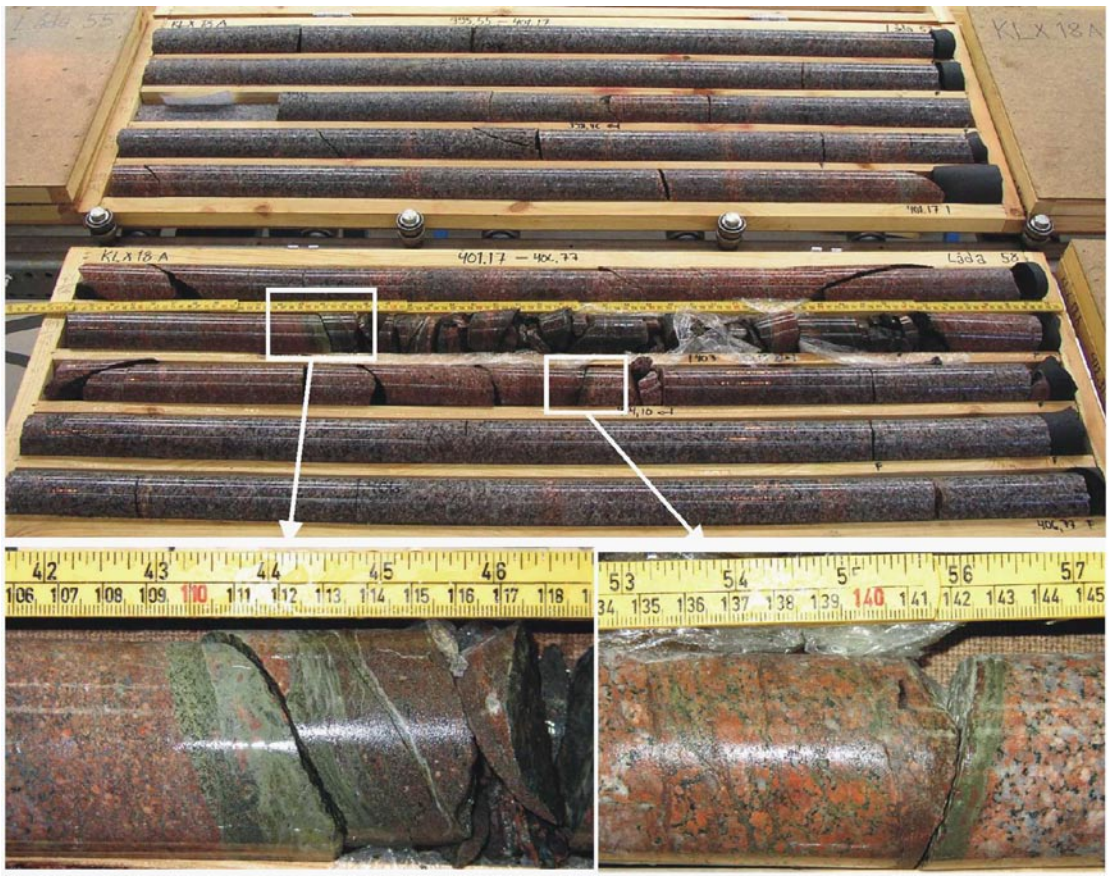

Figure 5-119. *A thin transition zone, which consists of a crush zone and a few cataclastic bands, defines DZ 6.*

Table 5-41. Summary of DZ 6.

Depth (m)	Box number	Interpretation	Description
395.55–402.498	57, 58	Host rock	Undeformed rock; red staining from depth 400.85 m extending down to 404.05 m.
402.498–403.324	58	Transition zone	Deformation zone characterized by highly fractured rock (25–30 f/m)/crush zone and red staining. Occurrence of a few cataclastic bands/networks with epidote. This transition zone could be due to a lithological change from granite to quartz monzodiorite.
403.324	58	Host rock	Undeformed rock with localized red staining.

5.9.7 DZ 7: depth interval 428–434 m

This section does not contain particularly relevant structural features. Localized red staining and a few, scattered, sealed epidote networks are the only aspects worth mentioning (Figure 5-120).

The highly fractured interval shown in the bottom left photograph of Figure 5-120 contains epidote and chlorite-coated open fractures that dip shallowly to the SSW/SW (Figure 5-121).

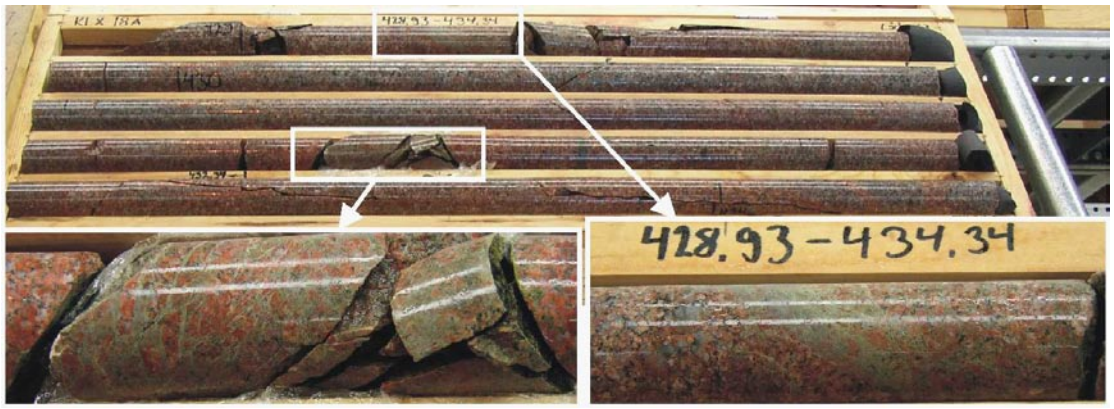

Figure 5-120. *DZ 7 in KLX18A is characterized by diffuse red staining and localized bands and sealed networks of epidotization.*

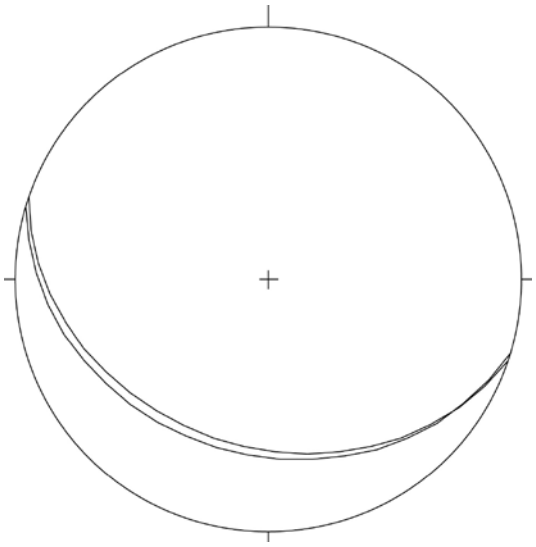

Figure 5-121. *Orientation of epidote- and chlorite-coated open fractures in DZ 7.*

Table 5-42. Summary of DZ 7.

Depth (m)	Box number	Interpretation	Description
423.39–434.34	62, 63	Host rock	Undeformed rock with red staining and a few epidote sealed networks.

5.9.8 DZ 8: depth interval 448.35–456.55 m

DZ 8 does not contain particularly relevant structural features. Red staining and a few, scattered, sealed epidote networks characterize the depth interval (Figure 5-122). These networks vary in thickness from millimetric to centimetric.

Table 5-43. Summary of DZ 8.

Depth (m)	Box number	Interpretation	Description
445.32–456.20	66, 67	Host rock	Undeformed rock characterized by red staining and a few epidotized cataclastic networks (from a few mm to cm thick).

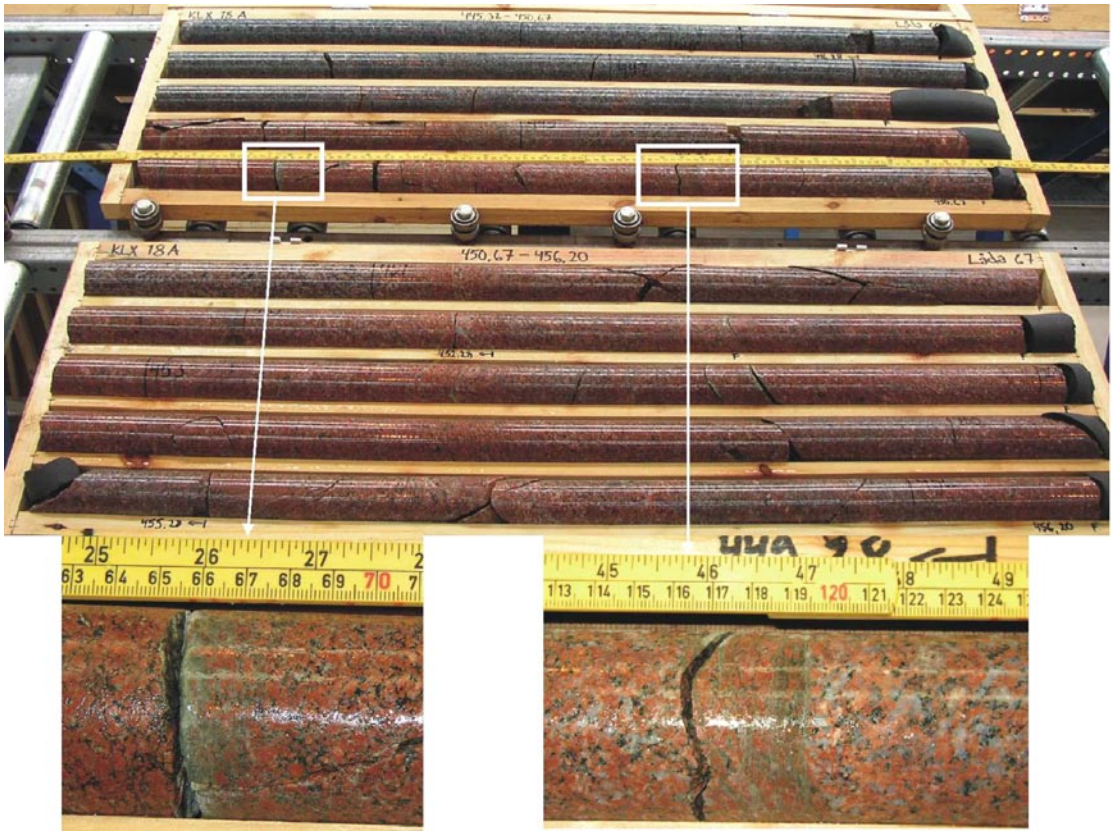

Figure 5-122. *DZ 8 is characterized by red staining and discrete bands and networks of epidotization with minor cataclasis associated with them.*

5.9.9 DZ 9: depth interval 471.9–488.9 m

DZ 9 contains a brittle deformation zone defined by an upper transition zone and a proper cataclastic fault core. The transition zone extends from ~483.92 to 485.491 m depth. It is defined by a progressive increase of the fracture frequency and the occurrence of cataclastic networks in the proximity of the fault core (red great circles in Figure 5-123). Fractures have a quite variable orientation, although most of them dip moderately to the S, SW (Figure 5-123) and exploit similarly oriented epidote veins and bands.

The fault core extends from 485.491 m to 485.730 m depth. It follows a c. 15 cm thick crush zone (Figure 5-124) and is characterized by a strongly fractured interval and the occurrence of c. 5 cm of proto-, cataclasites, ultracataclasites and a c. 2 cm thick gouge horizon (Figure 5-124). Cataclasites are oriented roughly EW and dip c. 50° to the S, thus not very dissimilar from the predominant orientation of fractures in the upper part of the DZ (Figure 5-125).

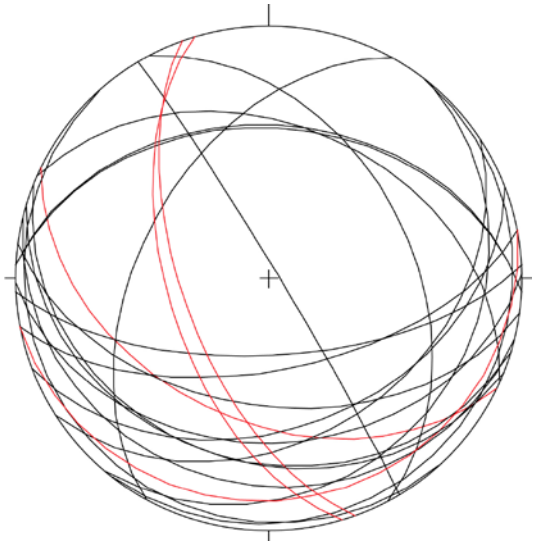

Figure 5-123. *Orientation of epidote bands and veins (red great circles) and open fractures within the upper transition zone of DZ 9.*

Figure 5-124. *DZ 9 is characterized by un upper transition zone extending from 471.9 to 488.9 m depth, which is defined by a progressive increase of the fracture frequency (upper photograph, two upper rows before the white boxes). The core (details shown in the two bottom pictures) consists of cataclasites, a gouge interval and a strongly fractured rock interval.*

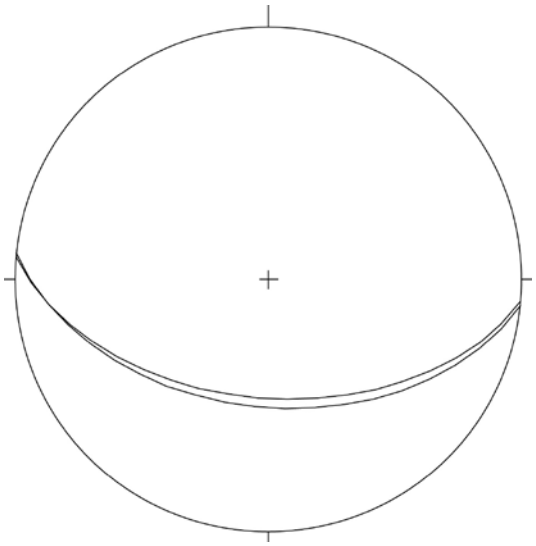

Figure 5-125. *Orientation of the DZ core cataclasites.*

The core is followed by a heavily fractured rock interval down to approximately 487.8 m depth. Fractures have a similar orientation to those of the upper transition zone, with an average EW/ENE-WSW strike and a c. 50° dip to the S/SSE (Figure 5-126). One SE-dipping striated plane indicates a dextral transtensional kinematics (red circle in Figure 5-126).

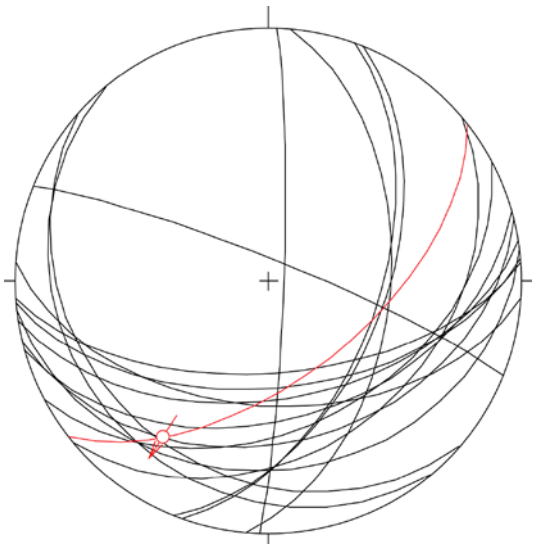

Figure 5-126. *Orientation of open fractures in the lower transition zone of DZ 9. The red great circle is a striated plane at depth 487.065 m.*

Table 5-44. Summary of DZ 9.

Depth (m)	Box number	Interpretation	Description
~483.92–485.491	73	Transition zone	Increase in fracture frequency and occurrence of epidote, sealed networks towards the core. The total thickness of the zone is 3.9 m.
485.491–485.730	73	Fault core	The brittle core is highly fractured and contains proto-cataclasites and a thin gouge horizon.
485.730– ~487.80	73	Transition zone	Decrease in fracture frequency away from the core.

5.10 KLX20A

This borehole is located in the westernmost part of the Laxemar investigation area (Figure 5-1), in the same locality of KLX11A. The drill hole is oriented 273/48 /Carlsten et al. 2007d/. We report here the characterization of four different deformation zones (DZ 1 to DZ 4) identified within depth interval 170 –418 m by /Carlsten et al. 2007d/ (Figure 5-127).

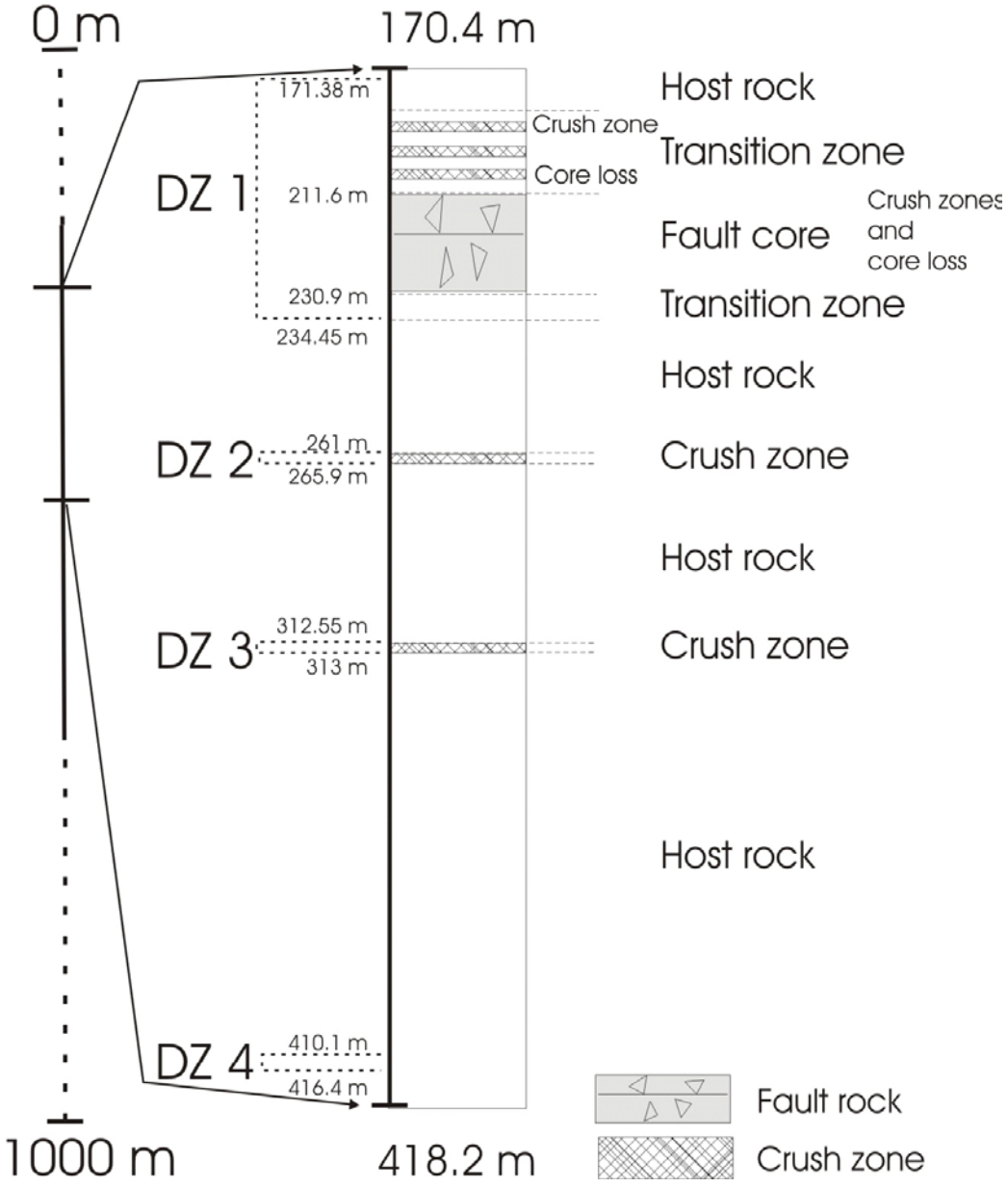

Figure 5-127. *Simplified structural log of depth interval 170–418 m of KLX20A. Four deformation zones (DZ 1 to DZ 4) are identified in this interval by the single-hole interpretation study of /Carlsten et al. 2007d/.*

5.10.1 DZ 1: depth interval 171.38–234.45 m

Deformation zone DZ1 is interesting due to the presence of a large dolerite dyke intruded upon quartz monzodiorite and of several brittle features. Brittle deformation features are widespread throughout the whole zone, with significant fracturing, crush zones and intervals of core loss. Of particular interest is the presence of many excellent quality striated planes, most of which are found within the mafic doleritic dyke (see an example in Figure 5-128).

Relatively undeformed rock and no significant structural features, except a few striated planes, characterize the upper granitic section of DZ 1 (Figure 5-129). In this section, a set of striated planes with normal kinematics dips moderately to the S, SW and coexists with two distinct sets of steep planes, which strike roughly NS and NE-SW and are transpressive sinistral. The striated planes are coated by chlorite, hematite, clay minerals and locally calcite.

At depth 182.37 there occurs the upper contact of a major doleritic dyke. This depth is also interpreted to correspond roughly to the upper limit of an upper transition zone within DZ 1, defined by pervasive fracture sets, several crush zones and core loss intervals. Striated planes are very common in this transition zone and are invariably coated by chlorite and clay minerals (Figure 5-128).

The fault-slip data measured within the transition zone down to depth 211 m are shown in Figure 5-130. The information-rich stereonet can be resolved into two main systematic sets of fractures: i) steep, predominantly strike-slip faults (top left stereonet in Figure 5-131), striking from NNW to NNE, which can be interpreted as belonging to a set of conjugate sinistral (red great circles) and dextral fault planes (black great circles); ii) moderately S- and N-dipping normal (blue great circles in the stereonet to the right) and reverse (black great circles) faults (Figure 5-131).

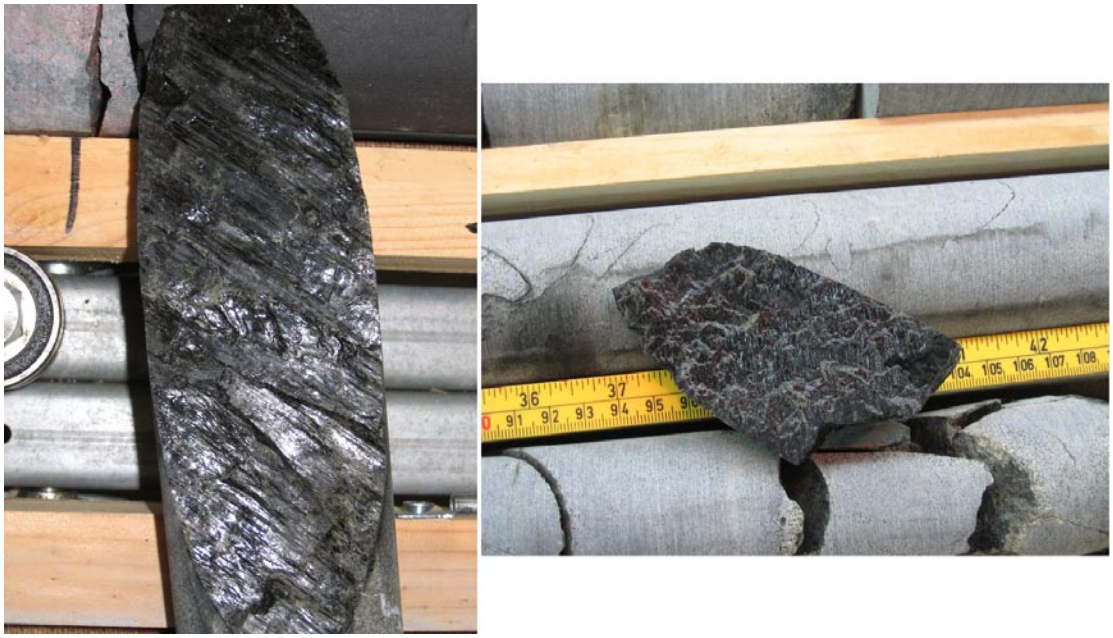

Figure 5-128. *Examples of the high quality striated surfaces within the doleritic dyke of DZ 1.*

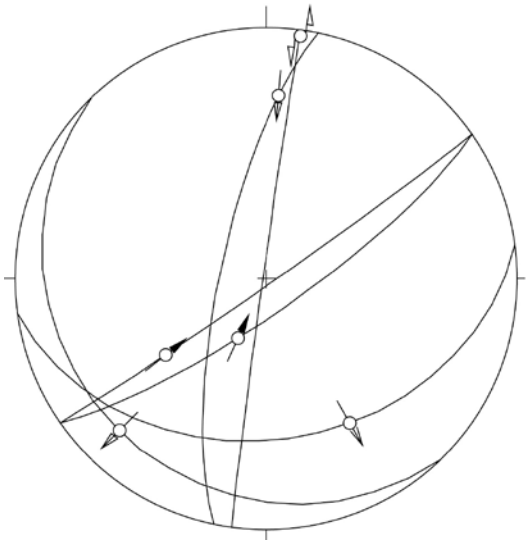

Figure 5-129. *Fault slip data for Ävrö granites in DZ 1 down to depth 183 m.*

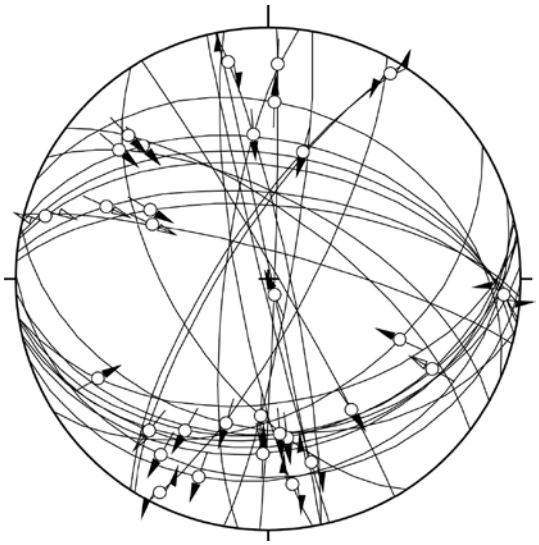

Figure 5-130. *Fault slip data for the upper transition zone (hosted in the dolerite dyke) of DZ 1. The dataset can be split in individual components, as shown in Figure 5-131.*

The orientation of these features is comparable to that of the striated planes from the upper granitic interval of DZ 1 (Figure 5-129). Crosscutting relationships are at times visible, as in Figure 5-131, where a steep fracture plane (shaded in white) truncates a flatter surface (shaded in red). This is however not a systematic relationship and we cannot establish a relative time sequence with confidence. Moreover, the moderately dipping surfaces are both normal and reverse fault planes and it is not clear from this section whether shortening or extension is the older tectonic regime that affected the rocks of DZ 1.

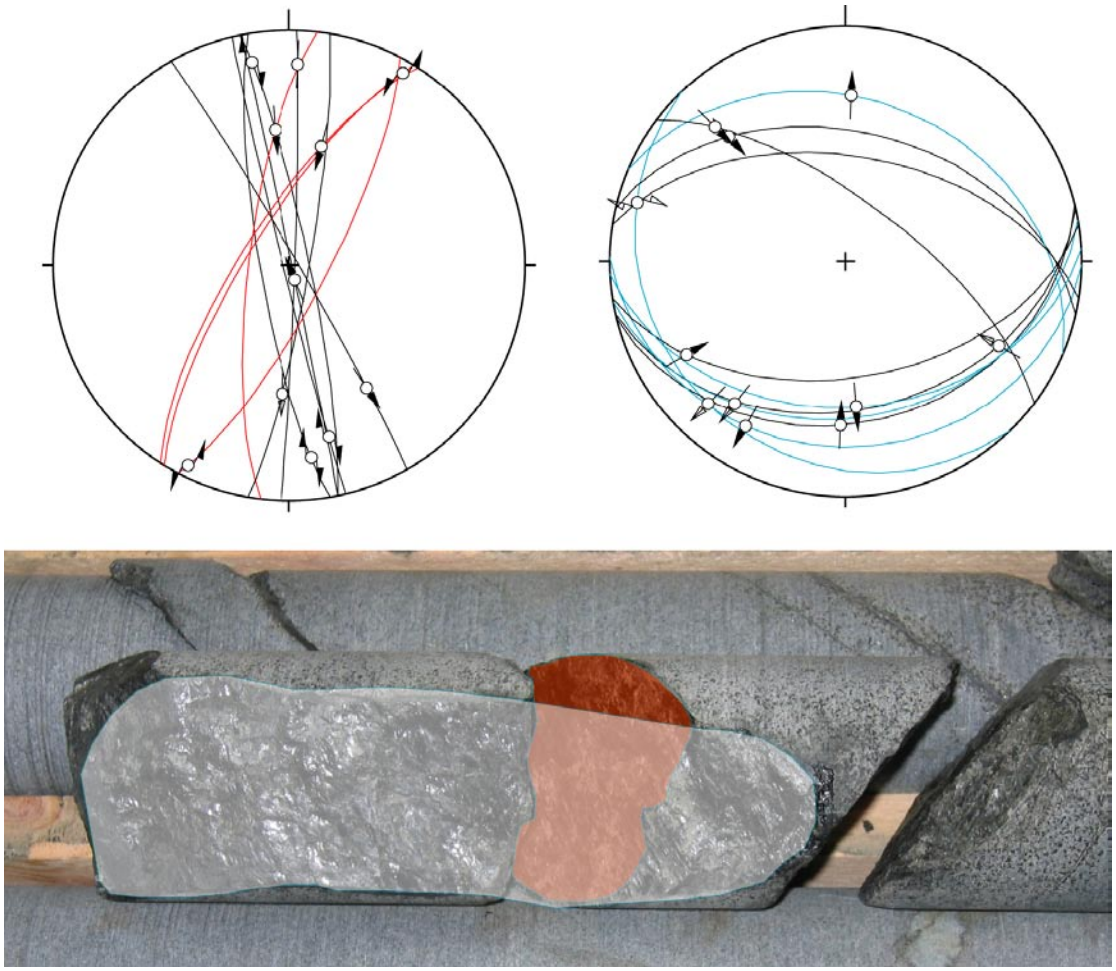

Figure 5-131. *The fault slip data can be resolved in several components. Steep, NNW- to NNE-striking sinistral (red great circles) and dextral (black circles) striated faults (top left stereonet) are separated from moderately N and S dipping normal (blue) and reverse (black) faults. The steep surfaces locally cut across the flatter ones (shaded in white and red, respectively, in the photograph at the bottom), although it remains undetermined whether these are normal or reverse structures.*

The occurrence of technical problems reported during recovery, core loss and crush zones increases with depth towards the fault core. There is major core loss from 215 to 224 m depth. The identification of the DZ core is based on the presence of numerous fractures sets and zones of crushed rock and core loss. The core extends from 211. 58 to 230 m depth and consists of several thinner cores, themselves defined by zones of crushed rock or very high fracture frequency. Numerous striated planes are present, but it was not possible to identify them in the BIPS image, thus precluding us from obtaining their orientation. A lower transition zone starts from depth 230.89 m. The zone is highly fractured, but the fracture frequency tends to decrease away from the core. Based on the fracture distribution, the upper transition zone is the more prominent of the two.

Table 5-45. Summary of DZ1.

Depth (m)	Box number	Interpretation	Description
182.37–211.58	16–22	Transition zone	Transition from granitic bedrock to dolerite. Progressive increase in fracture frequency. Numerous striated planes. Several narrow crush zones.
211.58–230.89	16	Fault core: crush zone	182.37–182.56 m heavily fractured rock/crush zone.
	20	Crush zone	~35 cm thick crush zone.
	21	Core loss	~10 cm core loss at 207.70 m.
	22–26	Fault core	Heavily fractured depth interval, with several crush zones and core loss. Major core loss between 215 m and 224 m.
230.89–234.31	26	Transition zone	Lithological change at 230.898 m from dolerite to granitic bedrock. High fracture frequency.

5.10.2 DZ 2: depth interval 261–265.9 m

This section consists of undeformed rock with low fracture frequency. A c. 30 cm thick crush zone occurs from 265.26 down to 265.54 m depth (Figure 5-132). The zone occurs within a sealed epidote network. We do not define this depth interval as a deformation zone due to the lack of relevant structural features (brittle or ductile) and/or fault rocks and transition zones.

Figure 5-132. *DZ 2 consists of relative undeformed rock with only a minor crush zone.*

Table 5-46. Summary of DZ 2.

Depth (m)	Box number	Interpretation	Description
257.12–268	31 –32	Host rock	Undeformed rock with low fracture frequency. No deformation zone.
265.26–265.54	32	Crush zone	Crush zone located within sealed epidote and calcite networks.

5.10.3 DZ 3: depth interval 312–313 m

DZ 3 is characterized by undeformed rock with low fracture frequency. A very minor crush zone extends from 312.54 to 312.91 m depth and overlaps with a doleritic dyke, whose contact to the granitic host rock is oriented 009/85 (Figure 5-133). The boundaries of the zone are sharp.

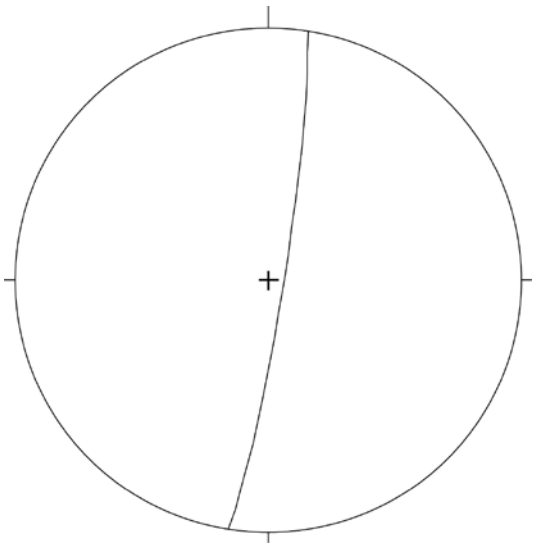

Figure 5-133. *Orientation of the doleritic dyke upper contact in DZ 3.*

Table 5-47. Summary of DZ 3.

Depth (m)	Box number	Interpretation	Description
312.06–312.54	41	Host rock	Undeformed rock with low fracture frequency.
312.54–312.91	41	Crush zone	Minor crush zone confined to a thin doleritic dyke.

5.10.4 DZ 4: depth interval 410–416 m

DZ 4 is in red stained granites and contains no relevant structural features apart from sporadic occurrences of centimetric dilational epidote and calcite bands (Figure 5-134). Minor cataclasis occured along their edges/walls. No systematic orientation is found for the veins (Figure 5-135). We do not interpret this depth interval as a deformation zone.

Figure 5-134. *DZ 4 consists of relatively undeformed rock with only a few epidote-calcite dilatant bands.*

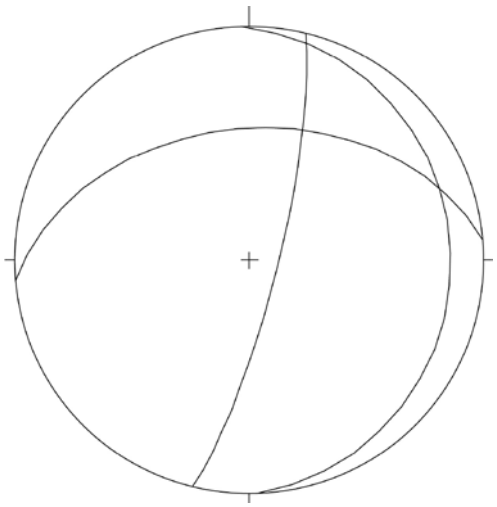

Figure 5-135. *Orientation of the epidote and calcite dilational veins found in DZ 4. No systematic orientation is observed.*

Table 5-48. Summary of DZ 4.

Depth (m)	Box number	Interpretation	Description
406.92–418.23	58–59	Host rock	Undeformed rock with low fracture frequency. A few occurrences of epidote-calcite veins. Red staining in the interval 410–416.45 m.

6 Field observations

The localities studied are shown in Figure 6-1, and their coordinates are listed in the Appendix. The data are displayed and analyzed site by site in the following subsections.

It is important to stress that the kinematic analysis of this section is based on the observation of reliable field brittle kinematic indicators and that reactivation is a common process that can easily lead to opposing kinematic evidence on the same structure. Caution is always needed when trying to unravel complex brittle kinematic patterns.

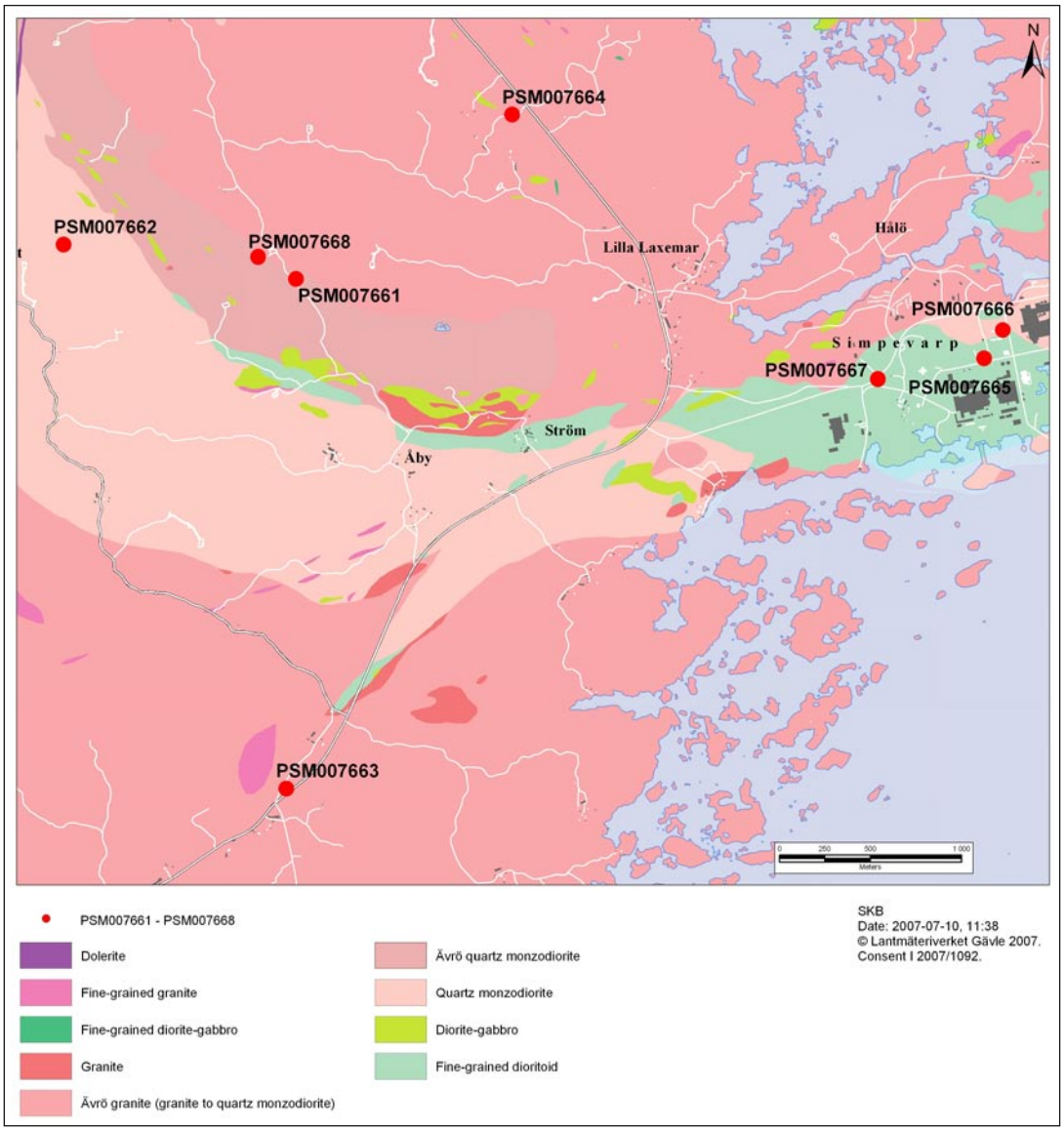

Figure 6-1. *Location of the outcrops studied and described in this report.*

6.1 PSM007661 (6366254/1548099)

The oucrop location is shown in Figure 6-1. The outcrop consists of a c. 50×3 m rock stripe cleaned from all its soil cover and vegetation in order to expose its highly fractured surface for a detailed fracture analysis. It corresponds to trench Gol 03 (ASM000116) of the detailed outcrop mapping study by /Forssberg et al. 2007/. The dominant lithology is the medium-grained porphyritic Ävrö granite. The granite is cut by fine-grained granite dykes, whose width varies between 1 and 10 cm. The outcrop is affected by systematic sets of hybrid fractures, showing variable amounts of shear and normal offsets. No fault rocks were found along these fractures. Unfortunately, no stretching lineations or striations could be measured or observed on the fractures' planes. We have therefore no direct constraints on the relative orientation of the sub-horizontal pavement (and thus the surface of observation) with respect to the shearing direction along the fractures. However, the many consistent kinematic observations at the outcrop scale make us confident that the observed structures have a predominantly strike-slip or low-obliquity character and that the kinematic interpretation here below is reliable.

The complexity of the fracture pattern of PSM007661 can be appreciated at a first glance from the stereonet of Figure 6-2, where a large number of fracture orientations are plotted in order to highlight possible systematic families of planar discontinuities.

Despite such complexity, detailed observations helped to identify a few key structural features and systematic sets of fractures.

A first major systematic fracture set trends roughly NS with subvertical dips to either the E or W (Figure 6-3). Epidote coating characterizes the fractures (Figure 6-4). The fractures' strikes are spread over a c. 30° interval about the NS direction.

Whereas in the westernmost sector of the trench the c. NS trending structures are interpreted to be predominantly sinistral (although field evidence remains at time ambiguous), in the eastern part their kinematics are consistently dextral and of easy and unambiguous interpretation due to obvious crosscutting relationships and dextral offsets of granitic dykes (Figure 6-5a). Examples of kinematic indicators associated with the NS striking set of fractures are shown in Figure 6-5. The overall impression is that of a predominantly dextral sense of shear, although locally sinistral kinematics are evident. Localized reactivation cannot be ruled out. Figure 6-5b actually supports the idea of structural reactivation. The large fracture on the right hand side of the image (oriented 179/87) is a clear example of contrasting kinematic indications along the same fracture plane/corridor.

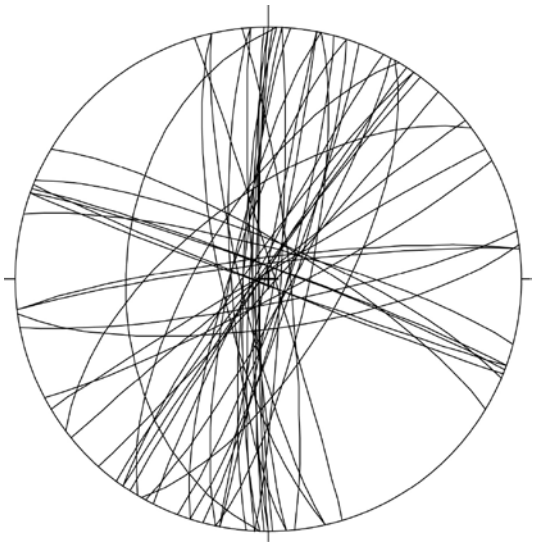

Figure 6-2. *Stereonet containing all the fractures measured at PSM007661.*

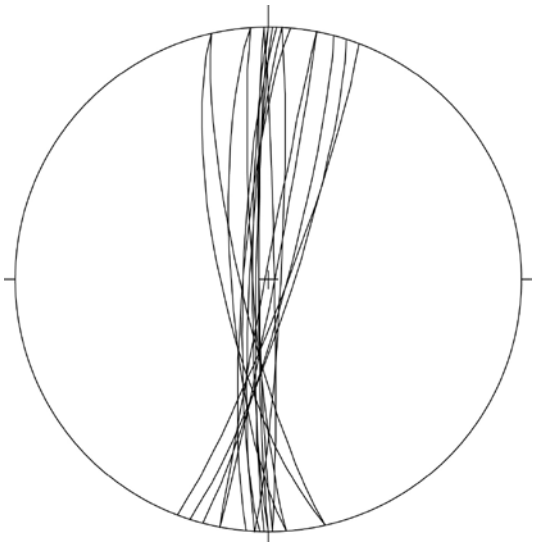

Figure 6-3. *A dominant fracture set (possibly representing two different conjugate orientations) strikes c. NS.*

Figure 6-4. *Epidote coating on a steep, NNE-striking fracture.*

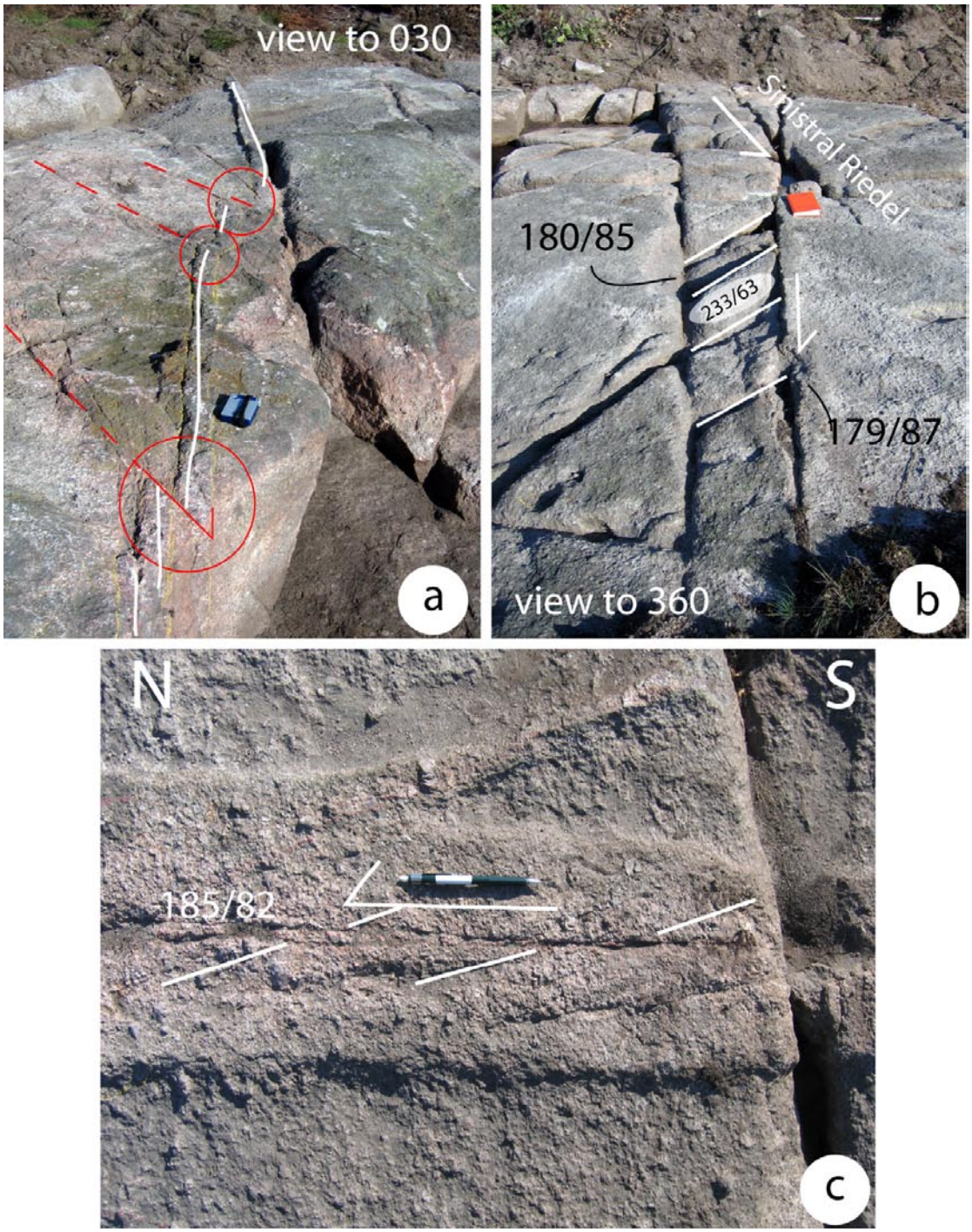

Figure 6-5. *Examples of kinematic indicators along the c. NS striking fractures. a): The fractures highlighted by the dashed red lines (oriented 354/83) cause several c. 10 cm dextral offsets of a microgranite dyke. b) Example of contrasting kinematic evidence along the same fracture plane. The fracture oriented 179/87 has an obvious sinistral Riedel shear in the upper part of the photograph, whereas in the lower part it seems responsible for the formation of a systematic set of dextral tension gashes, oriented 233/63. c) Sinistral kinematics along a fracture oriented 185/82 established from systematic sinistral Riedel shears.*

The northernmost segment of the fracture is associated with a very clear sinistral Riedel shear departing from the master plane, whereas to the S there occurs a series of four subparallel dilational gashes whose orientation is compatible with a dextral sense of shear (Figure 6-5b).

Structural analysis indicates that the generally dextral NS trending fractures are part of a conjugate set containing NE-SW striking sinistral fractures, as illustrated in Figure 6-6. The presence of secondary Riedel shears helps confirm the kinematics of the conjugate structures, as shown in the photograpgh to the right.

In addition to the main NS trending fractures, Figure 6-2 shows a systematic set of fractures oriented W/WNW-E/ESE. Secondary Riedel fractures indicate a consistent sinistral kinematics for the fractures (Figure 6-7). In general, as suggested by numerous abutting relationships, they appear to be post-dated by the NS fractures.

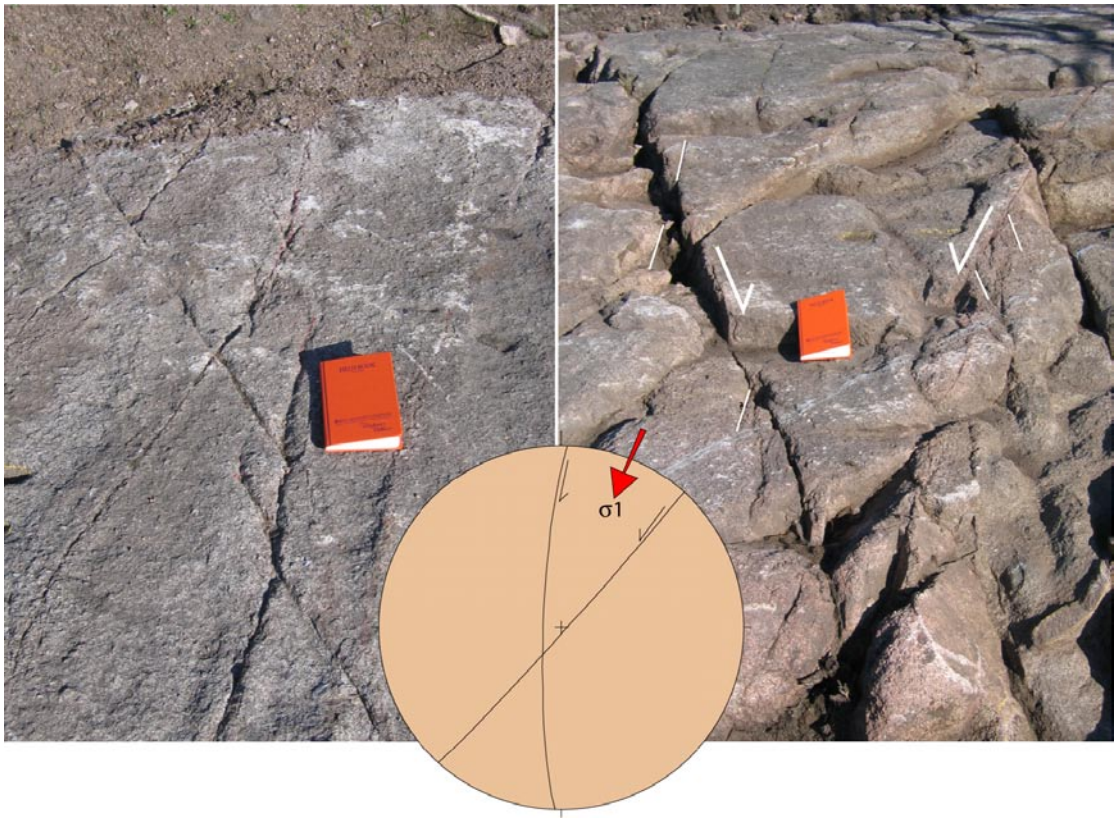

Figure 6-6. *Field evidence and stereonet of conjugate fracture sets. The acute angle defined by the intersection of the conjugate pairs is bisected by* σ_1.

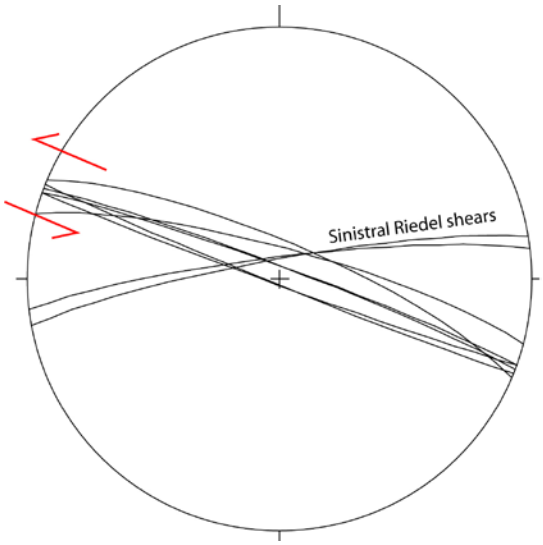

Figure 6-7. *A systematic set of W/WNW-E/ESE fractures is found in PSM007661. Sinistral kinematics is deduced from the presence of Riedel shears.*

6.2 PSM007662 (6366441/1546824)

The trench of PSM007662 corresponds to trench Gol 08 (ASM000121; Figure 6-8) of the study by /Forssberg et al. 2007/, and is located close to Lilla Basthult (Figure 6-1), in the western part of the Laxemar area. The dominant rock type exposed in the trench is grey, medium-grained quartz monzodiorite. Fine-grained granite dykes occur with sharp contacts to the host rock.

Two main systematic fracture sets were recognized at the outcrop (Figure 6-9). A first set strikes subvertically NNE-SSW, whereas a second family, also subvertical, strikes NW-SE. Fracture patterns at the outcrop scale are generally very complex, with many unsystematic fractures and second order Riedels creating schemes of difficult interpretation with respect to relative crosscutting relationships and kinematics (see for example Figure 6-10).

Figure 6-8. *View to the south of the trench investigated.*

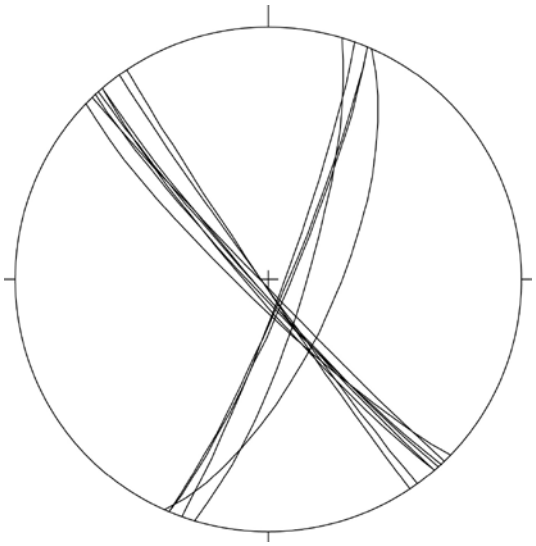

Figure 6-9. *Plot of the two systematic fracture sets observed at PSM007662.*

Figure 6-10. *Example of complex fracture pattern, which does not allow the establishment of the relative timing of fracture formation, their hierarchy nor their kinematics.*

The NNE-SSW striking set is suggested to be dextral on the basis of the spatial arrangement of its associated Riedel shears.

Riedel shears were also used in constraining the dextral kinematics of the NW-SE striking fractures (Figure 6-11). These fractures have centimetric apertures and have c. 1 m systematic spacing.

Figure 6-11. *Example of dextral Riedel along a NW-SE striking fracture.*

6.3 PSM007663 (6363455/1548045)

The outcrop, located along the main road between Lilla Laxemar and Figeholm (Figure 6-1), contains several striated planes. Figure 6-12 shows the fault-slip data collected. A rather complex kinematic pattern emerges, characterized by variably oriented fractures, generally dipping to the E, SE and S, indicating reverse, normal or strike-slip kinematics.

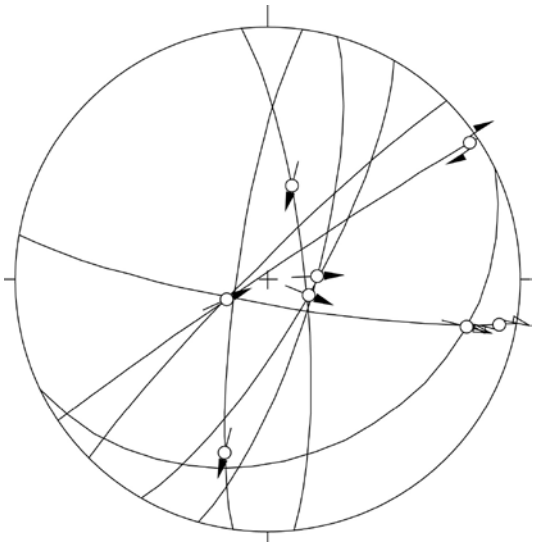

Figure 6-12. *Stereoplot of fault slip data for outcrop PSM007663.*

6.4 PSM007664 (6367156/1549283)

Outcrop PSM007664 is from the northermonst part of the Laxemar investigation area (Figure 6-1). It is a subhorizontal pavement that was stripped from its soil cover and vegetation to carry out detailed fracture mapping. The results are reported by /Cronquist et al. 2004/. In this section we rely on the geological and fracture mapping by the same authors and also use two of their figures to elaborate further the kinematics of the visible fracture sets. As shown in Figure 6-13 (Cronquist et al. 2004) the outcrop contains four different rock types, namely the Ävrö granite to quartz monzodiorite (generally porphyritic), fine-grained thin intrusive granite dykes and small bodies, a major dioritic body in the southern part of the outcrop and finally fine-grained mafic enclaves.

The detailed fracture map of /Cronquist et al. 2004/ is shown, in a modified version, in Figure 6-14. Our own detailed structural analysis shows that the highly fractured outcrop contains fractures that can be assigned to at least 5 systematic families. In order to facilitate recognition of these sets, we have highlighted selected fractures of each set with a different colour, which is also used to plot selected fracture planes of the same set in the stereonet at the bottom of Figure 6-14.

Following the key of the stereonet of Figure 6-14, each systematic set can be characterized as follows:

Set P:

P is possibly the most pervasive fracture set of the whole outcrop. It contains steep fractures that dip to the SSE. P fractures are thin and present a c. 3, 4 mm thick red staining halo along their walls. There are, however, also occurrences of very large, broken P fractures, with apertures up to several cm (Figure 6-15). The kinematics of P fractures are complex and there is evidence for structural reactivation under different kinematic conditions. Figure 6-15a, for example, shows sinistral stepping along a P fracture indicative of sinistral shearing. P fractures of Figure 6-15b, on the other hand, are interpreted as dextral fractures, as suggested by the presence of the intervening dextral dilatant fracture plane, which is interpreted as a tensional gash within a dextral shear corridor defined by bounding P fractures. No direct evidence for dextral shearing was however observed. The difference in style mentioned above for identically oriented P fractures (as actually visible in Figure 6-15) may suggest the presence of different generations of identically oriented fractures with different kinematics. No evidence was found, though, that could be used to establish a relative chronology between sinistral and dextral fractures within the P set.

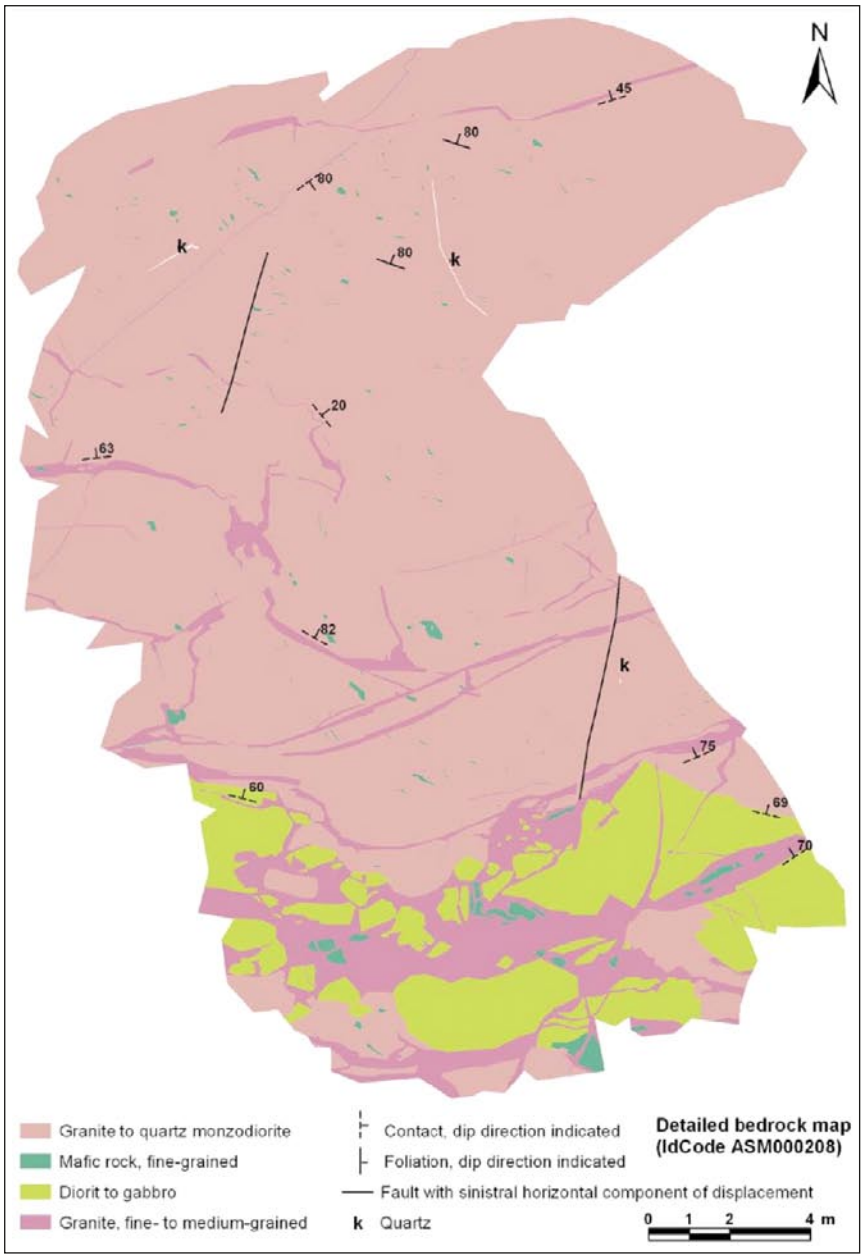

Figure 6-13. *Detailed geological map of outcrop PSM007664 taken from /Cronquist et al. 2004/.*

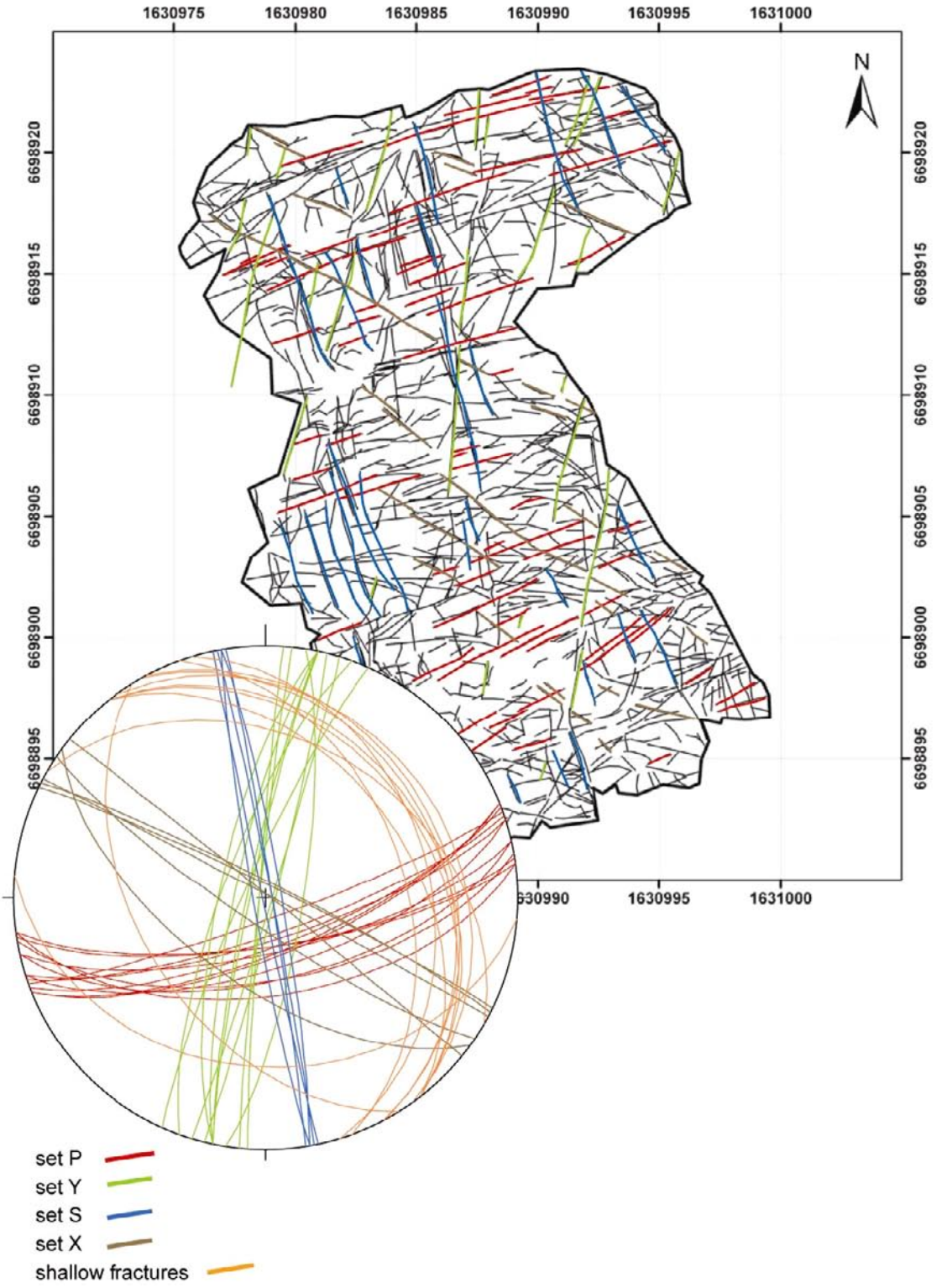

Figure 6-14. *Detailed fracture map for PSM007664 by /Cronquist et al, 2004/. Colours have been added to highlight systematic fracture sets, whose orientation is shown by the identically coloured great circles in the stereonet. Five systematic sets are highlighted.*

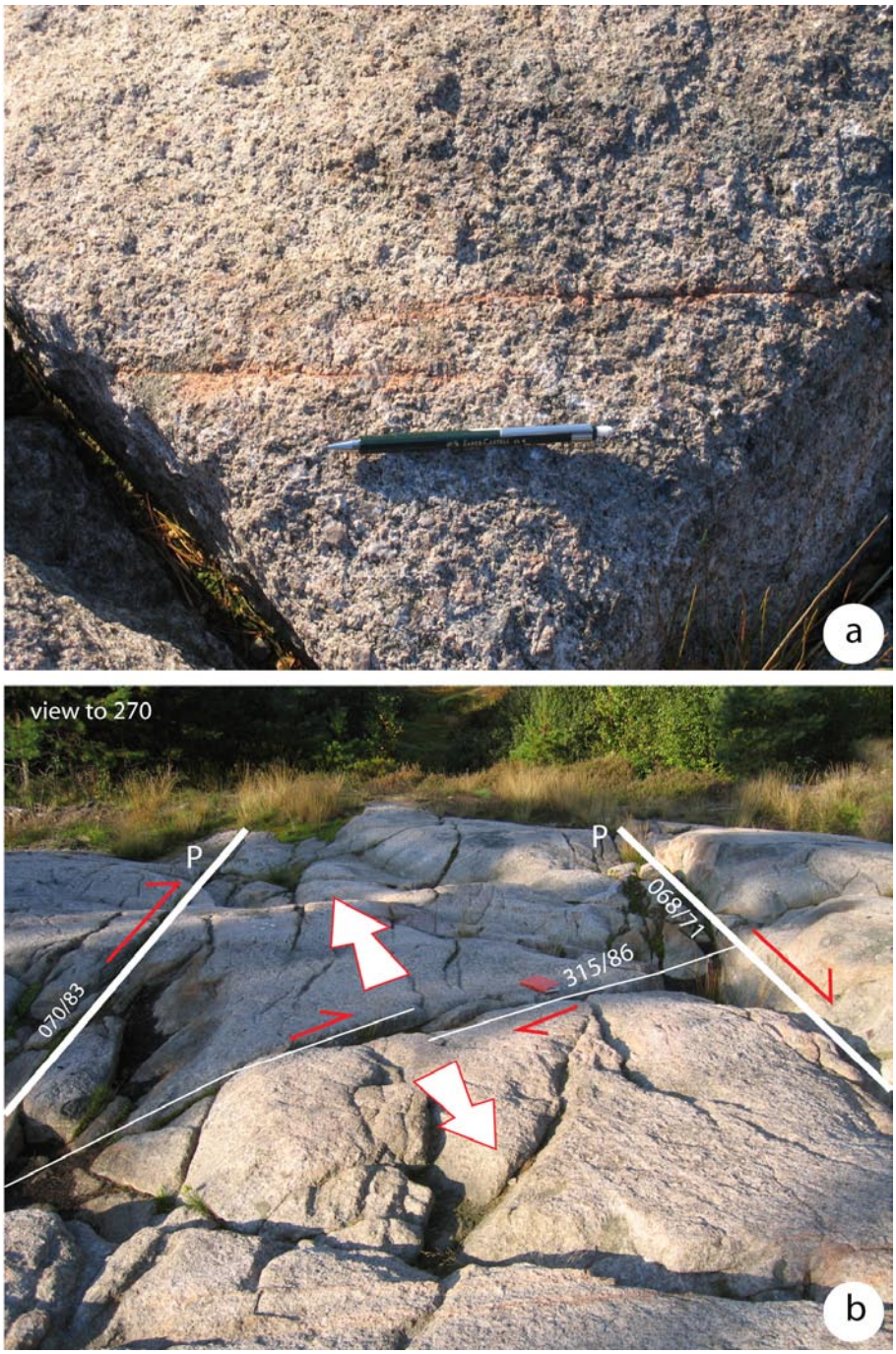

Figure 6-15. *Different style and contrasting kinematic evidence for fractures of the P set. The picture above shows a set of sinistrally stepped, thin fractures, whose walls are decorated by a thin red halo. The photograph at the bottom suggests instead possible evidence for dextral shearing along two large P fractures characterized by centimetric apertures. Reactivation and multiple shearing along the strike of set P are suggested.*

Set Y:

Set Y is coarsely spaced (c. 3 m) and cuts across the whole outcrop. It is mapped in green on the fracture map and on the stereonet of Figure 6-14. Fractures strike NNE-SSW and are subvertical. Fractures Y are consistently sinistral, as demonstrated, for example, by the sinistral 20 cm lateral offset of a granitic dyke (Figure 6-16).

An epidote-coated striated fracture of the Y set bears a lineation plunging sub horizontally to the SSW (Figure 6-17).

Figure 6-16. *Sinistral displacement of a granitic dyke across a fracture of set Y.*

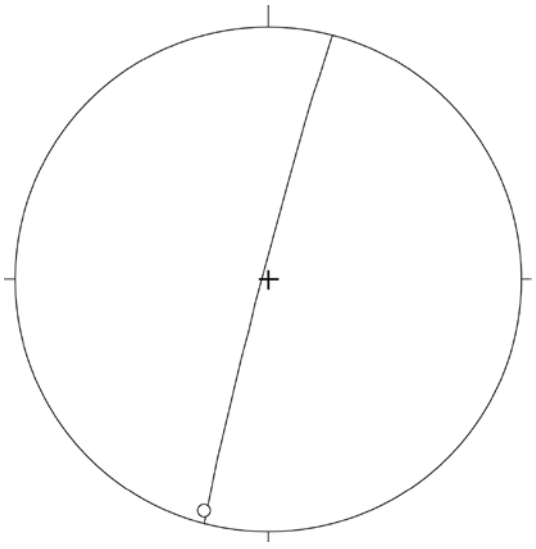

Figure 6-17. *Subhorizontal, SSW-plunging stretching lineation along an epidote-coated fracture of the Y set.*

Set S:

Set S, plotted in blue in Figure 6-14, is formed by generally thin fractures whose walls are stained by a millimetric red halo. No direct kinematic constraints were established for the fracture set. As shown in Figure 6-14, however, set S has similar spacing as set Y and occurs throughout the outcrop invariably together with Y. Their mutual angular relationship is typical of a conjugate set, with the acute angle centred roughly on the NS axis. It is tentatively suggested that sets Y and S are thus part of a conjugate system, which in turn requires set S to be dextral, given the sinistral kinematics established for set Y.

Set X:

No specific structural features characterize the NW-SE trending set X (plotted in brown in Figure 6-14).

Low-angle fractures:

An interesting feature is the presence of several low-angle fractures (in orange in the stereonet of Figure 6-14). They dip shallowly to the NE, with a couple of conjugate structures dipping to the SW. Due to their relatively low dip angle, their intersection with the rough outcrop surface generates very irregular trend lines. Their surfaces are generally smooth and polished. We could not establish their kinematics.

6.5 PSM007665 (6365817/1551870)

This dioritic outcrop (see Figure 6-1 for its location, at the entrance of the “Bergrunnslager”) contains several good-quality striated planes and a distinct ductile shear zone. Several striated planes dipping moderately to the SE and S show consistent reverse kinematics, with top-to-the-N/NW sense of shear and a low degree of obliquity (Figure 6-18). A well-preserved set of steep strike-slip conjugate fractures (purple great circles in Figure 6-18) constraints a N/NNW oriented greatest horizontal shortening direction (Figure 6-19). The NE-striking dashed great circle bears two resolvable slickenline directions and kinematics, namely dextral strike-slip and reverse top-to-the-N. Striated planes are invariably coated by epidote and chlorite.

The red great circles plot the orientation of the protomylonitic foliation of a discrete shear zone that dissects the outcrop with a NE/ENE-SW/WSW orientation (Figure 6-19). Foliation planes bear a gently WSW-plunging stretching lineation, which suggests a predominantly strike-slip character for the shear zone.

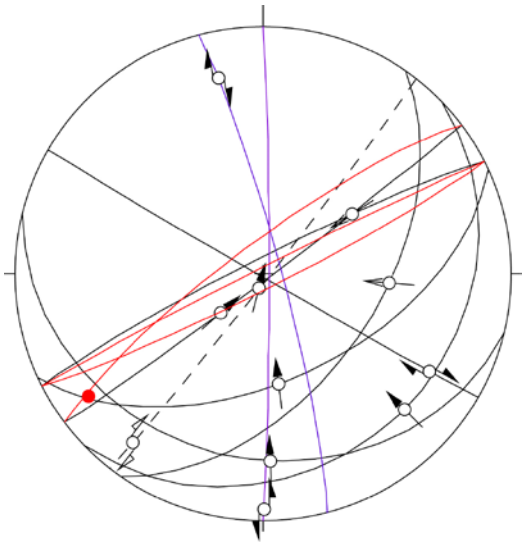

Figure 6-18. *Fault slip data for outcrop PSM007665. The dashed great circle is a plane containing two generations of slickenlines. The pair of purple great circles plots a well-defined conjugate set of steep strike-slip faults (see also Figure 6-19). The red great circles are the foliation of a minor ductile shear zone cutting across the outcrop. A gently SW-plunging stretching lineation suggests a principally strike-slip kinematics for the shear zone.*

Figure 6-19. *Left: the shaded white area highlights the width and the trend of the protomylonitic shear zone that dissects outcrop PSM007665 and whose orientation is shown by red great circles in Figure 6-18. In the background is visible Block 3 of the atomic power plant. Right: detail of the striated dextral fault oriented 345/84.*

6.6 PSM007666 (6365972/1551972)

Outcrop PSM007666 is a road outcrop located opposite to the western entrance of Block 3 of the atomic power plant (see Figure 6-1 for its exact geographical location). Diorites contain several epidote- and epidote/calcite-coated striated planes. Calcite is found along steep, generally strike-slip, N-S trending fractures (green great circles in Figure 6-20), whereas epidote coats SE- to S-dipping normal or reverse faults (black circles in Figure 6-20).

Red circles represent the orientation of a ductile (possibly strike-slip) shear zone (Figure 6-21) oriented ENE-WSW, which is very likely the along-strike continuation of the shear zone described in the previous section.

6.7 PSM007667 (6365704/1551288)

This fine-grained dioritoid oucrop contains several epidote-coated striated surfaces. Steep sinistral NW-SE fractures characterize the outcrop.

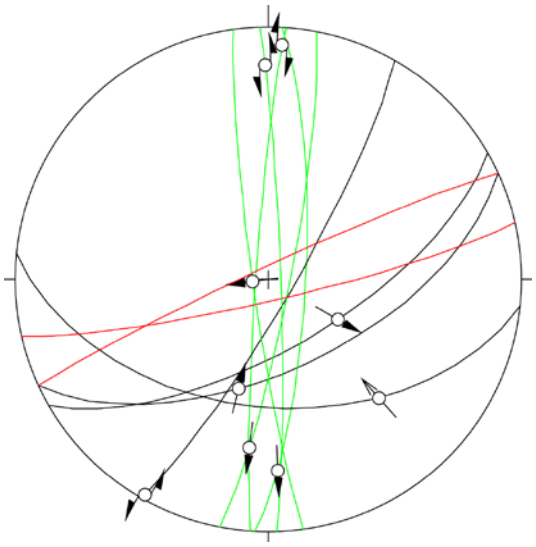

Figure 6-20. *Fault slip data for PSM007666. In green are calcite-coated striated planes, in black epidote-coated planes, whereas the red great circles show the orientation of a ductile shear zone that deforms the outcrop.*

Figure 6-21. *Steep protomylonitic shear zone in the outcrop opposite to the western entry of Block 3. Granitic slivers are visible in the deformed part.*

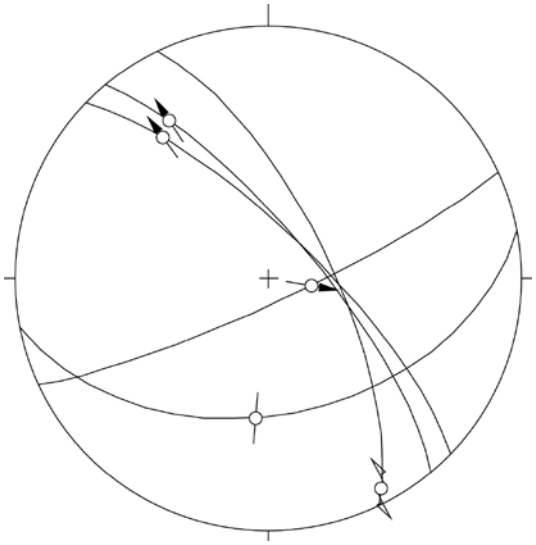

Figure 6-22. *Fault slip data from the dioritic rocks of outcrop PSM007667.*

6.8 PSM007668 (6366375/1547890)

The outcrop is the westernmost trench of a series of roughly E-W striking trenches, whose easternmost component has been discussed and analyzed in PSM007661 (Figure 6-1). The outcrop corresponds to trench Gol 02 (ASM000115) of the detailed outcrop mapping study by /Forssberg et al. 2007/. The dominant lithology at the outcrop is the medium-grained porphyritic Ävrö granite. The granite is cut by fine-grained granite dykes, whose width varies between 1 and 10 cm. The oucrop is characterized by 3 systematic sets of fractures.

A first set strikes E/ESE-W/WSW and dips very steeply to the NNE and SSW (Figure 6-23). Fractures have exactly the same orientation as PSM007661 fractures plotted in Figure 6-7. They are usually very straight, but become slightly curvilinear close to their terminations.

Kinematic indicators, such as systematic Riedel shears and tension gashes, suggest sinistral sense of shear, thus consistent with the observations made at PSM007661.

A second systematic set contains subvertical fractures oriented N/NNE-S/SSW (Figure 6-24). Orientation similarities suggest that these fractures belong to the same set of Figure 6-3 for PSM007661. Unfortunately, no kinematic indicators were observed in at PSM007668 to help constrain the sense of shear along these fractures.

A last set of fractures is shown in Figure 6-25. ENE/WSW striking fractures are observed throughout the outcrop, but unfortunately no clear and consistent kinematic indicators could be seen, although some minor Riedel shears suggest an overall dextral sense of shear. It remains also undetermined what the relative timing of this fracture set is with respect to the other sets observed at the outcrop.

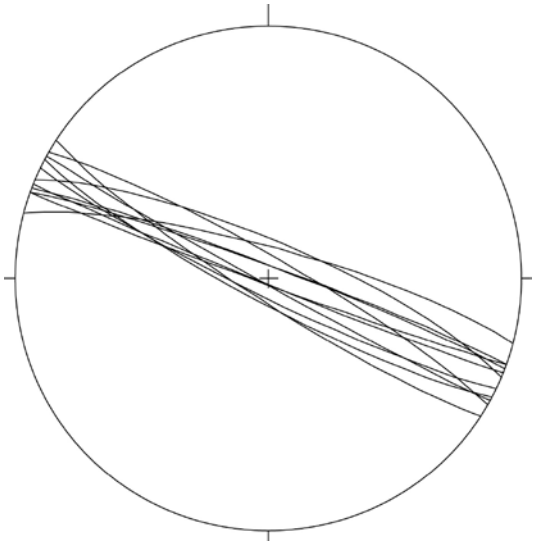

Figure 6-23. *ESE/WNW striking fractures characterize PSM007668. Kinematic indicators suggest sinistral sense of shear along these fractures.*

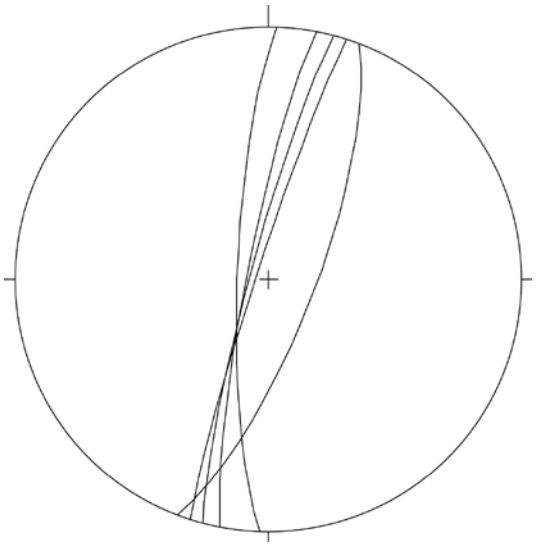

Figure 6-24. *A second systematic fracture set contains NNE/SSW striking fractures.*

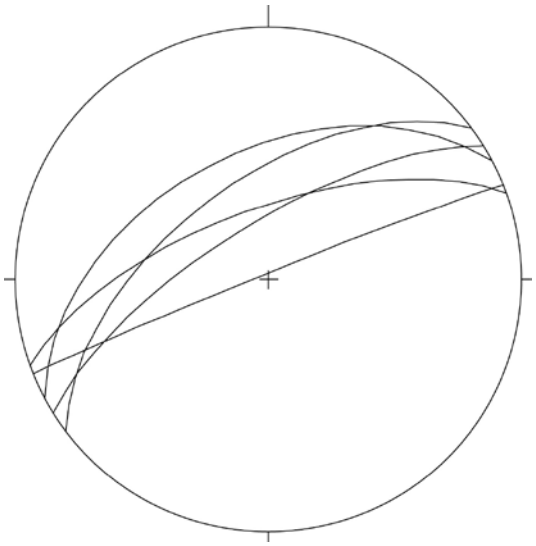

Figure 6-25. *A third systematic set at PSM007668 contains ENE/WSW fractures.*

The easternmost part of the trench contains sets of conjugate fractures (Figure 6-26), which constrain σ_1 along the E-ESE/W-WNW direction. On the ground of similar orientation, the ESE/WNW striking fractures can be part of the first systematic sinistral fracture set described for PSM007668 and shown in Figure 6-23.

The orientation of the fractures forming the conjugate pairs is also identical to the orientation of the fractures of Figure 6-7 for PSM007661. In that case, however, the ESE/WSW striking fractures are interpreted as master fractures, whereas the c. E-W features are Riedel shears whose spatial arrangement indicates the sinistral kinematics of the master fractures. In the case of PSM007668, instead, there does not seem to exist a hierarchical relationship between the fractures, which, as shown by Figure 6-26, are instead truly part of a conjugate set.

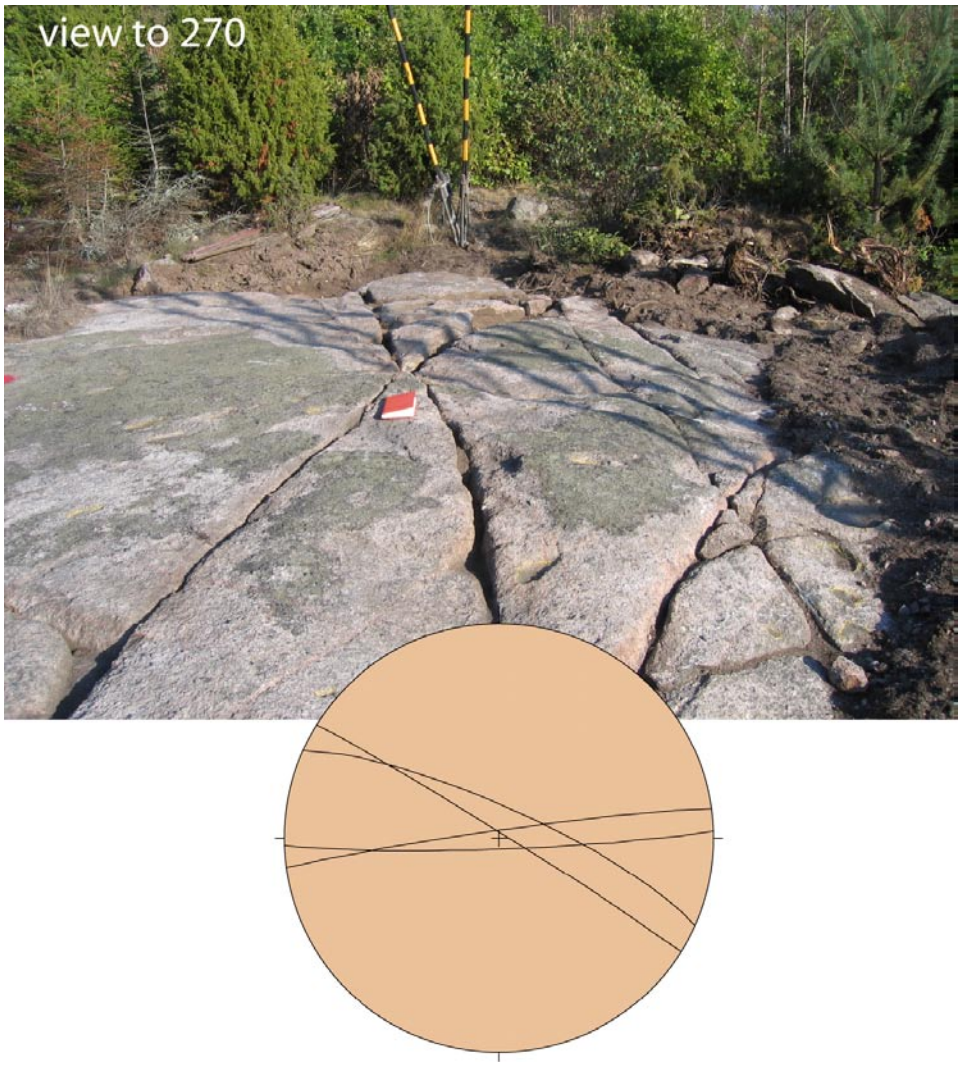

Figure 6-26. *Field view and orientation of conjugate fractures in PSM007668.*

6.9 Summary and discussion of field data

The structural field data discussed in this section is summarized in Figure 6-27. In order to integrate the results obtained by /Viola and Venvik Ganerød 2007/ and to allow for an easy visual comparison, Figure 6-28 reports the summary of the field observations of that study.

Outcrops containing striated planes and kinematic information will be used in a separate report for a detailed study of the paleostress evolution in the region and are therefore not used here to elaborate on local trends or models. The trenches and the polished outcrops studied during this study generally lack striated fault planes and kinematic inferences were therefore made on the basis of displaced structural markers or geometric relationships involving Riedel shears. Outcrops PSM007661, 2, 4 and 8 are heavily fractured and often of difficult interpretation. However, in several cases the sense of shear of specific sets of systematic fractures could be determined with confidence, as discussed in the individual sections on each outcrop. This is shown and summarized by the red arrows drawn on top of the stereonets in Figure 6-27.

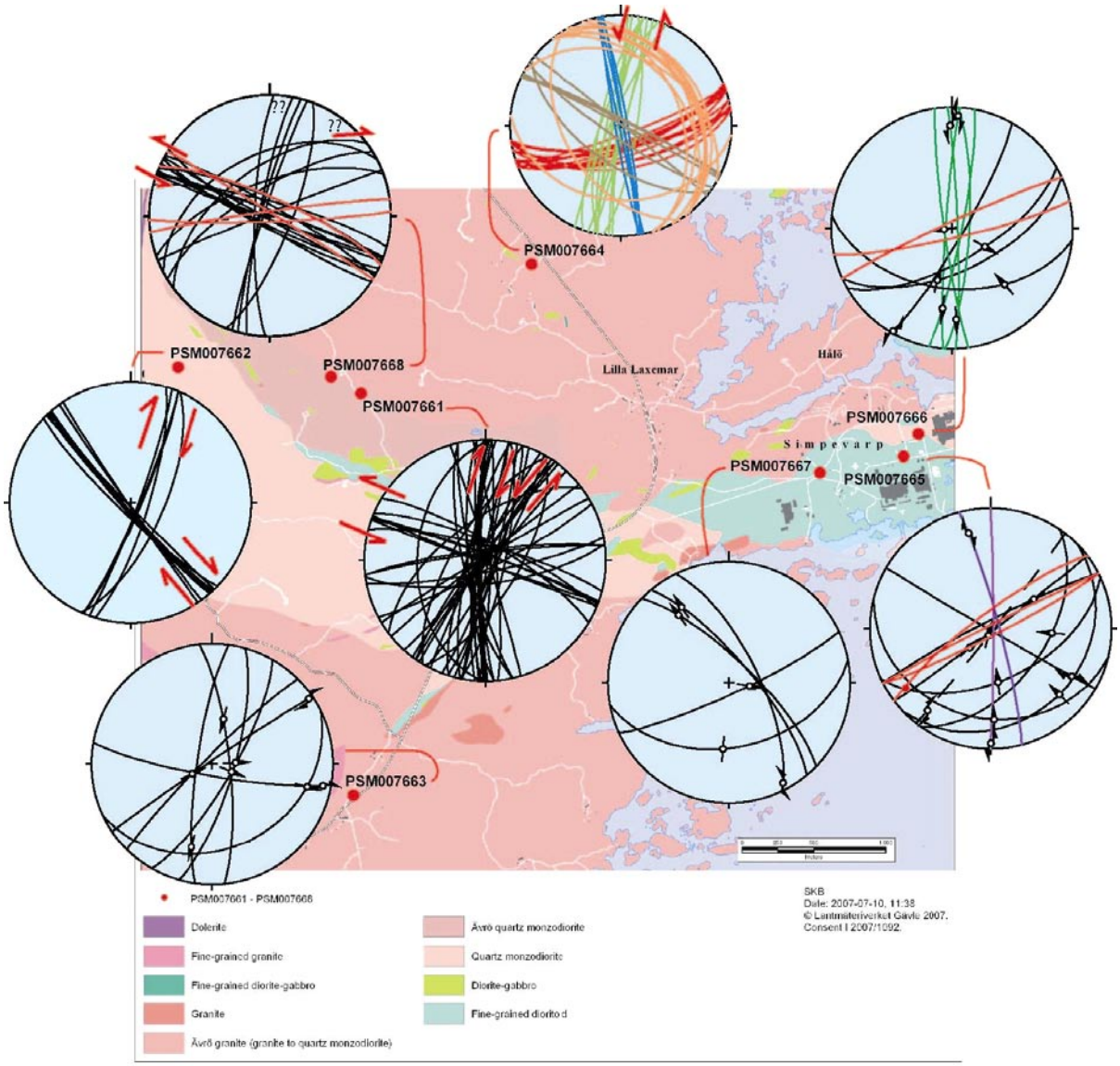

Figure 6-27. *Summary of field structural observations. Detailed information on each of the stereonets can be found in the descriptive section of each field locality.*

PSM007661 and PSM007668, for example, integrate well and confirm the sinistral kinematics of the WNW-ESE trending fractures. Stereonet 2 of Figure 6-28 shows a large number of similarly oriented fractures that were observed and measured by /Viola and Venvik Ganerød 2007/ in a series of outcrops in the same area. Unfortunately, no direct kinematic constraints on those fractures were observed in that study, and their sense of shear was thus suggested to be sinistral only on the basis of larger-scale correlations. The results of this study are therefore of great utility to help build kinematic models at a larger scale.

Reactivation has been shown to be common throughout the area and kinematic complexities can be the result of multiple shearing events, with different senses of shear along the same fracture planes. For example, there exist many steep fractures, striking roughly N-S, which have either sinistral or dextral kinematics (PSM007661, 62, 64 and 68). No clear kinematic picture emerges, with both sinistral and dextral shear, and in addition fractures do not seem to belong to clear conjugate sets.

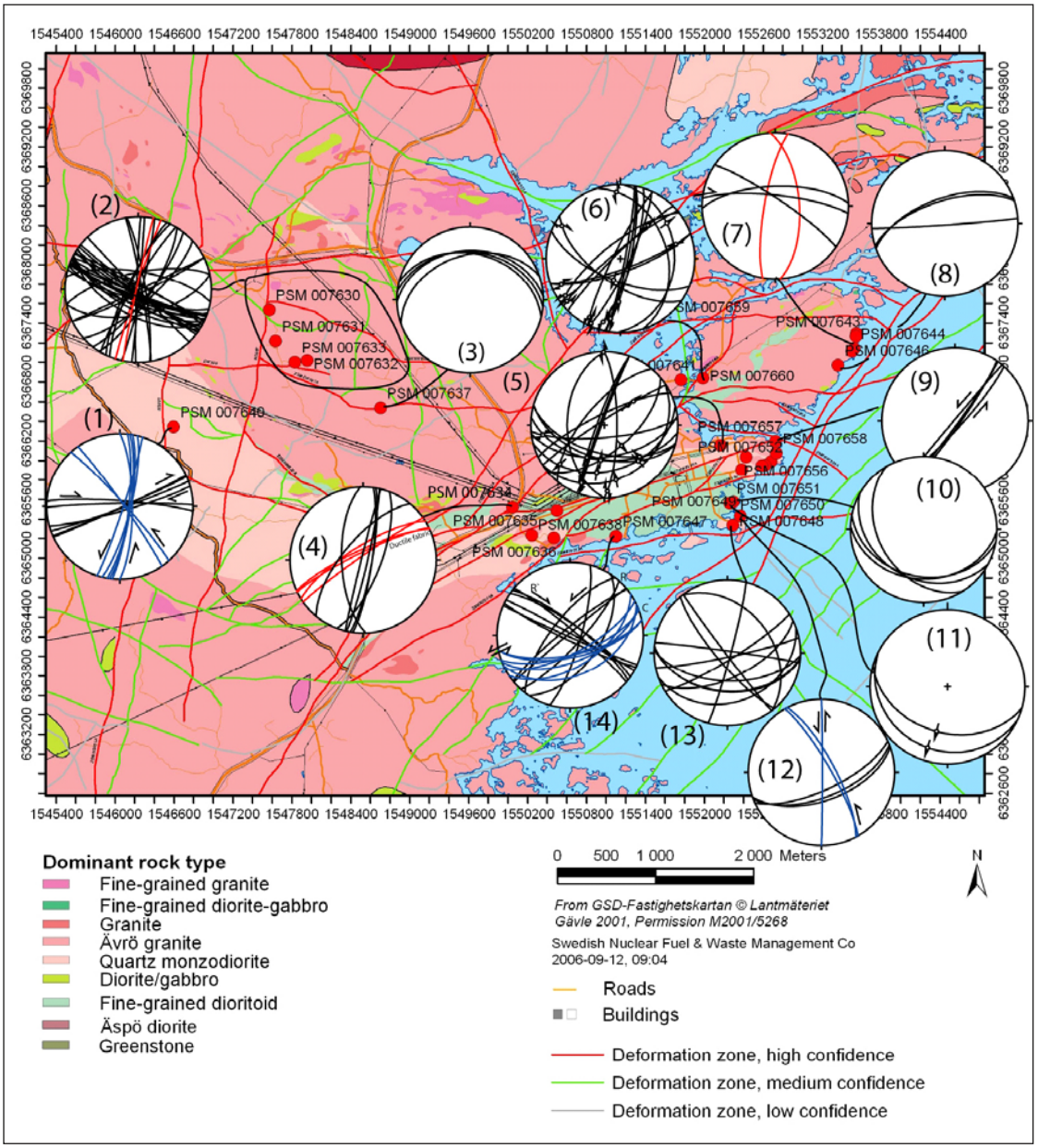

Figure 6-28. *Summary of field data from /Viola and Venvik Ganerød 2007/.*

7 References

Braathen A, 1999. Kinematics of brittle faulting in the Sunnfjord region, western Norway. Tectonophysics 302, 99–121.

Braathen A, Gabrielsen R H, 2000. Bruddsoner i fjell – oppbygning og definisjoner. Gråstein, 7, 1–20. Norges geologiske undersøkelse, ISSN 0807-4801.

Braathen A, Osmundsen P T, Nordgulen Ø, Roberts D, Meyer G B, 2002. Orogen-parallel extension of the Caledonides in northern Central Norway: an overview. Norwegian Journal of Geology, 82, 225–241.

Braathen A, Osmundsen P T, Gabrielsen R, 2004. Dynamic development of fault rocks in a crustal-scale detachment; an example from western Norway. Tectonics, 23, TC4010, doi:10.1029/2003TC001558.

Caine J S, Evans J P, Forster C B, 1996. Fault zone architecture and permeability structure. Geology, 24, 11, 1025–1028.

Carlsten S, Hultgren P, Mattsson H, Stanfors R, Wahlgren C-H, 2004. Geological single-hole interpretation of KLX04, HLX21 and HLX23, HLX24 and HLX25. SKB P-04-309, Svensk Kärnbränslehantering AB.

Carlsten S, Hultgren P, Mattsson H, Stanfors R, Wahlgren C-H, 2005. Geological single-hole interpretation of KLX03, HLX26 and HLX27. SKB P-05-038, Svensk Kärnbränslehantering AB.

Carlsten S, Hultgren P, Keisu M, Stråhle A, Wahlgren C-H, 2007a. Geological single-hole interpretation of KLX11A. SKB P-07-69, Svensk Kärnbränslehantering AB.

Carlsten S, Hultgren P, Mattsson H, Stanfors R, Stråhle A, Wahlgren C-H, 2007b. Geological single-hole interpretation of KLX10, HLX20 and HLX36. SKB P-07-66, Svensk Kärnbränslehantering AB.

Carlsten S, Hultgren P, Mattsson H, Stråhle A, Wahlgren C-H, 2007c. Geological single-hole interpretation of KLX12A, KLX09G, KLX10B and KLX10C. SKB P-07-68, Svensk Kärnbränslehantering AB.

Carlsten S, Hultgren P, Mattsson H, Stråhle A, Wahlgren C-H, 2007d. Geological single-hole interpretation of KLX18A and KLX20A. SKB P-07-70, Svensk Kärnbränslehantering AB.

Carlsten S, Hultgren P, Thunehed H H, Stanfors R, Stråhle A, Wahlgren C-H, 2007e. Geological single-hole interpretation of KLX09 and HLX37. SKB P-07-67, Svensk Kärnbränslehantering AB.

Cronquist T, Forssberg O, Hansen L M, Johnsson A, Koyi S, Leiner P, Sävås J, Vestgård J, 2004. Detailed fracture mapping of two outcrops at Laxemar. SKB P-04-274, Svensk Kärnbränslehantering AB.

Evens J P, Forster C B, Goddard J V, 1997. Permeability of fault-related rocks, and implications for hydraulic structure of fault zones. Journal of Structural Geology, 19, 1393–1404.

Forssberg O, Cronquist T, Vestgård J, Bergkvist L, Hermanson J, Öhman J, Pettersson A, Koyi S, Bergman T, 2007. Oskarshamn site investigation: detailed outcrop mapping in trenches. SKB P-07-29, Svensk Kärnbränslehantering AB.

Gudmundsson A, Berg S S, Lyslo K B, Skurtveit E, 2001. Fracture networks and fluid transport in active fault zones. Journal of Structural Geology 23, 343–353.

Higgings M W, 1971. Cataclastic Rocks. Geological Survey Professional Paper, 687, 1–97.

Munier R, Stanfors R, Milnes A G, Hermanson J, Triumf C-A, 2003. Geological Site Descriptive Model. A strategy for the development during site investigations. SKB R-03-07, Svensk Kärnbränslehantering AB.

Nordgulen Ø, **Braathen A, Corfu F, Osmundsen P T, Husmo T, 2002.** Polyphase kinematics and geochronology of the Kollstraumen detachment, north-central Norway. Norwegian Journal of Geology, 82, 299–316.

Osmundsen P T, Braathen A, Nordgulen Ø, Roberts D, Meyer G B, Eide E A, 2003. The Nesna shear zone and adjacent gneiss-cored culminations, North-central Norwegian Caledonides. Journal of the Geological Society, London 160*,* 1–14.

Petit J P, 1987. Criteria for the sense of movement on fault surfaces in brittle rocks. Journal of Structural Geology 9, 597–608.

Sibson R H, 1977. Fault rocks and fault mechanisms. J Geol Soc London, 133, 191–213.

Viola G, Venvik Ganerød G, 2007. Structural analysis of brittle deformation zones in the Simpevarp-Laxemar area, Oskarshamn, southeast Sweden. Report from Phase 1. SKB P-07-41, Svensk Kärnbränslehantering AB.

Appendix

Cores and core sections logged

Drill core	Sec-Up (m)	Sec-Low (m)	DZ	Meters
KLX03	722.5	814	DZ1	91.5
KLX04	227	230	DZ1	3
KLX04	254	258	DZ2	4
KLX04	295	298	DZ3	3
KLX04	325	326	DZ4	1
KLX04	346	355	DZ5	9
KLX 08	385	427	DZ6	42
KLX 08	476.5	487.5	DZ 7	10
KLX09	105.8	106	DZ1	0.2
KLX09	137.6	138	DZ2	0.4
KLX09	147	148	DZ3	1
KLX09	206	209	DZ4	3
KLX09	261.8	264	DZ5	2.2
KLX09	272	276	DZ6	4
KLX09	313	323.2	DZ7	10.2
KLX09	440	446	DZ8	6
KLX09	492.4	509	DZ9	16.6
KLX09	520	554	DZ10	34
KLX09	611	618.3	DZ11	7.3
KLX09	648.6	649.6	DZ12	1
KLX09	682	722	DZ13	40
KLX09	744.5	761	DZ14	16.5
KLX09	799.6	803	DZ15	3.4
KLX09	815	815.25	DZ16	0.25
KLX09	848.7	852.6	DZ17	3.9
KLX09	867.8	869.7	DZ18	1.9
KLX 10	690.5	706	DZ 9	16.5
KLX11A	142.25	142.9	DZ1	0.65
KLX11A	162.75	163.267	DZ2	0.52
KLX11A	168.7	169.9	DZ3	1.2
KLX11A	247.67	272	DZ4	24.5
KLX11A	285.4	286.4	DZ5	1
KLX11A	306.22	308.78	DZ6	2.75
KLX11A	345.3	348.03	DZ7	2.5
KLX11A	417.26	418.1	DZ8	2.7
KLX11A	430.56	432.2	DZ9	0.85
KLX11A	473.62	475.7	DZ10	1.65
KLX11A	486.1	513.15	DZ11	2.1
KLX11A	522.85	528.66	DZ12	27
KLX11A	577.9	586.16	DZ13	5.8
KLX11A	593.9	602.27	DZ14	8.3
KLX11A	689.06	689.86	DZ15	8.4
KLX11A	853	860	DZ16	0.8
KLX11A	906.84	907.6	DZ17	7
KLX11A	974.1	975.2	DZ18	0.8

Drill core	Sec-Up (m)	Sec-Low (m)	DZ	Meters
KLX 12A	445.6	447.55	DZ10	1.1
KLX 12A	498.85	499.54	DZ11	0.69
KLX 12A	596.5	600.8	DZ12	4.3
KLX18A	137.8	143.9	DZ1	6.1
KLX18A	148.6	149.4	DZ2	0.8
KLX18A	283.75	291.6	DZ3	7.85
KLX18A	359.6	366.2	DZ4	6.5
KLX18A	378.6	378.85	DZ5	0.25
KLX18A	401	404.2	DZ6	3.2
KLX18A	428	434	DZ7	6
KLX18A	448.35	456.55	DZ8	8.2
KLX18A	471.9	488.9	DZ9	17
KLX20A	171.38	234.45	DZ1	63.1
KLX20A	261	265.9	DZ2	5
KLX20A	312.55	313	DZ3	0.5
KLX20A	410.1	416.4	DZ4	6.3
Total (m)				**674.41**

List of field localities

Field localities			Swedish grid, RT 90	
Name	Northing (m)	Easting (m)	Accuracy	Area
PSM 007661	6366254	1548099	7 m	Laxemar
PSM 007662	6366441	1546824	7 m	Laxemar, Lilla Basthult
PSM 007663	6363455	1548045	8 m	Laxemar
PSM 007664	6367156	1549283	9 m	Laxemar
PSM 007665	6365817	1551870	9 m	Laxemar
PSM 007666	6365972	1551972	7 m	Laxemar
PSM 007667	6365704	1551288	5 m	Laxemar
PSM 007668	6366375	1547890	7 m	Laxemar